
Unitary Renormalization Group Solution of the Extended Anderson Impurity Model

MS Project Report

submitted in partial fulfillment of the requirements for the degree of

Master of Science

by

Abhirup Mukherjee
(18IP014)

under the supervision of

Dr. Siddhartha Lal

July 25, 2022

Emergent Phenomena and Quantum Matter Group
Department of Physical Sciences
Indian Institute of Science Education and Research Kolkata



Contents

Contents	i
1 Introduction	1
1.1 What is the minimal impurity model for a Mott metal-insulator transition?	1
1.2 Summary of the Anderson impurity problem	2
1.3 Some outstanding questions	3
1.4 Salient features of the method	4
1.5 Layout of the thesis	5
1.6 Summary of main results	5
2 Unitary Renormalization Group Method	7
2.1 Formalism	7
2.2 Prescription	16
2.3 URG analysis of the star graph model	18
2.4 URG analysis of the single-channel Kondo model	21
3 Connection between URG and Other Canonical Transformations	25
3.1 Poor man's scaling (PMS)	25
3.2 Schrieffer-Wolff transformation (SWT)	35
3.3 A comparison of URG, SWT and PMS on the Anderson model	39
3.4 Deriving the Kondo model from the Anderson model via a one-shot URG	40
3.5 Continuous unitary transformation RG	44
3.6 Comparison of the Canonical Transformations	48
4 URG of the single-impurity Anderson model: RG flows and fixed point Hamiltonian	51
4.1 Brief description of the single-impurity Anderson model	51
4.2 Calculation of renormalisation	51
4.3 Scaling equations for the SIAM	52
4.4 Connection to poor man's scaling	52
4.5 Preservation of particle-hole symmetry	53
4.6 Numerical analysis of the particle-hole symmetric RG equations	54
5 Physics of the extended single-impurity Anderson model	56
5.1 Introduction of spin-exchange and charge isospin-exchange interactions: the origin of the extended SIAM	56
5.2 RG equations for extended SIAM	58
5.3 Nature of coupling RG flows	58
5.4 Effective Hamiltonian and ground state	60
5.5 Approach towards the thermodynamic limit	61
5.6 Effective temperature scale at the fixed point	63
5.7 Impurity susceptibilities	64
5.8 Specific heat	67
5.9 Renormalization of impurity spectral function	68
5.10 Effective Hamiltonian for excitations of the Kondo cloud	71
5.11 Obtaining the real space low energy Hamiltonian: the local Fermi liquid	77

5.12	Destruction of the Abrikosov-Suhl resonance: passage from strong coupling to local moment	83
5.13	Calculating the $T = 0$ Wilson ratio from low energy excitations	87
5.14	Luttinger's and Friedel's sum rules	90
5.15	Reverse RG analysis	93
6	Effect of minimal attractive correlation in the bath	97
6.1	The modified hamiltonian	97
6.2	RG Equations	97
6.3	Phase diagram	98
6.4	Evolution of the groundstate across the transition	99
6.5	Evolution of various correlation measures and other quantities	100
6.6	Presence of sub-dominant pair fluctuations	103
6.7	Spectral functions	103
6.8	Bath spectral function $A_{00}(\omega)$ and the relation to DMFT	106
6.9	What, then, are the minimal ingredients for a metal-insulator transition?	109
	Appendix A Zero temperature Greens function in frequency domain	113
	Appendix B Derivation of RG equations for the impurity model with U, V, J, K, U_b, η	116
B.1	The full UV Hamiltonian	116
B.2	Renormalisation in the absence of U_b	117
B.3	Renormalisation in the presence of U_b	121
	Bibliography	125

Chapter 1

Introduction

1.1 What is the minimal impurity model for a Mott metal-insulator transition?

The Hubbard model is one of the fundamental models for strong electronic correlation; in its simplest form, it features a single band of conduction electrons hopping on a lattice and interacting via local correlations that provide a cost U if any site is doubly occupied:

$$H_{\text{hubb}} = -t \sum_{\langle i,j \rangle, \sigma} \left(c_{i\sigma}^\dagger c_{j\sigma} + \text{h.c.} \right) + U \sum_i \hat{n}_{i\uparrow} \hat{n}_{i\downarrow} - \mu \sum_{i,\sigma} \hat{n}_{i\sigma}$$

The model can be made particle-hole symmetric by choosing $\mu = U/2$:

$$H_{\text{hubb}} = -t \sum_{\langle i,j \rangle, \sigma} \left(c_{i\sigma}^\dagger c_{j\sigma} + \text{h.c.} \right) - \frac{U}{2} \sum_i \left(\hat{n}_{i\uparrow} - \hat{n}_{i\downarrow} \right)^2$$

There are two trivial limits of the model. At $U = 0$, the bath consists of just a kinetic energy part, and the ground state is just a filled Fermi sea. At $t = 0$, each lattice site decouples from the rest and becomes a local moment, which under symmetry-breaking becomes a Neel antiferromagnet. This suggests that on increasing U/t beyond some critical value, the system might undergo a phase transition from a metallic state to an insulating state [1]. This transition is reflected in the local spectral function - while it has a well-defined zero energy peak in the metallic phase, it is gapped in the insulating phase.

One method of studying Hubbard models is through auxiliary models, described in the next section. Auxiliary models are simpler versions of the full Hamiltonian that are able to capture the essential physics. For eg, a correlated impurity interacting with a conduction bath is a potential auxiliary model for the Hubbard Hamiltonian:

$$\mathcal{H}_{\text{SIAM}} = \epsilon_d \hat{n}_d + U \hat{n}_{d\uparrow} \hat{n}_{d\downarrow} - t \sum_{\langle i,j \rangle, \sigma} \left(c_{i\sigma}^\dagger c_{j\sigma} + \text{h.c.} \right) + V \sum_{\sigma} \left(c_{d\sigma}^\dagger c_{0\sigma} + \text{h.c.} \right) \quad (1.1.1)$$

The impurity has onsite energy ϵ_d and an onsite correlation U . It hybridises into the bath through V .

If the impurity site hybridises with a *non-interacting* bath defined by a uniform density of states, the impurity spectral function is found to have a well-defined Kondo resonance at low temperatures. Increasing the impurity correlation U only serves to reduce the width of the central peak at the cost of the appearance of side bands at energy scales of the order of U , but the resonance never dies. The situation is however different if the impurity is embedded in a correlated conduction bath with a non-trivial density of states. For the case of a conduction band with the DOS shown in the right of the figure below, the impurity hybridises into a reduced bandwidth because of the correlation on the lattice [2].

This difference in the type of conduction baths is utilised in dynamical mean-field theory to describe various phases of the bulk system. This is done through the DMFT algorithm: one starts with a non-interacting bath, but depending on the value of U , the conduction bath then gets modified and we ultimately end up with something that is different from what we started with. For small U , the bath does not change much and we retain the central

resonance of the impurity spectral function. This then describes a metal in the bulk. For larger values of U , however, the bath changes significantly such that its density of states becomes non-constant. Above a critical U_c , the impurity spectral function gets gapped out, and that then describes the insulating phase in the bulk. *This leaves open the following question: What is the minimal correlation one can insert into the non-interacting bath (of a single-impurity Anderson model) that can capture both the metallic and insulating phases of the bulk model?*

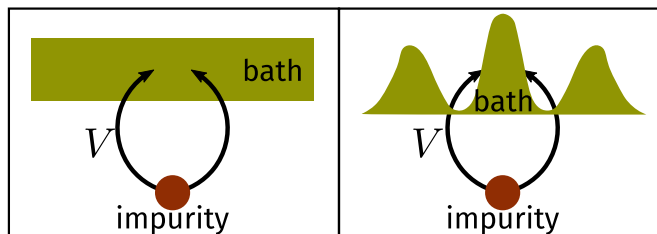


Figure 1.1: Various kinds of bath that an impurity can hybridise into. The left panel shows a non-interacting conduction band with a flat density of states. The right panel shows an interacting bath with an energy-dependent density of states. In the latter case, the impurity "feels" a reduced effective bandwidth defined by the width of the central peak.

1.2 Summary of the Anderson impurity problem

The single-impurity Anderson model (SIAM) is one of the most well-studied models in condensed matter physics and is the prototypical model for magnetism. It shows how strong correlations can give rise to a residual local moment. Friedel [1], in 1958, gave a phenomenological theory in which a local impurity developed an effective repulsion which forced the formation of bound states; those bound states where the up and down states became non-degenerate would correspond to the local moment. Taking inspiration from this, P.W.Anderson [3] in 1961 designed a model for the formation of local moment in second quantization. The model consisted of a bath of mobile electrons which interacted with the local impurity. The engine of magnetism was the local onsite Coulomb repulsion on the impurity site. This repulsion favours the formation of local moments because it makes it harder for the impurity to be doubly-occupied. Mean-field calculations of the impurity occupation reveal a criterion for the formation of local moments; this criterion is similar to the Stoner criterion for ferromagnetism. This mean-field analysis is of course only valid at high temperatures where electron-correlations are not so important. At low temperatures, it was found that the resistivity of the material reaches a minimum at some temperature, and then increases as $\ln T$ as we further reduce the temperature. This is in contrast to the previous results. And that was not all; at a sufficiently low temperature, it was found that the $\ln T$ -dependence disappears and the susceptibility became constant, implying the formation of a singlet state.

The fact that this logarithmic dependence vanishes once the singlet is formed suggests that it arises from the local moment on the impurity; once the local moment disappears (singlet), the log dependence vanishes as well. This led people to design a model in which the impurity interacted with the conduction bath through a Heisenberg-like spin-spin interaction. This model can be related to the SIAM through a canonical transformation followed by a projection to the low energy subspace [4]. In 1964, Jun Kondo [5, 6] found that a perturbative calculation of the transition probability of electrons from scattering via the impurity, up to second order in the exchange coupling J , revealed a logarithmic dependence of the resistivity on temperature. The crucial scattering process was that in which the spin of the incoming electron flipped (the S^+s^- and S^-s^+ terms). This explained the mystery of the resistivity minimum and the logarithmic dependence. But the mystery of the singlet state at very low temperatures still remained. The perturbative analysis would break down at low temperatures, so it was unreliable. The log term showed that the physics of the singlet involved all energy scales; one could not hope to capture it simply by taking the first few terms of a perturbative expansion. This problem came to be known as the Kondo problem. Notable attempts to solve this problem include the Coulomb gas approach by Anderson and Yuval [7, 8]. In 1970, Anderson attacked this problem by a renormalization group approach to account for all energy scales. In his "Poor Man's Scaling" approach, he progressively reduced the bandwidth while taking account of the eliminated states into the couplings via second order perturbation theory. This showed how the couplings would flow as we went to low temperatures, but it still could not remove the divergence as it was perturbative.

Anderson found that the exchange coupling increased as we go to lower temperatures, so he surmised that the

low energy theory was one where $J = \infty$. In 1975, Kenneth Wilson solved the problem by using his numerical renormalization group method in which he iteratively diagonalized chains of increasing length to go to the low energy physics [9, 10]. He proved that Anderson's guess was right and the low energy Hamiltonian was the same as that with $J = \infty$. Later calculations with Bethe ansatz in 1980 by Andrei and Wiegmann [11, 12] corroborated Wilson's findings. Other methods like the conformal field theory [13, 14] and bosonisation [15] have also been applied to this problem. Another important strong-coupling approach based on arguments of scattering phase shifts is that of the local Fermi liquid theory [16, 17] by Nozières. The low-temperature properties were found to be universal functions of a single energy scale, the Kondo temperature T_K [9, 18–21]. All the predicted aspects of the Kondo effect, including the existence of the Kondo cloud [22–26], were observed experimentally in quantum dot systems [27–31]. Scanning tunneling spectroscopy (STS) measurements have revealed that the Kondo effect often depends on the neighborhood of the impurities, in *Cu* and *Co* atoms [32, 33]. It was also shown [34], using quantum dots, that the out of equilibrium Kondo effect also displays universality, the physics at low temperatures being decided by only two energy scales, the frequency and amplitude of the perturbation. The impurity spectral function has been calculated using NRG [35], both at $T = 0$ [36, 37] as well as $T > 0$ [38], as well as using diagrammatic methods [39]. The electrical resistivity was found to obey single-parameter scaling behavior in T/T_K [40]. Nozières went further and analyzed a more realistic model, the multi-channel Kondo problem in which multiple conduction bath channels interact with quantum impurity at the center [41]. Such a model was found, through methods like the Bethe ansatz, CFT and bosonization among others, to host a non-Fermi liquid low energy phase [41–52]. Kondo effect also occurs in light quark matter which interact with heavy quark impurities through gluon-exchange interactions; the scattering amplitude goes through a similar logarithmic divergence and renormalisation group calculations reveal a Kondo scale in such systems [53, 54]. Kondo effect can also be realized for other fermionic systems like graphene [55], Dirac/Weyl semi-metals [56, 57] and dense nuclear matter [53, 58, 59].

A similar sequence of events also happened in the context of the Anderson model. In 1977 and 1978, Jefferson and Haldane independently calculated the "Poor Man's" scaling equations for the asymmetric SIAM, in the limit of infinitely large onsite repulsion. They were unable to access the strong-coupling fixed point (analogous to the $J = \infty$ fixed point in Kondo model), but their equations revealed which were the important regimes to consider. Later, in 1975, Krishnamurthy, Wilkins and Wilson applied the NRG method to the symmetric Anderson model and obtained the non-perturbative fixed points and susceptibility [35]. Their calculations were again supported by later Bethe ansatz calculations by Wiegmann and Tsvelick [12]. The physics of the Anderson model and the Kondo model has connotations with quantum field theory. The numerical renormalization group methods ushered in a revolution. The idea that physics on all length scales affect the low energy physics was very deep and has far-reaching consequences. The phenomenon in which the impurity electron strongly couples to one real space lattice site at low temperatures resulting in the screening of the local moment via spin-flip scatterings with the mobile electrons at that site is analogous to the phenomenon of quark confinement in which the quarks become bound at low energies. The high energy fixed point, $J = 0$, corresponds to the phenomenon of asymptotic freedom in which the interactions between particles become asymptotically weaker at high temperatures.

1.3 Some outstanding questions

Even though the problem of the SIAM has been essentially solved, some questions and clarifications still remain. In this work, we explore some of these questions.

- **Is it possible to get non-perturbative scaling equations for the whole journey?**

Neither NRG nor Bethe ansatz gives us scaling equations for the RG flows. Poor Man's scaling only gives perturbative ones which are valid close to the high energy theories. In the absence of scaling equations that show the complete crossover from the high energy to the low energy theory, it is difficult to visualize how the Hamiltonian is precisely chaining.

- **Is it possible to show the transfer of spectral weight along the flow, possibly by tracking the spectral function?**

Such an exercise will require the entire spectrum to be preserved along the flow. NRG, being projective will not work here. If the entire spectrum is available, computing the spectral function along the flow should indicate how the spectral weight is being distributed between the impurity and the conduction bath, or between various states of the impurity. It can also shed light on which terms or processes in the Hamiltonian contribute to which parts of the spectral function.

- **How does NRG obtain the local moment in the absence of hybridisation?** For the symmetric mode, NRG results show that in the absence of any interaction between the bath and the impurity, the value of the onsite repulsion flows to a large value and we end up with a local moment. The obvious question is, how does the impurity coupling renormalize when there is no term connecting the bath with the impurity?
- **Are there any interesting topological aspects of the fixed points?** We also intend to search for the existence of and possible changes in topological quantities at the fixed points. Since this is a zero-dimensional phenomenon, there will not be any gapping out of the Fermi surface, but there might be changes in topological quantities related to the Fermi surface or in the analyticity of the Green's function due to the presence of the coupling between the bath and the impurity. A strong indication of this is the change in the Wilson ratio from the non-interacting value of $R = 1$ to the local-Fermi liquid fixed point value of $R = 2$ obtained by Nozières [16].
- **What is the nature of the Kondo cloud that screens the spin(charge) of the impurity?** We do not yet have a theory for the excitations of the cloud of electrons at the zeroth site that couple to the impurity at the fixed point. The local Fermi liquid sits just outside the cloud and is able to "feel" its effects and gauge certain gross quantities like the Wilson ratio, but it does not have the excitations of the cloud because that part, along with the impurity, has been assumed to be "frozen" into the singlet configuration. A recent result in this context [60] is the effective Hamiltonian of the Kondo model cloud, also obtained using the same method that has been used in this thesis. The goal here is to do something similar for the SIAM as well.
- **How do entanglement measures respond to the RG flow?** Can we find a reflection of the screening mechanism in something like the mutual information or correlations? This requires a knowledge of the wavefunctions at the fixed point. Does the enhanced scattering of the electrons off the impurity lead to an increase in the entanglement between various electrons of the bath? It will also be interesting to check how various correlation functions vary across the RG flow.

1.4 Salient features of the method

The method employed in this work is a unitary renormalization group (URG) technique which progressively block-diagonalizes the Hamiltonian in the space of single high energy electrons. At each step of the process, the highest electron is decoupled from the system and it becomes an integral of motion, and the lower electronic system gets rotated to account for the decoupled electron. In this way, the RG goes on resolving the number fluctuations of the electrons. A fixed point is reached when the off-diagonal terms can no longer be removed. Since the method is unitary, it preserves the spectrum and allows calculating effective eigenvalues and eigenstates. It has some characteristic features:

- *Presence of a quantum fluctuation energy scale ω :* The URG process involves a parameter ω which contains the off-diagonal terms in the Hamiltonian. It quantifies the quantum fluctuation still unresolved in the system. Exactly at the fixed point, when the fluctuations are resolved, it assumes the value of one of the energies of the Hamiltonian. By probing the values of ω , all regions of the spectrum can, at least in principle, be accessed.
- *Presence of finite-valued fixed points:* The URG has a definite prescription for reaching the fixed point and it terminates after a finite number of steps (for a finite system). This leads to finite values of the fixed point couplings. This is also in accordance with our intuition that finite systems should not have diverging couplings.
- *Spectrum-preserving transformations:* Since the RG transformations are unitary, all eigenvalues and eigenstates are kept track of in the process. This allows us to calculate exact quantities for simple systems like the Kondo model.
- *Tractable low-energy effective Hamiltonians:* The final Hamiltonians obtained at the fixed point are usually tractable and allow us to extract information.

1.5 Layout of the thesis

Chapter ?? goes over the available work on the single-impurity Anderson model and its derivative - Kondo model. We go over the mean-field calculation of the Anderson model which gives a criteria for magnetism in terms of the onsite repulsion parameter U and the hybridisation parameter Δ . We then derive the Kondo model from the SIAM by way of a Schrieffer-Wolff transformation, which we solve using NRG. We also spend some time on the Poor Man's scaling approaches of both the SIAM and the Kondo model, and end the chapter with some discussions on the local Fermi liquid aspects of the fixed point theory.

Chapter 2 lays out the URG formalism and prescription. We derive the URG effective Hamiltonian and the unitaries that perform the RG transformations. We discuss several important features of the method and provide a prescription for applying it on models. We also perform the URG explicitly on two models - the star graph model and the Kondo model. We discuss various subtleties, especially the quantum fluctuation parameter ω and show that the URG actually diagonalizes the Hamiltonian. We derive many-body creation and annihilation operators η^\dagger and η which rotate the full Hamiltonian into successively more block-diagonal form.

Chapter 3 is closely tied to the formalism chapter and develops the connections between URG and other canonical transformations in the literature. We first define and setup each of the other transformations - the Schrieffer-Wolff transformation (SWT), Poor Man's scaling (PMS) and the Continuous Unitary Transformation (CUT) RG. We show that all of these are in some sense perturbative derivatives of URG. A byproduct of the discussion is a demonstration of the fact that PMS and SWT are exactly identical and differ only in the contexts in which they are applied. We also discuss the differences between URG and CUT-RG, and show that URG behaves like a generalized double-bracket flow [61]. Chapter 4 contains the URG analysis of the standard SIAM, and it shows that such a model cannot display a phase transition and is hence not the appropriate auxiliary model for DMFT.

Chapter 5 contains the URG analysis of the extended SIAM, obtained by adding spin-spin and charge-charge interactions to the SIAM. The RG equations are derived in detail. We focus mostly on the generalised version. We discuss both the positive and the negative regimes of the impurity correlation U . From the RG fixed point, we write down the fixed point Hamiltonian, and then discuss the spectrum of this Hamiltonian. We also compute some important quantities from the fixed point theory like the specific heat, magnetic susceptibility, charge susceptibility, Wilson ratio, Kondo cloud Hamiltonian, entanglement and correlation measures of the Kondo cloud electrons and change in the Luttinger's count of the bath. The Kondo cloud Hamiltonian is obtained by tracing out the impurity operators from the fixed point Hamiltonian. We compute the mutual information between various members of the fixed point Hamiltonian, as well as some off-diagonal correlations. We extract a low temperature local Fermi liquid from the Hamiltonian which we then use to calculate the zero temperature Wilson ratio for the Kondo regime of the SIAM. We also calculate the change in Luttinger's volume between the fixed points.

Chapter 6 contains the URG analysis of another extended SIAM obtained by adding an s-d coupling and an attractive local correlation in the bath. This model is shown to have a phase transition between local moment and singlet phases.

1.6 Summary of main results

The first of the main results in this work is the connection between URG and other canonical transformations. It is shown that URG is a non-perturbative variation of the most general unitary transformation. Other unitary transformations like the Schrieffer-Wolff transformation and Poor Man's scaling are simpler forms of URG, obtained by trivializing one of the terms in the Green's function that comes up in the URG formalism. CUT-RG is still more different from URG, since it is not only perturbative but also philosophically different in that it gradually suppresses the off-diagonal terms rather than killing more and more terms progressively. URG is thus different in two major ways - it provides non-perturbative equations because of the specific denominator structure as well as accommodates, at least in principle, the feedback effects of the off-diagonal terms through a quantum fluctuation operator in the denominator. We next look at the results concerning the SIAM. In the absence of any spin-exchange or charge isospin-exchange scattering, we do not see any renormalization in the hybridisation and the only flow is towards a local moment fixed point with large impurity onsite energy U . In the presence of those additional exchange scattering terms, the corresponding couplings J (spin exchange) and K (isospin exchange) flow to large values for low values of ω , signaling strong-coupling fixed points. At the spin-screened strong-coupling fixed point ($J > K$), the ground state wavefunction is a superposition of a spin singlet and a charge-isospin triplet. The ground state for the isospin-dominated fixed point ($K > J$) is an isospin singlet. Thermodynamic quantities are

now calculated using zero-mode Hamiltonians of the low energy effective theories. The impurity susceptibility χ_{imp} goes to the Curie-Weiss value of a four-fold degenerate system at large temperatures, and becomes constant (paramagnetic) at very low temperatures. With T_K defined suitably, χ_{imp} takes the zero temperature value of $(2\pi T_K)^{-1}$. The impurity specific heat has also been calculated, and reveals a two-peak structure. The fixed-point Hamiltonian further allows us to calculate the impurity spectral function. For very small U we obtain a single-peak structure corresponding to a single spin-spin or isospin-isospin excitation at the Fermi surface, while two other side-peaks emerge at large U that correspond to excitations between the spin and charge sectors. By tweaking the values of the couplings in the fixed-point Hamiltonian, we can mimic the reverse RG flow and see how the impurity spectral function morphs along this journey. Both the single-peak and three-peak structures revert back to a two-peak spectral function corresponding to that of a local moment. We then extract the effective Hamiltonian for the Kondo cloud, up to two particle interactions, by tracing out the impurity from the coupled Hamiltonian. The Hamiltonian has both a Fermi liquid piece of the form $\hat{n}_{k\sigma}\hat{n}_{q\sigma'}$ and a two-particle off-diagonal scattering piece of the form $c_{k\uparrow}^\dagger c_{k'\downarrow}^\dagger c_{q\uparrow} c_{q'\downarrow}$. It is the latter which is responsible for the screening mechanism. This conclusion is further strengthened by the studies of entanglement measures and correlations. The mutual information between the impurity and a cloud electron, as well as that between two cloud electrons increases as we go from the UV towards the IR fixed point. The off-diagonal correlation also increases from the UV towards the IR, which shows that the growth of the off-diagonal term is concomitant with the screening. We also obtain the Wilson ratio of the impurity by creating a local Fermi liquid from the fixed point Hamiltonian. Using the zero charge susceptibility at $T = 0$ in the Kondo regime of the SIAM, we can show that the Wilson ratio goes to 2 at the fixed point. We also calculate the change in Luttinger's volume along the RG flow. At the free orbital or local moment fixed points, the Luttinger's volume is measured purely by the number of conduction electrons, but we see that at the strong-coupling fixed point, the correct Luttinger's volume is given by the total number of electrons in the conduction bath as well as the impurity. This is also connected to the increase in Wilson ratio from 1 to 2.

Chapter 2

Unitary Renormalization Group Method

The URG method was introduced and formalised in refs. [62–65]. This section is adapted from those references and expanded wherever required.

2.1 Formalism

2.1.1 Description of the problem

We are given a Hamiltonian \mathcal{H} which is not completely diagonal in the occupation number basis of the electrons, \hat{n}_k : $[\mathcal{H}, n_k] \neq 0$. k labels any set of quantum numbers depending on the system. For spin-less Fermions it can be the momentum of the particle, while for spin-full Fermions it can be the set of momentum and spin. There are terms that scatter electrons from one quantum number k to another quantum number k' .

We take a general Hamiltonian,

$$\mathcal{H} = H_e \hat{n}_{q\beta} + H_h (1 - \hat{n}_{q\beta}) + c_{q\beta}^\dagger T + T^\dagger c_{q\beta} \quad (2.1.1)$$

Formally, we can decompose the entire Hamiltonian in the subspace of the electron we want to decouple ($q\beta$).

$$\mathcal{H} = \begin{pmatrix} |1\rangle & |0\rangle \\ H_1 & T \\ T^\dagger & H_0 \end{pmatrix} \quad (2.1.2)$$

The basis in which this matrix is written is $\{|1\rangle, |0\rangle\}$ where $|i\rangle$ is the set of all states where $\hat{n}_{q\beta} = i$. The aim of one step of the URG is to find a unitary transformation U such that the new Hamiltonian $U\mathcal{H}U^\dagger$ is diagonal in this already-chosen basis.

$$\tilde{\mathcal{H}} \equiv U\mathcal{H}U^\dagger = \begin{pmatrix} |1\rangle & |0\rangle \\ \tilde{H}_1 & 0 \\ 0 & \tilde{H}_0 \end{pmatrix} \quad (2.1.3)$$

U_q is defined by

$$\tilde{\mathcal{H}} = U_q \mathcal{H} U_q^\dagger \text{ such that } [\tilde{\mathcal{H}}, n_q] = 0 \quad (2.1.4)$$

It is clear that U is the diagonalizing matrix for \mathcal{H} . Hence we can frame this problem as an eigenvalue equation as well. Let $|\psi_1\rangle, |\psi_0\rangle$ be the basis in which the original Hamiltonian \mathcal{H} has no off-diagonal terms corresponding to $q\beta$. Hence, we can write

$$\mathcal{H} |\psi_i\rangle = \tilde{H}_i |\psi_i\rangle, i \in \{0, 1\} \quad (2.1.5)$$

Since $|\psi_i\rangle$ is the set of eigenstates of \mathcal{H} and $|i\rangle$ is the set of eigenstates in which $U\mathcal{H}U^\dagger$ has no off-diagonal terms corresponding to $q\beta$, we can relate $|\psi_i\rangle$ and $|i\rangle$ by the same transformation : $|\psi_i\rangle = U^\dagger |i\rangle$. We can expand the

state $|\psi_i\rangle$ in the subspace of $q\beta$:

$$|\psi_i\rangle = \sum_{j=0,1} |j\rangle \langle j| |\psi_i\rangle \equiv |1\rangle |\phi_1^i\rangle + |0\rangle |\phi_0^i\rangle \quad (2.1.6)$$

where $|\phi_j^i\rangle = \langle j| |\psi_i\rangle$. If we substitute the expansion 2.1.2 into the eigenvalue equation 2.1.5, we get

$$\left[H_e \hat{n}_{q\beta} + H_h \left(1 - \hat{n}_{q\beta} \right) + c_{q\beta}^\dagger T + T^\dagger c_{q\beta} \right] |\psi_i\rangle = \tilde{H}_i |\psi_i\rangle \quad (2.1.7)$$

The diagonal parts $H_e = \text{tr} [\mathcal{H} \hat{n}_{q\beta}]$ and $H_h = \text{tr} [\mathcal{H} (1 - \hat{n}_{q\beta})]$ can be separated into a purely diagonal part \mathcal{H}^d that contains the single-particle energies and the multi-particle correlation energies or Hartree-like contributions, and an off-diagonal part \mathcal{H}^i that scatters between the remaining degrees of freedom $k\sigma \neq q\beta$. That is,

$$H_e \hat{n}_{q\beta} + H_h (1 - \hat{n}_{q\beta}) = \mathcal{H}^d + \mathcal{H}^i$$

This gives

$$\left[c_{q\beta}^\dagger T + T^\dagger c_{q\beta} \right] |\psi_i\rangle = (\tilde{H}_i - \mathcal{H}^i - \mathcal{H}^d) |\psi_i\rangle \quad (2.1.8)$$

2.1.2 Obtaining the decoupling transformation

We now define a new operator $\hat{\omega}_i = \tilde{H}_i - \mathcal{H}^i$, such that

$$\left[c_{q\beta}^\dagger T + T^\dagger c_{q\beta} \right] |\psi_i\rangle = (\hat{\omega}_i - \mathcal{H}^d) |\psi_i\rangle \quad (2.1.9)$$

From the definition of $\hat{\omega}_i$, we can see that it is Hermitian and has no term that scatters in the subspace of $q\beta$, so it is diagonal in $q\beta$ and we can expand it as $\hat{\omega}_i = \hat{\omega}_i^1 \hat{n}_{q\beta} + \hat{\omega}_i^0 (1 - \hat{n}_{q\beta})$. Using the expansion 2.1.6, we can write

$$\hat{\omega}_i |\psi_i\rangle = \hat{\omega}_i^1 |1\rangle |\phi_1^i\rangle + \hat{\omega}_i^0 |0\rangle |\phi_0^i\rangle \quad (2.1.10)$$

Since the only requirement on $|\psi_i\rangle$ is that it diagonalize the Hamiltonian in the subspace of $q\beta$, there is freedom in the choice of this state. We can exploit this freedom and choose the $|\phi_0^i\rangle$ to be an eigenstates of $\hat{\omega}_i^{1,0}$ corresponding to real eigenvalues $\omega_i^{1,0}$:

$$\left[\mathcal{H}^d + c_{q\beta}^\dagger T + T^\dagger c_{q\beta} \right] |\psi_i(\omega_i)\rangle = (\omega_i^1 - \mathcal{H}^d) |1\rangle |\phi_1^i\rangle + (\omega_i^0 - \mathcal{H}^d) |0\rangle |\phi_0^i\rangle \quad (2.1.11)$$

If we now substitute the expansion 2.1.6 and gather the terms that result in $\hat{n}_{q\beta} = 1$, we get

$$c_{q\beta}^\dagger T |0\rangle |\phi_0^i\rangle = (\omega_i^1 - \mathcal{H}^d) |1\rangle |\phi_1^i\rangle \quad (2.1.12)$$

Similarly, gathering the terms that result in $\hat{n}_{q\beta} = 0$ gives

$$T^\dagger c_{q\beta} |1\rangle |\phi_1^i\rangle = (\omega_i^0 - \mathcal{H}^d) |0\rangle |\phi_0^i\rangle \quad (2.1.13)$$

We now define two many-particle transition operators:

$$\begin{aligned} \eta^\dagger(\omega_i^1) &= \frac{1}{\omega_i^1 - \mathcal{H}^d} c_{q\beta}^\dagger T \equiv G_1 c_{q\beta}^\dagger T \\ \eta(\omega_i^0) &= \frac{1}{\omega_i^0 - \mathcal{H}^d} T^\dagger c_{q\beta} \equiv G_0 T^\dagger c_{q\beta} \end{aligned} \quad (2.1.14)$$

wher G_j is the propagator $\frac{1}{\omega_i^j - \mathcal{H}^d}$. We can write this compactly as

$$\eta(\hat{\omega}) = GT^\dagger c_{q\beta} = \frac{1}{\hat{\omega}_i - \mathcal{H}^d} T^\dagger c_{q\beta} \quad (2.1.15)$$

where $\hat{\omega}_i = \omega_i^0 (1 - \hat{n}_{q\beta}) + \omega_i^1 \hat{n}_{q\beta} = \begin{pmatrix} \omega_i^1 & \\ & \omega_i^0 \end{pmatrix}$ is a 2x2 matrix and $\mathcal{H}^d = \mathcal{H}_0^d (1 - \hat{n}_{q\beta}) + \mathcal{H}_1^d \hat{n}_{q\beta}$ and $G = (\hat{\omega} - \mathcal{H}^d)^{-1}$. It is easy to check that this reproduces the previous forms of η_0 and η_1^\dagger . We will later find that it is important to demand that these two be Hermitian conjugates of each other; that constraint is imposed on the denominators:

$$\eta^\dagger(\omega_i^0) = \eta^\dagger(\omega_i^1) \implies \frac{1}{\omega_i^1 - \mathcal{H}^d} c_{q\beta}^\dagger T = c_{q\beta}^\dagger T \frac{1}{\omega_i^0 - \mathcal{H}^d} \quad (2.1.16)$$

Henceforth we will assume that this constraint has been imposed.

In terms of these operators, eq. 2.1.13 becomes

$$|1\rangle |\phi_1^i\rangle = \eta^\dagger |0\rangle |\phi_0^i\rangle, \quad |0\rangle |\phi_0^i\rangle = \eta |1\rangle |\phi_1^i\rangle \quad (2.1.17)$$

These allow us to write

$$|\psi_1\rangle = |1\rangle |\phi_1^i\rangle + |0\rangle |\phi_0^i\rangle = (1 + \eta) |1\rangle |\phi_1^i\rangle, \quad |\psi_0\rangle = (1 + \eta^\dagger) |0\rangle |\phi_0^i\rangle \quad (2.1.18)$$

Recalling that $|\psi_i\rangle = U^\dagger |i\rangle$, we can read off the required transformation:

$$U_1 = 1 + \eta \quad (2.1.19)$$

2.1.3 Properties of the many-body transition operators

The operators η have some important properties. First is the Fermionic nature:

$$\eta^2 = \eta^{\dagger 2} = 0 \quad \left[c^{\dagger 2} = c^2 = 0 \right] \quad (2.1.20)$$

Second is:

$$\begin{aligned} |1\rangle |\phi_1^i\rangle &= \eta^\dagger |0\rangle |\phi_0^i\rangle = \eta^\dagger \eta |1\rangle |\phi_1^i\rangle \implies \eta^\dagger \eta = \hat{n}_{q\beta} \\ |0\rangle |\phi_0^i\rangle &= \eta |1\rangle |\phi_1^i\rangle = \eta \eta^\dagger |0\rangle |\phi_0^i\rangle \implies \eta \eta^\dagger = 1 - \hat{n}_{q\beta} \end{aligned} \quad (2.1.21)$$

and hence the anticommutator

$$\implies \{\eta, \eta^\dagger\} = 1 \quad (2.1.22)$$

Note that the three equations in 2.1.21 work only when applied on the eigenstate $|\psi_i\rangle$ and not any arbitrary state.

$$\begin{aligned} \eta^\dagger \eta |\psi_i\rangle &= |1\rangle |\phi_1^i\rangle = \hat{n}_{q\beta} |\psi_i\rangle \\ \eta \eta^\dagger |\psi_i\rangle &= |0\rangle |\phi_0^i\rangle = (1 - \hat{n}_{q\beta}) |\psi_i\rangle \\ \{\eta^\dagger, \eta\} |\psi_i\rangle &= |\psi_i\rangle \end{aligned}$$

2.1.4 Form of the unitary operators

Although we have found the correct similarity transformations U_i (eqs. 2.1.19), we need to convert them into a unitary transformation. Say we are trying to rotate the eigenstate $|\psi_1\rangle$ into the state $|1\rangle$. We can then work with the transformation

$$U_1 = 1 + \eta \quad (2.1.23)$$

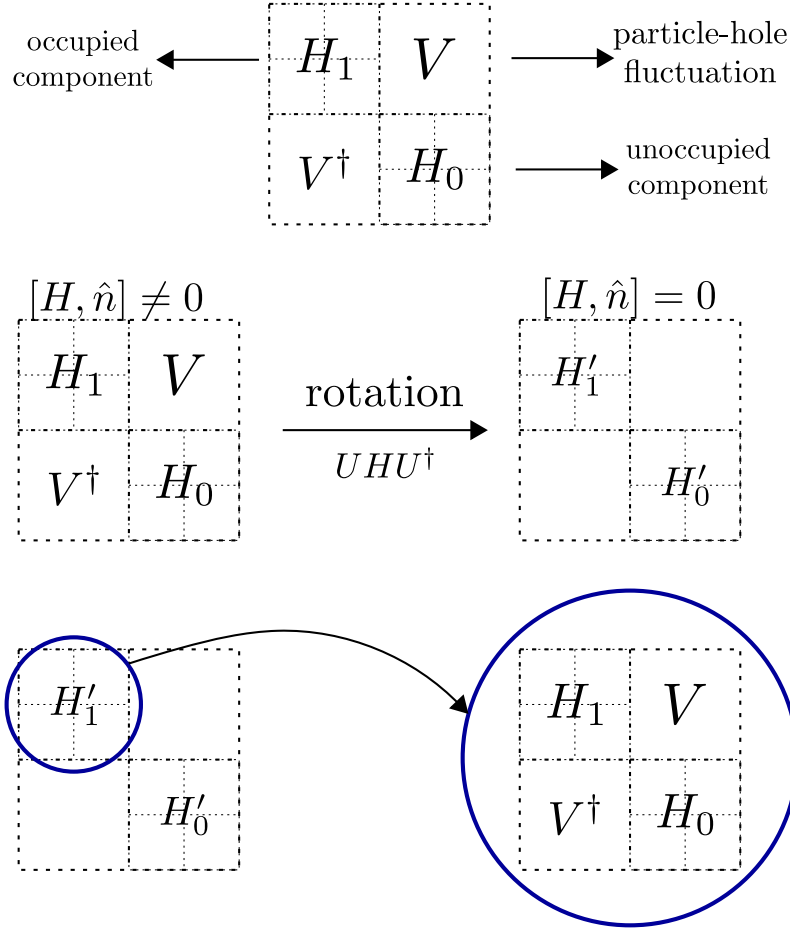


Figure 2.1: Three steps of the URG: Decompose the Hamiltonian in a 2×2 matrix, apply the unitary operator to rotate it, then repeat these steps with one of the rotated blocks.

In this form, this transformation is not unitary. It can however be written in an exponential form:

$$U_1 = e^\eta \quad (2.1.24)$$

using the fact that $\eta^2 = 0$. It is shown in ref. [66] that corresponding to a similarity transformation e^ω , there exists a unitary transformation e^G where

$$G = \tanh^{-1}(\omega - \omega^\dagger) \quad (2.1.25)$$

Applying that to the problem at hand gives

$$U_1^\dagger = \exp \left\{ \tanh^{-1}(\eta - \eta^\dagger) \right\} \quad (2.1.26)$$

Let $x = \tanh y$. Then,

$$x = \frac{e^{2y} + 1}{e^{2y} - 1} \implies y = \frac{1}{2} \log \frac{1+x}{1-x} \implies e^y = e^{\tanh^{-1} x} = \sqrt{\frac{1+x}{1-x}} \quad (2.1.27)$$

Therefore,

$$\exp \left\{ \tanh^{-1}(\eta - \eta^\dagger) \right\} = \frac{1 + \eta - \eta^\dagger}{\sqrt{(1 + \eta^\dagger - \eta)(1 - \eta^\dagger + \eta)}} = \frac{1 + \eta - \eta^\dagger}{\sqrt{1 + \{\eta, \eta^\dagger\}}} = \frac{1}{\sqrt{2}} (1 + \eta - \eta^\dagger) \quad (2.1.28)$$

The *unitary* operator that transforms the entangled eigenstate $|\psi_1\rangle$ to the state $|1\rangle$ is thus

$$U_1 = \frac{1}{\sqrt{2}} (1 + \eta^\dagger - \eta) \quad (2.1.29)$$

It can also be written as $\exp \left\{ \frac{\pi}{4} (\eta^\dagger - \eta) \right\}$ because

$$\begin{aligned} \exp \left\{ \frac{\pi}{4} (\eta^\dagger - \eta) \right\} &= 1 + (\eta^\dagger - \eta) \frac{\pi}{4} + \frac{1}{2!} (\eta^\dagger - \eta)^2 \left(\frac{\pi}{4} \right)^2 + \frac{1}{3!} (\eta^\dagger - \eta)^3 \left(\frac{\pi}{4} \right)^3 + \dots \\ &= 1 + (\eta^\dagger - \eta) \frac{\pi}{4} - \frac{1}{2!} \left(\frac{\pi}{4} \right)^2 - \frac{1}{3!} (\eta^\dagger - \eta) \left(\frac{\pi}{4} \right)^3 + \frac{1}{4!} \left(\frac{\pi}{4} \right)^4 + \dots \\ &= \cos \frac{\pi}{4} + (\eta^\dagger - \eta) \sin \frac{\pi}{4} \\ &= \frac{1}{\sqrt{2}} (1 + \eta^\dagger - \eta) \end{aligned} \quad (2.1.30)$$

There we used

$$(\eta^\dagger - \eta)^2 = \eta^{\dagger 2} + \eta^2 - \{ \eta^\dagger, \eta \} = -1 \quad \left[\because \eta^2 = \eta^{\dagger 2} = 0 \right] \quad (2.1.31)$$

and hence

$$(\eta^\dagger - \eta)^3 = -1 (\eta^\dagger - \eta) \quad (2.1.32)$$

and so on.

2.1.5 Effective Hamiltonian

We can now compute the form of the effective Hamiltonian that comes about when we apply U_1 - that is - when we rotate one exact eigenstate $|\psi_1\rangle$ into the occupied Fock space basis $|1\rangle$. From eq. 2.1.29,

$$\begin{aligned} U_1 \mathcal{H} U_1^\dagger &= \frac{1}{2} (1 + \eta^\dagger - \eta) \mathcal{H} (1 + \eta - \eta^\dagger) \\ &= \frac{1}{2} (1 + \eta^\dagger - \eta) (\mathcal{H} + \mathcal{H}\eta - \mathcal{H}\eta^\dagger) \\ &= \frac{1}{2} (\mathcal{H} + \mathcal{H}\eta - \mathcal{H}\eta^\dagger + \eta^\dagger \mathcal{H} + \eta^\dagger \mathcal{H}\eta - \eta^\dagger \mathcal{H}\eta^\dagger - \eta \mathcal{H} - \eta \mathcal{H}\eta + \eta \mathcal{H}\eta^\dagger) \\ &= \frac{1}{2} (\mathcal{H}^d + \mathcal{H}^i + \mathcal{H}^I + \mathcal{H}\eta - \mathcal{H}\eta^\dagger + \eta^\dagger \mathcal{H} + \eta^\dagger \mathcal{H}\eta - \eta^\dagger \mathcal{H}\eta^\dagger - \eta \mathcal{H} - \eta \mathcal{H}\eta + \eta \mathcal{H}\eta^\dagger) \\ &= \frac{1}{2} (\mathcal{H}^d + \mathcal{H}^i + \mathcal{H}^I + [\eta^\dagger - \eta, \mathcal{H}] + \eta^\dagger \mathcal{H}\eta - \eta^\dagger \mathcal{H}\eta^\dagger - \eta \mathcal{H}\eta + \eta \mathcal{H}\eta^\dagger) \end{aligned} \quad (2.1.33)$$

In the last two lines, we expanded the Hamiltonian into the three parts $\mathcal{H}^d, \mathcal{H}^i$ and a third piece $\mathcal{H}^I \equiv c_{q\beta}^\dagger T + T^\dagger c_{q\beta}$.

For reasons that will become apparent, we will split the terms into two groups:

$$\tilde{\mathcal{H}} = \frac{1}{2} \left(\underbrace{\mathcal{H}^d + \mathcal{H}^i + [\eta^\dagger - \eta, \mathcal{H}]}_{\text{group 1}} + \underbrace{\eta^\dagger \mathcal{H}\eta + \eta \mathcal{H}\eta^\dagger + \mathcal{H}^I - \eta^\dagger \mathcal{H}\eta^\dagger - \eta \mathcal{H}\eta}_{\text{group 2}} \right) \quad (2.1.34)$$

Group 2 can be easily shown to be 0. Note that terms that have two η or two η^\dagger sandwiching a \mathcal{H} can only be nonzero if the intervening \mathcal{H} has an odd number of creation or destruction operators.

$$\eta \mathcal{H} \eta = \eta c_q^\dagger T \eta \quad (2.1.35)$$

and

$$\eta^\dagger \mathcal{H} \eta^\dagger = \eta^\dagger T^\dagger c_q \eta^\dagger \quad (2.1.36)$$

Group 2 becomes

$$\text{group 2} = \mathcal{H}^I - \eta^\dagger T^\dagger c_q \eta^\dagger - \eta c_q^\dagger T \eta = c_q^\dagger T + T^\dagger c_q - \eta^\dagger T^\dagger c_q \eta^\dagger - \eta c_q^\dagger T \eta \quad (2.1.37)$$

To simplify this, we use the relation

$$\begin{aligned} \eta c_q^\dagger T \eta &= \frac{1}{\omega_i^0 - \mathcal{H}^d} T^\dagger c_q c_q^\dagger T \eta \\ &= T^\dagger c_q \frac{1}{\omega_i^1 - \mathcal{H}^d} c_q^\dagger T \eta \quad [\text{eq. 2.1.16}] \\ &= T^\dagger c_q \eta^\dagger \eta \quad [\text{eq. 2.1.15}] \\ &= T^\dagger c_q \hat{n}_q \quad [\text{eq. 2.1.21}] \end{aligned} \quad (2.1.38)$$

which gives

$$\eta c_q^\dagger T \eta = T^\dagger c_q \quad (2.1.39)$$

Taking the Hermitian conjugate of eq. 2.1.39 gives

$$\eta^\dagger T^\dagger c_q \eta^\dagger = c_q^\dagger T \quad (2.1.40)$$

Substituting the expressions 2.1.39 and 2.1.40 into the expression for group 2, 2.1.37, shows that it vanishes. This leaves us only with group 1:

$$\tilde{\mathcal{H}} = \frac{1}{2} \left(\mathcal{H}^d + \mathcal{H}^i + \overbrace{\eta^\dagger \mathcal{H} \eta + \eta \mathcal{H} \eta^\dagger}^{\text{group A}} + \underbrace{[\eta^\dagger - \eta, \mathcal{H}]}_{\text{group B}} \right) \quad (2.1.41)$$

Group A simplifies in the following way. First note that $\eta^\dagger \mathcal{H}^I \eta = \eta^\dagger \mathcal{H}^I \eta = 0$ must be 0 because it will involve consecutive $c_{q\beta}$ or consecutive $c_{q\beta}^\dagger$. We are therefore left with the diagonal part of \mathcal{H} , which is $H_e \hat{n}_{q\beta} + H_h (1 - \hat{n}_{q\beta})$.

$$\eta^\dagger \left[H_e \hat{n}_{q\beta} + H_h (1 - \hat{n}_{q\beta}) \right] \eta + \eta \left[H_e \hat{n}_{q\beta} + H_h (1 - \hat{n}_{q\beta}) \right] \eta^\dagger = \eta^\dagger H_h \eta + \eta H_e \eta^\dagger \quad (2.1.42)$$

This can be shown to be equal to the diagonal part:

$$\text{group A} = \eta^\dagger H_h \eta + \eta H_e \eta^\dagger = H_e \hat{n}_{q\beta} + H_h (1 - \hat{n}_{q\beta}) = \mathcal{H}^d + \mathcal{H}^i \quad (2.1.43)$$

It can also be shown that

$$\text{group B} = [\eta^\dagger - \eta, \mathcal{H}] = 2 [c_{q\beta}^\dagger T, \eta] \quad (2.1.44)$$

Putting it all together,

$$\tilde{\mathcal{H}} = \mathcal{H}^d + \mathcal{H}^i + [c_{q\beta}^\dagger T, \eta] \quad (2.1.45)$$

The renormalizing in the Hamiltonian is

$$\Delta \mathcal{H} = \tilde{\mathcal{H}} - \mathcal{H}^d - \mathcal{H}^i = [c_{q\beta}^\dagger T, \eta] \quad (2.1.46)$$

Because of eq. 2.1.44, it can also be written as

$$\Delta \mathcal{H} = \frac{1}{2} [\eta^\dagger - \eta, \mathcal{H}_X] = \frac{1}{2} [\eta^\dagger - \eta, \mathcal{H}] \quad (2.1.47)$$

This form will be useful later when we make the connection with one-shot Schrieffer-Wolff transformation and CUT RG.

To check that the renormalised Hamiltonian indeed commutes with $\hat{n}_{q\beta}$,

$$\begin{aligned} [\tilde{\mathcal{H}}, \hat{n}_{q\beta}] &= \left[\left[c_{q\beta}^\dagger T, \eta \right], \hat{n}_{q\beta} \right] = \left[c_{q\beta}^\dagger T \eta, \hat{n}_{q\beta} \right] - \left[\eta c_{q\beta}^\dagger T, \hat{n}_{q\beta} \right] \\ &= c_{q\beta}^\dagger T \eta \hat{n}_{q\beta} - \hat{n}_{q\beta} c_{q\beta}^\dagger T \eta \quad \left[2^{\text{nd}} [\cdot] \text{ is } 0, \because c_{q\beta}^\dagger \hat{n}_{q\beta} = \hat{n}_{q\beta} \eta = 0 \right] \\ &= c_{q\beta}^\dagger T \eta - c_{q\beta}^\dagger T \eta = 0 \end{aligned} \quad (2.1.48)$$

2.1.6 Fixed point condition

Within the URG, it is a prescription that the fixed point is reached when the denominator of the RG equation vanishes. This is equivalent to either $\omega_i^1 = \mathcal{H}_1^d$ or $\omega_i^0 = \mathcal{H}_0^d$. This shows that at the fixed point, one of the eigenvalues of $\hat{\omega}_i$ matches the corresponding eigenvalue of the diagonal blocks. This also leads to the vanishing of the off-diagonal block, because eqs. 2.1.12 and 2.1.13 gives

$$c_{q\beta}^\dagger T |0\rangle |\phi_0^i\rangle = (\omega_i^1 - \mathcal{H}_1^d) |1\rangle |\phi_1^i\rangle = 0 \implies c_{q\beta}^\dagger T = 0 \quad (2.1.49)$$

2.1.7 Multiple off-diagonal terms

There is a subtle assumption in the definitions eq. 2.1.14. In order for η to be the Hermitian conjugate of η^\dagger , \mathcal{H}_d cannot have any information that relates to the structure of T . To see why, say the total off-diagonal term is composed of two parts: $T = T_1 + T_2$.

$$\begin{aligned} \eta &= \frac{1}{\omega_0 - \mathcal{H}_d} (T_1^\dagger + T_2^\dagger) c = \left[\frac{1}{\omega^0 - E_1^0} T_1^\dagger c + \frac{1}{\omega^0 - E_2^0} T_2^\dagger c \right] \\ \eta^\dagger &= \frac{1}{\omega^1 - \mathcal{H}_d} c^\dagger (T_1 + T_2) = \left[\frac{1}{\omega^1 - E_1^1} c^\dagger T_1 + \frac{1}{\omega^1 - E_2^1} c^\dagger T_2 \right] \end{aligned} \quad (2.1.50)$$

where $\mathcal{H}_d T_i^\dagger c = E_i^0 T_i^\dagger c$ and $\mathcal{H}_d c^\dagger T_i = E_i^1 c^\dagger T_i$. We can now see that in order for $\eta = (\eta^\dagger)^\dagger$ to hold, two conditions must be met:

$$\omega^0 - E_1^0 = \omega^1 - E_1^1, \quad \omega^0 - E_2^0 = \omega^1 - E_2^1 \quad (2.1.51)$$

This will not hold generally. The correct solution is to realize that each such off-diagonal term T_i will come with its own quantum fluctuation scale ω_i .

$$\begin{aligned} \eta &= \sum_i \frac{1}{\omega_i^0 - E_i^0} T_i^\dagger c \\ \eta^\dagger &= \sum_i \frac{1}{\omega_i^1 - E_i^1} c^\dagger T_i \end{aligned} \quad (2.1.52)$$

If we now impose the condition that $\eta = (\eta^\dagger)^\dagger$, we get the relations

$$\omega_i^0 - \omega_i^1 = E_i^0 - E_i^1 \quad (2.1.53)$$

and so

$$\eta^\dagger - \eta = \sum_i \frac{1}{\omega_i^0 - E_i^0} (c^\dagger T_i - T_i^\dagger c) \quad (2.1.54)$$

The expression for the renormalization will not be just $[c^\dagger T, \eta]$ in this case. That form will be non-Hermitian. The correct form is obtained from the more general form $[\eta^\dagger - \eta, \mathcal{H}_X]$:

$$\begin{aligned}\Delta\mathcal{H} &= \frac{1}{2} [\eta^\dagger - \eta, c^\dagger T + T^\dagger c] = \frac{1}{2} \sum_{ij} \frac{1}{\omega_i^0 - E_i^0} [c^\dagger T_i - T_i^\dagger c, c^\dagger T_j + T_j^\dagger c] \\ &= \frac{1}{2} \sum_{ij} \frac{1}{\omega_i^0 - E_i^0} \left[\hat{n} (T_i T_j^\dagger + T_j T_i^\dagger) - (1 - \hat{n}) (T_i^\dagger T_j + T_j^\dagger T_i) \right] \\ &= \frac{1}{2} \sum_{ij} \left(\frac{1}{\omega_i^0 - E_i^0} + \frac{1}{\omega_j^0 - E_j^0} \right) [\hat{n} T_i T_j^\dagger - (1 - \hat{n}) T_i^\dagger T_j]\end{aligned}\tag{2.1.55}$$

2.1.8 Equivalence of the two unitaries and preservation of partial trace

In the subsection 2.1.4, we determined the form of the operator U_1 that unitarily decouples the node $q\beta$ from the other degrees of freedom. Eq. 2.1.29 was derived by reading off the transformation of $|1\rangle$ to $|\psi_1\rangle$, the first equation in 2.1.18. We could easily have chosen the other equation in the same equation set,

$$|\psi_0\rangle = (1 + \eta^\dagger) |0\rangle |\phi_0^i\rangle$$

which gives a similarity transformation $1 + \eta^\dagger$ and hence a unitary

$$U_0 = \frac{1}{\sqrt{2}} (1 + \eta - \eta^\dagger)\tag{2.1.56}$$

This η will however be different from the η in eq. 2.1.29. The reason is, in order to get U_1 , we must start from the eigenvalue equation $\mathcal{H}|\psi_1\rangle = \tilde{H}_1|\psi_1\rangle$. This means that the corresponding $\hat{\omega}$ will be defined as $\hat{\omega}_1 = \tilde{H}_1 - \mathcal{H}^i$. On the other hand, in order to get U_0 we must start with $\mathcal{H}|\psi_0\rangle = \tilde{H}_0|\psi_0\rangle$, and hence this $\hat{\omega}$ will be $\hat{\omega}_0 = \tilde{H}_0 - \mathcal{H}^i$. This difference in the $\hat{\omega}$ will define two different sets of η :

$$\begin{aligned}\text{Starting from } |\psi_1\rangle: \eta_1 &= \frac{1}{\omega_1^0 - \mathcal{H}^d} T^\dagger c_{q\beta} \quad \text{and} \quad \eta_1^\dagger = \frac{1}{\omega_1^1 - \mathcal{H}^d} T^\dagger c_{q\beta} \\ \text{Starting from } |\psi_0\rangle: \eta_0 &= \frac{1}{\omega_0^0 - \mathcal{H}^d} T^\dagger c_{q\beta} \quad \text{and} \quad \eta_0^\dagger = \frac{1}{\omega_0^1 - \mathcal{H}^d} T^\dagger c_{q\beta}\end{aligned}\tag{2.1.57}$$

The ω_j^i eigenvalues have both upper and lower indices. The upper index i signifies which eigenstate it relates to - $\omega_j |i\rangle = \omega_j^i |i\rangle$. The lower index refers to the exact eigenstate we started with - starting with $\mathcal{H}|\psi_j\rangle = \tilde{H}_j|\psi_j\rangle$ leads to ω_j . The two unitaries are

$$\begin{aligned}U_1 &= \frac{1}{\sqrt{2}} (1 + \eta_1^\dagger - \eta_1) \\ U_0 &= \frac{1}{\sqrt{2}} (1 + \eta_0 - \eta_0^\dagger)\end{aligned}\tag{2.1.58}$$

Since the two unitaries should give the same effective Hamiltonian, we require $U_1 = U_0$. That requires $\eta_1 = -\eta_0$. Comparing the expressions of the η s, we get

$$\omega_1^0 - \mathcal{H}_0^d = -(\omega_0^0 - \mathcal{H}_0^d)\tag{2.1.59}$$

This is the constraint that ensures that both unitaries give the same effective Hamiltonian. The condition $\eta_1 + \eta_0 = 0$, when expressed without resolving $\hat{\omega}$ into its eigenvalues can also be shown to be a statement of the preservation of

the partial trace under the RG flow.

$$\begin{aligned}
\eta_1 &= \frac{1}{\tilde{H}_1 - \mathcal{H}^i - \mathcal{H}^d} T^\dagger c_{q\beta}, \quad \eta_0 = \frac{1}{\tilde{H}_0 - \mathcal{H}^i - \mathcal{H}^d} T^\dagger c_{q\beta} \\
\implies \eta_1 + \eta_0 &= \left[\frac{1}{\tilde{H}_1 - \mathcal{H}^i - \mathcal{H}^d} + \frac{1}{\tilde{H}_0 - \mathcal{H}^i - \mathcal{H}^d} \right] T^\dagger c_{q\beta} = 0 \\
\implies \tilde{H}_1 - \mathcal{H}^i - \mathcal{H}^d &= - \left[\tilde{H}_0 - \mathcal{H}^i - \mathcal{H}^d \right] \\
\implies \tilde{H}_1 + \tilde{H}_0 &= 2\mathcal{H}_0
\end{aligned} \tag{2.1.60}$$

$\mathcal{H}_0 = \mathcal{H}^i + \mathcal{H}^d$ is the total diagonal part of the bare model. To match the dimensions, we must take $\tilde{H}_1 = E_1 \otimes I$ and similarly $\tilde{H}_0 = E_0 \otimes I$, where the rotated Hamiltonian is

$$\tilde{H} = \begin{pmatrix} E_1 & 0 \\ 0 & E_0 \end{pmatrix} \tag{2.1.61}$$

Therefore, the trace of the rotated Hamiltonian is $t_{\text{new}} = E_1 + E_0$. The trace of the LHS in the final equation of 2.1.60 is $\text{tr}(\tilde{H}_1 + \tilde{H}_0) = \text{tr}(E_1 \otimes I + E_0 \otimes I) = 2(E_1 + E_0) = 2t_{\text{new}}$. The trace of the RHS in final equation of 2.1.60 is $2 \times \text{tr}(\mathcal{H}_0) = 2t_{\text{old}}$ where $t_{\text{old}} = \text{tr}(\mathcal{H}_0)$ is the trace of the old Hamiltonian. Equating the LHS and RHS gives $t_{\text{new}} = t_{\text{old}}$.

2.1.9 Complete generator for the unitary transformation

Given some operator O_0 , we can generate a family of unitarily-connected operators O_j using a unitary operator $U(t)$:

$$O_j = U_j O(0) U_j^\dagger, \quad j = 1, 2, \dots \tag{2.1.62}$$

The discrete change equation for O_j can be represented in the form of a commutator:

$$\Delta O_j \equiv O_{j+1} - O_j = [O_j, S_j] \tag{2.1.63}$$

where

$$S_j = U_j \Delta U_j^\dagger. \tag{2.1.64}$$

Note that because $\Delta(U_j U_j^\dagger) = 0$, we have $(\Delta U_j) U_j^\dagger = -U_j (\Delta U_j^\dagger)$ and so S_j is anti-Hermitian. To verify that eq. 2.1.62 is indeed the solution of eq. 2.1.63, we differentiate eq. 2.1.62:

$$O_{j+1} - O_j = \Delta U_j O(0) U_j^\dagger + U_j O(0) \Delta U_j^\dagger = \Delta U_j U_j^\dagger O_j + O_j U_j \Delta U_j^\dagger = [O_j, S_j] \tag{2.1.65}$$

This shows that given a family of operators eq. 2.1.62 connected through U_j , we can obtain a generator S_j that defines the flow equation of O_j .

Since the URG is unitary, we should be able to obtain such a generator for it as well. From the expression of the unitary transformation of URG:

$$U_j = \frac{1}{\sqrt{2}} \begin{pmatrix} 1 + \eta_j^\dagger - \eta_j \end{pmatrix} \tag{2.1.66}$$

From the definition of the generator S_j , we then get

$$S_j = \frac{1}{2} \begin{pmatrix} 1 + \eta_j^\dagger - \eta_j \end{pmatrix} \begin{pmatrix} \eta_{j+1} - \eta_{j+1}^\dagger - \eta_j + \eta_j^\dagger \end{pmatrix} \tag{2.1.67}$$

The operators η_j and its hermitean conjugate can be thought of as angular momentum creation and annihilation

operators acting on the 2×2 Hilbert space of the occupied and vacant states $|1\rangle |\phi_1\rangle, |0\rangle |\phi_0\rangle$:

$$\eta_j |1\rangle |\phi_1\rangle = |0\rangle |\phi_0\rangle, \quad \eta_j |0\rangle |\phi_0\rangle = 0, \quad \eta_j^\dagger |0\rangle |\phi_0\rangle = |1\rangle |\phi_1\rangle, \quad \eta_j^\dagger |1\rangle |\phi_1\rangle = 0, \quad (2.1.68)$$

$$(2.1.69)$$

To check whether they have the correct algebra, we design the three spin operators $S^i, i = \{x, y, z\}$.

$$\begin{aligned} S^x &= \frac{1}{2} (S^+ + S^-) = \frac{1}{2} (\eta_j^\dagger + \eta_j) \\ S^y &= \frac{1}{2i} (S^+ - S^-) = \frac{1}{2i} (\eta_j^\dagger - \eta_j) \\ S^z &= \hat{n} - \frac{1}{2} \end{aligned} \quad (2.1.70)$$

The commutation relations give

$$\begin{aligned} [S^x, S^y] &= \frac{1}{4i} [\eta_j^\dagger + \eta_j, \eta_j^\dagger - \eta_j] = \frac{1}{2i} [\eta_j, \eta_j^\dagger] = \frac{1}{2i} (1 - \hat{n} - \hat{n}) = \frac{-1}{i} \left(\hat{n} - \frac{1}{2} \right) = iS^z \\ [S^y, S^z] &= \frac{1}{2i} \left[\eta_j^\dagger - \eta_j, \hat{n} - \frac{1}{2} \right] = \frac{1}{2i} [-\eta_j \hat{n} - \hat{n} \eta_j^\dagger] = \frac{1}{2i} (-\eta_j - \eta_j^\dagger) = \frac{i}{2} (\eta_j^\dagger + \eta_j) = iS^x \\ [S^z, S^x] &= \frac{1}{2} \left[\hat{n} - \frac{1}{2}, \eta_j^\dagger + \eta_j \right] = \frac{1}{2} [\hat{n} \eta_j^\dagger - \eta_j \hat{n}] = \frac{1}{2} (\eta_j^\dagger - \eta_j) = i \frac{1}{2i} (\eta_j^\dagger - \eta_j) = iS^y \end{aligned} \quad (2.1.71)$$

These operators therefore satisfy the commutation algebra of angular momentum operators $[S^i, S^j] = i\epsilon^{ijk} S^k$.

2.1.10 A note on the various quantum fluctuation scales ω_i^j

At a particular step of the URG, there are two quantum fluctuation energy scales associated with each sector. If we rotate $|\psi_1\rangle$ to $|1\rangle$ (particle/occupied sector), the corresponding unitary will be a function of $\omega_1^{0,1}$. If we, on the other hand, rotate $|\psi_0\rangle$ to $|0\rangle$ (hole/unoccupied sector), the unitary will be a function of $\omega_0^{0,1}$. The superscript j signifies whether this particular ω_i^j is an eigenvalue corresponding to $|1, \phi_i\rangle$ or $|0, \phi_i\rangle$. ω_i^0 occurs in the many-body transition operator η , because η is preceded by c and hence it picks out the eigenstate $|0, \phi_i\rangle$. On the other hand, ω_i^1 occurs in the many-body transition operator η^\dagger , because that is preceded by c^\dagger . This constrains these two values, because we must have $\eta(\omega_i^0) = \left(\eta^\dagger(\omega_i^1) \right)^\dagger$ (eq. 2.1.16), for each value of i , giving us two constraints in total. The subscript i signifies whether ω_i^j is a part of the particle sector unitary $U_1(\omega_1^j)$ or the hole sector unitary $U_0(\omega_0^j)$. As mentioned in the previous section, since both ways are equivalent, we must have $U_1 = U_0$ which leads to the constraints $\eta(\omega_0^j) = -\eta(\omega_1^j)$. All the independent constraints are listed below.

$$\begin{aligned} \omega_1^0 - \omega_1^1 &= \mathcal{H}_d^0 - \mathcal{H}_d^1 \\ \omega_0^0 - \omega_0^1 &= \mathcal{H}_d^0 - \mathcal{H}_d^1 \\ \omega_1^0 + \omega_0^0 &= 2\mathcal{H}_d^0 \end{aligned} \quad (2.1.72)$$

The first two come from $\eta(\omega_i^0) = \left(\eta^\dagger(\omega_i^1) \right)^\dagger$ while the last comes from $\eta(\omega_0^j) = -\eta(\omega_1^j)$. These are the only independent relations. Other relations like the one between ω_1^0 and ω_0^1 can be derived from these. This means that we have four ω and three constraints, such that each step of the URG is characterized by just a single independent quantum fluctuation scale.

2.2 Prescription

Given a Hamiltonian

$$\mathcal{H} = \mathcal{H}_1 + \mathcal{H}_0 + c^\dagger T + T^\dagger c \quad (2.2.1)$$

the goal is to look at the renormalization of the various couplings in the Hamiltonian as we decouple high energy electron states. Typically we have a shell of electrons at some energy D . During the process, we make one simplification. We assume that there is only one electron on that shell at a time, say with quantum numbers q, σ , and calculate the renormalization of the various couplings due to this electron. We then sum the momentum q over the shell and the spin β , and this gives the total renormalization due to decoupling the entire shell.

From eq. 2.1.45, the first two terms in the rotated Hamiltonian are just the diagonal parts of the bare Hamiltonian; they are unchanged in that part. The renormalization comes from the third term. For one electron $q\beta$ on the shell, the renormalization is

$$\Delta\mathcal{H} = \left[c_{q\beta}^\dagger \text{Tr} \left(\mathcal{H} c_{q\beta} \right), \eta \right] = c_{q\beta}^\dagger \text{Tr} \left(\mathcal{H} c_{q\beta} \right) \eta - \eta c_{q\beta}^\dagger \text{Tr} \left(\mathcal{H} c_{q\beta} \right) \quad (2.2.2)$$

Since this assumes we have obtained this from U_1 , it is fair to tag the η with a suitable label:

$$\Delta\mathcal{H} = c_{q\beta}^\dagger \text{Tr} \left(\mathcal{H} c_{q\beta} \right) \eta_1 - \eta_1 c_{q\beta}^\dagger \text{Tr} \left(\mathcal{H} c_{q\beta} \right) \quad (2.2.3)$$

It is clear that the first term takes into account virtual excitations that start from a filled state ($\hat{n}_{q\beta} = 1$ initially) - such a term is said to be a part of the *particle sector*.

$$\Delta_1\mathcal{H} = c_{q\beta}^\dagger \text{Tr} \left(\mathcal{H} c_{q\beta} \right) \eta_1 \quad (2.2.4)$$

The second term, on the other hand, considers excitations that start from an empty state. They constitute the *hole sector*.

$$\Delta_0\mathcal{H} = -\eta_1 c_{q\beta}^\dagger \text{Tr} \left(\mathcal{H} c_{q\beta} \right) \quad (2.2.5)$$

To write the total renormalization in a particle-hole symmetric form, we can use the relation $\eta_0 = -\eta_1$, such that both the terms will now come with a positive sign:

$$\Delta\mathcal{H} = c_{q\beta}^\dagger \text{Tr} \left(\mathcal{H} c_{q\beta} \right) \eta_1 + \eta_0 c_{q\beta}^\dagger \text{Tr} \left(\mathcal{H} c_{q\beta} \right) \quad (2.2.6)$$

We can make one more manipulation: using eq. 2.1.16, we get

$$\Delta\mathcal{H} = c_{q\beta}^\dagger \text{Tr} \left(\mathcal{H} c_{q\beta} \right) \eta_1 + \text{Tr} \left(c_{q\beta}^\dagger \mathcal{H} \right) c_{q\beta} \eta_0^\dagger \quad (2.2.7)$$

This form of the total renormalization is identical to the one we use in the "Poor Man's scaling"-type of renormalization that was used to get the scaling equations in the Kondo and Anderson models [3, 67]. Writing down the forms of η and η^\dagger explicitly, we get

$$\Delta\mathcal{H} = c_{q\beta}^\dagger \text{Tr} \left(\mathcal{H} c_{q\beta} \right) \frac{1}{\omega_1^0 - \mathcal{H}_0^d} \text{Tr} \left(c_{q\beta}^\dagger \mathcal{H} \right) c_{q\beta} + \text{Tr} \left(c_{q\beta}^\dagger \mathcal{H} \right) c_{q\beta} \frac{1}{\omega_0^1 - \mathcal{H}_1^d} c_{q\beta}^\dagger \text{Tr} \left(\mathcal{H} c_{q\beta} \right) \quad (2.2.8)$$

The renormalization due to the entire shell is obtained by summing over all states on the shell.

$$\Delta\mathcal{H} = \sum_{q\beta} \left[c_{q\beta}^\dagger \text{Tr} \left(\mathcal{H} c_{q\beta} \right) \frac{1}{\omega_1^0 - \mathcal{H}_0^d} \text{Tr} \left(c_{q\beta}^\dagger \mathcal{H} \right) c_{q\beta} + \text{Tr} \left(c_{q\beta}^\dagger \mathcal{H} \right) c_{q\beta} \frac{1}{\omega_0^1 - \mathcal{H}_1^d} c_{q\beta}^\dagger \text{Tr} \left(\mathcal{H} c_{q\beta} \right) \right] \quad (2.2.9)$$

These equations will now need to be simplified. For example, in the particle sector, we can set $\hat{n}_{q\beta} = 0$ in the numerator, because there is no such excitation in the initial state. Similarly, in the hole sector, we can set $\hat{n}_{q\beta} = 1$ because that state was occupied in the initial state. Another simplification we typically employ is that $\mathcal{H}_{0,1}^d$ will, in general, have the energies of all the electrons. But we consider only the energy of the on-shell electrons in the denominator. After integrating out these electrons, we can rearrange the remaining operators to determine which term in the Hamiltonian it renormalizes and what is the renormalization.

At first sight, one might think that we must evaluate lots of traces to obtain the terms in $\Delta\mathcal{H}$. A little thought reveals that the terms in the numerator are simply the off-diagonal terms in the Hamiltonian; $\text{Tr} \left(c_{q\beta}^\dagger \mathcal{H} \right) c_{q\beta}$ is the off-diagonal term that has $c_{q\beta}$ in it, and $c_{q\beta}^\dagger \text{Tr} \left(\mathcal{H} c_{q\beta} \right)$ is the off-diagonal term that has $c_{q\beta}^\dagger$ in it. \mathcal{H}^D is just the

diagonal part of the Hamiltonian.

2.3 URG analysis of the star graph model

The star graph problem has already been analyzed using URG and an extensive study of its entanglement properties has already been carried out, in ref. [68]. Here we focus on just deriving the RG equations. The system consists of N spin-like degrees of freedom (labeled 1 through N) individually talking to a spin at the center (labeled 0). Each spin i ($i \in [0, N]$) has an on-site energy ϵ_i . The coupling strength between 0 and i ($i \in [1, N]$) is J_i . We choose the on-site energies such that $\epsilon_{i+1} > \epsilon_i, i \in [N-1, 1]$. In this way, ϵ_1 is the infrared limit and ϵ_N is the ultraviolet limit.

$$\mathcal{H} = \epsilon_0 S_0^z + \sum_{i=1}^N \left[\epsilon_i S_i^z + J_i \vec{S}_0 \cdot \vec{S}_i \right] \quad (2.3.1)$$

By converting the last term into S^z and S^\pm , we can write the Hamiltonian as

$$\mathcal{H} = \epsilon_0 S_0^z + \sum_{i=1}^N \left[\epsilon_i S_i^z + J_i \left(S_0^z S_i^z + \frac{1}{2} (S_0^+ S_i^- + S_0^- S_i^+) \right) \right] \quad (2.3.2)$$

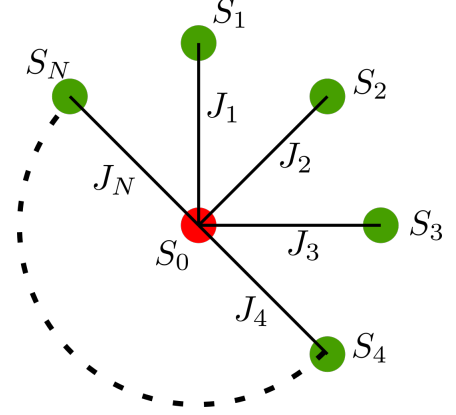


Figure 2.2: Star Graph model

2.3.1 Calculation of Renormalization

The RG involves decoupling the nodes N through 1, and looking at the resultant renormalization in ϵ_i and J_i . As a simplification, we will ignore the lower nodes in the denominator and keep only the node currently being decoupled, ie node N . Since node 0 is connected to node N , we will keep node 0 in the denominator as well. Making this simplification gives

$$\mathcal{H}^D = \epsilon_0 S_0^z + \epsilon_N S_N^z + J_N S_0^z S_N^z \quad (2.3.3)$$

The off-diagonal part in the subspace of the node N is

$$\mathcal{H}_X = S_N^+ T + T^\dagger S_N^- = \frac{1}{2} J_N (S_N^+ S_0^- + S_N^- S_0^+) \quad (2.3.4)$$

The renormalization on doing one step of the URG is given by

$$\begin{aligned} \Delta \mathcal{H} &= S_N^+ T \frac{1}{\omega_0^1 - \mathcal{H}^D} T^\dagger S_N^- + T^\dagger S_N^- \frac{1}{\omega_1^0 - \mathcal{H}^D} S_N^+ T \\ &= \frac{J_N^2}{4} S_N^+ S_0^- \frac{1}{\omega_0^1 - \epsilon_0 S_0^z - \epsilon_N S_N^z - J_N S_0^z S_N^z} S_0^+ S_N^- + \frac{J_N^2}{4} S_0^+ S_N^- \frac{1}{\omega_1^0 - \epsilon_0 S_0^z - \epsilon_N S_N^z - J_N S_0^z S_N^z} S_N^+ S_0^- \end{aligned} \quad (2.3.5)$$

There, N refers to the spin being decoupled. The first Greens function has S_0^+ and S_N^- in front of it, so we substitute $S_0^z = \frac{1}{2}, S_N^z = -\frac{1}{2}$ in that Greens function. For the other Greens function we do the opposite.

$$\Delta \mathcal{H} = \frac{J_N^2}{4} S_N^+ S_0^- \frac{1}{\omega_1^0 - \frac{1}{2}\epsilon_0 + \frac{1}{2}\epsilon_N + \frac{1}{4}J_N} S_0^+ S_N^- + \frac{J_N^2}{4} S_0^+ S_N^- \frac{1}{\omega_0^1 + \frac{1}{2}\epsilon_0 - \frac{1}{2}\epsilon_N + \frac{1}{4}J_N} S_N^+ S_0^- \quad (2.3.6)$$

To relate ω_1^0 and ω_0^1 , we use eq. 2.1.72:

$$\omega_1^0 + \omega_0^1 = \mathcal{H}_0^D + \mathcal{H}_1^D = -\frac{1}{2} J_N \implies \omega_1^0 \equiv \omega, \quad \omega_0^1 \equiv \omega' = -\frac{1}{2} J_N - \omega \quad (2.3.7)$$

So, the renormalization becomes

$$\Delta\mathcal{H} = \frac{J_N^2}{4} \frac{1}{\omega - \frac{1}{2}\epsilon_0 + \frac{1}{2}\epsilon_N + \frac{1}{4}J_N} \left(S_N^+ S_0^- S_0^+ S_N^- - S_0^+ S_N^- S_N^+ S_0^- \right) = \frac{J_N^2}{4} \frac{1}{\omega - \frac{1}{2}\epsilon_0 + \frac{1}{2}\epsilon_N + \frac{1}{4}J_N} (S_N^z - S_0^z) \quad (2.3.8)$$

There we used $S^+ S^- = \frac{1}{2} + S^z$ and $S^- S^+ = \frac{1}{2} - S^z$.

We can now read off the renormalizations in ϵ_N and ϵ_0 .

$$\begin{aligned} \Delta\epsilon_N &= \frac{1}{4} J_N^2 \frac{1}{\omega - \frac{1}{2}\epsilon_0 + \frac{1}{2}\epsilon_N + \frac{1}{4}J_N} \\ \Delta\epsilon_0 &= -\frac{1}{4} J_N^2 \frac{1}{\omega - \frac{1}{2}\epsilon_0 + \frac{1}{2}\epsilon_N + \frac{1}{4}J_N} \end{aligned} \quad (2.3.9)$$

2.3.2 Nature of flows

We are interested in looking at the renormalization of the central node energy ϵ_0 , upon removing the nodes N through 1. We will hence concentrate on the second RG equation. We first make some simplifying assumptions: $J_i = J, \epsilon_i = \epsilon$ for all $i \in \{1, N\}$.

$$\Delta\epsilon_0 = -\frac{1}{4} J^2 \frac{1}{\omega - \frac{1}{2}\epsilon_0 + \frac{1}{2}\epsilon + \frac{1}{4}J} \quad (2.3.10)$$

Define $\tilde{\omega} = \omega + \frac{1}{2}\epsilon + \frac{1}{4}J$.

$$\Delta\epsilon_0 = -\frac{1}{4} J^2 \frac{1}{\tilde{\omega} - \frac{1}{2}\epsilon_0} \quad (2.3.11)$$

Our goal here is to look for a fixed-point condition such that the denominator vanishes at some point of the RG. If we start with a bare of ϵ_0 such that $\tilde{\omega} - \frac{1}{2}\epsilon_0 > 0$, the denominator will be positive and the RG equation will be irrelevant. This means that ϵ_0 will keep on decreasing, and the denominator will keep on becoming more and more positive, meaning there cannot be a fixed point in this situation.

If, on other hand, we start with a bare of ϵ_0 such that $\tilde{\omega} - \frac{1}{2}\epsilon_0 < 0$, the denominator will be negative and the RG equation will be relevant. This means that ϵ_0 will keep on increasing, and the denominator will keep on becoming more and more negative, meaning there cannot be a fixed point in this situation either. These situations are depicted in figure 2.3.

Since we cannot find a fixed point, we will use a different ω . Instead of ω_1^0 , we will use ω_1^1 . From eq. 2.1.72, we have

$$\omega_1^0 - \omega_1^1 = \mathcal{H}_0^D - \mathcal{H}_1^D = \epsilon_0 - \epsilon_N = \epsilon_0 - \epsilon \quad (2.3.12)$$

Defining $\omega_1^1 = \omega'$ and substituting this in eq. 2.3.10 gives

$$\Delta\epsilon_0 = -\frac{1}{4} J^2 \frac{1}{\omega' - \frac{1}{2}\epsilon + \frac{1}{2}\epsilon_0 + \frac{1}{4}J} \quad (2.3.13)$$

We again define $-\tilde{\omega} = \omega' - \frac{1}{2}\epsilon + \frac{1}{4}J$.

$$\Delta\epsilon_0 = \frac{1}{4} J^2 \frac{1}{\tilde{\omega} - \frac{1}{2}\epsilon_0} \quad (2.3.14)$$

We now repeat the exercise of determining the relevance of the flows under various regime. If we start with a bare ϵ_0 such that $\tilde{\omega} + \frac{1}{2}\epsilon_0 > 0$, then the denominator is positive so the renormalization will be irrelevant. ϵ_0 will decrease until we reach $\tilde{\omega} + \frac{1}{2}\epsilon_0 = 0$. This will be a fixed point. However, if we start with a bare ϵ_0 such that $\tilde{\omega} + \frac{1}{2}\epsilon_0 < 0$, then the denominator is negative so the renormalization will be relevant. ϵ_0 will increase until we reach $\tilde{\omega} + \frac{1}{2}\epsilon_0 = 0$. This will again be a fixed point. This new situation is depicted in right panel of figure 2.3.

2.3.3 Effective Hamiltonians

If $\tilde{\omega}$ and ϵ_0 are of the same sign at the bare level, then it is easy to see that since the fixed point is defined by $\tilde{\omega} = \frac{1}{2}\epsilon_0^*$ (* denotes value at fixed point), the effective Hamiltonian at the fixed point will be

$$\mathcal{H}^* = 2\tilde{\omega} S_0^z + \epsilon \sum_i S_i^z + J \sum_i \vec{S}_i \cdot \vec{S}_0, \quad \text{if } \tilde{\omega}\epsilon_0 > 0 \quad (2.3.15)$$

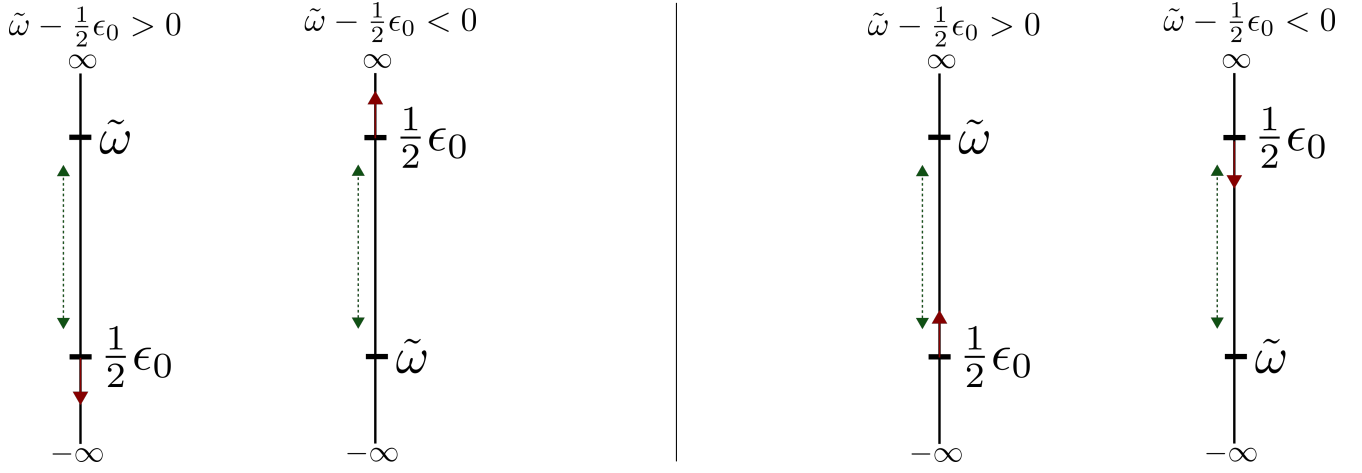


Figure 2.3: Left: RG flow for the two cases. The green line is the distance between the bare values of the two couplings, and hence also the magnitude of the denominator. The red arrow denotes the direction in which ϵ_0 will flow. Upward flow is increase. In both cases, the flow is such that the distance between the two quantities (and hence the magnitude of the denominator) increases. The RG fixed point occurs when the magnitude of the denominator goes to 0. This happens if the distance vanishes. Since the distance necessarily increases, we cannot get a fixed point in this way. Right: RG flow for the two cases with the new $-\tilde{\omega} = \omega' - \frac{1}{2}\epsilon + \frac{1}{4}J$. Now we can see that in both cases, the flow is such that the distance (green dotted line) between the couplings decreases. A fixed point is reached when this distance vanishes.

If, at the bare level, ϵ_0 and $\tilde{\omega}$ are of opposite signs, then ϵ_0 would undergo a change in sign at some point as it flows towards $\tilde{\omega}$. Since we do not expect a coupling to change sign under RG, we will restrict it to 0 in such cases.

$$\mathcal{H}^* = \epsilon \sum_i S_i^z + J \sum_i \vec{S}_i \cdot \vec{S}_0, \quad \text{if } \tilde{\omega}\epsilon_0 < 0 \quad (2.3.16)$$

Things get much more simpler if we assume the onsite energies of the surrounding nodes are zero.

$$\begin{aligned} \mathcal{H}^* &= 2\tilde{\omega}S_0^z + J \sum_i \vec{S}_i \cdot \vec{S}_0, & \text{if } \tilde{\omega}\epsilon_0 > 0 \\ \mathcal{H}^* &= J \sum_i \vec{S}_i \cdot \vec{S}_0, & \text{if } \tilde{\omega}\epsilon_0 < 0 \end{aligned} \quad (2.3.17)$$

2.3.4 Fixed points

The fixed points are obtained numerically by solving the RG equation. As mentioned before, there are two types of solutions: The first kind is those in which ϵ_0 and $\tilde{\omega}$ are of the same sign, and the former flows to the latter without crossing the 0 axis. These flows are shown (obtained numerically) in fig. 2.4. The second kind are those where the two couplings have different signs, and so ϵ_0 flows to 0. These are shown in fig. 2.5.

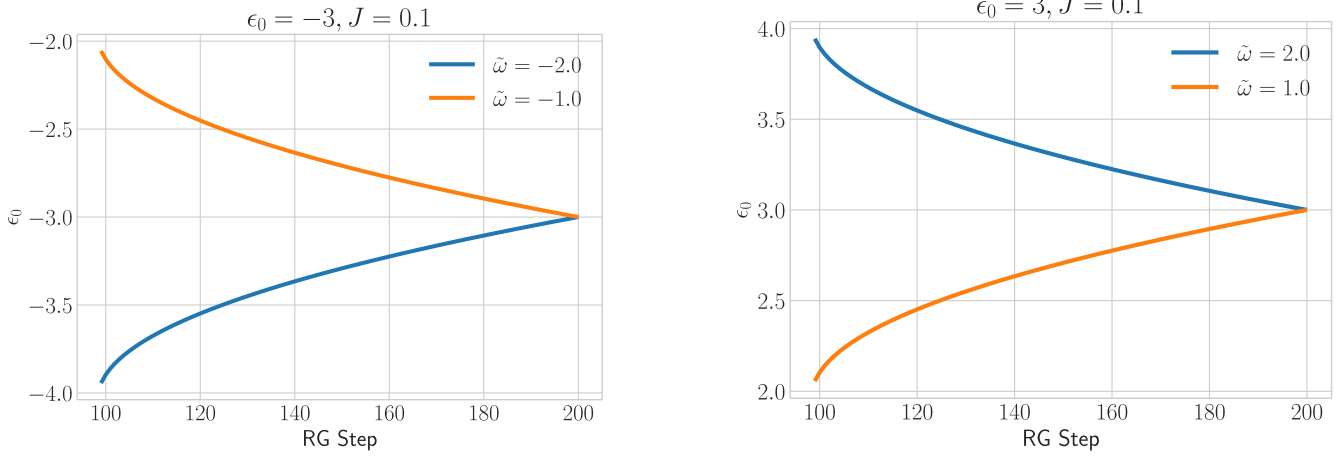


Figure 2.4: Flows where ϵ_0 and $\tilde{\omega}$ have same sign. The left and right panels show flows starting from negative and positive values respectively. The two plots in each panel correspond to different values of $\tilde{\omega}$, one greater than the bare ϵ_0 , the other less than that. The fixed point value is $2\tilde{\omega}$.

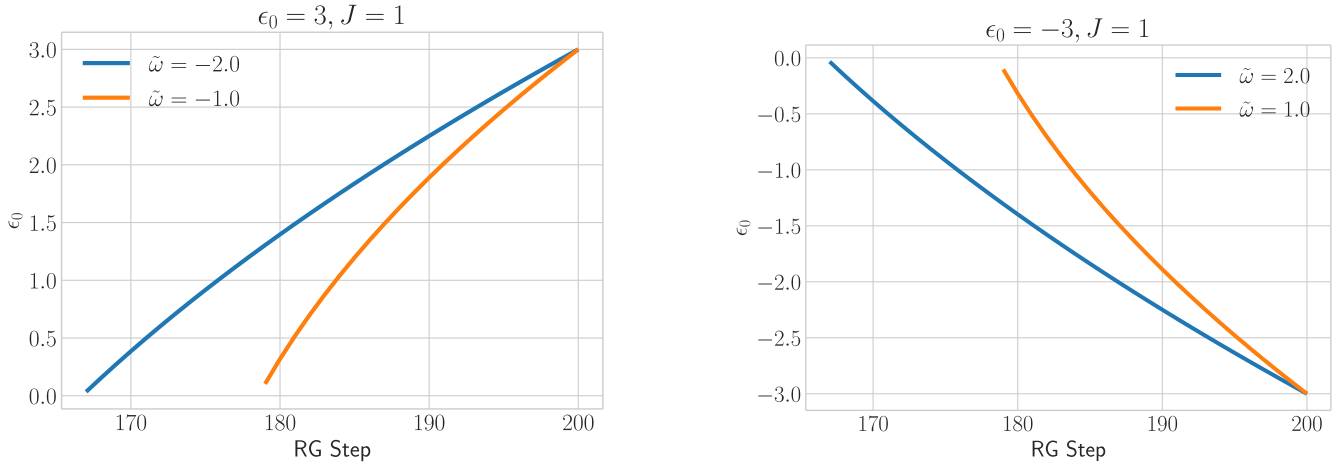


Figure 2.5: Flows where ϵ_0 and $\tilde{\omega}$ have opposite sign. The left and right panels show flows starting from negative and positive values respectively. The two plots in each panel correspond to different values of $\tilde{\omega}$, one greater than the bare ϵ_0 , the other less than that. The fixed point value is 0.

2.4 URG analysis of the single-channel Kondo model

The Kondo model URG analysis was originally carried out in ref. [1]. A specific version of the model is described by the Hamiltonian

$$\mathcal{H} = \sum_{k\sigma} \epsilon_k \tau_{k\sigma} + \sum_{k,l} J^z S_d^z s_{kl}^z + \frac{1}{2} \sum_{k,l} J^t \left(S_d^+ s_{kl}^- + S_d^- s_{kl}^+ \right) \quad (2.4.1)$$

where $s_{kl}^z = \frac{1}{2} (c_{k\uparrow}^\dagger c_{l\uparrow} - c_{k\downarrow}^\dagger c_{l\downarrow})$, $s_{kl}^- = c_{k\downarrow}^\dagger c_{l\uparrow}$ and $s_{kl}^+ = s_{lk}^-^\dagger$. Also, $\tau = \hat{n} - \frac{1}{2}$. k, l sum over the momentum states. \vec{S}_d is the impurity spin operator.

The scheme is that we will disentangle an electron $q\beta$ from the Hamiltonian, q being the momentum and β the spin. The diagonal part of the Hamiltonian under this scheme is

$$H_{q\beta}^D = \epsilon_q \tau_{q\beta} + J^z S_d^z s_{qq}^z \quad (2.4.2)$$

The off-diagonal parts at a particular RG step H_1^I and H_0^I , that start from particle and hole states respectively,

are

$$\begin{aligned} H_1^I &= \sum_{|k| < \Lambda, q} J^z S_d^z s_{kq}^z + \frac{1}{2} \sum_{|k| < \Lambda, q} J^t \left(S_d^+ s_{kq}^- + S_d^- s_{kq}^+ \right) \\ H_0^I &= \sum_{|k| < \Lambda, q} J^z S_d^z s_{qk}^z + \frac{1}{2} \sum_{|k| < \Lambda, q} J^t \left(S_d^+ s_{qk}^- + S_d^- s_{qk}^+ \right) \end{aligned} \quad (2.4.3)$$

H_1^I is the Hamiltonian term that scatters from the occupied configuration of q , H_0^I is the same from the unoccupied configuration. These are the terms that appear in the numerator.

2.4.1 Particle sector

The particle sector involves integrating out those states which are occupied ($\hat{n}_{q\beta} = 1$). We will work at an energy shell $\epsilon_q = -D$. The renormalization is

$$H_0^I \frac{1}{\omega - H_{q\beta}^D} H_1^I \quad (2.4.4)$$

Both H_0^I and H_1^I have all three operators S_d^z, S_d^\pm . We call S_d^z the spin-keep term and the others spin-flip terms. The entire product will thus have $3 \times 3 = 9$ terms. Not all terms however renormalize the Hamiltonian. Those terms that have identical operators on both sides can be ignored because $S_d^{z2} = \text{constant}$ and $S^\pm{}^2 = 0$. The other six terms will renormalize the Hamiltonian. This brings in one more simplification: all the six terms that *will* renormalize the Hamiltonian have a spin flip operator on at least one side of the Greens function. This means that in the denominator of the Greens function, S_d^z and s_{qq}^z have to be anti-parallel in order to produce a non-zero result for that term. This means we can identically replace $S_d^z s_{qq}^z = -\frac{1}{4}$. Also, in the particle sector, the Greens function always has $c_{q\beta}$ in front of it, so $\epsilon_q \tau_{q\beta} = D/2$. Substituting all this, we get

$$\begin{aligned} \frac{1}{\omega - D/2 + J/4} \sum_{|k, k'| < \Lambda, q} \left[\frac{1}{2} J^z J^t \left(S_d^z S_d^+ s_{qk'}^- s_{kq}^- + S_d^z S_d^- s_{qk'}^z s_{kq}^+ \right) + \frac{1}{2} J^t J^z \left(S_d^+ S_d^z s_{qk'}^- s_{kq}^z + S_d^- S_d^z s_{qk'}^+ s_{kq}^z \right) \right. \\ \left. + \frac{1}{4} J^{t2} \left(S_d^- S_d^+ s_{qk'}^+ s_{kq}^- + S_d^+ S_d^- s_{qk'}^- s_{kq}^+ \right) \right] \end{aligned} \quad (2.4.5)$$

We now simplify the products and keep only terms diagonal in q . For example: $s_{qk'}^z s_{kq}^+ = \frac{1}{2} \hat{n}_{q\downarrow} s_{kk'}^+$ and $s_{qk'}^z s_{kq}^- = -\frac{1}{2} \hat{n}_{q\uparrow} s_{kk'}^-$. The renormalization becomes

$$\frac{1}{\omega - D/2 + J/4} \sum_{|k, k'| < \Lambda, q} \left[\frac{1}{4} J^z J^t \left(-\frac{1}{2} S_d^+ \hat{n}_q s_{kk'}^- - \frac{1}{4} S_d^- \hat{n}_q s_{kk'}^z \right) - \frac{1}{4} J^{t2} S_d^z \left(-\hat{n}_{q\uparrow} c_{k\downarrow}^\dagger c_{k'\downarrow} + \hat{n}_{q\downarrow} c_{k\uparrow}^\dagger c_{k'\uparrow} \right) \right] \quad (2.4.6)$$

We now replace $\sum_q \hat{n}_{q\sigma} = n(D)$. The renormalization due to excitations coming from the particle sector is

$$\Delta H_1 = -\frac{1}{2} \frac{n(D)}{\omega - D/2 + J/4} \sum_{|k, k'| < \Lambda} \left[J^z J^t \frac{1}{2} \left(S_d^+ s_{kk'}^- + S_d^- s_{kk'}^z \right) + J^{t2} S_d^z s_{kk'}^z \right] \quad (2.4.7)$$

The renormalization in the couplings coming from the particle sector is therefore,

$$\Delta J^z = -\frac{1}{2} \frac{J^{t2} n(D)}{\omega - D/2 + J/4}, \quad \Delta J^t = -\frac{1}{2} \frac{J^z J^t n(D)}{\omega - D/2 + J/4} \quad (2.4.8)$$

2.4.2 Hole sector

The hole sector involves integrating out those states which are vacant ($\hat{n}_{q\beta} = 1$). We will work at an energy shell $\epsilon_q = D$. The renormalization is

$$H_1^I \frac{1}{\omega - H_{q\beta}^D} H_0^I \quad (2.4.9)$$

The same considerations as those in the particle sector apply here, and the denominator becomes $\omega - D/2 + J/4$, while the numerator is $H_1^I H_0^I$. Since this is just the Hermitian conjugate of the particle sector form, we do not

need to calculate this separately, because the renormalization here will be $\Delta H_0 = \Delta H_1^\dagger = \Delta H_1$.

2.4.3 Scaling equations

Since the renormalization in the hole sector is equal to that in the particle sector, the total renormalization is simply twice that in the particle sector (eqs. 2.4.8):

$$\Delta J^z = -\frac{J^{t^2}n(D)}{\omega - D/2 + J/4}, \quad \Delta J^t = -\frac{J^z J^t n(D)}{\omega - D/2 + J/4} \quad (2.4.10)$$

If we set $J_z = J_t = J$, we have an SU(2)-symmetric Kondo model $J\vec{S}_d \cdot \vec{s}$.

$$\Delta J = -\frac{J^2 n(D)}{\omega - D/2 + \frac{1}{4}J} \quad (2.4.11)$$

To recover the one-loop form, we can replace ω with the bare value $-D/2$ and ignore the J in the denominator (small J).

$$\Delta J \approx \frac{J^2 n(D)}{D} \quad (2.4.12)$$

2.4.4 Numerical Solutions

The symmetric scaling equation 2.4.11 was solved numerically with the choice $\omega = -\frac{\epsilon_q}{2}$, for both positive and negative bare values of J . For sufficiently low values of ω , the Kondo coupling J flows to the strong-coupling limit. This limit, as obtained from the URG, is of course finite. This can be reconciled with the NRG result $J^* = \infty$ by noting the fact that increasing the bare bandwidth D does increase the value of URG J^* , such that in the thermodynamic limit $D \rightarrow \infty$, URG should give $J^* \rightarrow \infty$. This is shown in fig. 2.7

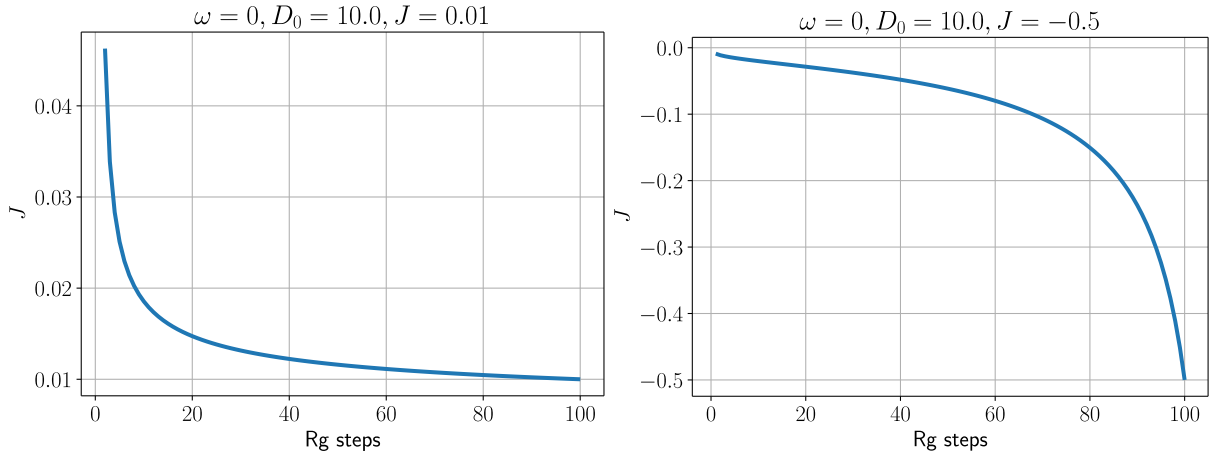


Figure 2.6: Flow of J towards the strong-coupling fixed point (right) and the weak coupling saddle-point (left). The x-axis indicates the index of the energy shell being decoupled. The largest value (UV) is the first step, and we go towards the left (IR).

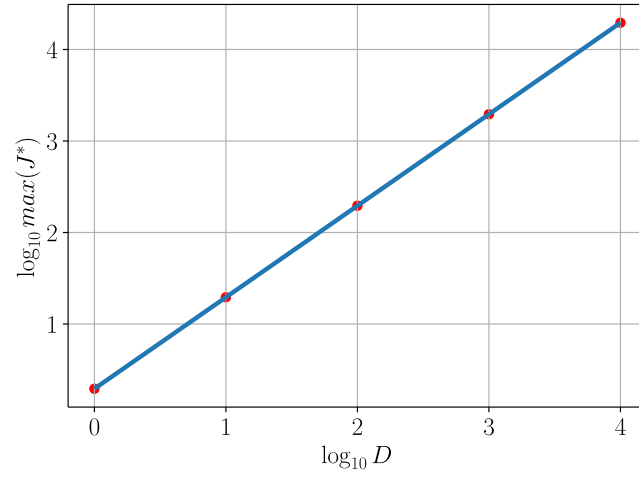


Figure 2.7: Variation of the fixed point value J^* against the bare bandwidth, in log scale.

Chapter 3

Connection between URG and Other Canonical Transformations

3.1 Poor man's scaling (PMS)

3.1.1 Formalism

We first describe the formalism of the poor man's scaling (PMS) method, first formulated by Anderson [3]. The problem is defined as

$$\mathcal{H}|\Psi\rangle = E|\Psi\rangle \quad (3.1.1)$$

\mathcal{H} is the total Hamiltonian and $|\Psi\rangle$ and E are the exact eigenstate and eigenvalue of \mathcal{H} . We imagine a separation of the total Hilbert space into two set of states, and we call these two states $|0\rangle$ and $|1\rangle$. This separation depends on which scattering term we want to kill by this transformation. For example, in the URG, we typically select a particular electron $q\beta$ and then kill the scattering terms that change the number of this state. In that case, $|0\rangle$ will refer to the set of states $\{|\hat{n}_{q\beta} = 0\rangle \otimes |\phi_0\rangle\}$ and $|1\rangle$ will refer to the set of states $\{|\hat{n}_{q\beta} = 1\rangle \otimes |\phi_1\rangle\}$. $|\phi_{0,1}\rangle$ refer to the states of all the other electrons. As another example, if we wanted to separate the charge-Kondo and the spin-Kondo from the SIAM, we would want to kill the terms that scatter between the spin-full subspace $\hat{n}_d = 1$ to the spin-less subspace $\hat{n}_d = 0, 2$. These two will then be the $|0\rangle$ and $|1\rangle$ sets.

Keeping this separation in mind, the exact eigenstate $|\Psi\rangle$ can be split as

$$|\Psi\rangle = \sum_i |\phi_0^i\rangle + \sum_i |\phi_1^i\rangle \quad (3.1.2)$$

The Hamiltonian can also be split as

$$\mathcal{H} = H_0 + V_+ + V_- \quad (3.1.3)$$

H_0 does not scatter between $\{|0\rangle\}$ and $\{|1\rangle\}$. It contains the diagonal parts as well as scatterings inside the subspaces. V_{\pm} scatter between the subspaces:

$$\begin{aligned} V_+ \{|0\rangle\} &\mapsto \{|1\rangle\}, & V_+ |1\rangle &\rightarrow 0 \\ V_- \{|1\rangle\} &\mapsto \{|0\rangle\}, & V_- |0\rangle &\rightarrow 0 \end{aligned} \quad (3.1.4)$$

The Schrodinger equation can thus be split into

$$\begin{aligned} H_0 \sum_i |\phi_0^i\rangle + V_- \sum_i |\phi_1^i\rangle &= E \sum_i |\phi_0^i\rangle \\ H_0 \sum_i |\phi_1^i\rangle + V_+ \sum_i |\phi_0^i\rangle &= E \sum_i |\phi_1^i\rangle \end{aligned} \quad (3.1.5)$$

Eliminating $\sum_i |\phi_1^i\rangle$ gives

$$H_0 \sum_i |\phi_0^i\rangle + V_- \frac{1}{E_1 - H_0} V_+ \sum_i |\phi_0^i\rangle = E \sum_i |\phi_0^i\rangle \quad (3.1.6)$$

The effective Hamiltonian in this subspace is therefore

$$\tilde{\mathcal{H}}_0 = H_0 + V_- \frac{1}{E - H_0} V_+ \quad (3.1.7)$$

Similarly, eliminating $\sum_i |\phi_0^i\rangle$ gives the effective Hamiltonian in the other subspace,

$$\tilde{\mathcal{H}}_1 = H_0 + V_+ \frac{1}{E - H_0} V_- \quad (3.1.8)$$

The total effective Hamiltonian that does not scatter between the two subspaces is

$$\tilde{\mathcal{H}}(E) = H_0 + \underbrace{V_- \frac{1}{E - H_0} V_+ + V_+ \frac{1}{E - H_0} V_-}_{\text{renormalization}} \quad (3.1.9)$$

This is of course a function of whatever exact energy eigenvalue we chose, E . Different choices will give different effective Hamiltonians. The renormalization will now be written in terms of the matrix elements. Since the entire \mathcal{H}_X must be Hermitian, we must have $V_- = V_+^\dagger \equiv V$.

$$\Delta\mathcal{H}(E) = V \frac{1}{E - H_0} V^\dagger + V^\dagger \frac{1}{E - H_0} V \quad (3.1.10)$$

Now take the first term and insert complete bases on both sides of V and V^\dagger .

$$V \frac{1}{E - H_0} V^\dagger = \sum_{ijk} |\phi_0^i\rangle \langle \phi_0^i| V |\phi_1^j\rangle \langle \phi_1^j| \frac{1}{E - H_0} |\phi_1^j\rangle \langle \phi_1^j| V^\dagger |\phi_0^k\rangle \langle \phi_0^k| = \sum_{ijk} |\phi_0^i\rangle V_{ij} \langle \phi_1^j| \frac{1}{E - H_0} |\phi_1^j\rangle V_{kj}^\dagger \langle \phi_0^k| \quad (3.1.11)$$

where we defined $\langle \phi_0^i| V |\phi_1^j\rangle = V_{ij}$. We now approximate H_0 by keeping just the diagonal part, and allowing the balance to redefine E into ω . Then, $(E - H_0) |\phi_{0,1}^j\rangle \equiv (\omega_{0,1} - E_{0,1}^j) |\phi_{0,1}^j\rangle$. That gives

$$V \frac{1}{E - H_0} V^\dagger = \sum_{ijk} |\phi_0^i\rangle \langle \phi_0^k| \frac{V_{ij} V_{kj}^\dagger}{\omega_1 - E_1^j} \quad (3.1.12)$$

The second term similarly gives

$$V^\dagger \frac{1}{E - H_0} V = \sum_{ijk} |\phi_1^i\rangle \langle \phi_1^k| \frac{V_{ji}^\dagger V_{jk}}{\omega_0 - E_0^j} \quad (3.1.13)$$

The total renormalization becomes

$$\Delta\mathcal{H}(E) = \sum_{ijk} \left(\frac{1}{\omega_1 - E_1^j} |\phi_0^i\rangle \langle \phi_0^k| V_{ij} V_{kj}^\dagger + \frac{1}{\omega_0 - E_0^j} |\phi_1^i\rangle \langle \phi_1^k| V_{ji}^\dagger V_{jk} \right) \quad (3.1.14)$$

This is a general expression that would work irrespective of whether you are decoupling multiple electrons or a single electron. However, the ω are unknown and we need some prescription for replacing them. Since the E is the eigenstate of the initial state on which the scattering terms act, it makes sense to replace them with the initial state energy.

$$\Delta\mathcal{H}(E) = \sum_{ijk} \left(\frac{1}{E_0^k - E_1^j} |\phi_0^i\rangle \langle \phi_0^k| V_{ij} V_{kj}^\dagger + \frac{1}{E_1^k - E_0^j} |\phi_1^i\rangle \langle \phi_1^k| V_{ji}^\dagger V_{jk} \right) \quad (3.1.15)$$

However, closer inspection reveals that this choice makes the renormalization non-Hermitian. So the correct choice

is to keep both the initial and final energies.

$$\begin{aligned}\Delta\mathcal{H} &= \frac{1}{2} \sum_{ijk} \frac{1}{\omega_1 - E_1^j} \left(|\phi_0^i\rangle \langle \phi_0^k| V_{ij} V_{kj}^\dagger + |\phi_0^k\rangle \langle \phi_0^i| V_{kj} V_{ij}^\dagger \right) + \frac{1}{2} \sum_{ijk} \frac{1}{\omega_0 - E_0^j} \left(|\phi_1^i\rangle \langle \phi_1^k| V_{ji}^\dagger V_{jk} + |\phi_1^k\rangle \langle \phi_1^i| V_{jk}^\dagger V_{ji} \right) \\ &= \frac{1}{2} \sum_{ijk} \left(\frac{1}{E_0^k - E_1^j} |\phi_0^i\rangle \langle \phi_0^k| V_{ij} V_{kj}^\dagger + \frac{1}{E_0^k - E_1^j} |\phi_0^k\rangle \langle \phi_0^i| V_{kj} V_{ij}^\dagger \right) + \frac{1}{2} \sum_{ijk} \left(\frac{1}{E_1^k - E_0^j} |\phi_1^i\rangle \langle \phi_1^k| V_{ji}^\dagger V_{jk} \right. \\ &\quad \left. + \frac{1}{E_1^k - E_0^j} |\phi_1^k\rangle \langle \phi_1^i| V_{jk}^\dagger V_{ji} \right)\end{aligned}\tag{3.1.16}$$

Therefore,

$$\Delta\mathcal{H} = \frac{1}{2} \sum_{ijk} \left(\frac{1}{E_0^k - E_1^j} + \frac{1}{E_0^i - E_1^j} \right) |\phi_0^i\rangle \langle \phi_0^k| V_{ij} V_{kj}^\dagger + \frac{1}{2} \sum_{ijk} \left(\frac{1}{E_1^k - E_0^j} + \frac{1}{E_1^i - E_0^j} \right) |\phi_1^i\rangle \langle \phi_1^k| V_{ji}^\dagger V_{jk}\tag{3.1.17}$$

In summary, the prescription of replacing all ω with the initial state energy will be correct only if the initial and final states are the same. This happens when we are decoupling a single-electron state - then the total renormalization is of the form $c^\dagger T^\dagger c$ such that we start from an initial state, scatter to an intermediate state and then go back to the initial state so that the final state is the same as the initial state. However, if we are using PMS to decouple states in one-shot, each subspace will have multiple states and there might be terms where we do not end up at the initial state we started with. Then the correct prescription would be to use the mean of the initial and final state denominators.

One might wonder how we can generate higher order terms in this method. Eq. 3.1.17, as it stands, has only $\mathcal{O}(V^2)$ terms. The higher order terms were actually dropped when we replaced H_0 with its diagonal part in eq. 3.1.12. To see the higher order term, we do not drop the off-diagonal part in the denominator, but split the total H_0 into a diagonal and an off-diagonal part: $H_0 = H_d + X$. Note that X is off-diagonal in the subspace of the states that have not been decoupled yet but will be decoupled later. They represent scattering between the lower energy states. X is still diagonal with respect to the states that we are decoupling presently. The total effective Hamiltonian becomes

$$\tilde{\mathcal{H}}(E) = H_0 + V \frac{1}{G_0(E)^{-1} - X} V^\dagger + V^\dagger \frac{1}{G_0(E)^{-1} - X} V\tag{3.1.18}$$

where $G_0(E)^{-1} = E - H_d$ is the inverse of the non-interacting Greens function. To allow computation, we can expand the denominator in powers of $XG_0(E)^{-1}$:

$$\begin{aligned}\Delta H \equiv \tilde{\mathcal{H}}(E) - H_0 &= VG_0(E) [1 + XG_0(E) + XG_0(E)XG_0(E) + \dots] V^\dagger + V^\dagger \frac{1}{G_0(E)^{-1} - X} V \\ &= \underbrace{VG_0(E)V^\dagger + V^\dagger G_0(E)V}_{\text{two vertex or one loop correction}} + \underbrace{VG_0(E)XG_0(E)V^\dagger + V^\dagger G_0(E)XG_0(E)V}_{\text{three vertex or two loop correction}} \\ &\quad + \text{higher loop corrections}\end{aligned}\tag{3.1.19}$$

3.1.2 PMS third order equations for symmetric multi-channel Kondo model

To get a clear idea of what the various terms in eq. 3.1.19 mean, we will calculate the multi-channel Kondo model RG equations up to third order. The model is

$$H = \sum_{k\sigma,\gamma} \epsilon_{k\sigma}^{(\gamma)} c_{k\sigma}^\dagger c_{k\sigma}^{(\gamma)} + \sum_{k\alpha,k'\alpha',\gamma,a} J^a S_d^a \sigma_{\alpha\alpha'}^a c_{k\alpha}^{(\gamma)\dagger} c_{k'\alpha'}^{(\gamma)}\tag{3.1.20}$$

a goes over x, y, z and represents the directions. S_d^a therefore represents the spin operators for the impurity along the x, y and z directions. The labels $k\alpha$ and $k'\alpha'$ sum over the conduction electrons, while the index γ represents the channel. We will first calculate the second order terms. The virtual particle term is

$$VG_0(E)V^\dagger = \sum_{k,k',\alpha,\alpha',q,\beta,\gamma,a,b} c_{q\beta}^{(\gamma)\dagger} c_{k\alpha}^{(\gamma)} S_d^a \sigma_{\beta\alpha}^a \frac{J^a J^b}{E - H_d} c_{k'\alpha'}^{(\gamma)\dagger} c_{q\beta}^{(\gamma)} S_d^b \sigma_{\alpha'\beta}^b\tag{3.1.21}$$

The label q sums over the momentum states being decoupled ($|\epsilon_q| \in [D - |\delta D|, D]$). The labels k, k' , on the other hand, sum over the momentum states that are not being decoupled, so they lie in the complimentary range. The denominator of the Greens function is the excitation energy $\epsilon_q - \epsilon_{k'}$. We will now simplify the term.

$$\begin{aligned}
VG_0(E)V^\dagger &= \sum_{k,k',\alpha,\alpha',q,\beta,\gamma,a,b} \frac{J^a J^b}{\epsilon_q - \epsilon_{k'}} S_d^a \sigma_{\beta\alpha}^a S_d^b \sigma_{\alpha'\beta}^b c_{q\beta}^{(\gamma)\dagger} c_{k\alpha}^{(\gamma)} c_{k'\alpha'}^{(\gamma)\dagger} c_{q\beta}^{(\gamma)} \\
&= \sum_{k,k',\alpha,\alpha',\beta,\gamma,a,b} \frac{J^a J^b}{\epsilon_q - \epsilon_{k'}} S_d^a \sigma_{\beta\alpha}^a S_d^b \sigma_{\alpha'\beta}^b c_{k\alpha}^{(\gamma)} c_{k'\alpha'}^{(\gamma)\dagger} \sum_q \hat{n}_{q\beta}^{(\gamma)} \\
&= \sum_{k,k',\alpha,\alpha',\beta,\gamma,a,b} S_d^a \sigma_{\beta\alpha}^a S_d^b \sigma_{\alpha'\beta}^b c_{k\alpha}^{(\gamma)} c_{k'\alpha'}^{(\gamma)\dagger} \int_{-D}^{-D+|\delta D|} d\epsilon \rho(\epsilon) \frac{J^a J^b \hat{n}^{(\gamma)}(\epsilon)_\beta}{\epsilon_q - \epsilon_{k'}} \\
&= \sum_{k,k',\alpha,\alpha',\beta,\gamma,a,b} S_d^a \sigma_{\beta\alpha}^a S_d^b \sigma_{\alpha'\beta}^b c_{k\alpha}^{(\gamma)} c_{k'\alpha'}^{(\gamma)\dagger} \frac{J^a J^b \rho(0)|\delta D|}{-D} [\hat{n}(\epsilon) = \theta(-\epsilon), |\epsilon_{k'}| \ll D] \\
&= \sum_{\alpha,\alpha',a,b} S_d^a S_d^b (\sigma^b \sigma^a)_{\alpha',\alpha} \sum_{k,k',\gamma} c_{k\alpha}^{(\gamma)} c_{k'\alpha'}^{(\gamma)\dagger} \frac{J^a J^b \rho(0)|\delta D|}{-D} \\
&= \sum_{\alpha,\alpha',a,b} \left(\frac{1}{4} \delta_{ab} + \frac{i}{2} \sum_c \epsilon^{abc} S_d^c \right) \left(\delta_{ab} + i \sum_c \epsilon^{bac} \sigma^c \right)_{\alpha',\alpha} \sum_{k,k',\gamma} c_{k\alpha}^{(\gamma)} c_{k'\alpha'}^{(\gamma)\dagger} \frac{J^a J^b \rho(0)|\delta D|}{-D}
\end{aligned} \tag{3.1.22}$$

The spin part can now be simplified:

$$\begin{aligned}
\sum_{a,b} J^a J^b \left(\frac{1}{4} \delta_{ab} + \frac{i}{2} \sum_c \epsilon^{abc} S_d^c \right) \left(\delta_{ab} + i \sum_c \epsilon^{bac} \sigma^c \right)_{\alpha',\alpha} &= \frac{\sum_a J^{a2}}{4} \delta_{\alpha,\alpha'} + \frac{1}{2} \sum_{a,b,c,c'} J^a J^b \epsilon^{abc} \epsilon^{abc'} S_d^c (\sigma^c)_{\alpha'\alpha} \\
&= \frac{\sum_a J^{a2}}{4} \delta_{\alpha,\alpha'} + \frac{1}{2} \sum_c S_d^c \sigma_{\alpha'\alpha}^c \left(\sum_{\substack{a,b, \\ a \neq b}} J^a J^b - 2J^c \sum_{\substack{a \\ a \neq c}} J^a \right)
\end{aligned} \tag{3.1.23}$$

The constant part renormalizes a potential scattering, so we drop that part. The renormalization from the other part is

$$\begin{aligned}
&\sum_{\alpha,\alpha',c} S_d^c \sigma_{\alpha'\alpha}^c \sum_{k,k',\gamma} c_{k\alpha}^{(\gamma)} c_{k'\alpha'}^{(\gamma)\dagger} \frac{\frac{1}{2} \left(\sum_{\substack{a,b, \\ a \neq b}} J^a J^b - 2J^c \sum_{\substack{a \\ a \neq c}} J^a \right) \rho(0)|\delta D|}{-D} \\
&= \sum_{\alpha,\alpha',c} S_d^c \sigma_{\alpha'\alpha}^c \sum_{k,k',\gamma} c_{k'\alpha'}^{(\gamma)\dagger} c_{k\alpha}^{(\gamma)} \frac{\frac{1}{2} \left(\sum_{\substack{a,b, \\ a \neq b}} J^a J^b - 2J^c \sum_{\substack{a \\ a \neq c}} J^a \right) \rho(0)|\delta D|}{D}
\end{aligned} \tag{3.1.24}$$

The virtual hole term $V^\dagger G_0(E)V$ gives the same contribution. The total renormalization at second order is therefore

$$\delta J^c = \frac{\left(\sum_{\substack{a,b, \\ a \neq b}} J^a J^b - 2J^c \sum_{\substack{a \\ a \neq c}} J^a \right) \rho(0)|\delta D|}{D} = \frac{2J^{c+1} J^{c-1} \rho(0)|\delta D|}{D} \tag{3.1.25}$$

where $\{c-1, c, c+1\}$ is a cyclic permutation of $\{x, y, z\}$. This reveals that the anisotropic Kondo coupling RG equations have a cyclic form:

$$\delta J^x = \frac{2J^y J^z \rho(0)|\delta D|}{D} \tag{3.1.26}$$

Cyclic permutations of the labels x, y, z produce the other equations. From here on, we will assume $J^a = J$ for simplicity. This gives, at second order,

$$\delta J = \frac{2J^2 \rho(0)|\delta D|}{D} \tag{3.1.27}$$

We now consider the third order term. The virtual hole three vertex term, $V^\dagger G_0(E) X G_0(E) V$, is of the form

$$J^3 \sum_{\substack{q, k_1, k_2, k, k', \\ \alpha, \alpha', \alpha_1, \alpha_2, \beta, \\ \gamma_1, \gamma_2}} c_{q\beta}^{(\gamma_1)\dagger} c_{k\alpha}^{(\gamma_1)} \vec{S}_d \cdot \vec{\sigma}_{\beta\alpha} \frac{1}{E - H_d} c_{k_1\alpha_1}^{(\gamma_2)\dagger} c_{k_2\alpha_2}^{(\gamma_2)} \vec{S}_d \cdot \vec{\sigma}_{\alpha_1\alpha_2} \frac{1}{E - H_d} c_{k'\alpha'}^{(\gamma_1)\dagger} c_{q\beta}^{(\gamma_1)} \vec{S}_d \cdot \vec{\sigma}_{\alpha'\beta} \quad (3.1.28)$$

The other term among the two third order terms is the virtual particle term. The labels q, k, k', k_1, k_2 run over the momentum states, $\alpha, \alpha', \alpha_1, \alpha_2, \beta$ run over the spin indices and γ_1, γ_2 run over the channel indices. q, β are the labels of the momentum states that are being decoupled. $|\epsilon_q|$ therefore lies in the range $[D, D - \delta D]$. The rest of the labels $(k, \alpha), (k_1, \alpha_1), (k_2, \alpha_2)$ lie in the compliment range and represent electrons that are not being decoupled at this step.

The denominator of the right-most Greens function measures the energy difference between the initial state and the state reached after the first excitation. This difference is $\epsilon_q - \epsilon_{k'}$. Similarly, the second Greens function has the energy difference between the initial state and the one obtained after two subsequent excitations. This difference is $\epsilon_q - \epsilon_{k'} + \epsilon_{k_2} - \epsilon_{k_1}$. With this substitution, we get

$$V^\dagger G_0(E) X G_0(E) V = J^3 \sum_{\substack{q, k_1, k_2, k, k', \\ \alpha, \alpha', \alpha_1, \alpha_2, \beta, \\ \gamma_1, \gamma_2}} \frac{c_{q\beta}^{(\gamma_1)\dagger} c_{k\alpha}^{(\gamma_1)} \vec{S}_d \cdot \vec{\sigma}_{\beta\alpha} c_{k_1\alpha_1}^{(\gamma_2)\dagger} c_{k_2\alpha_2}^{(\gamma_2)} \vec{S}_d \cdot \vec{\sigma}_{\alpha_1\alpha_2} c_{k'\alpha'}^{(\gamma_1)\dagger} c_{q\beta}^{(\gamma_1)} \vec{S}_d \cdot \vec{\sigma}_{\alpha'\beta}}{(\epsilon_q - \epsilon_{k'} + \epsilon_{k_2} - \epsilon_{k_1})(\epsilon_q - \epsilon_{k'})} \quad (3.1.29)$$

The sum over q can be performed in the usual manner.

$$\begin{aligned} \sum_q \frac{c_{q\beta}^{(\gamma_1)\dagger} c_{q\beta}^{(\gamma_1)}}{(\epsilon_q - \epsilon_{k'} + \epsilon_{k_2} - \epsilon_{k_1})(\epsilon_q - \epsilon_{k'})} &= \int_{-D}^{-D+|\delta D|} \frac{d\epsilon \rho(\epsilon) \hat{n}(\epsilon)}{(\epsilon - \epsilon_{k'} + \epsilon_{k_2} - \epsilon_{k_1})(\epsilon - \epsilon_{k'})} \\ &= \frac{\rho(0)|\delta D|}{(D + \epsilon_{k'} - \epsilon_{k_2} + \epsilon_{k_1})(D + \epsilon_{k'})} \end{aligned} \quad (3.1.30)$$

where we have taken $\rho(\epsilon) = \rho(0)$, $\hat{n}(\epsilon) = \theta(-\epsilon)$ and $\epsilon_q \simeq -D$.

For the next step, note that $\vec{S}_d \cdot \vec{\sigma}_{x,y} = \sum_a S_d^a \sigma_{x,y}^a$. Substituting this into $V^\dagger G_0(E) X G_0(E) V$ gives

$$\sum_{\gamma_1, \gamma_2} \sum_{k_1, k_2, k, k', \alpha, \alpha', \alpha_1, \alpha_2, \beta} \sum_{a, b, c} \frac{J^3 \rho(0) |\delta D|}{(D + \epsilon_{k'} - \epsilon_{k_2} + \epsilon_{k_1})(D + \epsilon_{k'})} S_d^a \sigma_{\beta\alpha}^a S_d^b \sigma_{\alpha_1\alpha_2}^b S_d^c \sigma_{\alpha'\beta}^c c_{k\alpha}^{(\gamma_1)\dagger} c_{k_1\alpha_1}^{(\gamma_2)\dagger} c_{k_2\alpha_2}^{(\gamma_2)} c_{k'\alpha'}^{(\gamma_1)} \quad (3.1.31)$$

Now, note that all not all combinations of the momenta will renormalize the $\vec{S}_d \cdot \vec{\sigma}$ term of the Hamiltonian. In order for such a term to come out, the four remaining momenta must be contracted to two. The first set of terms that satisfy this requirement is given by the condition $k'\alpha' = k\alpha$. The renormalization from this subset of terms is

$$\begin{aligned} &\sum_{\gamma_1, \gamma_2} \sum_{k_1, k_2, k} \sum_{\alpha, \alpha_1, \alpha_2, \beta} \sum_{a, b, c} \frac{J^3 \rho(0) |\delta D|}{(D + \epsilon_k - \epsilon_{k_2} + \epsilon_{k_1})(D + \epsilon_k)} S_d^a \sigma_{\beta\alpha}^a S_d^b \sigma_{\alpha_1\alpha_2}^b S_d^c \sigma_{\alpha\beta}^c c_{k_1\alpha_1}^{(\gamma_2)\dagger} c_{k_2\alpha_2}^{(\gamma_2)} c_{k\alpha}^{(\gamma_1)\dagger} c_{k\alpha}^{(\gamma_1)} \\ &= \sum_{\gamma_2} \sum_{k_1, k_2} \sum_{\alpha, \alpha_1, \alpha_2, \beta} \sum_{a, b, c} J^3 \rho(0) |\delta D| S_d^a \sigma_{\beta\alpha}^a S_d^b \sigma_{\alpha_1\alpha_2}^b S_d^c \sigma_{\alpha\beta}^c c_{k_1\alpha_1}^{(\gamma_2)\dagger} c_{k_2\alpha_2}^{(\gamma_2)} \sum_{\gamma_1} \int_0^{D-|\delta D|} \frac{d\epsilon \rho(\epsilon)}{(D + \epsilon - \epsilon_{k_2} + \epsilon_{k_1})(D + \epsilon)} \\ &\simeq \sum_{\gamma_2} \sum_{k_1, k_2} \sum_{\alpha, \alpha_1, \alpha_2, \beta} \sum_{a, b, c} J^3 \rho(0) |\delta D| S_d^a \sigma_{\beta\alpha}^a S_d^b \sigma_{\alpha_1\alpha_2}^b S_d^c \sigma_{\alpha\beta}^c c_{k_1\alpha_1}^{(\gamma_2)\dagger} c_{k_2\alpha_2}^{(\gamma_2)} \sum_{\gamma_1} \int_0^{D-|\delta D|} \frac{d\epsilon \rho(\epsilon)}{(D + \epsilon)^2} \\ &= \frac{K \rho^2(0) J^3 |\delta D|}{2D} \sum_{\alpha, \beta} \sum_{a, c, b} \sum_{\alpha_1, \alpha_2} S_d^a \sigma_{\beta\alpha}^a S_d^b \sigma_{\alpha_1\alpha_2}^b \sigma_{\alpha\beta}^c \sum_{k_1, k_2, \gamma_2} c_{k_1\alpha_1}^{(\gamma_2)\dagger} c_{k_2\alpha_2}^{(\gamma_2)}. \end{aligned} \quad (3.1.32)$$

$K = \sum_{\gamma_1}$ is the total number of channels. The other set of terms is given by the condition $k_1\alpha_1 = k_2\alpha_2$. The

renormalization from these terms can be calculated similarly:

$$\begin{aligned}
& \sum_{\gamma_1, \gamma_2} \sum_{k_1, k, k'} \sum_{\alpha, \alpha', \alpha_1, \beta} \sum_{a, b, c} \frac{J^3 \rho(0) |\delta D|}{(D + \epsilon_{k'})^2} S_d^a \sigma_{\beta\alpha}^a S_d^b \sigma_{\alpha_1 \alpha_1}^b S_d^c \sigma_{\alpha' \beta}^c c_{k\alpha}^{(\gamma_1)} c_{k_1 \alpha_1}^{(\gamma_2) \dagger} c_{k_1 \alpha_1}^{(\gamma_2)} c_{k' \alpha'}^{(\gamma_1) \dagger} \\
&= \sum_{\gamma_1} \sum_{k, k'} \sum_{\alpha, \alpha', \beta} \sum_{a, b, c} \frac{J^3 \rho(0) |\delta D|}{(D + \epsilon_{k'})^2} S_d^a \sigma_{\beta\alpha}^a S_d^b \text{Trace}(\sigma^b) S_d^c \sigma_{\alpha' \beta}^c c_{k\alpha}^{(\gamma_1)} \sum_{\gamma_2} \left[\int_{-D+|\delta D|}^0 d\epsilon \rho(\epsilon) \right] c_{k' \alpha'}^{(\gamma_1) \dagger} \\
&= 0
\end{aligned} \tag{3.1.33}$$

The spin products can be simplified using the identity

$$\sum_{\alpha\beta} \sigma_{\beta\alpha}^a \sigma_{\alpha\beta}^c = \text{Trace}[\sigma^a \sigma^c] = 2\delta_{ac} . \tag{3.1.34}$$

Using this identity, we get

$$V^\dagger G_0(E) X G_0(E) V = \frac{K \rho^2(0) J^3 |\delta D|}{D} \sum_{a, b} \sum_{\alpha_1, \alpha_2} S_d^a S_d^b S_d^a \sigma_{\alpha_1 \alpha_2}^b \sum_{k_1, k_2, \gamma_2} c_{k_1 \alpha_1}^{(\gamma_2) \dagger} c_{k_2 \alpha_2}^{(\gamma_2)} \tag{3.1.35}$$

The products of the impurity spin operators can now be simplified:

$$\sum_a S_d^a S_d^b S_d^a = \sum_a \left[S_d^b S_d^a + i \sum_c \epsilon^{abc} S_d^c \right] S_d^a = \frac{3}{4} S_d^b + i \sum_{a, c} \epsilon^{abc} S_d^c S_d^a = \frac{3}{4} S_d^b + \frac{1}{2} i^2 \sum_{a, c, e} \epsilon^{abc} \epsilon^{aec} S_d^e = -\frac{1}{4} S_d^b \tag{3.1.36}$$

Substituting this result in the renormalization gives

$$\begin{aligned}
V^\dagger G_0(E) X G_0(E) V &= -\frac{K \rho(0)^2 J^3 |\delta D|}{4D} \sum_{k_1, k_2, \alpha_1, \alpha_2, b, \gamma_2} S_d^b \sigma_{\alpha_1 \alpha_2}^b c_{k_1 \alpha_1}^{(\gamma_2) \dagger} c_{k_2 \alpha_2}^{(\gamma_2)} \\
&= -\frac{K \rho(0)^2 J^3 |\delta D|}{4D} \sum_{k_1 \alpha_1, k_2 \alpha_2, \gamma_2} \vec{S}_d \cdot \vec{\sigma}_{\alpha_1 \alpha_2} c_{k_1 \alpha_1}^{(\gamma_2) \dagger} c_{k_2 \alpha_2}^{(\gamma_2)}
\end{aligned} \tag{3.1.37}$$

The other term (virtual particle term) gives an equal contribution. The total renormalization is

$$\delta J = \frac{2J^2 \rho(0) |\delta D|}{D} \left(1 - \frac{K \rho(0) J}{4} \right) \tag{3.1.38}$$

3.1.3 PMS in the language of the URG - obtaining the η operators

To make a better connection with URG, we next show how the PMS formalism works out for a single-electron decoupling. The corresponding problem can be phrased in the following manner. We want to decouple one electron at momentum q from the full Hamiltonian. We can split the exact wavefunction as

$$|\Psi\rangle = |\Psi_0\rangle + |\Psi_1\rangle \tag{3.1.39}$$

where $|\Psi_0\rangle = (1 - \hat{n}_q) |\Psi^N\rangle$ is that part of the wavefunction where the state q is occupied. $|\Psi_1^N\rangle = \hat{n}_q |\Psi\rangle$ is that part of the wavefunction where the state q is occupied. We can also split the Hamiltonian as

$$\mathcal{H} = \mathcal{H}^d + V_0 + V_+ + V_- \tag{3.1.40}$$

\mathcal{H}^d is the diagonal part; it has the purely energy terms as well as self-energies that may arise from the diagonal parts of interactions; V_0 is the purely off-diagonal term that does not change \hat{n}_q ; it is the scattering *inside* the low energy subspace. V_+ and V_- are the purely off-diagonal terms that *do* change \hat{n}_q ; V_+ takes you from $\hat{n}_q = 0$ to $\hat{n}_q = 1$ and V_- does the opposite.

Substituting eqs. 3.1.40 and 3.1.39 in eq. 3.1.1 gives

$$\left(\mathcal{H}^d + V_0 + V_+ + V_-\right) (|\Psi_0\rangle + |\Psi_1\rangle) = E (|\Psi_0\rangle + |\Psi_1\rangle) \quad (3.1.41)$$

Gathering the kets with $\hat{n}_q = 0, 1$ gives

$$\begin{aligned} \left(\mathcal{H}_0^d + V_0\right) |\Psi_0\rangle + V_- |\Psi_1\rangle &= E |\Psi_0\rangle \\ \left(\mathcal{H}_1^d + V_0\right) |\Psi_1\rangle + V_+ |\Psi_0\rangle &= E |\Psi_1\rangle \end{aligned} \quad (3.1.42)$$

The second equation can be written as

$$|\Psi_1\rangle = \eta^\dagger |\Psi_0\rangle \quad (3.1.43)$$

where

$$\left(\eta^\dagger\right)_{\text{PMS}} = \frac{1}{E - \mathcal{H}_1^d - V_0} V_+ \quad (3.1.44)$$

Substituting this in the first equation gives

$$\left(\mathcal{H}_0^d + V_0 + V_- \eta^\dagger\right) |\Psi_0\rangle = E |\Psi_0\rangle \quad (3.1.45)$$

This new Hamiltonian,

$$\tilde{\mathcal{H}}_0 = \mathcal{H}_0^d + V_0 + V_- \eta^\dagger \quad (3.1.46)$$

has the high energy mode removed; the scattering terms start from the low energy subspace and end at the low energy subspace as well. The renormalization in the low energy subspace scatterings is

$$\Delta V_0 = V_- \eta^\dagger \quad (3.1.47)$$

If we eliminate $|\Psi_0\rangle$ instead of $|\Psi_1\rangle$, we get the renormalized equation in the high energy subspace:

$$|\Psi_0\rangle = \eta |\Psi_1\rangle \quad (3.1.48)$$

where

$$(\eta)_{\text{PMS}} = \frac{1}{E - \mathcal{H}_0^d - V_0} V_- \quad (3.1.49)$$

,so

$$\left(\mathcal{H}_1^d + V_0 + V_+ \eta\right) |\Psi_1\rangle = E |\Psi_1\rangle \quad (3.1.50)$$

The renormalized Hamiltonian in the high energy subspace is thus

$$\tilde{\mathcal{H}}_1 = \mathcal{H}_1^d + V_0 + V_+ \eta \quad (3.1.51)$$

If we want to keep both the high energy and low energy parts of the Hamiltonian, the new Hamiltonian is

$$\begin{aligned} \tilde{\mathcal{H}} &= \tilde{\mathcal{H}}_1 \hat{n} + \tilde{\mathcal{H}}_0 (1 - \hat{n}) \\ &= \mathcal{H}_0^d + \mathcal{H}_1^d + V_0 + V_+ \eta + V_- \eta^\dagger \end{aligned} \quad (3.1.52)$$

The total renormalization is

$$(\Delta \mathcal{H})_{\text{PMS}} = V_+ (\eta)_{\text{PMS}} + V_- (\eta^\dagger)_{\text{PMS}} \quad (3.1.53)$$

It can be shown that if we define a unitary operator $U = 1 - \eta + \eta^\dagger$, the transformed Hamiltonian $U \mathcal{H} U^\dagger$ is the same as eq. 3.1.52. This, along with the properties of η , have been shown in section 2. The important feature of eq. 3.1.52 is that there is no term in the transformed Hamiltonian which scatters between $|\Psi_0\rangle$ and $|\Psi_0\rangle$ - the two subspaces have been truly decoupled.

$$\left[U \mathcal{H} U^\dagger, n_q\right] = 0 \quad (3.1.54)$$

We can write down the renormalized Schrodinger equation in the low energy subspace, from eq. 3.1.45,

$$\tilde{\mathcal{H}}_0 |\Psi_0\rangle = E |\Psi_0\rangle \quad (3.1.55)$$

and again repeat the entire process. $\tilde{\mathcal{H}}_0$ now takes the place of \mathcal{H} and $|\Psi_0\rangle$ takes the place of $|\Psi\rangle$ in eq. 3.1.1.

The expression for URG is obtained in an almost identical way. The only difference is that instead of starting with the exact eigenpair $(E, |\Psi\rangle)$, we start with a more general pair $(\tilde{\mathcal{H}}, |\Phi\rangle)$ where $|\Phi\rangle$ is not necessarily an exact eigenstate of \mathcal{H} . It is defined by \mathcal{H}' , which is in turn defined as $\hat{n}_q \mathcal{H}' (1 - \hat{n}_q) = 0$. $|\Phi\rangle$ is then defined by

$$\mathcal{H} |\Phi\rangle = \mathcal{H}' |\Phi\rangle \quad (3.1.56)$$

This definition of \mathcal{H}' is the very minimum that we must have in order to fulfill our goal (decouple q).

The operators η and its conjugate change accordingly:

$$\begin{aligned} (\eta)_{\text{URG}} &= \frac{1}{\tilde{\mathcal{H}} - \mathcal{H}_0^d - V_0} V_- \\ &= \frac{1}{\hat{\omega} - \mathcal{H}_0^d} V_- \end{aligned} \quad (3.1.57)$$

where $\hat{\omega} \equiv \mathcal{H}' - V_0$ now embodies the quantum fluctuations inherent in the Hamiltonian through the scattering term V_0 . Similarly,

$$(\eta^\dagger)_{\text{URG}} = \frac{1}{\hat{\omega} - \mathcal{H}_1^d} V_+ \quad (3.1.58)$$

The renormalization is again

$$(\Delta\mathcal{H})_{\text{URG}} = V_+ (\eta)_{\text{URG}} + V_- (\eta^\dagger)_{\text{URG}} \quad (3.1.59)$$

This again allows us to write down a unitary operator that decouples the entangled state:

$$U = 1 - \eta + \eta^\dagger, \left[\hat{n}_q, U\mathcal{H}U^\dagger \right] = 0 \quad (3.1.60)$$

where $\tilde{\mathcal{H}} = U^\dagger \mathcal{H} U$. We can now write down a new problem in this decoupled space with the rotated items and attempt to decouple another electron q' . We will again choose some general eigenpair $(\mathcal{H}', |\Phi\rangle)$ such that $\tilde{\mathcal{H}} |\Phi\rangle = \mathcal{H}' |\Phi\rangle$ and $[\mathcal{H}', \hat{n}_{q'}] = 0$.

Summarizing, the general Hamiltonian is not diagonal in the Fock space basis. URG, in order to proceed, selects one non-Fock basis of states $|\Phi\rangle$ such that q is decoupled in that Hamiltonian. Since there can be lots of such basis, there is a freedom in this choice. With this basis in mind, URG then finds a unitary operator which when operated on the Hamiltonian takes us to the form in which it is diagonal in the Fock space basis. Note that this form is a function of the chosen $|\Phi\rangle$. We then select the second degree of freedom and repeat the process. What PMS does is, it exploits the freedom of choice and selects the exact eigenstate $|\Psi\rangle$ of the Hamiltonian as the non-Fock basis $|\Phi\rangle$. Doing that returns a rotated Hamiltonian which is diagonal in q , and is a function of the chosen state, same as URG. The conclusion is that depending on which state we choose as our diagonal non-Fock basis, URG and PMS will cause flows along different lines in general.

As the couplings flow, V_0 will also flow, leading to a flow of $\hat{\omega}$. Just at the fixed point, the denominator of URG vanishes, giving the equation

$$(\hat{\omega} - \mathcal{H}_1^d) V_+ |\Psi_0\rangle \text{ or } (\hat{\omega} - \mathcal{H}_1^d) V_- |\Psi_1\rangle \quad (3.1.61)$$

This means that one of the eigenvalues of $\hat{\omega}$ matches with the eigenvalue of the diagonal part \mathcal{H}^d , either in the occupied sector (\mathcal{H}_1^d) or unoccupied sector (\mathcal{H}_0^d). Since the eigenvalues are unchanged during the unitary renormalization, this implies that ω takes up one of the eigenvalues of the whole Hamiltonian \mathcal{H} . This will correspond to the fixed point obtained from PMS if we had started PMS with that eigenvalue.

In short, while the PMS flow is parametrised by one of the exact energy eigenvalues E , the URG flow is parametrised by a non-trivial operator $\hat{\omega}$ which incorporates both a diagonal part and an off-diagonal part and itself flows under the URG. At the fixed point, the off-diagonal part cancels out and the $\hat{\omega}$ finally flows to one of the energy eigenvalues and the URG fixed point matches with one of the PMS fixed points.

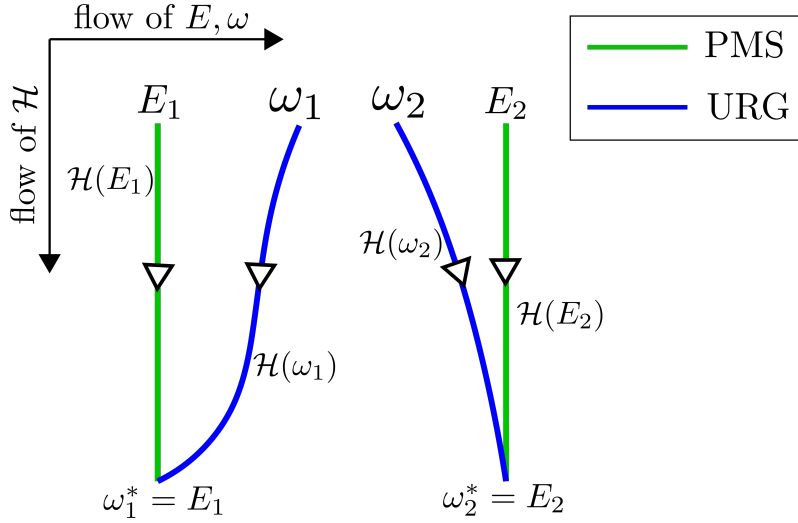


Figure 3.1: Flows of PMS(green) and URG(blue)

3.1.4 PMS for the single impurity Anderson model

To demonstrate the implementation, we can look at a specific model. For the SIAM,

$$\mathcal{H} = \sum_{k\sigma} \left(\epsilon_k \tau_{k\sigma} + V c_{k\sigma}^\dagger c_{d\sigma} + \text{h.c.} \right) \quad (3.1.62)$$

where $\tau = \hat{n} - \frac{1}{2}$. We want to decouple the state $q\beta$ from the rest of the electrons. We have $H_0 = \epsilon_d \hat{n}_d + U \hat{n}_{d\uparrow} \hat{n}_{d\downarrow} + \sum_{k\sigma} \epsilon_k \hat{n}_{k\sigma}$, $V_0 = \sum_{k<q,\sigma} c_{k\sigma}^\dagger c_{d\sigma} + \text{h.c.}$, $V_+ = V c_{q\beta}^\dagger c_{d\beta}$ and $V_- = V c_{d\beta}^\dagger c_{q\beta}$. The renormalization in particle sector

$$\Delta V_0 = c_{d\beta}^\dagger c_{q\beta} \frac{1}{(E - V_0) - \hat{\mathcal{H}}_0^d} c_{q\beta}^\dagger c_{d\beta} \quad (3.1.63)$$

The intermediate energy (at the propagator) is

$$\hat{\mathcal{H}}_0^d = \sum_{k,\sigma} \epsilon_k \tau_{k\sigma} + \epsilon_d \hat{n}_{d\bar{\beta}} \quad (3.1.64)$$

This is because the $c_{d\beta}$ at the right of the propagator ensures that we must have $\hat{n}_{d\beta} = 0$ at the propagator.

$$\Delta V_0 = c_{d\beta}^\dagger c_{q\beta} \frac{1}{(E - V_0) - \sum_{k,\sigma} \epsilon_k \tau_{k\sigma} - \epsilon_d \hat{n}_{d\bar{\beta}}} c_{q\beta}^\dagger c_{d\beta} \quad (3.1.65)$$

Since E is the exact eigenvalue, we do not have an expression for it. Instead, we approximate $E - V_0$ by substituting it with the current diagonal part corresponding to the initial state on which this entire term will act. The initial state is characterized by $\hat{n}_{q\beta} = 0$ and $\hat{n}_{d\beta} = 1$, so

$$E - V_0 = \sum_{k<q,\sigma} \epsilon_k \tau_{k\sigma} - \frac{1}{2} \epsilon_q + \epsilon_d + (\epsilon_d + U) \hat{n}_{d\bar{\beta}} \quad (3.1.66)$$

The $-\frac{1}{2} \epsilon_q$ comes from substituting $\hat{n}_{q\beta} = 0$ in $\epsilon_q \tau_{q\beta}$.

Substituting this in ΔV_0 gives

$$\begin{aligned}\Delta V_0 &= c_{d\beta}^\dagger c_{q\beta} \frac{1}{-\frac{1}{2}\epsilon_q - \epsilon_q \tau_{q\beta} + \epsilon_d + U \hat{n}_{d\bar{\beta}}} c_{q\beta}^\dagger c_{d\beta} = c_{d\beta}^\dagger c_{q\beta} \frac{1}{-\epsilon_q + \epsilon_d + U \hat{n}_{d\bar{\beta}}} c_{q\beta}^\dagger c_{d\beta} = c_{d\beta}^\dagger c_{q\beta} c_{q\beta}^\dagger c_{d\beta} \frac{1}{-\epsilon_q + \epsilon_d + U \hat{n}_{d\bar{\beta}}} \\ &= -c_{d\beta}^\dagger c_{q\beta} c_{q\beta}^\dagger c_{d\beta} \frac{1}{\epsilon_q - \epsilon_d - U \hat{n}_{d\bar{\beta}}} = (1 - \hat{n}_{q\beta}) \left(\frac{-\hat{n}_{d\beta} \hat{n}_{d\bar{\beta}}}{\epsilon_q - \epsilon_d - U} + \frac{-\hat{n}_{d\beta} (1 - \hat{n}_{d\bar{\beta}})}{\epsilon_q - \epsilon_d} \right)\end{aligned}\quad (3.1.67)$$

On the second line, we substituted $\tau_{q\beta} = \frac{1}{2}$ in the denominator, which is ensured by the $c_{q\beta}^\dagger$ to the right of the propagator. The first term renormalizes the energy of the doublon state and the second term renormalizes that of the singly-occupied state:

$$\Delta E_2 = \frac{-1}{\epsilon_q - \epsilon_d - U}, \quad \Delta E_1 = \frac{-1}{\epsilon_q - \epsilon_d} \quad (3.1.68)$$

The renormalization in the hole sector is

$$\Delta V_0 = c_{q\beta}^\dagger c_{d\beta} \frac{1}{(E - V_0) - \hat{\mathcal{H}}_0^d} c_{d\beta}^\dagger c_{q\beta} = c_{q\beta}^\dagger c_{d\beta} \frac{1}{(E - V_0) - \sum_{k,\sigma} \epsilon_k \tau_{k\sigma} - \epsilon_d - (\epsilon_d + U) \hat{n}_{d\bar{\beta}}} c_{d\beta}^\dagger c_{q\beta} \quad (3.1.69)$$

This time we substitute

$$E - V_0 = \sum_{k < q, \sigma} \epsilon_k \tau_{k\sigma} + \tau_{q\beta} \epsilon_q^- + \epsilon_d \hat{n}_{d\bar{\beta}} = \sum_{k < q, \sigma} \epsilon_k \tau_{k\sigma} + \frac{1}{2} \epsilon_q^- + \epsilon_d \hat{n}_{d\bar{\beta}} \quad (3.1.70)$$

In the last step we put $\tau_{q\beta} = \frac{1}{2}$ because the state is occupied in the initial configuratin. Note that since the electron $q\beta$ was occupied in the inital state, the energy ϵ_q^- in this sector must be opposite to that of the particle sector, ϵ_q . Hence $\epsilon_q^- = -\epsilon_q$, which gives

$$\begin{aligned}\Delta V_0 &= c_{q\beta}^\dagger c_{d\beta} \frac{1}{-\frac{1}{2}\epsilon_q - \epsilon_q^- \tau_{q\beta} - \epsilon_d - U \hat{n}_{d\bar{\beta}}} c_{d\beta}^\dagger c_{q\beta} = c_{q\beta}^\dagger c_{d\beta} c_{d\beta}^\dagger c_{q\beta} \frac{1}{-\epsilon_q - \epsilon_d - U \hat{n}_{d\bar{\beta}}} = \hat{n}_{q\beta} \left(\frac{-(1 - \hat{n}_{d\beta}) \hat{n}_{d\bar{\beta}}}{\epsilon_q + \epsilon_d + U} + \right. \\ &\quad \left. - \frac{(1 - \hat{n}_{d\beta}) (1 - \hat{n}_{d\bar{\beta}})}{\epsilon_q + \epsilon_d} \right)\end{aligned}\quad (3.1.71)$$

In the second line, we put $\epsilon_q^- = -\epsilon_q$ and $\tau_{q\beta} = -\frac{1}{2}$. The first term renormalizes the singly-occupied state while the second term renormalizes the holon state. Combining with the particle sector results, the total renormalization in all the three impurity states (holon, single and doublon) are

$$\begin{aligned}\Delta E_0 &= -\frac{1}{\epsilon_q + \epsilon_d} \\ \Delta E_1 &= -\frac{1}{\epsilon_q + \epsilon_d + U} - \frac{1}{\epsilon_q - \epsilon_d} \\ \Delta E_2 &= -\frac{1}{\epsilon_q - \epsilon_d - U}\end{aligned}\quad (3.1.72)$$

These results are also obtained in ref. [69]. The complete process is depicted in fig. 3.2.

Some conclusions:

- The *only* difference in the formalism of PMS and URG is that while PMS uses the exact energy eigenvalue E to parameterise the flow, URG uses a general intermediate decoupled Hamiltonian to do the same. Since the E is also, technically, an intermediate decoupled Hamiltonian (it is the final Hamiltonian), PMS can be seen as an URG but with a specific choice for the paramter.
- In practise, PMS replaces $E - V_0$ with the diagonal part of the initial state at the current step of the RG. We are talking about the energy of the initial state, not the intermediate state. This is because, from eq. 3.1.1,

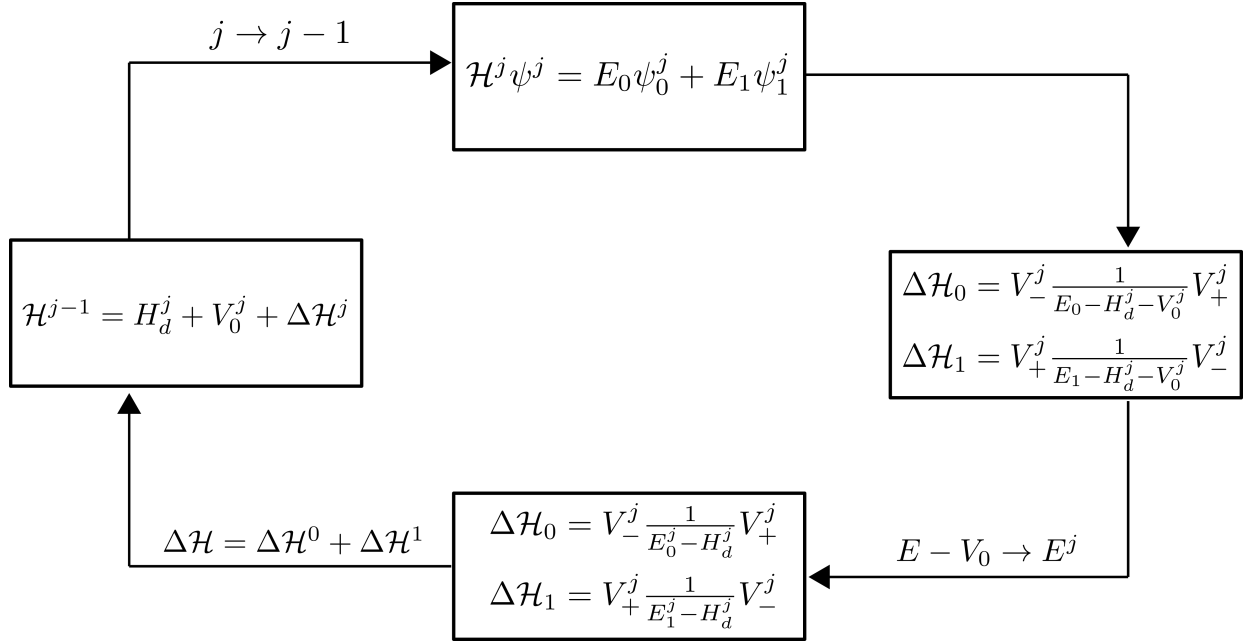


Figure 3.2: Flow chart of "Poor Man's" scaling algorithm

E is the energy of the initial state on which V_{\pm} act.

- The ideal solution would have been to substitute the exact energy and the total scattering term V , but since we do not know E and keeping the V would make the thing untractable, we use our current best guess (renormalised diagonal part). As the RG flows, both E_j and V flow, such that at the fixed point, V becomes zero (scattering terms get removed) and E_j morphs into the exact E .
- In practise, URG replaces the $\hat{\omega}$ with a guess for the final energy E . This however ignores the renormalization of $\hat{\omega}$. A better approach would be to replace it with E_j , following PMS. That would act like the one-particle renormalization of $\hat{\omega}$.
- PMS usually drops any diagonal component of the scattering from the denominator. For example, in the PMS of the Kondo model by Anderson [3] or that of the anisotropic power law Kondo model by Chenge et.al [70], they do not keep the term $J_z S_d^z s^z$ in the denominator although it is number (spin) conserving. Such terms are kept in the denominator of the URG though. It must be mentioned however that ref. [71] *does* bring a diagonal charge-charge interaction in the denominator in the PMS of the extended Anderson model.

3.2 Schrieffer-Wolff transformation (SWT)

3.2.1 Formalism

We have a general Hamiltonian

$$\mathcal{H} = \mathcal{H}_0 + \mathcal{H}_X \quad (3.2.1)$$

\mathcal{H}_0 is diagonal w.r.t a particular degree of freedom. V is off-diagonal w.r.t that same degree of freedom. Let S be an *anti-Hermitian* and *off-diagonal* operator. $U = e^S$ is then a unitary transformation.

$$\begin{aligned}
 U \mathcal{H} U^\dagger &= e^S (\mathcal{H}_0 + \mathcal{H}_X) e^{-S} \\
 &= \left(\cosh(S) + \sinh(S) \right) (\mathcal{H}_0 + \mathcal{H}_X) \left(\cosh(S) - \sinh(S) \right) \\
 &= H_1 + H_2
 \end{aligned} \quad (3.2.2)$$

where H_1 is diagonal and H_2 is off-diagonal.

$$\begin{aligned} H_1 &= \cosh(S) \mathcal{H}_0 \cosh(S) - \sinh(S) \mathcal{H}_0 \sinh(S) - \cosh(S) \mathcal{H}_X \sinh(S) \\ &\quad + \sinh(S) \mathcal{H}_X \cosh(S) \\ H_2 &= -\cosh(S) \mathcal{H}_0 \sinh(S) + \sinh(S) \mathcal{H}_0 \cosh(S) + \cosh(S) \mathcal{H}_X \cosh(S) \\ &\quad - \sinh(S) \mathcal{H}_X \sinh(S) \end{aligned} \quad (3.2.3)$$

The decoupling condition is $H_2 = 0$.

For small S , we have $\sinh S \sim S$ and $\cosh S \sim 1 + \frac{1}{2}S^2$. Therefore, the off-diagonal part, up to second order, is

$$H_2 = -\mathcal{H}_0 S + S \mathcal{H}_0 + \mathcal{H}_X + O(S^3) = [S, \mathcal{H}_0] + \mathcal{H}_X \quad (3.2.4)$$

The second order decoupling condition is thus

$$[S, \mathcal{H}_0] = -\mathcal{H}_X \quad (3.2.5)$$

The effective Hamiltonian is what remains, H_1 . That becomes, at second order,

$$\begin{aligned} H_1 &= \left(1 + \frac{1}{2}S^2\right) \mathcal{H}_0 \left(1 + \frac{1}{2}S^2\right) - S \mathcal{H}_0 S - \left(1 + \frac{1}{2}S^2\right) \mathcal{H}_X S + S \mathcal{H}_X \left(1 + \frac{1}{2}S^2\right) \\ &= \mathcal{H}_0 + \frac{1}{2} \{S^2, \mathcal{H}_0\} - S \mathcal{H}_0 S - \mathcal{H}_X S + S \mathcal{H}_X + O(S^3) \\ &= \mathcal{H}_0 + \frac{1}{2} S [S, \mathcal{H}_0] - \frac{1}{2} [S, \mathcal{H}_0] S + [S, \mathcal{H}_X] + O(S^3) \\ &= \mathcal{H}_0 + \frac{1}{2} [S, [S, \mathcal{H}_0]] + [S, \mathcal{H}_X] + O(S^3) \\ &= \mathcal{H}_0 + \frac{1}{2} [S, -\mathcal{H}_X] + [S, \mathcal{H}_X] + O(S^3) \\ &= \mathcal{H}_0 + \frac{1}{2} [S, \mathcal{H}_X] + O(S^3) \end{aligned} \quad (3.2.6)$$

Avoiding the perturbative route, we can take $S = \frac{\pi}{4} (\eta^\dagger - \eta)$, where η and its conjugate are non-perturbative and Fermionic - they satisfy $\eta^2 = \eta^{\dagger 2} = 0$ and $\{\eta, \eta^\dagger\} = 1$. We can then write

$$\begin{aligned} e^S &= \exp \left\{ \frac{\pi}{4} (\eta^\dagger - \eta) \right\} \\ &= 1 + (\eta^\dagger - \eta) \frac{\pi}{4} + \frac{1}{2!} (\eta^\dagger - \eta)^2 \left(\frac{\pi}{4}\right)^2 + \frac{1}{3!} (\eta^\dagger - \eta)^3 \left(\frac{\pi}{4}\right)^3 + \dots \\ &= 1 + (\eta^\dagger - \eta) \frac{\pi}{4} - \frac{1}{2!} \left(\frac{\pi}{4}\right)^2 - \frac{1}{3!} (\eta^\dagger - \eta) \left(\frac{\pi}{4}\right)^3 + \frac{1}{4!} \left(\frac{\pi}{4}\right)^4 + \dots \\ &= \cos \frac{\pi}{4} + (\eta^\dagger - \eta) \sin \frac{\pi}{4} \\ &= \frac{1}{\sqrt{2}} (1 + \eta^\dagger - \eta) \end{aligned} \quad (3.2.7)$$

There we used

$$(\eta^\dagger - \eta)^2 = \eta^{\dagger 2} + \eta^2 - \{\eta^\dagger, \eta\} = -1 \quad \left[\because \eta^2 = \eta^{\dagger 2} = 0 \right] \quad (3.2.8)$$

and hence

$$(\eta^\dagger - \eta)^3 = -1 (\eta^\dagger - \eta) \quad (3.2.9)$$

	renormalization	decoupling condition
SWT	$\frac{1}{2} [S, \mathcal{H}_X]$	$[S, \mathcal{H}_0] = -\mathcal{H}_X$
URG	$\frac{2}{\pi} [S, \mathcal{H}_X]$	$[S, \mathcal{H}_0] = -\frac{\pi}{4} \mathcal{H}_X + \frac{4}{\pi} S \mathcal{H}_X S$

Table 3.1: Comparison of perturbative and non-perturbative canonical transformations

and so on. This simplification allows us to write

$$\cosh S = \frac{1}{2} [e^S + e^{-S}] = \frac{1}{2\sqrt{2}} (1 + \eta^\dagger - \eta + 1 - \eta^\dagger + \eta) = \frac{1}{\sqrt{2}} \quad (3.2.10)$$

and

$$\sinh S = \frac{1}{2} [e^S - e^{-S}] = \frac{1}{2\sqrt{2}} (1 + \eta^\dagger - \eta - 1 + \eta^\dagger - \eta) = \frac{1}{\sqrt{2}} (\eta^\dagger - \eta) \quad (3.2.11)$$

The off-diagonal part now becomes

$$H_2 = \frac{1}{2} \left(\mathcal{H}_X - \eta^\dagger \mathcal{H}_X \eta^\dagger - \eta \mathcal{H}_X \eta + [\eta^\dagger - \eta, \mathcal{H}_0] \right) \quad (3.2.12)$$

The vanishing of this quantity is now the decoupling condition, and is also given in eq 16 of ref. [62].

To look for a decoupling condition similar to eq. 3.2.5, we can re-express the cosh and sinh in eq. 3.2.10 in terms of S , by substituting $\eta^\dagger - \eta = \frac{4}{\pi} S$:

$$\cosh S = \frac{1}{\sqrt{2}}, \text{ and } \sinh S = \frac{4}{\sqrt{2}\pi} S \quad (3.2.13)$$

That gives

$$H_2 = \frac{1}{2} \left(\frac{4}{\pi} [S, \mathcal{H}_0] + \mathcal{H}_X - \frac{16}{\pi^2} S \mathcal{H}_X S \right) \quad (3.2.14)$$

The decoupling condition becomes

$$[S, \mathcal{H}_0] = -\frac{\pi}{4} \mathcal{H}_X + \frac{4}{\pi} S \mathcal{H}_X S \quad (3.2.15)$$

This can be compared to the second order condition: $[S, \mathcal{H}_0] = -\mathcal{H}_X$. We can also write the effective Hamiltonian for this non-perturbative case.

$$U \mathcal{H} U^\dagger = H_1 = \frac{1}{2} \mathcal{H}_0 - \frac{4}{\pi^2} S \mathcal{H}_0 S + \frac{2}{\pi} [S, \mathcal{H}_X] \quad (3.2.16)$$

The differences between the perturbative and non-perturbative ways are summarized in table 3.1. There appear to be two differences between these decoupling conditions: (a) a pre-factor of $\frac{\pi}{4}$ for the first term on the right hand side, and (b) the altogether new second term on the right hand side. Both are outcomes of the non-perturbative nature of URG. This offers evidence that the physics captured by the effective Hamiltonian (and its associated low-energy many-particle Hilbert space) obtained from URG lies well beyond that obtained from SWT. Further, it shows that the SWT can only be justified as an expansion in a small parameter (say, $\frac{1}{U}$) in the Anderson impurity problem), followed by a truncation of the BCH expansion and a projection onto a particular low-energy subspace. The truncation and projection are adopted simultaneously, and appear to impose the limit of $U = \infty$ by hand. The URG flow never attains such a limit, thus suggesting that there exists a lot of interesting physics that could potentially be lost in the SWT procedure. Further, the projection finally applied within SWT means that we can never recover what is thrown away. This is again not the case with URG.

3.2.2 Obtaining renormalization via Schrieffer-Wolff transformation - comparison with "poor man's scaling" and URG

Similar to the situation in Poor Man's scaling, one can visualize two set of states and let $\mathcal{H}_X = V_+ + V_-$ be the scattering that connects them and hence the one we want to kill. Let S be of the form

$$S = \sum_{ij} \left[s |\phi_1^i\rangle \langle \phi_0^j| - s^\dagger |\phi_0^j\rangle \langle \phi_1^i| \right] \quad (3.2.17)$$

This form is of course chosen to make S anti-Hermitian and off-diagonal. The part s can be determined from the decoupling condition:

$$-\mathcal{H}_X = [S, H_0] = SH_0 - H_0S \quad (3.2.18)$$

Multiplying with $\langle \phi_0^a|$ and $|\phi_1^b\rangle$ from the left and right respectively gives

$$-\langle \phi_0^a| V + V^\dagger |\phi_1^b\rangle = \langle \phi_0^a| SH_0 - H_0S |\phi_1^b\rangle \quad (3.2.19)$$

Since V^\dagger acts on $|0\rangle$, it will not affect the LHS. Also, $\langle \phi_0^a| V |\phi_1^b\rangle = V_{ab}$. If we now consider only the diagonal part of H_0 , we can write $H_0(|\phi_0^a\rangle, |\phi_1^b\rangle) = (E_{0,a} |\phi_0^a\rangle, E_{1,b} |\phi_1^b\rangle)$. We then get

$$\begin{aligned} -V_{ab} &= \langle \phi_0^a| \sum_i \left[S |\phi_1^i\rangle \langle \phi_1^i| H_0 - H_0 |\phi_0^i\rangle \langle \phi_0^i| S \right] |\phi_1^b\rangle = \sum_i \left[S_{ai} E_1^i \delta_{bi} - E_0^i \delta_{ai} S_{ib} \right] = S_{ab} E_1^b - E_0^a S_{ab} \\ \Rightarrow S_{ab} &= \frac{V_{ab}}{E_0^a - E_1^b} \end{aligned} \quad (3.2.20)$$

where we defined $\langle \phi_0^x| S |\phi_1^y\rangle = S_{xy}$. The total generator is

$$S = \sum_{ij} \left[S_{ij} |\phi_0^i\rangle \langle \phi_1^j| - S_{ij}^\dagger |\phi_1^j\rangle \langle \phi_0^i| \right] = \sum_{ij} \frac{1}{E_0^i - E_1^j} \left[V_{ij} |\phi_0^i\rangle \langle \phi_1^j| - V_{ij}^\dagger |\phi_1^j\rangle \langle \phi_0^i| \right] \quad (3.2.21)$$

The renormalization is thus

$$\begin{aligned} \Delta \mathcal{H} &= \frac{1}{2} [S, \mathcal{H}_X] \\ &= \frac{1}{2} \sum_{ij,kl} \left[\frac{1}{E_0^i - E_1^j} \left(V_{ij} |\phi_0^i\rangle \langle \phi_1^j| - V_{ij}^\dagger |\phi_1^j\rangle \langle \phi_0^i| \right), V_{kl} |\phi_0^k\rangle \langle \phi_1^l| + V_{kl}^\dagger |\phi_1^l\rangle \langle \phi_0^k| \right] \\ &= \frac{1}{2} \sum_{ij,kl} \left[\frac{1}{E_0^i - E_1^j} \left(V_{ij} V_{kl}^\dagger |\phi_0^i\rangle \langle \phi_0^k| \delta_{jl} - V_{ij}^\dagger V_{kl} |\phi_1^j\rangle \langle \phi_1^l| \delta_{ik} \right. \right. \\ &\quad \left. \left. - V_{kl}^\dagger V_{ij} |\phi_1^l\rangle \langle \phi_1^j| \delta_{ki} + V_{kl} V_{ij}^\dagger |\phi_0^k\rangle \langle \phi_0^i| \delta_{lj} \right) \right] \\ &= \frac{1}{2} \sum_{ijk} \left[\frac{1}{E_0^i - E_1^j} \left(V_{ij} V_{kj}^\dagger |\phi_0^i\rangle \langle \phi_0^k| - V_{ij}^\dagger V_{ik} |\phi_1^j\rangle \langle \phi_1^k| - V_{ik}^\dagger V_{ij} |\phi_1^k\rangle \langle \phi_1^j| + V_{kj} V_{ij}^\dagger |\phi_0^k\rangle \langle \phi_0^i| \right) \right] \\ &= \frac{1}{2} \sum_{ijk} \left[\left(\frac{1}{E_0^i - E_1^j} + \frac{1}{E_0^k - E_1^j} \right) V_{ij} V_{kj}^\dagger |\phi_0^i\rangle \langle \phi_0^k| - \left(\frac{1}{E_0^i - E_1^j} + \frac{1}{E_0^i - E_1^k} \right) V_{ij}^\dagger V_{ik} |\phi_1^j\rangle \langle \phi_1^k| \right] \end{aligned} \quad (3.2.22)$$

This is the same as the PMS result eq. 3.1.17. It is easy to see that since this transformation is unitary, it has zero trace so as to preserve the trace of the Hamiltonian:

$$\text{Tr} [\mathcal{H}] = \sum_l \left(\langle \phi_0^l| + \langle \phi_1^l| \right) \Delta \mathcal{H} \left(|\phi_0^l\rangle + |\phi_1^l\rangle \right) = \frac{1}{2} \sum_{jl} \frac{2}{E_0^l - E_1^j} V_{lj} V_{lj}^\dagger - \frac{1}{2} \sum_{ji} \frac{2}{E_0^i - E_1^j} V_{ij}^\dagger V_{il} = 0 \quad (3.2.23)$$

We can also make a comparison to the renormalization obtained from URG.

$$\Delta\mathcal{H} = \frac{1}{2} [\eta^\dagger - \eta, \mathcal{H}] \quad (3.2.24)$$

where

$$\begin{aligned} \eta &= \frac{1}{\omega - \mathcal{H}^d} \sum_{ij} V_{ij} |\phi_0^i\rangle \langle \phi_1^j| = \sum_{ij} \frac{1}{\omega_1^j - E_0^i} V_{ij} |\phi_0^i\rangle \langle \phi_1^j| \\ \Rightarrow \eta^\dagger &= \sum_{ij} \frac{1}{\omega_1^j - E_0^i} V_{ij}^\dagger |\phi_1^j\rangle \langle \phi_0^i| \\ \Rightarrow \eta^\dagger - \eta &= \sum_{ij} \frac{1}{\omega_1^j - E_0^i} \left(V_{ij}^\dagger |\phi_1^j\rangle \langle \phi_0^i| - V_{ij} |\phi_0^i\rangle \langle \phi_1^j| \right) \end{aligned} \quad (3.2.25)$$

This can be thought of as the generator for the unitary transformations of URG. Comparing with the generator S of eq. 3.2.21, the prescription to go from URG to SWT is to replace $\omega_1^j \rightarrow E_1^j$. Doing a similar calculation gives

$$\Delta\mathcal{H}_{URG} = \frac{1}{2} \sum_{ijk} \left[\left(\frac{1}{E_0^i - \omega_1^j} + \frac{1}{E_0^k - \omega_1^j} \right) V_{ij} V_{kj}^\dagger |\phi_0^i\rangle \langle \phi_0^k| - \left(\frac{1}{E_0^i - \omega_1^j} + \frac{1}{E_0^i - \omega_1^k} \right) V_{ij}^\dagger V_{ik} |\phi_1^j\rangle \langle \phi_1^k| \right] \quad (3.2.26)$$

3.3 A comparison of URG, SWT and PMS on the Anderson model

The SWT for the single-impurity Anderson model is briefly sketched below. In order to decouple a state $q\beta$ from the SIAM ($\epsilon_q > 0$), we take an ansatz $S = (A + B\hat{n}_{d\bar{\beta}})(c_{q\beta}^\dagger c_{d\beta} - \text{h.c.})$. Plugging this into the decoupling condition gives

$$-\epsilon_q (A + B\hat{n}_{d\bar{\beta}}) + \epsilon_d (A + B\hat{n}_{d\bar{\beta}}) + U (A + B) \hat{n}_{d\bar{\beta}} = -V \quad (3.3.1)$$

which gives

$$S = V \left[\frac{1 - \hat{n}_{d\bar{\beta}}}{\epsilon_q - \epsilon_d} + \frac{\hat{n}_{d\bar{\beta}}}{\epsilon_q - \epsilon_d - U} \right] (c_{q\beta}^\dagger c_{d\beta} - \text{h.c.}) \quad (3.3.2)$$

The remaining diagonal part constitutes the effective Hamiltonian.

$$\begin{aligned} U\mathcal{H}U^\dagger &= H_1 = \mathcal{H}_0 + \frac{1}{2} \{ \mathcal{H}_0, S^2 \} - S\mathcal{H}_0S + [S, \mathcal{H}_X] \\ &= \mathcal{H}_0 + \frac{1}{2} [[\mathcal{H}_0, S], S] + [S, \mathcal{H}_X] \\ &= \mathcal{H}_0 + \frac{1}{2} [\mathcal{H}_X, S] + [S, \mathcal{H}_X] \\ &= \mathcal{H}_0 + \frac{1}{2} [S, \mathcal{H}_X] \end{aligned} \quad (3.3.3)$$

For the SIAM (and noting that we are decoupling $q\beta$), the two parts are

$$\begin{aligned} \mathcal{H}_0 &= \sum_{k\sigma} \epsilon_k \hat{n}_{k\sigma} + \epsilon_d \hat{n}_d + U \hat{n}_{d\uparrow} \hat{n}_{d\downarrow} + \sum_{k\sigma \neq q\beta} \left(c_{k\sigma}^\dagger c_{d\sigma} + \text{h.c.} \right) \\ \mathcal{H}_X &= c_{q\beta}^\dagger c_{d\beta} + \text{h.c.} \end{aligned} \quad (3.3.4)$$

The renormalization in the effective Hamiltonian from decoupling a high energy particle state is thus

$$\begin{aligned} \frac{1}{2} [S, \mathcal{H}_X] \Big|_{\hat{n}_{q\beta}=0} &= |V|^2 \left[\frac{1 - \hat{n}_{d\bar{\beta}}}{\epsilon_q - \epsilon_d} + \frac{\hat{n}_{d\bar{\beta}}}{\epsilon_q - \epsilon_d - U} \right] \left[\hat{n}_{q\beta} (1 - \hat{n}_{d\beta}) - \hat{n}_{d\beta} (1 - \hat{n}_{q\beta}) \right] \Big|_{\hat{n}_{q\beta}=0} \\ &= -\hat{n}_{d\beta} |V|^2 \left[\frac{1 - \hat{n}_{d\bar{\beta}}}{\epsilon_q - \epsilon_d} + \frac{\hat{n}_{d\bar{\beta}}}{\epsilon_q - \epsilon_d - U} \right] \end{aligned} \quad (3.3.5)$$

In the last step, we put $\hat{n}_{q\beta} = 0$ because previously we assumed $\epsilon_q > 0$ and high energy virtual excitations above the Fermi surface must necessarily be vacant in the initial state (at $T = 0$). We can obtain the renormalization from decoupling a high energy *hole* state directly from this expression, just by choosing $\hat{n}_{q\beta} = 1$ and setting $\epsilon_q \rightarrow -\epsilon_q$.

$$\left. \frac{1}{2} [S, \mathcal{H}_X] \right|_{\hat{n}_{q\beta}=1} = - \left(1 - \hat{n}_{d\beta} \right) |V|^2 \left[\frac{1 - \hat{n}_{d\bar{\beta}}}{\epsilon_q + \epsilon_d} + \frac{\hat{n}_{d\bar{\beta}}}{\epsilon_q + \epsilon_d + U} \right] \quad (3.3.6)$$

These two results - the renormalization in the particle and hole sectors - is identical to the result obtained from PMS of the SIAM [67, 72]. The renormalizations in the various energy levels of the impurity can be read off now, after summing over all states in the interval we are decoupling.

$$\begin{aligned} \Delta E_2 &= -2 \sum_q \frac{|V_q|^2}{\epsilon_q - \epsilon_d - U} \\ \Delta E_1 &= - \sum_q \frac{|V_q|^2}{\epsilon_q - \epsilon_d} - \sum_q \frac{|V_q|^2}{\epsilon_q + \epsilon_d + U} \\ \Delta E_0 &= -2 \sum_q \frac{|V_q|^2}{\epsilon_q + \epsilon_d} \end{aligned} \quad (3.3.7)$$

This can be compared with the URG result, eq. 4.3.1,

$$\begin{aligned} \Delta E_2 &= 2 \sum_q \frac{|V_q|^2}{\omega - \frac{1}{2}\epsilon_q + \epsilon_d + U} \\ \Delta E_1 &= \sum_q \frac{|V_q|^2}{\omega - \frac{1}{2}\epsilon_q - \epsilon_d - U} + \sum_q \frac{|V_q|^2}{\omega - \frac{1}{2}\epsilon_q + \epsilon_d} \\ \Delta E_0 &= 2 \sum_q \frac{|V_q|^2}{\omega - \frac{1}{2}\epsilon_q - \epsilon_d} \end{aligned} \quad (3.3.8)$$

We can transform the URG result to the SWT result if we ignore the effect of the quantum fluctuations in ω (arising from the presence of the off-diagonal term \mathcal{H}^i) and replace it with the renormalised diagonal value of $-\frac{1}{2}\epsilon_q$. This means that SWT tracks the effect of the off-diagonal terms only in the numerator. Of course, all this assumes we are doing an iterative SWT instead of a one-shot SWT; the latter is the conventional way. A second difference is that URG has a Green's function like structure in the renormalization such that a fixed point is reached when the diagonal part \mathcal{H}^d matches one of the eigenvalues of ω (see 2.1.6). SWT does not have such a fixed point structure.

Another point to note is that decoupling a single electron does not generate all the charge-charge or spin-spin interactions that come out when one performs a one-shot SWT. This implies that such terms are a result of decoupling the non-local interactions of the impurity (it is talking to all the mobile electrons), and cannot be generated when we remove just the local interactions of the mobile electrons. Instead, if one performs a URG in which we non-perturbatively kill the 2-point vertices in the SIAM, such 4-point vertices are generated. This is shown in the next subsection.

3.4 Deriving the Kondo model from the Anderson model via a one-shot URG

Here we will show how we can obtain the spin-spin interaction of the Kondo model by performing a one-shot URG on the SIAM. This should justify that the action of performing an SWT is analogous to decoupling the whole band via URG. There are three departures from the conventional way of doing URG (or PMS).

- We will be severing the connections of the impurity with all the mobile electrons in one-shot, and not iteratively.
- We will have to trivialize the quantum fluctuation operator $\hat{\omega}$ by replacing it with the diagonal part of the initial state energy.

Since we are decoupling the whole band, the off-diagonal part that we want to remove is

$$\mathcal{H}^I = \sum_{k\sigma} \left[V_k c_{k\sigma}^\dagger c_{d\sigma} + \text{h.c.} \right] \quad (3.4.1)$$

The diagonal part is the rest of the Hamiltonian.

$$\mathcal{H}^d = \sum_{k\sigma} \epsilon_k \hat{n}_{k\sigma} + \epsilon_d \hat{n}_d + U \hat{n}_{d\uparrow} \hat{n}_{d\downarrow} = \sum_{k\sigma} \epsilon_k \tau_{k\sigma} + \epsilon_d \hat{n}_d + U \hat{n}_{d\uparrow} \hat{n}_{d\downarrow} \quad (3.4.2)$$

Following eq. 2.1.47, the renormalization is

$$\Delta\mathcal{H} = \frac{1}{2} \left[\eta^\dagger - \eta, \mathcal{H}_X \right] \quad (3.4.3)$$

The transition operator η is

$$\begin{aligned} \eta &= \frac{1}{\omega - \mathcal{H}^d} \sum_{k\sigma} V_k^* c_{d\sigma}^\dagger c_{k\sigma} = \sum_{k\sigma} \frac{1}{\omega + \frac{1}{2}\epsilon_k - \epsilon_d - (\epsilon_d + U) \hat{n}_{d\bar{\sigma}}} V_k^* c_{d\sigma}^\dagger c_{k\sigma} \\ &= \sum_{k\sigma} \left[\frac{\hat{n}_{d\bar{\sigma}}}{\omega_1 + \frac{1}{2}\epsilon_k - 2\epsilon_d - U} + \frac{1 - \hat{n}_{d\bar{\sigma}}}{\omega_0 + \frac{1}{2}\epsilon_k - \epsilon_d} \right] V_k^* c_{d\sigma}^\dagger c_{k\sigma} = \sum_{k\sigma} \left[\frac{\hat{n}_{d\bar{\sigma}}}{E_k^1} + \frac{1 - \hat{n}_{d\bar{\sigma}}}{E_k^0} \right] V_k^* c_{d\sigma}^\dagger c_{k\sigma} \end{aligned} \quad (3.4.4)$$

where $E_k^1 = \omega_1 + \frac{1}{2}\epsilon_k - 2\epsilon_d - U$ and $E_k^0 = \omega_0 + \frac{1}{2}\epsilon_k - \epsilon_d$. The total generator is therefore

$$\eta^\dagger - \eta = \sum_{k\sigma} \left[\frac{\hat{n}_{d\bar{\sigma}}}{E_k^1} + \frac{1 - \hat{n}_{d\bar{\sigma}}}{E_k^0} \right] \left(V_k c_{k\sigma}^\dagger c_{d\sigma} - V_k^* c_{d\sigma}^\dagger c_{k\sigma} \right) \quad (3.4.5)$$

The renormalization is

$$\Delta\mathcal{H}(\omega_1, \omega_0) = \frac{1}{2} \sum_{kq\sigma\alpha} \left[\left(\frac{\hat{n}_{d\bar{\sigma}}}{E_k^1} + \frac{1 - \hat{n}_{d\bar{\sigma}}}{E_k^0} \right) \left(V_k c_{k\sigma}^\dagger c_{d\sigma} - V_k^* c_{d\sigma}^\dagger c_{k\sigma} \right), V_q c_{q\alpha}^\dagger c_{d\alpha} + V_q^* c_{d\alpha}^\dagger c_{q\alpha} \right] \quad (3.4.6)$$

The summation has two parts, $\Delta_{1,2}$ - one where $\sigma = \alpha$ and another where $\sigma = \bar{\alpha}$. The first part Δ_1 gives

$$\begin{aligned} \Delta_1 &= \frac{1}{2} \sum_{kq\sigma=\alpha} \left[\left(\frac{\hat{n}_{d\bar{\sigma}}}{E_k^1} + \frac{1 - \hat{n}_{d\bar{\sigma}}}{E_k^0} \right) \left(V_k c_{k\sigma}^\dagger c_{d\sigma} - V_k^* c_{d\sigma}^\dagger c_{k\sigma} \right), V_q c_{q\sigma}^\dagger c_{d\sigma} + V_q^* c_{d\sigma}^\dagger c_{q\sigma} \right] \\ &= \frac{1}{2} \sum_{kq\sigma} \left(\frac{\hat{n}_{d\bar{\sigma}}}{E_k^1} + \frac{1 - \hat{n}_{d\bar{\sigma}}}{E_k^0} \right) \left[V_k c_{k\sigma}^\dagger c_{d\sigma} - V_k^* c_{d\sigma}^\dagger c_{k\sigma}, V_q c_{q\sigma}^\dagger c_{d\sigma} + V_q^* c_{d\sigma}^\dagger c_{q\sigma} \right] \\ &= \frac{1}{2} \sum_{kq\sigma} \left(\frac{\hat{n}_{d\bar{\sigma}}}{E_k^1} + \frac{1 - \hat{n}_{d\bar{\sigma}}}{E_k^0} \right) \left\{ V_k V_q^* \left[c_{k\sigma}^\dagger c_{d\sigma}, V_q^* c_{d\sigma}^\dagger c_{q\sigma} \right] - V_k^* V_q \left[c_{d\sigma}^\dagger c_{k\sigma}, c_{q\sigma}^\dagger c_{d\sigma} \right] \right\} \\ &= \frac{1}{2} \sum_{kq\sigma} \left(\frac{\hat{n}_{d\bar{\sigma}}}{E_k^1} + \frac{1 - \hat{n}_{d\bar{\sigma}}}{E_k^0} \right) \left\{ V_k V_q^* \left[c_{k\sigma}^\dagger c_{d\sigma}, V_q^* c_{d\sigma}^\dagger c_{q\sigma} \right] + V_k^* V_q \left[c_{q\sigma}^\dagger c_{d\sigma}, c_{d\sigma}^\dagger c_{k\sigma} \right] \right\} \\ &= \frac{1}{2} \sum_{kq\sigma} \left[\hat{n}_{d\bar{\sigma}} \left(\frac{1}{E_k^1} + \frac{1}{E_q^1} \right) + (1 - \hat{n}_{d\bar{\sigma}}) \left(\frac{1}{E_k^0} + \frac{1}{E_q^0} \right) \right] V_k V_q^* \left[c_{k\sigma}^\dagger c_{d\sigma}, c_{d\sigma}^\dagger c_{q\sigma} \right] \\ &= \sum_{kq\sigma} \left[\frac{1}{2} V_k V_q^* \left(\frac{1}{E_k^0} + \frac{1}{E_q^0} \right) + \hat{n}_{d\bar{\sigma}} \frac{1}{2} V_k V_q^* \left(\frac{1}{E_k^1} + \frac{1}{E_q^1} - \frac{1}{E_k^0} - \frac{1}{E_q^0} \right) \right] \left(c_{k\sigma}^\dagger c_{q\sigma} - c_{d\sigma}^\dagger c_{d\sigma} \delta_{kq} \right) \end{aligned} \quad (3.4.7)$$

We can now define two new energy scales:

$$W_{kq} = \frac{1}{2} V_k V_q^* \left(\frac{1}{E_k^0} + \frac{1}{E_q^0} \right), \quad J_{kq} = \frac{1}{2} V_k V_q^* \left(\frac{1}{E_k^1} + \frac{1}{E_q^1} - \frac{1}{E_k^0} - \frac{1}{E_q^0} \right) \quad (3.4.8)$$

The renormalization Δ_1 becomes

$$\begin{aligned} \Delta_1 &= \sum_{kq\sigma} \left[W_{kq} + \hat{n}_{d\bar{\sigma}} J_{kq} \right] \left(c_{k\sigma}^\dagger c_{q\sigma} - c_{d\sigma}^\dagger c_{d\sigma} \delta_{kq} \right) \\ &= \sum_{kq\sigma} \left[W_{kq} + \hat{n}_{d\bar{\sigma}} J_{kq} \right] c_{k\sigma}^\dagger c_{q\sigma} - \sum_{k\sigma} \left[W_{kk} + \hat{n}_{d\bar{\sigma}} J_{kk} \right] \hat{n}_{d\sigma} \\ &= \sum_{kq\sigma} \left[W_{kq} + \frac{1}{2} \hat{n}_d J_{kq} \right] c_{k\sigma}^\dagger c_{q\sigma} - \sum_{kq\sigma} \sigma J_{kq} S_d^z c_{k\sigma}^\dagger c_{q\sigma} - \sum_{k\sigma} \left[W_{kk} + \hat{n}_{d\bar{\sigma}} J_{kk} \right] \hat{n}_{d\sigma} \end{aligned} \quad (3.4.9)$$

There we exchanged $\hat{n}_{d\bar{\sigma}}$ for S_d^z and \hat{n}_d , in the first term, by using the definitions $\hat{n}_{d\sigma} + \hat{n}_{d\bar{\sigma}} = \hat{n}_{d\sigma}$ and $\hat{n}_{d\sigma} - \hat{n}_{d\bar{\sigma}} = 2\sigma S_d^z$.

The second term in the summation comes from the choice $\sigma = \bar{\alpha}$.

$$\begin{aligned} \Delta_2 &= \frac{1}{2} \sum_{kq\bar{\sigma}=\alpha} \left[\left(\frac{\hat{n}_{d\bar{\sigma}}}{E_k^1} + \frac{1 - \hat{n}_{d\bar{\sigma}}}{E_k^0} \right) \left(V_k c_{k\sigma}^\dagger c_{d\sigma} - V_k^* c_{d\sigma}^\dagger c_{k\sigma} \right), V_q c_{q\bar{\sigma}}^\dagger c_{d\bar{\sigma}} + V_q^* c_{d\bar{\sigma}}^\dagger c_{q\bar{\sigma}} \right] \\ &= \frac{1}{2} \sum_{kq\sigma} \left(V_k c_{k\sigma}^\dagger c_{d\sigma} - V_k^* c_{d\sigma}^\dagger c_{k\sigma} \right) \left[\frac{\hat{n}_{d\bar{\sigma}}}{E_k^1} + \frac{1 - \hat{n}_{d\bar{\sigma}}}{E_k^0}, V_q c_{q\bar{\sigma}}^\dagger c_{d\bar{\sigma}} + V_q^* c_{d\bar{\sigma}}^\dagger c_{q\bar{\sigma}} \right] \\ &= \frac{1}{2} \sum_{kq\sigma} \left(V_k c_{k\sigma}^\dagger c_{d\sigma} - V_k^* c_{d\sigma}^\dagger c_{k\sigma} \right) \left(V_q^* c_{d\bar{\sigma}}^\dagger c_{q\bar{\sigma}} - V_q c_{q\bar{\sigma}}^\dagger c_{d\bar{\sigma}} \right) \left(\frac{1}{E_k^1} - \frac{1}{E_k^0} \right) \\ &= \frac{1}{2} \sum_{kq\sigma} \left(V_k V_q^* c_{k\sigma}^\dagger c_{d\sigma} c_{d\bar{\sigma}}^\dagger c_{q\bar{\sigma}} - V_k V_q c_{k\sigma}^\dagger c_{d\sigma} c_{q\bar{\sigma}}^\dagger c_{d\bar{\sigma}} - V_k^* V_q^* c_{d\sigma}^\dagger c_{k\sigma} c_{d\bar{\sigma}}^\dagger c_{q\bar{\sigma}} + V_k^* V_q c_{d\sigma}^\dagger c_{k\sigma} c_{q\bar{\sigma}}^\dagger c_{d\bar{\sigma}} \right) \\ &\quad \times \left(\frac{1}{E_k^1} - \frac{1}{E_k^0} \right) \end{aligned} \quad (3.4.10)$$

We now use the following trick to combine the first and fourth terms:

$$\begin{aligned} &\frac{1}{2} \sum_{kq\sigma} \left(V_k V_q^* c_{k\sigma}^\dagger c_{d\sigma} c_{d\bar{\sigma}}^\dagger c_{q\bar{\sigma}} + V_k^* V_q c_{d\sigma}^\dagger c_{k\sigma} c_{q\bar{\sigma}}^\dagger c_{d\bar{\sigma}} \right) \times \left(\frac{1}{E_k^1} - \frac{1}{E_k^0} \right) \\ &= \frac{1}{2} \sum_{kq\sigma} V_k V_q^* c_{k\sigma}^\dagger c_{d\sigma} c_{d\bar{\sigma}}^\dagger c_{q\bar{\sigma}} \left(\frac{1}{E_k^1} - \frac{1}{E_k^0} \right) + \frac{1}{2} \sum_{kq\sigma} V_k^* V_q c_{d\sigma}^\dagger c_{k\sigma} c_{q\bar{\sigma}}^\dagger c_{d\bar{\sigma}} \left(\frac{1}{E_k^1} - \frac{1}{E_k^0} \right) \\ &= \frac{1}{2} \sum_{kq\sigma} V_k V_q^* c_{k\sigma}^\dagger c_{d\sigma} c_{d\bar{\sigma}}^\dagger c_{q\bar{\sigma}} \left(\frac{1}{E_k^1} - \frac{1}{E_k^0} \right) + \frac{1}{2} \sum_{qk\sigma} V_q^* V_k c_{d\bar{\sigma}}^\dagger c_{q\bar{\sigma}} c_{k\sigma}^\dagger c_{d\sigma} \left(\frac{1}{E_q^1} - \frac{1}{E_q^0} \right) \\ &= - \sum_{kq\sigma} J_{kq} c_{k\sigma}^\dagger c_{q\bar{\sigma}} c_{d\bar{\sigma}}^\dagger c_{d\sigma} \end{aligned} \quad (3.4.11)$$

In the penultimate step, we interchanged the dummy indices k and q and changed $\sigma \leftrightarrow \bar{\sigma}$ in the second term.

Similarly, for the second term, we get

$$\frac{1}{2} \sum_{kq\sigma} V_k V_q c_{k\sigma}^\dagger c_{d\sigma} c_{q\bar{\sigma}}^\dagger c_{d\bar{\sigma}} \left(\frac{1}{E_k^1} - \frac{1}{E_k^0} \right)$$

$$\begin{aligned}
&= \frac{1}{4} \sum_{kq\sigma} \left[V_k V_q \left(\frac{1}{E_k^1} - \frac{1}{E_k^0} \right) c_{k\sigma}^\dagger c_{d\sigma} c_{q\bar{\sigma}}^\dagger c_{d\bar{\sigma}} + \underbrace{V_k V_q \left(\frac{1}{E_k^1} - \frac{1}{E_k^0} \right) c_{k\bar{\sigma}}^\dagger c_{d\bar{\sigma}} c_{q\sigma}^\dagger c_{d\sigma}}_{\sigma \leftrightarrow \bar{\sigma}} \right] \\
&= \frac{1}{4} \sum_{kq\sigma} \left[V_k V_q \left(\frac{1}{E_k^1} - \frac{1}{E_k^0} \right) c_{k\sigma}^\dagger c_{d\sigma} c_{q\bar{\sigma}}^\dagger c_{d\bar{\sigma}} + \underbrace{V_q V_k \left(\frac{1}{E_q^1} - \frac{1}{E_q^0} \right) c_{q\bar{\sigma}}^\dagger c_{d\bar{\sigma}} c_{k\sigma}^\dagger c_{d\sigma}}_{k \leftrightarrow q} \right] \\
&= \sum_{kq\sigma} V_k V_q \frac{1}{4} \left(\frac{1}{E_k^1} - \frac{1}{E_k^0} + \frac{1}{E_q^1} - \frac{1}{E_q^0} \right) c_{k\sigma}^\dagger c_{d\sigma} c_{q\bar{\sigma}}^\dagger c_{d\bar{\sigma}} \\
&= \frac{1}{2} \sum_{kq\sigma} K_{kq} c_{k\sigma}^\dagger c_{d\sigma} c_{q\bar{\sigma}}^\dagger c_{d\bar{\sigma}}
\end{aligned}$$

where K_{kq} is yet another energy scale.

$$K_{kq} = \frac{1}{2} V_k V_q \left(\frac{1}{E_k^1} - \frac{1}{E_k^0} + \frac{1}{E_q^1} - \frac{1}{E_q^0} \right) \quad (3.4.12)$$

The third term gives

$$\frac{1}{2} \sum_{kq\sigma} V_k^* V_q^* c_{d\sigma}^\dagger c_{k\sigma} c_{d\bar{\sigma}}^\dagger c_{q\bar{\sigma}} \left(\frac{1}{E_k^1} - \frac{1}{E_k^0} \right) = \sum_{kq\sigma} K_{kq} c_{d\sigma}^\dagger c_{k\sigma} c_{d\bar{\sigma}}^\dagger c_{q\bar{\sigma}} \quad (3.4.13)$$

The total renormalization can thus be written as

$$\begin{aligned}
\Delta \mathcal{H}(\omega_1, \omega_0) &= - \sum_{k\sigma} [W_{kk} + \hat{n}_{d\bar{\sigma}} J_{kk}] \hat{n}_{d\sigma} && [\text{renormalization in } \epsilon_d, U] \\
&+ \sum_{kq\sigma} \left[W_{kq} + \frac{1}{2} \hat{n}_d J_{kq} \right] c_{k\sigma}^\dagger c_{q\sigma} && [\text{potential scattering}] \\
&- \sum_{kq\sigma} J_{kq} \left[S_d^z \sigma c_{k\sigma}^\dagger c_{q\sigma} + \sum_{kq\sigma} J_{kq} c_{k\sigma}^\dagger c_{q\bar{\sigma}} c_{d\bar{\sigma}}^\dagger c_{d\sigma} \right] && [\text{spin Kondo}] \\
&+ \sum_{kq\sigma} K_{kq} c_{k\sigma}^\dagger c_{d\sigma} c_{q\bar{\sigma}}^\dagger c_{d\bar{\sigma}} + \text{h.c.} && [\text{charge Kondo}]
\end{aligned} \quad (3.4.14)$$

Note that this renormalization is in a particular eigendirection of the total quantum fluctuation operator $\hat{\omega}$. In other words, the single perturbative J_{kq} has been replaced with 2^N scales, each with its own value of ω . This is where the complexity has been transferred in going from the second-order SWT to the non-perturbative URG. The

new energy scales are thus the non-perturbative variants of the ones generated in SWT.

$$\begin{aligned}
W_{kq}^{SWT} &= \frac{1}{2} V_k V_q^* \left(\frac{1}{\epsilon_k - \epsilon_d} + \frac{1}{\epsilon_q - \epsilon_d} \right) \\
J_{kq}^{SWT} &= \frac{1}{2} V_k V_q^* \left(\frac{1}{\epsilon_k - \epsilon_d - U} + \frac{1}{\epsilon_q - \epsilon_d - U} - \frac{1}{\epsilon_k - \epsilon_d} - \frac{1}{\epsilon_q - \epsilon_d} \right) \\
W_{kq}^{URG}(\omega) &= \frac{1}{2} V_k V_q^* \left(\frac{1}{\omega_0 + \frac{1}{2}\epsilon_k - \epsilon_d} + \frac{1}{\omega_0 + \frac{1}{2}\epsilon_q - \epsilon_d} \right) \\
J_{kq}^{URG}(\omega) &= \frac{1}{2} V_k V_q^* \left(\frac{1}{\omega_1 + \epsilon_k - \epsilon_d - U} + \frac{1}{\omega_1 + \epsilon_q - \epsilon_d - U} - \frac{1}{\omega_0 + \epsilon_k - \epsilon_d} - \frac{1}{\omega_0 + \epsilon_q - \epsilon_d} \right)
\end{aligned} \tag{3.4.15}$$

To recover the SWT scales from the URG ones, we have to substitute each ω_i by the energy of the initial state to which it corresponds. From eq. 3.4.4, we note that ω_1 refers to the initial state in which $\hat{n}_{k\sigma} = \hat{n}_{d\bar{\sigma}} = 1 - \hat{n}_{d\sigma} = 1$. Therefore, $\omega_1 = \frac{1}{2}\epsilon_k + \epsilon_d$. Similarly, ω_0 refers to the initial state in which $\hat{n}_{k\sigma} = 1 - \hat{n}_{d\bar{\sigma}} = 1 - \hat{n}_{d\sigma} = 1$. Therefore, $\omega_0 = \frac{1}{2}\epsilon_k$. Substituting these into the URG energy scales gives back the SWT scales.

3.5 Continuous unitary transformation RG

3.5.1 Formalism

The following equation generates a family of unitary Hamiltonians.

$$\frac{d\mathcal{H}(l)}{dl} = [\mathcal{H}, \eta(l)] \tag{3.5.1}$$

To prove the unitarity [73], we construct the unitary operator $U(l)$ that connects the Hamiltonians $\mathcal{H}(l)$ and $\mathcal{H}(l=0)$. Let $\mathcal{H}(l) = U(l)\mathcal{H}(l=0)U^\dagger(l)$, where $U(l)$ is defined by

$$\eta(l) = \frac{dU}{dl}U^\dagger = -U\frac{dU^\dagger}{dl} \left[UU^\dagger = 1 \implies \frac{d(UU^\dagger)}{dl} = 0 \right] \tag{3.5.2}$$

This will give

$$\begin{aligned}
\frac{d\mathcal{H}(l)}{dl} &= \frac{dU}{dl}\mathcal{H}(0)U^\dagger(l) + U\mathcal{H}(0)\frac{dU^\dagger}{dl} \\
&= \frac{dU}{dl}U^\dagger\mathcal{H}(l) + \mathcal{H}(l)U\frac{dU(l)^\dagger}{dl} \\
&= \eta(l)\mathcal{H}(l) - \mathcal{H}(l)\eta(l) \\
&= [\eta(l), \mathcal{H}(l)]
\end{aligned} \tag{3.5.3}$$

This proves that the family of Hamiltonians $\mathcal{H}(l)$ satisfy the flow equation eq. 3.5.1. $\eta(l)$ is referred to as the generator of the flow equation. It is chosen so as to reduce the off-diagonal part of the Hamiltonian, either progressively or in one shot. In Schrieffer-Wolff transformation, the transformation is one-shot, and the η there is the S that sits on top of the exponential in the unitary transformation. In URG, the generator to decouple one electron $q\beta$ is $\eta_{q\beta}^\dagger - \eta_{q\beta}$.

In Continuous unitary transformation (CUT) RG [74], we progressively block-diagonalize the Hamiltonian by removing off-diagonal terms that are farthest from the diagonal, through infinitesimal unitary transformations. The change is described as a flow against the parameter l . The canonical choice of the generator is $\eta(l) = [\mathcal{H}_d, \mathcal{H}_X]$, where \mathcal{H}_d is the diagonal part of the Hamiltonian and $\mathcal{H}_X = \mathcal{H} - \mathcal{H}_d$ is the off-diagonal part of the Hamiltonian. Therefore,

$$\frac{d\mathcal{H}}{dl} = [[\mathcal{H}_d(l), \mathcal{H}_X(l)], \mathcal{H}(l)] \tag{3.5.4}$$

To see how this choice of the generator results in a decay of the off-diagonal terms, we can consider a simple

2-particle Hamiltonian:

$$\mathcal{H} = \sum_i \epsilon_i \hat{n}_i + \sum_{i \neq j} g_{ij} c_i^\dagger c_j \quad (3.5.5)$$

where $g_{ij}^* = g_{ji}$. The canonical generator then turns out to be

$$\eta = \left[\sum_i \epsilon_i \hat{n}_i, \sum_{j \neq k} g_{jk} c_j^\dagger c_k \right] = \sum_{k \neq i} \epsilon_i \left[g_{ik} c_i^\dagger c_k - g_{ki} c_k^\dagger c_i \right] = \sum_{k \neq i} g_{ik} c_i^\dagger c_k (\epsilon_i - \epsilon_k) \quad (3.5.6)$$

and the renormalization in the Hamiltonian is

$$\frac{d\mathcal{H}}{dl} = [\eta, \mathcal{H}] = \left[\sum_{k \neq i} g_{ik} c_i^\dagger c_k (\epsilon_i - \epsilon_k), \sum_i \epsilon_i \hat{n}_i + \sum_{i \neq j} g_{ij} c_i^\dagger c_j \right] \quad (3.5.7)$$

The first commutator gives

$$- \sum_{i \neq k} g_{ik} (\epsilon_i - \epsilon_k)^2 c_i^\dagger c_k \quad (3.5.8)$$

The second commutator gives

$$\sum_{\substack{k \neq i \\ j}} \left[g_{kj} g_{ik} (\epsilon_i - \epsilon_k) c_i^\dagger c_j + g_{ji} g_{ik} (\epsilon_k - \epsilon_i) c_j^\dagger c_k \right] = \sum_{\substack{k \neq i \\ j}} g_{ik} g_{kj} (\epsilon_i + \epsilon_j - 2\epsilon_k) c_i^\dagger c_j \quad (3.5.9)$$

The total renormalization is

$$\frac{d\mathcal{H}}{dl} = - \sum_{i \neq j} g_{ij} (\epsilon_i - \epsilon_j)^2 c_i^\dagger c_j + \sum_{\substack{k \neq i \\ j}} g_{ik} g_{kj} (\epsilon_i + \epsilon_j - 2\epsilon_k) c_i^\dagger c_j \quad (3.5.10)$$

The couplings renormalize as

$$\begin{aligned} \frac{d\epsilon_i}{dl} &= \sum_{k \neq i} 2|g_{ik}|^2 (\epsilon_i - \epsilon_k) \\ \frac{dg_{ij}}{dl} &= -g_{ij} (\epsilon_i - \epsilon_j)^2 + \sum_{k \neq i} g_{ik} g_{kj} (\epsilon_i + \epsilon_j - 2\epsilon_k) \end{aligned} \quad (3.5.11)$$

To see the decay of the off-diagonal terms, first we will relate the off-diagonal flow to the diagonal flow using the invariance of the trace under a unitary transformation:

$$0 = \frac{d\text{Tr}(\mathcal{H})^2}{dl} = \frac{d\text{Tr}(\mathcal{H})^2}{dl} = \sum_i \frac{d\epsilon_i^2}{dl} + \sum_{i \neq j} \frac{d|g_{ij}|^2}{dl} \implies \sum_{i \neq j} \frac{d|g_{ij}|^2}{dl} = - \sum_i \frac{d\epsilon_i^2}{dl} \quad (3.5.12)$$

From the flow equation, we can see that

$$\sum_i \frac{d\epsilon_i^2}{dl} = 2 \sum_{i \neq k} \epsilon_i \frac{d\epsilon_i}{dl} = 2 \sum_i |g_{ik}|^2 (\epsilon_i - \epsilon_k)^2 \geq 0 \quad (3.5.13)$$

Therefore,

$$\sum_{i \neq j} \frac{d|g_{ij}|^2}{dl} \leq 0 \quad (3.5.14)$$

This implies that at $l \rightarrow \infty$, the only off-diagonal terms that survive are those with g_{ij} that scatter between degenerate states, that is, those with $\epsilon_i - \epsilon_j = 0$.

3.5.2 CUT-RG for the Fröhlick Hamiltonian

To get a feel for the method, we will apply it on the Fröhlick Hamiltonian to remove the electron-phonon coupling term.

$$\mathcal{H} = \mathcal{H}_d + \mathcal{H}_X \quad (3.5.15)$$

where \mathcal{H}_X is the electron-phonon coupling term

$$\sum_{kq} g_q b_{-q}^\dagger c_{k+q,\sigma}^\dagger c_{k\sigma} + \text{h.c.} \quad (3.5.16)$$

and-1 $\mathcal{H}_d = \sum_{k\sigma} \epsilon_k \hat{n}_{k\sigma} + \sum_q \hbar\omega_q b_q^\dagger b_q$ is the kinetic energy of the electron and phonons. We assume time-reversal invariance such that $\omega_q = \omega_{-q}$. We choose

$$\eta(l) = [\mathcal{H}_d, \mathcal{H}] = [\mathcal{H}_d, \mathcal{H}_X] \quad (3.5.17)$$

It is easy to compute the commutators.

$$\begin{aligned} \left[\sum_{k\sigma} \epsilon_k \hat{n}_{k\sigma}, \sum_{kq\sigma} b_{-q}^\dagger c_{k+q,\sigma}^\dagger c_{k\sigma} \right] &= \sum_{kq\sigma} g_q (\epsilon_{k+q} - \epsilon_k) g_q b_{-q}^\dagger c_{k+q,\sigma}^\dagger c_{k\sigma} \\ \left[\sum_q \hbar\omega_q b_q^\dagger b_q, \sum_{kq} g_q b_{-q}^\dagger c_{k+q,\sigma}^\dagger c_{k\sigma} \right] &= \sum_{kq} g_q \hbar\omega_q b_{-q}^\dagger c_{k+q,\sigma}^\dagger c_{k\sigma} \end{aligned} \quad (3.5.18)$$

Therefore,

$$\eta = \sum_{kq\sigma} g_q (\epsilon_{k+q} - \epsilon_k + \hbar\omega_q) b_{-q}^\dagger c_{k+q,\sigma}^\dagger c_{k\sigma} - \text{h.c.} \quad (3.5.19)$$

We define $\xi \equiv \epsilon_{k+q} - \epsilon_k + \hbar\omega_q$. The renormalization in the total Hamiltonian becomes

$$\frac{d\mathcal{H}}{dl} = [\eta, \mathcal{H}] \quad (3.5.20)$$

The flow equation for the electron-phonon coupling is

$$\frac{dg_q}{dl} = -\xi^2 g_q \implies g_q(l) = g_q(0) \exp \left\{ -\xi^2 l \right\} \quad (3.5.21)$$

A new electron-electron coupling $V_{kk'q} c_{k+q}^\dagger c_{k'-q}^\dagger c_{k'} c_k$ is also generated. For the Cooper channel ($k' = -k$), the flow equation is

$$V_{k,-k,q}(\infty) = V_{k,-k,-q}(0) - \frac{g_q^2 \omega_q}{\omega_q^2 + (\epsilon_{k+q} - \epsilon_k)^2} \quad (3.5.22)$$

Off-diagonal terms that connect larger energy differences ξ decay the fastest.

3.5.3 Deriving CUT RG from URG

We will now see that the renormalization in URG can also be put into a similar form. From eq. 2.1.47, we can write the URG renormalization in the diagonal part as

$$\Delta\mathcal{H}^0 = \frac{1}{2} [\eta^\dagger - \eta, \mathcal{H}] \quad (3.5.23)$$

where $\mathcal{H}^0 = \mathcal{H}^d + \mathcal{H}^i$. The URG generator can be recast (starting from the definitions of η , eqs. 2.1.14) as

$$\begin{aligned}\eta^\dagger - \eta &= G_1 c^\dagger T - G_0 T^\dagger c \\ &= \frac{1}{\omega_1 - \omega_0} \left[G_1 (\omega_1 - \omega_0) c^\dagger T - G_0 (\omega_1 - \omega_0) T^\dagger c \right] \\ &= \frac{1}{\omega_1 - \omega_0} \left[G_1 \omega_1 c^\dagger T - c^\dagger T \omega_0 G_0 - T^\dagger c \omega_1 G_1 + G_0 \omega_0 T^\dagger c \right]\end{aligned}\tag{3.5.24}$$

In the last step, we changed the second and fourth terms using the constraints $G_1 c^\dagger T = c^\dagger T G_0$ and $G_0 T^\dagger c = T^\dagger c G_1$, eq. 2.1.16. We now add and subtract $G_1 G_1^{-1} c^\dagger T = c^\dagger T$ and $G_0 G_0^{-1} T^\dagger c = T^\dagger c$ for each term.

$$\begin{aligned}\eta^\dagger - \eta &= \frac{1}{\omega_1 - \omega_0} \left[G_1 (\omega_1 - G_1^{-1}) c^\dagger T + c^\dagger T - c^\dagger T (\omega_0 - G_0^{-1}) G_0 - c^\dagger T \right. \\ &\quad \left. - T^\dagger c (\omega_1 - G_1^{-1}) G_1 - T^\dagger c + G_0 (\omega_0 - G_0^{-1}) T^\dagger c + T^\dagger c \right] \\ &= \frac{1}{\omega_1 - \omega_0} \left[G_1 (\omega_1 - G_1^{-1}) c^\dagger T - c^\dagger T (\omega_0 - G_0^{-1}) G_0 \right. \\ &\quad \left. - T^\dagger c (\omega_1 - G_1^{-1}) G_1 + G_0 (\omega_0 - G_0^{-1}) T^\dagger c \right]\end{aligned}\tag{3.5.25}$$

In the last step, the extra $c^\dagger T$ and $T^\dagger c$ terms canceled out. In the second and third terms, we can bring the Greens function closer to the operators $c^\dagger T$ and $T^\dagger c$ because $(\omega_j - G_j^{-1}) G_j = G_j (\omega_j - G_j^{-1})$:

$$\begin{aligned}\eta^\dagger - \eta &= \frac{1}{\omega_1 - \omega_0} \left[G_1 (\omega_1 - G_1^{-1}) c^\dagger T - c^\dagger T G_0 (\omega_0 - G_0^{-1}) \right. \\ &\quad \left. - T^\dagger c G_1 (\omega_1 - G_1^{-1}) + G_0 (\omega_0 - G_0^{-1}) T^\dagger c \right] \\ &= \frac{1}{\omega_1 - \omega_0} \left[G_1 (\omega_1 - G_1^{-1}) c^\dagger T - G_1 c^\dagger T (\omega_0 - G_0^{-1}) \right. \\ &\quad \left. - G_0 T^\dagger c (\omega_1 - G_1^{-1}) + G_0 (\omega_0 - G_0^{-1}) T^\dagger c \right]\end{aligned}\tag{3.5.26}$$

In the last step, we again used the constraint $G_1 c^\dagger T = c^\dagger T G_0$ and its partner. From the definition of the Green's function $G = (\omega - \mathcal{H}^d)^{-1}$, we can write $\omega_j - G_j^{-1} = \mathcal{H}_j^d$. Therefore,

$$\begin{aligned}\eta^\dagger - \eta &= \frac{1}{\omega_1 - \omega_0} \left[G_1 \mathcal{H}_1^d c^\dagger T - G_1 c^\dagger T \mathcal{H}_0^d - G_0 T^\dagger c \mathcal{H}_1^d + G_0 \mathcal{H}_0^d T^\dagger c \right] \\ &= \frac{1}{\omega_1 - \omega_0} \left[G \mathcal{H}^d c^\dagger T - G c^\dagger T \mathcal{H}^d - G T^\dagger c \mathcal{H}^d + G \mathcal{H}^d T^\dagger c \right] \\ &= \frac{1}{\omega_1 - \omega_0} G \left[\mathcal{H}^d, c^\dagger T + T^\dagger c \right]\end{aligned}\tag{3.5.27}$$

where $\mathcal{H}^d = \mathcal{H}_1^d \hat{n} + \mathcal{H}_0^d (1 - \hat{n})$ and $G = G_1 \hat{n} + G_0 (1 - \hat{n}) = (\hat{\omega} - \mathcal{H}^d)^{-1}$. For URG, the relevant off-diagonal part of the Hamiltonian for the current node is $\mathcal{H}^I = c^\dagger T + T^\dagger c$. Therefore,

$$\eta^\dagger - \eta = \frac{1}{\omega_1 - \omega_0} G \left[\mathcal{H}^d, \mathcal{H}^I \right] = \left[\mathcal{H}^d, \frac{1}{\omega_1 - \omega_0} G \mathcal{H}^I \right]\tag{3.5.28}$$

The last equality comes about because both G and \mathcal{H}^d are completely diagonal and hence commute. The renormalization in the Hamiltonian under URG, which is a function of both the quantum fluctuation scale ω and the

running bandwidth D , can thus be written as

$$\Delta\mathcal{H}(\omega, D) = \left[\left[\mathcal{H}^d, \tilde{\mathcal{H}}^I \right], \mathcal{H} \right] - \mathcal{H}_X \quad (3.5.29)$$

The most obvious difference with the CUT version is the presence of the off-diagonal piece $-\mathcal{H}_X$. This is a result of the philosophical difference between URG and CUT-RG - while CUT-RG gradually suppresses the off-diagonal matrix elements, URG makes the off-diagonal components in each 2×2 block vanish completely. We can instead look at the renormalization in the diagonal part of the Hamiltonian under URG:

$$\Delta\mathcal{H}^0(\omega, D) = \left[\left[\mathcal{H}^d, \tilde{\mathcal{H}}^I \right], \mathcal{H} \right] \quad (3.5.30)$$

where $\tilde{\mathcal{H}}^I = \frac{1}{\omega_1 - \omega_0} G \mathcal{H}^I$. This can be compared to the analogous equation for CUT (eq. 3.5.4),

$$\Delta\mathcal{H}(\lambda) = \Delta\lambda \left[\left[\mathcal{H}_d, \mathcal{H}_X \right], \mathcal{H} \right] \quad (3.5.31)$$

Leaving aside the obvious differences in the philosophies (the presence of ω in URG or the fact that while URG decouples as a flow in the bandwidth, CUT uses a general parameter λ or the algorithmic difference that while URG decouples one specific node, CUT tries to make the Hamiltonian band-diagonal), the major physical difference is the presence of the total Green's function in the URG equation. It must be noted that while CUT employs the entire off-diagonal part in \mathcal{H}_X , the \mathcal{H}^I of URG contains only those parts that are off-diagonal with respect to the node being decoupled at this step.

To bring the URG form closer to CUT, we can make some approximations.

$$G = \left(\hat{\omega} - \mathcal{H}^d \right)^{-1} \approx - \left(\mathcal{H}^d \right)^{-1} \quad (3.5.32)$$

where we assumed that the quantum fluctuations are small and can be ignored w.r.t the diagonal contribution \mathcal{H}^d . This gives

$$\frac{\Delta\mathcal{H}^0(\omega, D)}{\left[\mathcal{H}_1^d (\omega_0 - \omega_1) \right]^{-1}} = \left[\left[\mathcal{H}^d, \mathcal{H}^I \right], \mathcal{H} \right] \quad (3.5.33)$$

We can thus make the connection,

$$\Delta\lambda \sim \left[\mathcal{H}_1^d (\omega_0 - \omega_1) \right]^{-1} \quad (3.5.34)$$

Note that in going from eq. 3.5.30 to the simplified form eq. 3.5.33, we had to drop all quantum fluctuations in the denominator and we lose the fixed point structure in the process. This results in the distinction that while URG can reach a fixed point theory in a finite number of steps, CUT cannot do so.

3.6 Comparison of the Canonical Transformations

We have considered three canonical transformations in this section: the Poor Man's scaling (PMS), the Schrieffer-Wolff transformation (SWT) and the continuous unitary transformation renormalization group (CUT-RG). PMS and SWT are more or less identical; they differ in the context in which they are used. PMS is used when there is an entire spectrum of energies in the model, ranging from a low energy limit to a high energy; it is then employed to decouple the highest energy modes in an iterative fashion. SWT is used when the Hamiltonian can be split into one high and one low energy part, and we need to decouple these two modes. It is clear when seen from this perspective that SWT is like a one-shot PMS; it decouples the UV from the IR in one step, compared to the iterative approach of PMS. However, as has been shown in the previous subsections, both PMS and SWT can be formalized in an identical fashion, so that one can be switched for the other in both contexts.

Now that we have established that PMS and SWT are formally identical, we can relate them to URG. URG is similar in philosophy to PMS in the fact that URG also successively decouples high energy modes from the low energy ones. The difference is that URG takes care of the quantum fluctuations, at least in principle, by introducing a new set of energy scales ω . These ω then parameterise the RG flows of URG, compared to the single RG flow of PMS. Since SWT is formally the same as PMS, there is also a comparison between SWT and URG. Both PMS

and SWT trivialize the quantum fluctuation scales of URG by replacing it with the bare energy values.

CUT-RG is philosophically different from the other transformations. Its goal is to gradually reduce the contributions of the off-diagonal terms by making them decay along a certain scale l . Off-diagonal terms that connect states with large energy differences decay faster. In this sense, there is no sequential dropping out of off-diagonal terms; all off-diagonal terms disappear at $l = \infty$. In this sense, it is like a continuous version of SWT. While SWT strives to remove an entire off-diagonal term in one-shot, CUT RG does this gradually by introducing a scale l . This separation of scales is absent in SWT. It does exist in URG and PMS, albeit in a different fashion. There, the separation comes in when we decouple single electron states starting from the Brillouin zone boundary Λ_N and come down to the Fermi surface Λ_0 . Each Λ provides a natural energy scale for separating the high and low energy physics.

If one integrates the continuum generator η over all the scales, one should recover something analogous to the SWT generator. This generator is however necessarily perturbative in the off-diagonal term, since by definition η will only be of first order in \mathcal{H}_X . This is in contrast to the non-perturbative generators in URG and, at least in principle, PMS. This non-perturbative form is encapsulated in the presence of a second completely different set of energy scales ω (or E in PMS). This second energy scale is absent in CUT RG because it takes care of at most the second order term.

Another point to note is that since SWT keeps the entire off-diagonal piece in the generator, new terms will almost certainly be generated at every step, and they have to be truncated. This is not the case with URG or PMS, because in those methods, we decouple just a single-electron at each step, and so those electrons become integrals of motion at that step, leading to their removal from the off-diagonal piece, and very often the Hamiltonian retains the same form as the bare model. This makes the philosophy of URG and PMS easier to work with. Tied to this is the fact that CUT RG often takes a certain type of interaction in the generator part, and not the entire off-diagonal piece. Hence, at the limit of the flow parameter going to ∞ , the chosen off-diagonal piece goes to zero but the remaining off-diagonal pieces still remain. As a result, the Hamiltonian is at most block diagonal at this stage. On the other hand, URG progressively decouples single electrons, meaning all scattering terms corresponding to that electron vanish at each step.

One last thing to note is that URG, being unitarily implemented with a well-defined generator, does not accommodate for spontaneous symmetry breaking (SSB). In order to see SSB, the symmetry-breaking term has to be added to the bare model explicitly; if this term grows under the RG, then the ground state will be symmetry-broken. CUT RG, however, does allow for SSB through the idea that the generator is not uniquely defined. If the generator commutes with a particular symmetry, then the family of Hamiltonians will also have the symmetry [73]. However, if the generator is replaced by something that is normal ordered w.r.t a particular expectation value, then the CUT RG flow will usually be towards either the symmetry-preserved state or the symmetry-broken state, depending on whichever is stable [75].

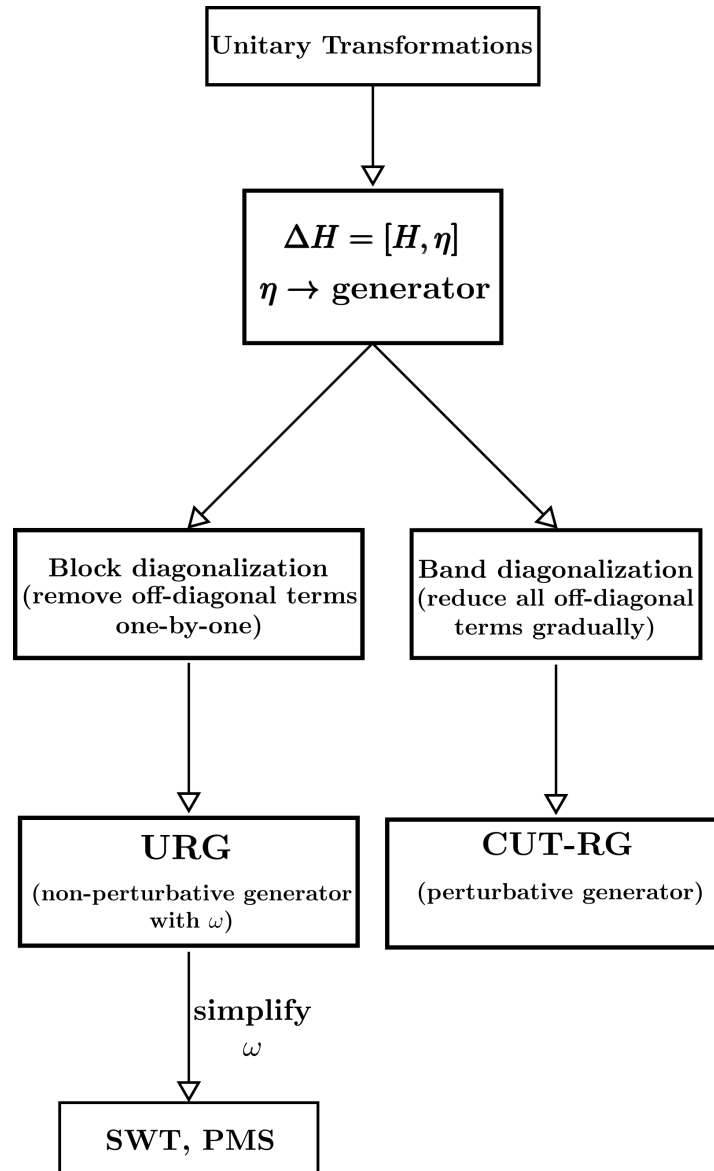


Figure 3.3: Comparison of the various unitary transformations and their relationships to each other.

Chapter 4

URG of the single-impurity Anderson model: RG flows and fixed point Hamiltonian

4.1 Brief description of the single-impurity Anderson model

The model is the usual single-impurity Anderson model Hamiltonian.

$$\mathcal{H} = \sum_{k\sigma} \epsilon_k \hat{n}_{k\sigma} + \sum_{k\sigma} \left(V_k c_{k\sigma}^\dagger c_{d\sigma} + h.c. \right) + \epsilon_d \sum_{\sigma} \hat{n}_{d\sigma} + U \hat{n}_{d\uparrow} \hat{n}_{d\downarrow} \quad (4.1.1)$$

To allow the calculation of both particle and hole kinetic energies, we will write the kinetic energy part as $\sum_{k\sigma} \epsilon_k \tau_{k\sigma}$, where $\tau = \hat{n} - \frac{1}{2}$ and drop the extra constant part.

$$\mathcal{H} = \sum_{k\sigma} \epsilon_k \tau_{k\sigma} + \sum_{k\sigma} \left(V_k c_{k\sigma}^\dagger c_{d\sigma} + h.c. \right) + \epsilon_d \sum_{\sigma} \hat{n}_{d\sigma} + U \hat{n}_{d\uparrow} \hat{n}_{d\downarrow} \quad (4.1.2)$$

4.2 Calculation of renormalisation

The renormalisation is

$$c_{q\beta}^\dagger T \frac{1}{\omega - H^D} T^\dagger c_{q\beta} + T^\dagger c_{q\beta} \frac{1}{\omega' - H^D} c_{q\beta}^\dagger T \quad (4.2.1)$$

We will be decoupling an electron $q\beta$ at the energy shell $\epsilon_q = \pm D$. The diagonal part (that comes down in the denominator) is

$$H^D = \epsilon_q \tau_{q\beta} + \epsilon_d \hat{n}_{d\beta} + U \hat{n}_{d\beta} \hat{n}_{d\bar{\beta}} \quad (4.2.2)$$

The off-diagonal part is

$$c_{q\beta}^\dagger T = V_q c_{q\beta}^\dagger c_{d\beta} \quad (4.2.3)$$

The renormalisation from a single electron $q\beta$ is

$$\begin{aligned} \Delta H &= c_{q\beta}^\dagger c_{d\beta} \frac{1|V_q|^2}{\omega - H^D} c_{d\beta}^\dagger c_{q\beta} + c_{d\beta}^\dagger c_{q\beta} \frac{1|V_q|^2}{\omega' - H^D} c_{q\beta}^\dagger c_{d\beta} \\ &= c_{q\beta}^\dagger c_{d\beta} \frac{|V_q|^2}{\omega - D/2 - \epsilon_d - U \hat{n}_{d\bar{\beta}}} c_{d\beta}^\dagger c_{q\beta} + c_{d\beta}^\dagger c_{q\beta} \frac{|V_q|^2}{\omega' - D/2} c_{q\beta}^\dagger c_{d\beta} \\ &= \frac{\hat{n}_{q\beta} (1 - \hat{n}_{d\beta}) |V_q|^2}{\omega - D/2 - \epsilon_d - U \hat{n}_{d\bar{\beta}}} + \frac{\hat{n}_{d\beta} (1 - \hat{n}_{q\beta}) |V_q|^2}{\omega' - D/2} \end{aligned} \quad (4.2.4)$$

For comparing the two ω s, we will use the relation eq. 2.1.72: $\omega_0^1 + \omega_0^1 = H_0^D + H_1^D$ where $\omega_0^1 = \omega'$. ω_0^1 however is not ω . This is because the relation assumes the ω s to be calculated at the same energy - while ω' is calculated

at energy $-D$, ω is at energy D . The ω_0^1 should hence be the ω at energy $-D$, which is $-\omega$. With this in mind, the relation says

$$\omega' - \omega = D/2 + \epsilon_d + U\hat{n}_{d\beta} - D/2 \quad (4.2.5)$$

This gives an expression of ω' in terms of ω . Substituting this into ΔH gives

$$\Delta H = \frac{\hat{n}_{q\beta}(1 - \hat{n}_{d\beta})|V_q|^2}{\omega - D/2 - \epsilon_d - U\hat{n}_{d\beta}} + \frac{\hat{n}_{d\beta}(1 - \hat{n}_{q\beta})|V_q|^2}{\omega - D/2 + \epsilon_d + U\hat{n}_{d\beta}} \quad (4.2.6)$$

The total renormalisation from the entire shell $\pm D$ is

$$\begin{aligned} \Delta H &= \sum_{q\beta} |V_q|^2 \left[\frac{\hat{n}_{q\beta}(1 - \hat{n}_{d\beta})}{\omega - D/2 - \epsilon_d - U\hat{n}_{d\beta}} + \frac{\hat{n}_{d\beta}(1 - \hat{n}_{q\beta})}{\omega - D/2 + \epsilon_d + U\hat{n}_{d\beta}} \right] \\ &= \sum_q |V_q|^2 \left[\frac{(1 - \hat{n}_{d\beta})\hat{n}_{d\bar{\beta}}}{\omega - \frac{1}{2}\epsilon_q - \epsilon_d - U} + \frac{(1 - \hat{n}_{d\beta})(1 - \hat{n}_{d\bar{\beta}})}{\omega - \frac{1}{2}\epsilon_q - \epsilon_d} + \frac{\hat{n}_{d\beta}\hat{n}_{d\bar{\beta}}}{\omega - \frac{1}{2}\epsilon_q + \epsilon_d + U} + \frac{\hat{n}_{d\beta}(1 - \hat{n}_{d\bar{\beta}})}{\omega - \frac{1}{2}\epsilon_q + \epsilon_d} \right] \end{aligned} \quad (4.2.7)$$

4.3 Scaling equations for the SIAM

Once we have the renormalisation for decoupling one electronic or hole state, we can just sum over the spins and momenta to get the total renormalisation upon decoupling the entire shells $\pm\epsilon_q$. From the structure of ΔH in eq. 4.2.7, we can see that there are renormalisations to all three configuration energies of the impurity: the doublon energy E_2 corresponding to the state $\hat{n}_{d\beta}\hat{n}_{d\bar{\beta}}$, the single energy E_1 corresponding to $(\hat{n}_{d\beta}(1 - \hat{n}_{d\bar{\beta}}) + \hat{n}_{d\bar{\beta}}(1 - \hat{n}_{d\beta}))$, and the holon energy E_0 corresponding to $(1 - \hat{n}_{d\beta})(1 - \hat{n}_{d\bar{\beta}}) + \hat{n}_{d\bar{\beta}}(1 - \hat{n}_{d\beta})$.

$$\begin{aligned} \Delta E_2 &= +2 \sum_q \frac{|V_q|^2}{\omega - \frac{1}{2}\epsilon_q + \epsilon_d + U} \\ \Delta E_1 &= + \sum_q \frac{|V_q|^2}{\omega - \frac{1}{2}\epsilon_q + \epsilon_d} + \sum_q \frac{|V_q|^2}{\omega - \frac{1}{2}\epsilon_q - \epsilon_d - U} \\ \Delta E_0 &= +2 \sum_q \frac{|V_q|^2}{\omega - \frac{1}{2}\epsilon_q - \epsilon_d} \end{aligned} \quad (4.3.1)$$

Using the relations $\epsilon_d = E_1 - E_0$ and $U = E_2 + E_0 - 2E_1$, we can write

$$\begin{aligned} \Delta\epsilon_d &= + \sum_q \frac{|V_q|^2}{\omega - \frac{1}{2}\epsilon_q + \epsilon_d} + \sum_q \frac{|V_q|^2}{\omega - \frac{1}{2}\epsilon_q - \epsilon_d - U} - 2 \sum_q \frac{|V_q|^2}{\omega - \frac{1}{2}\epsilon_q - \epsilon_d} \\ \Delta U &= \sum_q \frac{2|V_q|^2}{\omega - \frac{1}{2}\epsilon_q + \epsilon_d + U} + \sum_q \frac{2|V_q|^2}{\omega - \frac{1}{2}\epsilon_q - \epsilon_d} - \sum_q \frac{2|V_q|^2}{\omega - \frac{1}{2}\epsilon_q + \epsilon_d} - \sum_q \frac{2|V_q|^2}{\omega - \frac{1}{2}\epsilon_q - \epsilon_d - U} \end{aligned} \quad (4.3.2)$$

4.4 Connection to poor man's scaling

To obtain the results of Poor Man's scaling [67] [72], we can look at various regimes. First we look at the case when both ϵ_d and U are small such that both the singly-occupied and doubly-occupied subspaces of the impurity are comfortably inside the bandwidth, $U, \epsilon_d \ll \epsilon_q$. We can then ignore the ϵ_d and U in the denominator compared to the ϵ_q .

$$\begin{aligned} \Delta\epsilon_d &= \sum_q \frac{|V_q|^2}{\omega - \frac{1}{2}\epsilon_q} + \sum_q \frac{|V_q|^2}{\omega - \frac{1}{2}\epsilon_q} - 2 \sum_q \frac{|V_q|^2}{\omega - \frac{1}{2}\epsilon_q} \\ \Delta U &= 2 \sum_q \frac{|V_q|^2}{\omega - \frac{1}{2}\epsilon_q} + 2 \sum_q \frac{|V_q|^2}{\omega - \frac{1}{2}\epsilon_q} - 2 \sum_q \frac{|V_q|^2}{\omega - \frac{1}{2}\epsilon_q} - 2 \sum_q \frac{|V_q|^2}{\omega - \frac{1}{2}\epsilon_q} \end{aligned} \quad (4.4.1)$$

Assuming the upper and lower band edges are symmetrical such that $\sum_{-D} = \sum_D$, we get $\Delta\epsilon_d = \Delta U = 0$.

In the regime $U \gg \epsilon_q \gg \epsilon_d$, the doubly-occupied state is far above the bandwidth. We can now ignore the terms that have U in the denominator. We get

$$\begin{aligned}\Delta\epsilon_d &= \sum_q \frac{|V_q|^2}{\omega - \frac{1}{2}\epsilon_q} - 2 \sum_q \frac{|V_q|^2}{\omega - \frac{1}{2}\epsilon_q} \\ \Delta U &= 2 \sum_q \frac{|V_q|^2}{\omega - \frac{1}{2}\epsilon_q} - 2 \sum_q \frac{|V_q|^2}{\omega - \frac{1}{2}\epsilon_q}\end{aligned}\tag{4.4.2}$$

Again assuming symmetrical upper and lower edges, and isotropic dispersion $\epsilon_q = D$ and $\sum_q |V|^2 = \frac{\Delta}{\pi} |\delta D|$, we get

$$\begin{aligned}\Delta U &= 0 \\ \delta\epsilon_d &= -\frac{\Delta}{\pi} \frac{1}{\omega - \frac{1}{2}D}\end{aligned}\tag{4.4.3}$$

There we replaced the difference symbol Δ with δ to avoid confusion with the hybridisation $\Delta \sim \sum V^2$. For low quantum fluctuations, we can ignore the renormalisation in the couplings and replace ω with the initial conduction electron energy: $\omega = \epsilon_q \tau_{q\beta} = -\frac{1}{2}D$.

$$\delta\epsilon_d = \frac{\Delta}{\pi} \frac{\delta D}{D}\tag{4.4.4}$$

This is the one-loop scaling equation.

4.5 Preservation of particle-hole symmetry

The Anderson model Hamiltonian, eq. 4.1.1, has an impurity particle-hole symmetry for a certain condition of the couplings. To see this, we apply the particle-hole transformation $c_k \rightarrow c_k^\dagger, c_d \rightarrow -c_d^\dagger$ to the Hamiltonian. Since we are looking at the impurity symmetry, we will only look at the terms involving the impurity. The particle-hole symmetry of the conduction bath is a separate thing and that requires a specific lattice. Hence we will not consider kinetic energy term in this discussion. The rest of the terms transform as

$$\epsilon_d \sum_\sigma \hat{n}_{d\sigma} \rightarrow 2\epsilon_d - \epsilon_d \sum_\sigma \hat{n}_{d\sigma}\tag{4.5.1}$$

$$U \hat{n}_{d\uparrow} \hat{n}_{d\downarrow} \rightarrow U \hat{n}_{d\uparrow} \hat{n}_{d\downarrow} - U \sum_\sigma \hat{n}_{d\sigma} + U\tag{4.5.2}$$

$$\sum_{k\sigma} V(k) c_{k\sigma}^\dagger c_{d\sigma} + hc \rightarrow \sum_{k\sigma} -V(k) c_{k\sigma} c_{d\sigma}^\dagger + hc = \sum_{k\sigma} V^*(k) c_{k\sigma}^\dagger c_{d\sigma} + hc\tag{4.5.3}$$

The impurity-bath hopping term can be made symmetric by making $V(k)$ real; we would then have, from eq. 4.5.3,

$$V(k) \left(c_{k\sigma}^\dagger c_{d\sigma} + c_{d\sigma}^\dagger c_{k\sigma} \right) \rightarrow V(k) \left(c_{d\sigma}^\dagger c_{k\sigma} + c_{k\sigma}^\dagger c_{d\sigma} \right)\tag{4.5.4}$$

The impurity diagonal terms, ϵ_d and U , require a specific condition. Combining eqs. 4.5.1 and 4.5.2,

$$\epsilon_d \hat{n}_{d\sigma} + U \hat{n}_{d\uparrow} \hat{n}_{d\downarrow} \rightarrow (-\epsilon_d - U) \hat{n}_{d\sigma} + U \hat{n}_{d\uparrow} \hat{n}_{d\downarrow}\tag{4.5.5}$$

We dropped some constant terms in the transformed Hamiltonian. For particle-hole symmetry, the left and right hand sides must be same. The required condition is thus

$$\epsilon_d = -\epsilon_d - U \implies \epsilon_d + \frac{1}{2}U = 0\tag{4.5.6}$$

This same condition can be obtained in a more physical way. If we consider the singly-occupied state of the impurity as the reference state, the doubly-occupied state is the particle-excitation and the vacant state is the hole excitation. The energy of this particle state is $E_2 = 2\epsilon_d + U$ and that of the hole state is $E_0 = 0$. Particle-hole symmetry then requires the particle and hole levels to be degenerate, which means $E_2 = E_0$, and we recover the condition eq. 4.5.6.

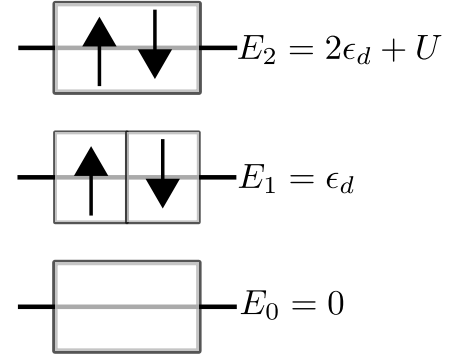


Figure 4.1: Particle and hole excitations of the impurity

Since the URG is unitary, if we start from a model that is particle-hole symmetric, the RG equations should uphold that symmetry. What this means is that if we have $\epsilon_d + \frac{1}{2}U = 0$ in the bare model, the new couplings should also satisfy $\epsilon'_d + \frac{1}{2}U' = 0$. This means we must have

$$\Delta \left(\epsilon_d + \frac{1}{2}U \right) = 0 \quad (4.5.7)$$

The quantity $\gamma = \epsilon_d + \frac{1}{2}U$ is thus an RG-invariant for the particle-hole symmetric model; it does not change under the RG flow. It is often referred to as the asymmetry parameter; it quantifies the asymmetry in the model. We need to check if our equations satisfy this. Looking at the RG equations for ϵ_d and U , we can find the RG equation for the asymmetry parameter. The slightly easier way is to just note that the renormalisation in E_2 should be equal to the renormalisation in E_0 , in order for p-h symmetry to hold.

$$\Delta E_2 = 2 \frac{\Delta}{\pi} \frac{1}{\omega - D + \epsilon_d + U}, \Delta E_0 = 2 \frac{\Delta}{\pi} \frac{1}{\omega - D - \epsilon_d} \quad (4.5.8)$$

If we start with a particle-hole symmetric model, we will have $-\epsilon_d = \epsilon_d + U$. Substituting that gives $\Delta E_2 = \Delta E_0$. This shows that the doublon and holon states remain equidistant from the single-particle level, thus maintaining particle-hole symmetry along the flow.

4.6 Numerical analysis of the particle-hole symmetric RG equations

We will specialize to the particle-hole symmetric case, $2\epsilon_d + U = 0$, and a symmetric energy shell $\epsilon_q = D$, and look at the scaling behavior of ϵ_d .

$$\Delta \epsilon_d = -4|V|^2 \frac{\epsilon_d}{\left(\omega - \frac{1}{2}D \right)^2 - \epsilon_d^2} \quad (4.6.1)$$

Since the equation is symmetric under $\epsilon_d \rightarrow -\epsilon_d$, we might as well work with the magnitude of the onsite energy:

$$\Delta |\epsilon_d| = -4|V|^2 \frac{|\epsilon_d|}{\left(\omega - \frac{1}{2}D \right)^2 - \epsilon_d^2} \quad (4.6.2)$$

Depending on the signature of the denominator, the flows will be either relevant or irrelevant. For the flow to the local moment fixed point, the fixed point value of $|\epsilon_d|$ grows as we increase the bandwidth. This implies that for a thermodynamically large system, the local moment fixed point will be at $-\epsilon_d \rightarrow \infty$. This behavior is shown in fig. 4.3.

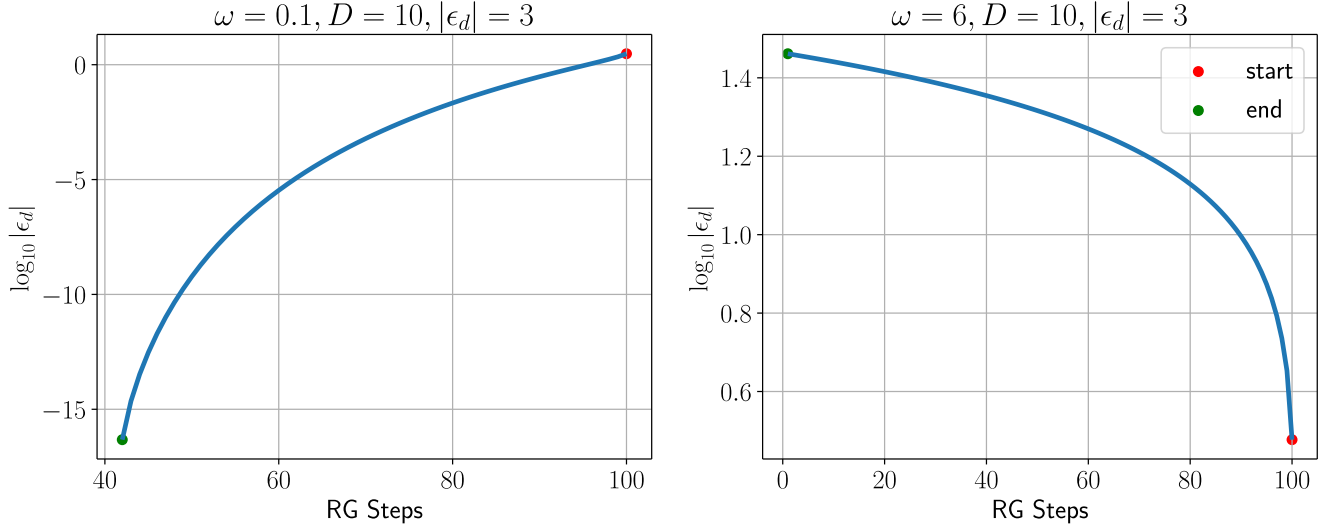


Figure 4.2: Left: Irrelevant flow towards $|\epsilon_d| = 0$, at low ω . Right: Relevant flow towards large $|\epsilon_d|$, at large ω . The former can be thought of as the projection of the strong-coupling flow on to the $\epsilon_d - D$ plane. The latter is the flow towards the local moment fixed point, if we start from a negative ϵ_d .

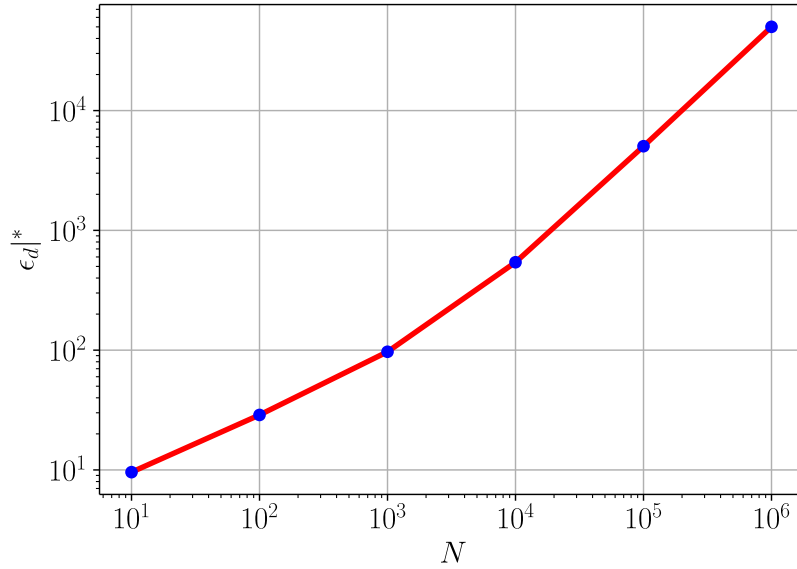


Figure 4.3: Change in fixed point value of $|\epsilon_d|$ with system size.

Chapter 5

Physics of the extended single-impurity Anderson model

5.1 Introduction of spin-exchange and charge isospin-exchange interactions: the origin of the extended SIAM

We will now study the *extended* SIAM obtained by introducing spin-exchange and charge isospin-exchange interactions between the impurity and the conduction bath [76]. Such terms are generated when one does a Schrieffer-Wolff transformation on the SIAM, but we will find it prudent to keep these terms in the bare model itself.

The spin-exchange interaction has the form

$$J\vec{S}_d \cdot \vec{s} = J \left[S_d^z s^z + \frac{1}{2} (S_d^+ s^- + S_d^- s^+) \right], \quad (5.1.1)$$

where $\vec{S}_d = (S_d^x, S_d^y, S_d^z) = \sum_{\alpha\beta} \vec{\sigma}_{\alpha\beta} c_{d\alpha}^\dagger c_{d\beta}$ is the impurity spin operator, $\vec{s} = \sum_{kk'\alpha\beta} \vec{\sigma}_{\alpha\beta} c_{k\alpha}^\dagger c_{k'\beta}$ is the spin operator for the conduction bath and J is the spin-exchange coupling. The bath spin operator actually acts locally, as can be seen by Fourier transforming to real space (using the definition $f(k) = \frac{1}{\sqrt{N}} \sum_r g(r) \exp(ikr)$):

$$\vec{s} = \sum_{kk'rr'} \frac{1}{N} e^{ikr - ik'r'} \vec{\sigma}_{\alpha\beta} c_{r\alpha}^\dagger c_{r'\beta} = \sum_{rr'} \frac{1}{N} \vec{\sigma}_{\alpha\beta} c_{r\alpha}^\dagger c_{r'\beta} N \delta(r) \delta(r') = \vec{\sigma}_{\alpha\beta} c_{0\alpha}^\dagger c_{0\beta} \quad (5.1.2)$$

In order to introduce the charge isospin coupling, we define the Nambu spinor [77, 78] $\psi^k = \begin{pmatrix} c_{k\uparrow} & c_{k\downarrow}^\dagger \end{pmatrix}$, and the charge isospin [76] for the mobile conduction electrons

$$\vec{C} = \sum_{kk'} \psi^k \vec{C} \psi^{k'} = \frac{1}{2} \sum_{kk'\alpha\beta} \psi_\alpha^k \vec{\sigma}_{\alpha\beta} \psi_\beta^{k'} \quad (5.1.3)$$

The various components of the isospin are

$$\begin{aligned} C^z &= \sum_{kk'\sigma} \frac{1}{2} \psi_\sigma^k \sigma_{\sigma\sigma}^z \psi_\sigma^{k'} = \frac{1}{2} \sum_{kk'\sigma} \left(c_{k\sigma}^\dagger c_{k'\sigma} - \frac{1}{2} \delta_{kk'} \right) \\ C^x &= \sum_{kk'\sigma} \frac{1}{2} \psi_\sigma^k \sigma_{\sigma\bar{\sigma}}^x \psi_{\bar{\sigma}}^{k'} = \sum_{kk'\sigma} \frac{\sigma}{4} \left(c_{k\sigma}^\dagger c_{k'\bar{\sigma}} + \text{h.c.} \right) \\ C^y &= \sum_{kk'\sigma} \frac{1}{2} \psi_\sigma^k \sigma_{\sigma\bar{\sigma}}^y \psi_{\bar{\sigma}}^{k'} = \sum_{kk'\sigma} -\frac{i\sigma}{4} \left(c_{k\sigma}^\dagger c_{k'\bar{\sigma}} - \text{h.c.} \right) \end{aligned} \quad (5.1.4)$$

It is easy to verify that these operators satisfy the SU(2) commutation algebra. For example, if we write $C^x = A + A^\dagger$

and $C^y = B + B^\dagger$, then $[C^x, C^y] = [A, B^\dagger] - \text{h.c.}$, where

$$[A, B^\dagger] = \frac{1}{4} \sum_{kk', qq'} [c_{k\uparrow}^\dagger c_{k'\downarrow}^\dagger, i c_{q'\downarrow} c_{q\uparrow}] = \frac{i}{4} \sum_{kq} (c_{k\uparrow}^\dagger c_{q\uparrow} - c_{k\downarrow} c_{q\downarrow}^\dagger) \quad (5.1.5)$$

and therefore

$$\Rightarrow [C^x, C^y] = \frac{i}{2} \sum_{kq} (c_{k\uparrow}^\dagger c_{q\uparrow} - c_{k\downarrow} c_{q\downarrow}^\dagger) = iC^z \quad (5.1.6)$$

There are similar operators for the impurity electron:

$$\psi_d = \begin{pmatrix} c_{d\uparrow} & c_{d\downarrow}^\dagger \end{pmatrix}, \quad \vec{C}_d = \frac{1}{2} \sum_{\beta} \psi_{d,\alpha}^\dagger \vec{\sigma}_{\alpha\beta} \psi_{d,\beta} \quad (5.1.7)$$

The full charge-Kondo interaction can now be written down in terms of these isospins:

$$K \vec{C}_d \cdot \vec{C} = K \left[C_d^z C^z + \frac{1}{2} (C_d^+ C^- + C_d^- C^+) \right] \quad (5.1.8)$$

where $C^\pm \equiv C^x \pm iC^y$.

$$C^+ = \sum_{kk'} c_{k\uparrow}^\dagger c_{k'\downarrow}^\dagger, \quad C^- = \sum_{kk'} c_{k'\downarrow} c_{k\uparrow} \quad (5.1.9)$$

The full extended Anderson model Hamiltonian, at particle-hole symmetry, is

$$\mathcal{H} = \sum_{k\sigma} \epsilon_k \tau_{k\sigma} + \epsilon_d (\hat{n}_{d\uparrow} - \hat{n}_{d\downarrow})^2 + \sum_{k\sigma} (V_k c_{k\sigma}^\dagger c_{d\sigma} + \text{h.c.}) + J \vec{S}_d \cdot \vec{s} + K \vec{C}_d \cdot \vec{C} \quad (5.1.10)$$

For the URG analysis, at each RG step, we decouple the electronic states $q\beta$ on the k -space shell of radius Λ_j . For simplicity, we will only consider those diagonal terms in the denominator that either have both $q\beta$ and $q\bar{\beta}$ or both $q\beta$ and d or both $q\bar{\beta}$ and d . Terms that have purely $q\bar{\beta}$ will not be considered. Also, the scattering between just d and $q\bar{\beta}$ can be ignored since it is diagonal in $q\beta$. The diagonal (number-preserving) part is

$$H_D = \sum_{\beta} \epsilon_q \tau_{q\beta} + \epsilon_d (\hat{n}_{d\uparrow} - \hat{n}_{d\downarrow})^2 + J S_d^z s_q^z + K C_d^z C_q^z \quad (5.1.11)$$

where $s_q^z = \frac{1}{2} (\hat{n}_{q\uparrow} - \hat{n}_{q\downarrow})$ and $C_q^z = \frac{1}{2} (\hat{n}_{q\uparrow} + \hat{n}_{q\downarrow} - 1)$. The off-diagonal part is:

$$H_X = \sum_{\beta=\uparrow,\downarrow} \left[V c_{d\beta}^\dagger c_{q\beta} + \frac{1}{2} J \sum_{k < \Lambda_N} \left\{ (\hat{n}_{d\beta} - \hat{n}_{d\bar{\beta}}) \frac{1}{2} c_{k\beta}^\dagger c_{q\beta} + c_{d\beta}^\dagger c_{d\bar{\beta}} c_{k\bar{\beta}}^\dagger c_{q\beta} \right\} + \frac{1}{2} K \sum_{k < \Lambda_N} \left\{ (\hat{n}_d - 1) \frac{1}{2} c_{k\beta}^\dagger c_{q\beta} + c_{d\beta}^\dagger c_{d\bar{\beta}}^\dagger c_{k\bar{\beta}} c_{q\beta} \right\} \right] + \text{h.c.} \quad (5.1.12)$$

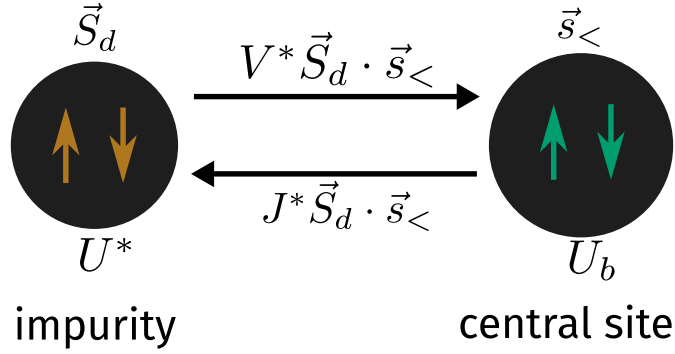


Figure 5.1: While we have studied the full model under renormalisation group, often we will turn to a simplified zero-bandwidth version of the model that is obtained by ignoring the kinetic energy part of the Hamiltonian. This zero-bandwidth model is effectively a two site model.

5.2 RG equations for extended SIAM

The derivation of the RG equations are shown in appendix B.

$$\begin{aligned}
 \Delta\epsilon_d &= 2V^2 n_j \left(\frac{1}{\omega - \frac{D}{2} + \epsilon_d + \frac{K}{4}} - \frac{1}{\omega - \frac{D}{2} - \epsilon_d + \frac{J}{4}} \right) + \frac{n_j}{2} \left(\frac{J^2}{\omega - \frac{D}{2} + \frac{J}{4}} - \frac{K^2}{\omega - \frac{D}{2} + \frac{K}{4}} \right), \\
 \Delta V &= -\frac{3n_j V}{8} \left[J \left(\frac{1}{\omega - \frac{D}{2} + \frac{J}{4}} + \frac{1}{\omega - \frac{D}{2} - \epsilon_d + \frac{J}{4}} \right) + K \left(\frac{1}{\omega - \frac{D}{2} + \frac{K}{4}} + \frac{1}{\omega - \frac{D}{2} + \epsilon_d + \frac{K}{4}} \right) \right], \\
 \Delta J &= -\frac{n_j J^2}{\omega - \frac{D}{2} + \frac{J}{4}}, \\
 \Delta K &= -\frac{n_j K^2}{\omega - \frac{D}{2} + \frac{K}{4}}
 \end{aligned} \tag{5.2.1}$$

In terms of $U = -2\epsilon_d$, the equations become

$$\Delta U = 4V^2 n_j \left(\frac{1}{d_1} - \frac{1}{d_0} \right) - n_j \left(\frac{J^2}{d_2} - \frac{K^2}{d_3} \right), \tag{5.2.2}$$

$$\Delta V = -\frac{3n_j V}{8} \left[J \left(\frac{1}{d_2} + \frac{1}{d_1} \right) + K \left(\frac{1}{d_3} + \frac{1}{d_0} \right) \right], \tag{5.2.3}$$

$$\Delta J = -\frac{n_j J^2}{d_2}, \quad \Delta K = -\frac{n_j K^2}{d_3} \tag{5.2.4}$$

d_i are the denominators:

$$d_0 = \omega - \frac{D}{2} - \frac{U}{2} + \frac{K}{4}, \quad d_1 = \omega - \frac{D}{2} + \frac{U}{2} + \frac{J}{4}, \quad d_2 = \omega - \frac{D}{2} + \frac{J}{4}, \quad d_3 = \omega - \frac{D}{2} + \frac{K}{4} \tag{5.2.5}$$

5.3 Nature of coupling RG flows

5.3.1 Repulsive interaction on impurity: $U > 0$

For the Hamiltonians with positive on-site correlation, we will assume that the spin-exchange coupling is positive and charge isospin-exchange coupling is negative: $J > 0, K < 0$. This choice is motivated by the signs of the corresponding terms when they are generated via a Schrieffer-Wolff transformation [4]. The impurity-bath hybridisation V is always positive. The sign of the couplings lead to inequalities among the denominators which we will utilise at various points. First of all, since $U > 0$, we have $d_1 - d_2 = \frac{U}{2} > 0$. Secondly, since $K < 0$, we have

$d_2 - d_3 = \frac{J-K}{4} > 0$. And finally, we have $d_3 - d_0 = \frac{U}{2} > 0$. Combining these, we can write

$$d_1 > d_2 > d_3 > d_0 \quad (5.3.1)$$

The strong coupling regime is defined as the range of values of ω where the hybridisation is relevant. This is ensured by the assumption $d_1 < 0$. From eq. 5.3.1, we can then conclude that all denominators are negative: $d_i = -|d_i|$. The simplest consequence of this is the RG flow of K :

$$\Delta K = -\frac{n_j K^2}{d_3} = \frac{n_j K^2}{|d_3|} > 0 \implies K_{j+1} > K_j \implies K_0 = -|K_0|, K^* \rightarrow 0 \quad (5.3.2)$$

K_j is the value of K after the j^{th} RG step, K_0 representing the bare value. In other words, since $d_3 < 0$, the RG equation for K provides an algebraic increment, and the negative K increases and flows towards zero. The $*$ indicates a fixed point value. The isospin coupling is irrelevant in this regime, and we will ignore it.

The coupling J , on the other hand, is relevant and flows from a small positive value towards a large value at strong coupling.

$$\Delta J = -\frac{n_j J^2}{d_2} = \frac{n_j J^2}{|d_2|} > 0 \implies J_{j+1} > J_j \implies J_0 \rightarrow \text{large } J^* \text{ (strong coupling)} \quad (5.3.3)$$

The value of J^* is obtained when the denominator d_2 vanishes.

Because of the RG irrelevance of K , we can simplify the RG equation for V :

$$\Delta V = -\frac{3n_j V J}{8} \left(\frac{1}{d_2} + \frac{1}{d_1} \right) = \frac{3n_j V J}{8} \left(\frac{1}{|d_2|} + \frac{1}{|d_1|} \right) > 0 \quad (5.3.4)$$

Since both the denominators are positive, V is relevant. The fixed point value V^* is attained when the denominator d_1 vanishes (d_1 will vanish earlier than d_2).

We can compare the rate of flows of V and J :

$$\frac{\Delta V}{\Delta J} = \frac{3V}{8J} \left(1 + \frac{|d_2|}{|d_1|} \right) > \frac{3V}{4J} \quad (5.3.5)$$

There we used the fact that $|d_2| > |d_1|$. We finally come to the RG equation for U :

$$\Delta U = 4V^2 n_j \left(\frac{1}{d_1} - \frac{1}{d_0} \right) - n_j \frac{J^2}{d_2} = -4V^2 \left(U + \frac{J}{4} \right) \frac{n_j}{d_0 d_1} - \frac{n_j J^2}{d_2} \quad (5.3.6)$$

For $V > J$, we can expect U to be irrelevant. On the other hand, $V < J$ makes U relevant.

In short, the $U > 0$ regime is characterised by an irrelevant isospin-exchange coupling K and a relevant spin-exchange coupling J , and the following set of RG equations for the remaining couplings U and V :

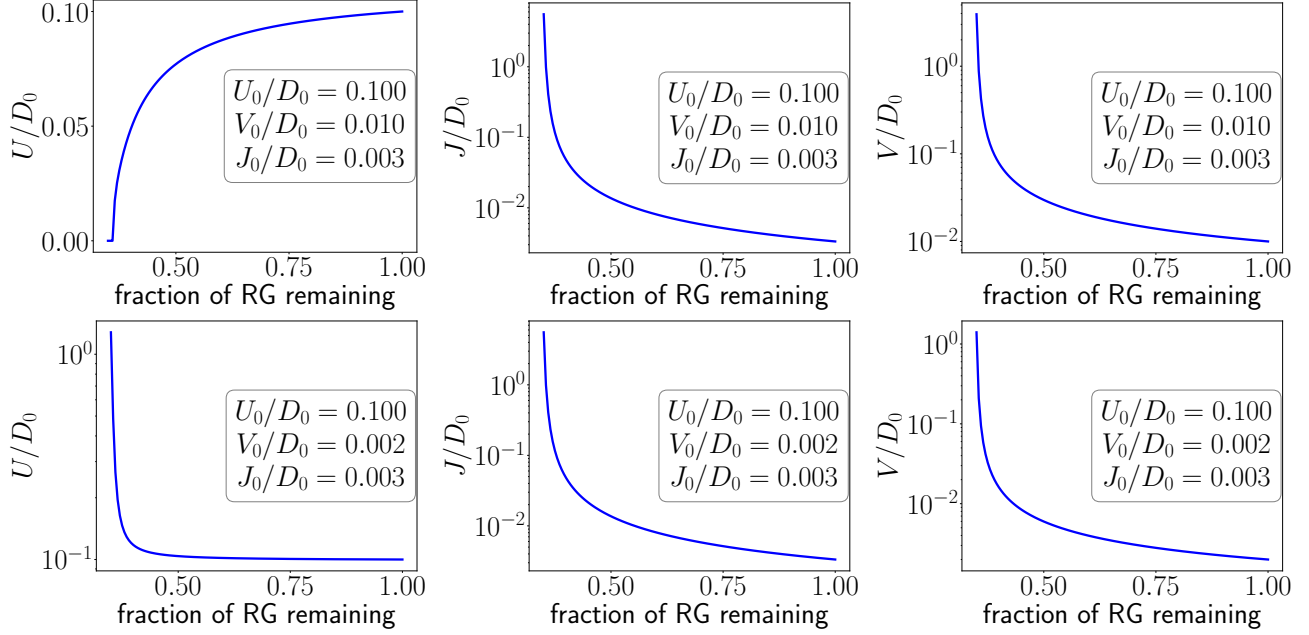
$$\Delta U = 4V^2 n_j \left(\frac{1}{d_1} - \frac{1}{d_0} \right) - n_j \frac{J^2}{d_2}, \quad \Delta V = -\frac{3n_j V J}{8} \left(\frac{1}{d_2} + \frac{1}{d_1} \right) \quad (5.3.7)$$

5.3.2 Attractive interaction on impurity: $U < 0$

Here, we have $J < 0$ and $K > 0$. The denominators satisfy the following inequality in this regime:

$$d_0 > d_3 > d_2 > d_1 \quad (5.3.8)$$

The strong coupling regime here corresponds to $d_0 < 0$. This again means that all the denominators are negative. The spin-exchange coupling J is now irrelevant, because its bare value is negative while its RG equation is positive: $\Delta J > 0$. Moreover, the isospin coupling K is now positive and so is its RG equation: $\Delta K > 0$, which



means it flows to strong coupling. V also flows to strong coupling. The RG equation for U can be written as

$$\Delta U = 4V^2 \left(\frac{K}{4} - U \right) \frac{n_j}{d_0 d_1} + \frac{n_j K^2}{d_3} \quad (5.3.9)$$

The first term is necessarily positive, while the second term is negative. This means that for roughly $V_0 > J_0$, we will have $\Delta U > 0$, and since $U_0 < 0$, this amounts to an irrelevant flow of U towards zero. On the other hand, for $J_0 > V_0$, we will have $\Delta U < 0$, and this corresponds to a relevant flow of U towards large negative value.

In other words, the RG flows in this regime can be exactly mapped to those in the positive U regime. The general statement is: in the strong coupling regime of positive(negative) U , V is always relevant, $J(K)$ is relevant, $K(J)$ is irrelevant, and U is relevant when $J(K) > V$, otherwise U is irrelevant.

5.4 Effective Hamiltonian and ground state

The fixed point Hamiltonian can, in general, be written as

$$\mathcal{H}^* = \sum_{\sigma, k} \epsilon_k T_{k\sigma} - \frac{U^*}{2} (\hat{n}_{d\uparrow} - \hat{n}_{d\downarrow})^2 + \sum_{\sigma, k < \Lambda^*} \left(V^* c_{k\sigma}^\dagger c_{d\sigma} + \text{h.c.} \right) + J^* \vec{S}_d \cdot \vec{s} + K^* \vec{C}_d \cdot \vec{C} \quad (5.4.1)$$

The first term is the kinetic energy of all the electrons. The next two terms are the impurity-diagonal pieces, featuring the renormalised interaction U^* . The next three terms are the residual interactions between the impurity and the metal, with the renormalised couplings V^* , J^* and K^* . The summations in these terms extend from the fixed point momentum cutoff Λ^* to 0. This is the region of momentum space which the URG was unable to decouple. The operators \vec{s} and \vec{C} represent the macroscopic magnetic and charge spins formed by the remaining electrons that are lying inside the window $[0, \Lambda^*]$:

$$\vec{s} = \sum_{\substack{k, k' < \Lambda^* \\ \alpha, \beta}} c_{k\alpha}^\dagger \vec{\sigma}_{\alpha\beta} c_{k'\beta} \quad (5.4.2)$$

Our goal here is to write down the ground state wavefunction for this low-energy Hamiltonian.

To make progress, we will simplify the effective Hamiltonian by taking the zero bandwidth limit. This reduces it to a two-site problem. One site is of course the impurity site, and this site will be labeled as site 1. The other site will be formed by the center of mass degree of freedom of the conduction electrons, and will be labeled as site

2. The Hamiltonian for this two-site problem is

$$\mathcal{H}_{IR} = -\frac{U^*}{2} (\hat{n}_{1\uparrow} - \hat{n}_{1\downarrow})^2 + V^* \sum_{\sigma} (c_{1\sigma}^{\dagger} c_{2\sigma} + \text{h.c.}) + J^* \vec{S}_1 \cdot \vec{S}_2 + K^* \vec{C}_1 \cdot \vec{C}_2 \quad (5.4.3)$$

The subscripts on the operators designate the site on which they act; \hat{n}_1 is the number operator for the first site.

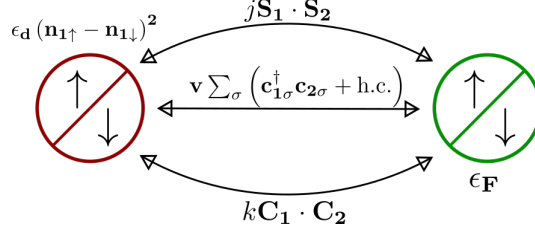


Figure 5.2: Two-site effective problem of fixed point Hamiltonian

We will adopt the following notation to represent the states in this Hilbert space. A general state will be represented in the Fock space basis as $|n_{1\uparrow} n_{1\downarrow} n_{2\uparrow} n_{2\downarrow}\rangle$. For example,

$$|1101\rangle = c_{1\uparrow}^{\dagger} c_{1\downarrow}^{\dagger} c_{2\downarrow}^{\dagger} |-\rangle \quad (5.4.4)$$

$|-\rangle$ is the vacuum state.

For $U > 0$, the ground state is given by

$$|\Psi\rangle_1 = c_s \frac{1}{\sqrt{2}} (|\uparrow, \downarrow\rangle - |\downarrow, \uparrow\rangle) + c_c \frac{1}{\sqrt{2}} (|\uparrow\downarrow, 0\rangle + |0, \uparrow\downarrow\rangle), \quad E_1 = -V^* \sqrt{\gamma^2 + 4} - \frac{1}{4} U^* - \frac{3}{8} J^* \quad (5.4.5)$$

where $\gamma = \frac{1}{2V^*} \left[\frac{1}{4} (3J^* + K^*) + \frac{1}{2} U^* \right]$. The probabilities for the spin and charge sectors for the ground state are

$$(c_s)^2 = \frac{1}{2\sqrt{\gamma^2 + 4}} (\sqrt{\gamma^2 + 4} + \gamma), \quad (c_c)^2 = \frac{1}{2\sqrt{\gamma^2 + 4}} (\sqrt{\gamma^2 + 4} - \gamma). \quad (5.4.6)$$

For (roughly) $J_0 > V_0$, we get $J^* \gg V^*$ and $U^* \gg U_0$ so that $\gamma \gg 1$. This gives $(c_s)^2 \sim 1$ and $(c_c)^2 \sim 0$. The entire contribution to the ground state then comes from the spin sectors of the two sites. This is calculated numerically in fig. 5.3.

In the other regime of $U < 0$, the two competing states are $|\Psi\rangle_1$ defined above (with energy E_1), and $|\Psi_2\rangle$, the charge singlet: $|\Psi\rangle_2 = \frac{1}{\sqrt{2}} (|2, 0\rangle - |0, 2\rangle)$ having energy E_2 .

$$E_2 = -\frac{3}{4} K^*, \quad E_1 - E_2 = -\frac{1}{4} \sqrt{\left(\frac{1}{2} K^* + U^* \right)^2 + (4V^*)^2} - \frac{1}{4} U^* + \frac{3}{4} K^* \quad (5.4.7)$$

For $V_0 \gg K_0$, the largest energy scale will be V^* , and we can then approximate this difference as

$$E_1 - E_2 \simeq -V^* < 0 \quad (5.4.8)$$

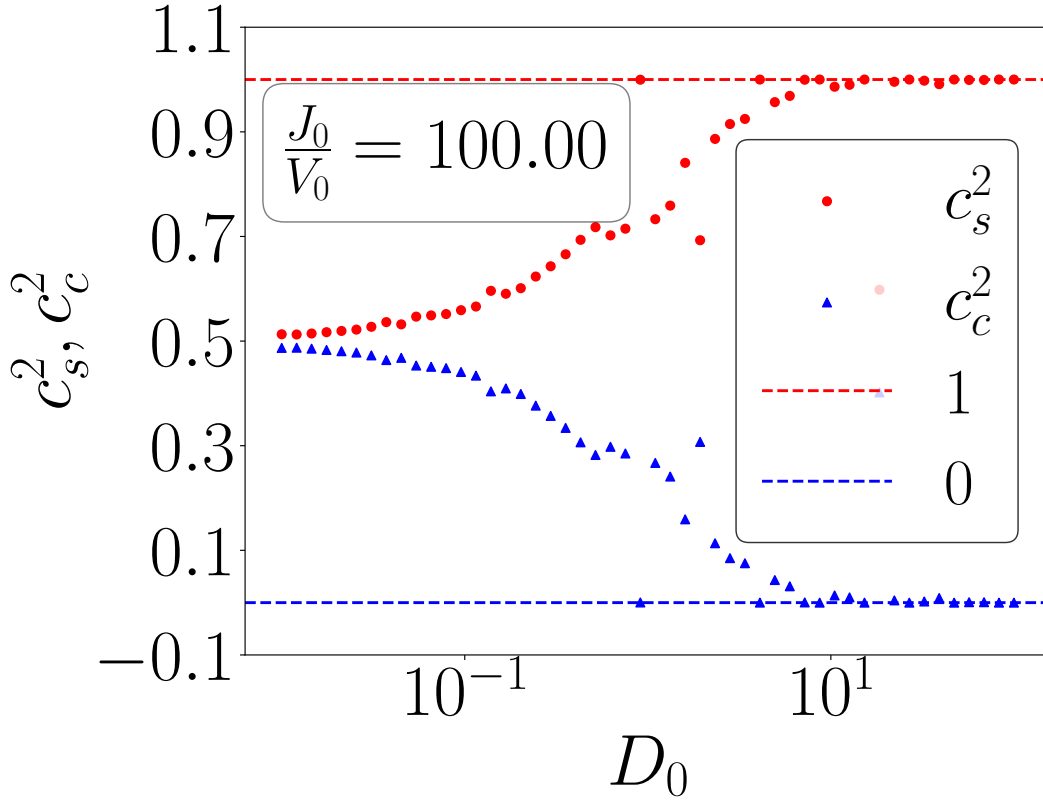
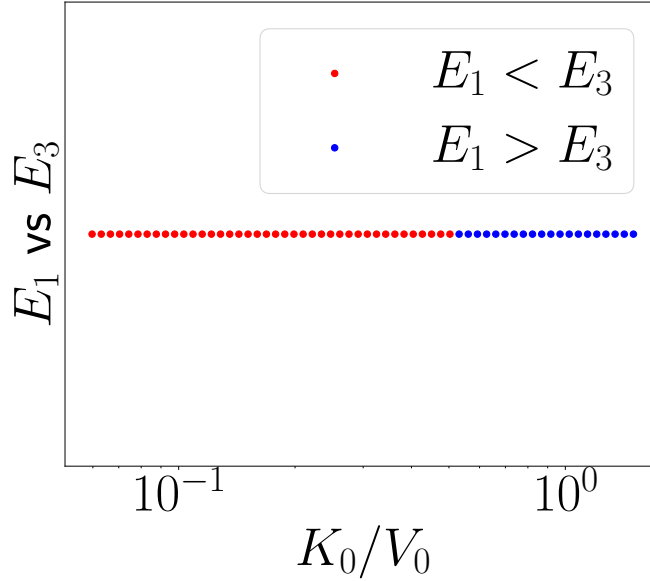
In such a case, $|\Psi\rangle_1$ will therefore be the ground state. In the other regime $V_0 \ll K_0$, the largest energy scale will be K^* , and we can then write

$$E_1 - E_2 \simeq -\frac{1}{8} K^* + \frac{3}{4} K^* > 0 \quad (5.4.9)$$

In this case, the ground state will be $|\Psi\rangle_2$. There exists, therefore, a phase transition at a critical plane (U_c, K_c, V_c) , where the ground state changes between the charge singlet $|\Psi\rangle_2$ and the spin singlet + charge triplet $|\Psi\rangle_1$.

5.5 Approach towards the thermodynamic limit

[Update with V vs D plots]

Figure 5.3: Variation of relative weights c_s and c_c with J_0 

The URG method works strictly on finite systems and leads to finite values of fixed point couplings. The behaviour of the Hamiltonian in the thermodynamic limit can then be determined using finite-size scaling where we increase the bandwidth and decrease the width of each RG step. When applied to the fixed point value of the impurity-bath hybridisation parameter V (fig. 5.4), it can be seen that the fixed point value increases as the system size is increased, implying that the continuum limit of V^* is ∞ . This holds for both $V_0 > J_0$ and $V_0 < J_0$, as shown in the two panels of fig. 5.4.

In a similar manner, we checked the variation of the spin and charge probabilities, c_s and c_c , in the ground

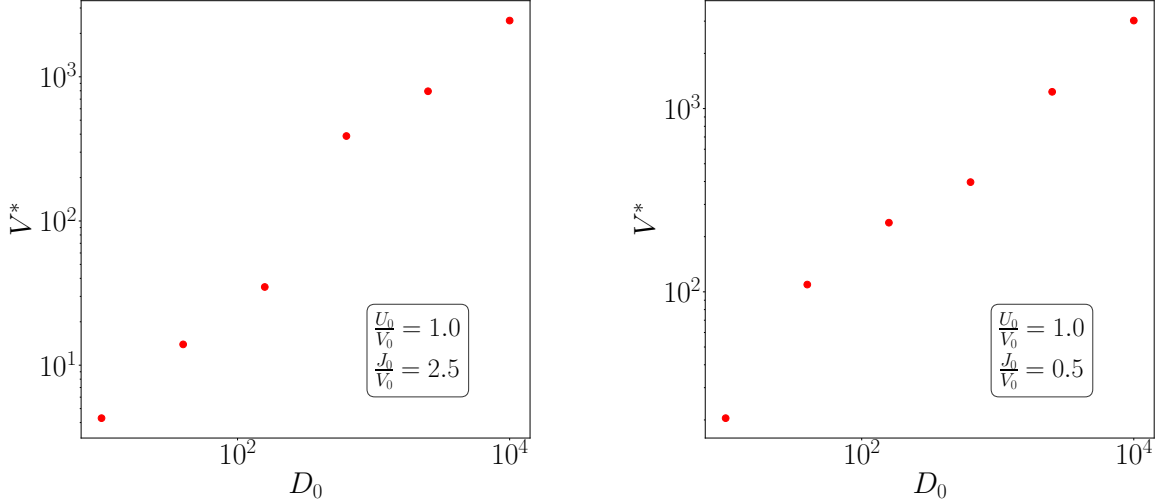


Figure 5.4: Variation of fixed point value V^* with increasing bandwidth D_0 , for both $V_0 > J_0$ and $V_0 < J_0$.

state, with increasing bandwidth. The result is shown in fig. 5.5. For both $V_0 < J_0$ and $V_0 > J_0$, we see that

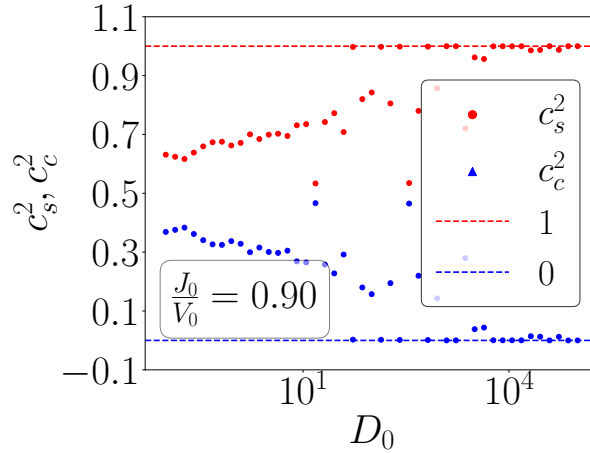


Figure 5.5: Variation of spin and charge fractions, c_s and c_c , of the ground state, as a function of bare bandwidth D_0 . Left and right panels show the cases of $J_0 < V_0$ and $J_0 > V_0$ respectively.

the spin contribution increases towards unity while the charge contribution vanishes. This indicates that at large bandwidth, the ground state becomes purely a spin singlet, formed purely by singly-occupied impurity states.

$$\lim_{D_0 \rightarrow \infty} |\Psi\rangle_1 = \frac{1}{\sqrt{2}} (|\uparrow, \downarrow\rangle - |\downarrow, \uparrow\rangle) \quad (5.5.1)$$

5.6 Effective temperature scale at the fixed point

We will first change the discrete RG equation to a continuum equation by interpreting ΔJ as $\frac{\Delta J}{\Delta \ln D}$, where the denominator is unity: $\Delta \ln D = 1$. Now, since the bandwidth is decreasing under the RG, we can write $\Delta \ln D = -d \ln D$. The continuum equation (for $K = 0$) becomes

$$\frac{dJ}{d \ln D} = n(0) J^2 \frac{1}{\omega - \frac{D}{2} + \frac{J}{4}} \quad (5.6.1)$$

where we have replaced by the number of states at each shell with that at the Fermi surface (uniform DOS). We can define a dimensionless quantity $g \equiv \frac{J}{2} - \omega$. In terms of g , the continuum RG equation becomes

$$-\frac{dg}{d \ln D} + \frac{Dg}{2\omega - D} = \frac{n(0)g^2}{1 - \frac{g}{4}} \quad (5.6.2)$$

Now, for the specific case where D is small ($D \rightarrow 0$), we can simplify and integrate this equation:

$$\begin{aligned} \frac{dg}{d \ln D} &= \frac{n(0)g^2}{\frac{g}{4} - 1} \\ \Rightarrow \left[\frac{1}{g} + \frac{1}{4} \ln g \right]_{g_0}^{g^*} &= n(0) \ln D \Big|_{D_0}^{D^*} \end{aligned} \quad (5.6.3)$$

$g^*(0), D^*(0)$ are the fixed point (bare) values of g, D . From the denominator structure, the fixed-point value is $g^* = 4$. This gives an estimate of the bandwidth of the emergent window:

$$D^* = D_0 \left(\frac{4}{g_0} \right)^{\frac{1}{4n(0)}} \exp \left\{ -\frac{1}{n(0)} \left(\frac{1}{g_0} - \frac{1}{4} \right) \right\} \quad (5.6.4)$$

We can now define a temperature scale [9, 35] for the fixed-point theory:

$$T_K \equiv \frac{2N^*}{\pi} D^* = \frac{2N^*}{\pi} D_0 \left(\frac{4}{g_0} \right)^{\frac{1}{4n(0)}} \exp \left\{ -\frac{1}{n(0)} \left(\frac{1}{g_0} - \frac{1}{4} \right) \right\} \quad (5.6.5)$$

The factor of $2N^*$ is inserted to make the Kondo temperature intensive (we will see below that the N^* allows it to be written in terms of parameters of the two-site Hamiltonian) - $2N^*$ is the total number of momentum states in the fixed point theory. The factor of $\frac{1}{\pi}$ is for aesthetic reasons. Since we have and will primarily work with $\omega = 0$, the fixed point condition can be used to write $D^* = \frac{J^* + K^*}{2}$.

$$T_K = \frac{2N^*}{\pi} \frac{1}{2} (J^* + K^*) = \frac{1}{\pi} (j + k) \quad (5.6.6)$$

5.7 Impurity susceptibilities

5.7.1 Spin susceptibility

The spin susceptibility is defined as

$$\chi(\beta) = \beta \left(\left\langle (S_d^z)^2 \right\rangle - \left\langle S_d^z \right\rangle^2 \right) \quad (5.7.1)$$

There is an alternate way of calculating this. We insert a fictitious magnetic field that couples only to the impurity site. The Hamiltonian in the presence of this field is

$$\mathcal{H}'(B) = \mathcal{H} + BS_d^z \quad (5.7.2)$$

The susceptibility is then given by

$$\chi(\beta) = \lim_{B \rightarrow 0} \frac{1}{\beta} \left[\frac{1}{Z(B)} \frac{\partial^2 Z(B)}{\partial B^2} - \frac{1}{Z(B)^2} \left(\frac{\partial Z(B)}{\partial B} \right)^2 \right] \quad (5.7.3)$$

where $Z(B)$ is the partition function of the Hamiltonian $\mathcal{H}'(B)$. The following is to prove that the RHS of eqs. 5.7.1 and 5.7.3 are the same. We start with 5.7.3. The first derivative can be written as

$$\frac{\partial Z(B)}{\partial B} = \text{Trace} \left[\frac{\partial}{\partial B} \exp \left\{ -\beta (\mathcal{H} + BS_d^z) \right\} \right] = \text{Trace} \left[-\beta S_d^z \exp \left\{ -\beta (\mathcal{H} + BS_d^z) \right\} \right] \quad (5.7.4)$$

which means the first term becomes

$$\lim_{B \rightarrow 0} -\frac{1}{Z(B)^2} \left(\frac{\partial Z(B)}{\partial B} \right)^2 = - \left(\beta \frac{1}{\text{Trace} [\exp \{-\beta \mathcal{H}\}]} \text{Trace} [S_d^z \exp \{-\beta \mathcal{H}\}] \right)^2 = -\beta^2 \langle S_d^z \rangle^2 \quad (5.7.5)$$

The second derivative is

$$\frac{\partial^2 Z(B)}{\partial B^2} = \text{Trace} \left[-\beta S_d^z \frac{\partial}{\partial B} \exp \left\{ -\beta (\mathcal{H} + BS_d^z) \right\} \right] = \text{Trace} \left[\beta^2 (S_d^z)^2 \exp \left\{ -\beta (\mathcal{H} + BS_d^z) \right\} \right] \quad (5.7.6)$$

so the second term becomes

$$\lim_{B \rightarrow 0} \frac{1}{Z(B)} \frac{\partial^2 Z(B)}{\partial B^2} = \beta^2 \frac{1}{\text{Trace} [\exp \{-\beta \mathcal{H}\}]} \text{Trace} [(S_d^z)^2 \exp \{-\beta \mathcal{H}\}] = \beta^2 \langle (S_d^z)^2 \rangle \quad (5.7.7)$$

The full thing becomes

$$\begin{aligned} \lim_{B \rightarrow 0} \frac{1}{\beta} \left[\frac{1}{Z(B)} \frac{\partial^2 Z(B)}{\partial B^2} - \frac{1}{Z(B)^2} \left(\frac{\partial Z(B)}{\partial B} \right)^2 \right] &= \frac{1}{\beta} \left(-\beta^2 \langle S_d^z \rangle^2 + \beta^2 \langle (S_d^z)^2 \rangle \right) \\ &= \beta \left(\langle (S_d^z)^2 \rangle - \langle S_d^z \rangle^2 \right) \end{aligned} \quad (5.7.8)$$

This completes the proof.

To calculate the impurity susceptibility, we take the zero bandwidth Hamiltonian \mathcal{H}_{IR} and insert a magnetic field to obtain the Hamiltonian in eq. (5.7.2). For a particular regime of U , only one of J or K will be non-zero. We then numerically diagonalise this Hamiltonian to obtain the partition function $Z(B)$ and its derivatives. The spin susceptibility can then be calculated using eq. (5.7.3). The results for $U > 0$ are shown in fig. 5.6.

5.7.2 Charge susceptibility

We can similarly define the charge susceptibility as

$$\chi(\beta) = \beta \left(\langle (C_d^z)^2 \rangle - \langle C_d^z \rangle^2 \right) = \lim_{B_c \rightarrow 0} \frac{1}{\beta} \left[\frac{1}{Z(B_c)} \frac{\partial^2 Z(B_c)}{\partial B_c^2} - \frac{1}{Z(B_c)^2} \left(\frac{\partial Z(B_c)}{\partial B_c} \right)^2 \right] \quad (5.7.9)$$

where B_c is now a field that couples to the impurity charge-isospin:

$$\mathcal{H}'(B_c) = \mathcal{H} + B_c C_d^z \quad (5.7.10)$$

The charge susceptibility for $U < 0$ is shown in fig. 5.7.

It is interesting to look at the behaviour of the charge susceptibility in the positive U regime, fig. 5.8. It is seen that for $J_0 < V_0$, the charge susceptibility is very similar to the spin susceptibility, with a reduced saturation value. This is because, for that range of bare values, the ground state consists of a comparable mixture of the spin and charge states (see fig. 5.3). This means that the magnetic field term in eq. (5.7.10) can couple to the charge component of the ground state, and give a non-zero charge susceptibility at zero temperature. On the other hand, for $J_0 > V_0$, we see that χ_c vanishes at low temperatures. This can again be understood from the ground state. For

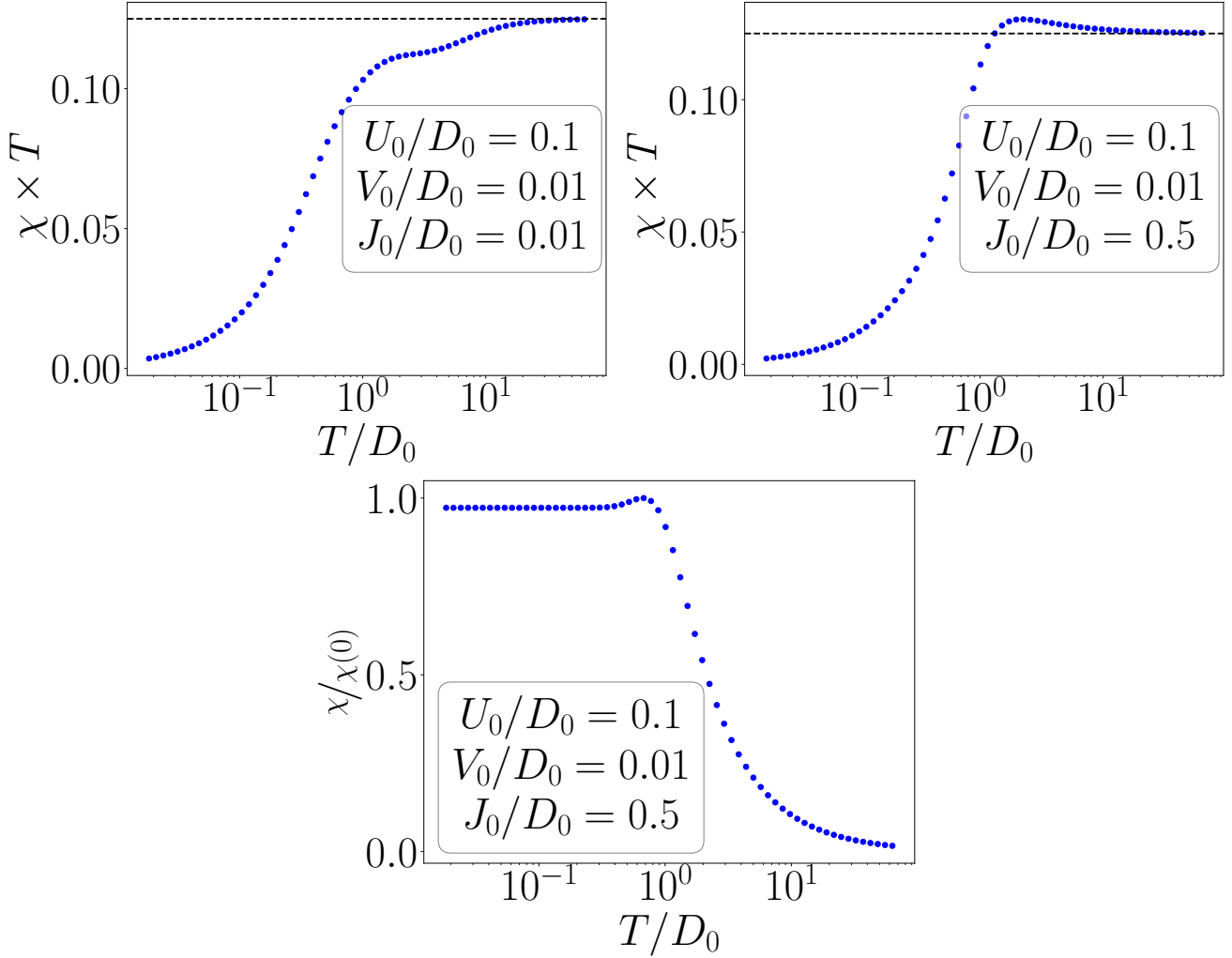


Figure 5.6: Spin susceptibility of the impurity times temperature, for two sets of bare parameters, in $U > 0$. At low temperatures, it becomes linear because χ itself becomes constant (screening), while at high temperatures, $\chi \times T$ becomes constant because of the paramagnetic $\sim 1/T$ form of χ . For the right panel with a larger value of the spin-exchange coupling, the χ tries to go towards the local moment value of $1/4$ but eventually drops back to the free orbital value of $1/8$.

that range of bare values, the ground state can be approximated by purely the singlet, because the charge fraction c_-^c becomes very small. This means that the field B_c has nothing to couple with. Alternatively, it can be said that since the ground state has only terms with $\hat{n}_d = 1$, no number fluctuation is possible, and the impurity isospin is not susceptible at all to charge polarisation.

From eq. (5.5.1), we know that in the thermodynamic limit, the ground state of $U > 0$ regime reduces to a screened local moment. That then implies that the charge susceptibility vanishes at low temperatures, owing to lack of any charge content in the ground state in the large bandwidth limit.

$$\lim_{D_0 \rightarrow \infty} \chi_c(U > 0, T \rightarrow 0) = 0 \quad (5.7.11)$$

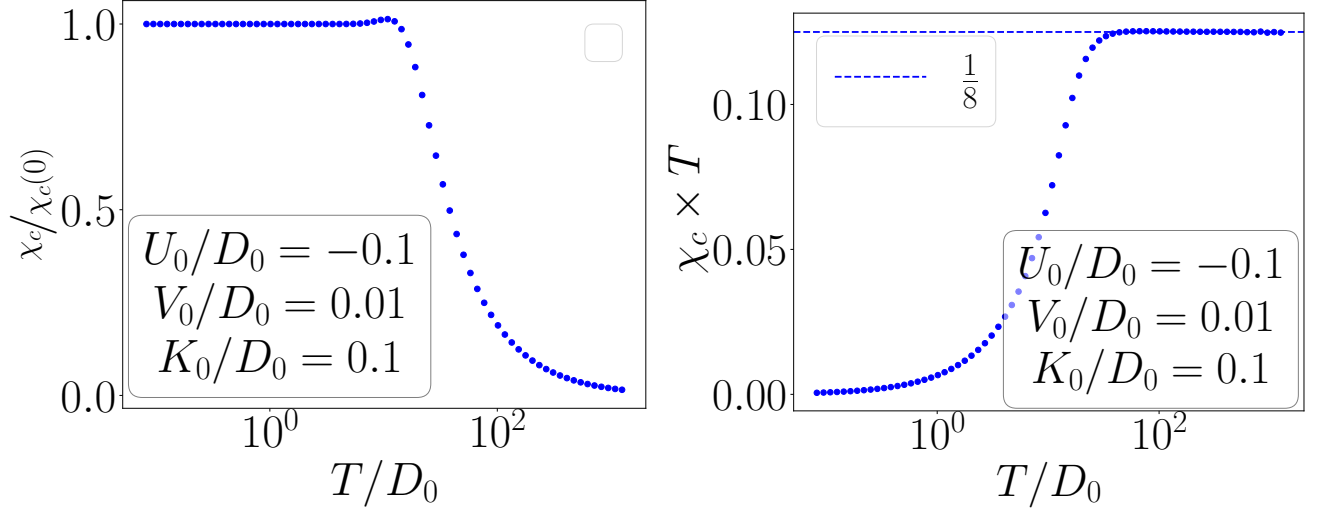


Figure 5.7: Charge susceptibility for the impurity at $U < 0$, for two sets of bare parameters. The physics is very similar to that of the spin susceptibility in $U > 0$.

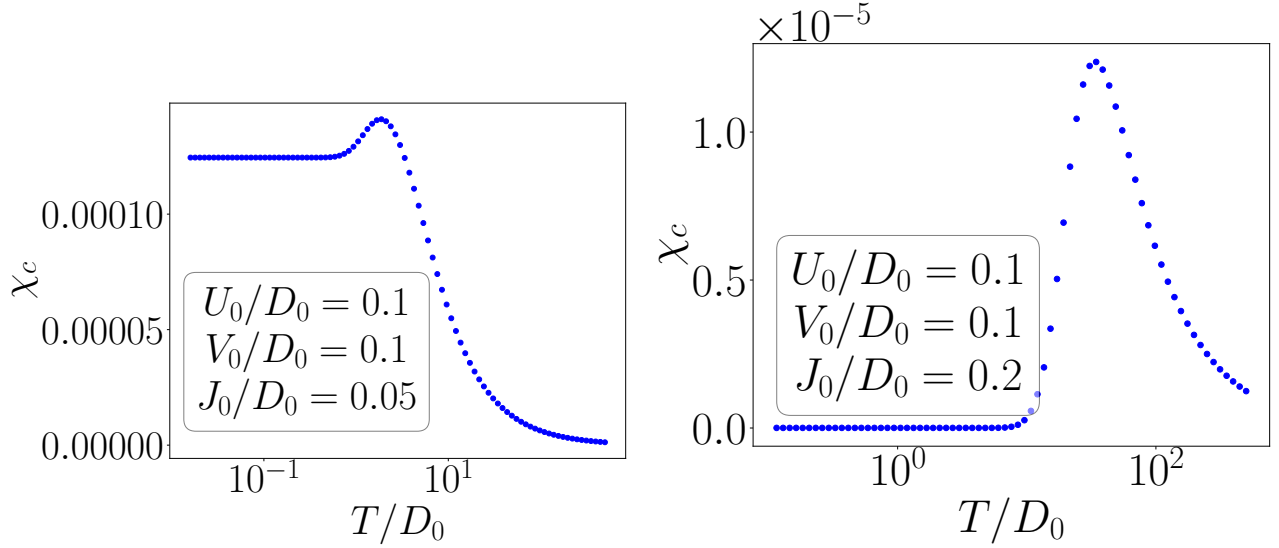


Figure 5.8: Charge susceptibility of the impurity in the positive U regime, for two values of J_0 . The smaller bare value leads to a spin+charge mixed ground state, and hence a non-zero χ_c at zero temperature. The larger J_0 , however, leads to a purely spin ground state without any number fluctuation, and this gives vanishing χ_c at zero temperature.

5.8 Specific heat

The specific heat is calculated by diagonalizing the fixed point Hamiltonian, numerically. The obtained spectrum is denoted by $\{\mathcal{E}_i\}$. The total average energy of the impurity+cloud at temperature T is then

$$\langle \mathcal{E} \rangle = \frac{1}{Z} \sum_i \mathcal{E}_i e^{-\beta \mathcal{E}_i} \quad (5.8.1)$$

where $Z = \sum_i e^{-\beta E_i}$ is the partition function. The specific heat of this system is thus

$$\begin{aligned} C_V &= \frac{\partial \langle \mathcal{E} \rangle}{\partial T} \\ &= -\frac{1}{k_B T^2} \frac{\partial \langle \mathcal{E} \rangle}{\partial \beta} \\ &= \frac{1}{k_B T^2} \left[\frac{1}{Z} \sum_i \mathcal{E}_i^2 e^{-\beta \mathcal{E}_i} - \left(\frac{1}{Z} \sum_i \mathcal{E}_i e^{-\beta \mathcal{E}_i} \right)^2 \right] \end{aligned} \quad (5.8.2)$$

In the absence of impurity, the eigenvalues of the Hamiltonian are $\{\mathcal{E}_i^0\}$ with a partition function $Z^0 = \sum_i e^{-\beta \mathcal{E}_i^0}$, so the bath specific heat is

$$C_V^0 = \frac{1}{k_B T^2} \left[\frac{1}{Z_0} \sum_i \mathcal{E}_i^2 e^{-\beta \mathcal{E}_i^0} - \left(\frac{1}{Z_0} \sum_i \mathcal{E}_i^0 e^{-\beta \mathcal{E}_i^0} \right)^2 \right] \quad (5.8.3)$$

The impurity specific heat is the difference.

$$C_V^{\text{imp}} = C_V - C_V^0 \quad (5.8.4)$$

These values were calculated numerically and plotted against temperature in fig. 5.9.

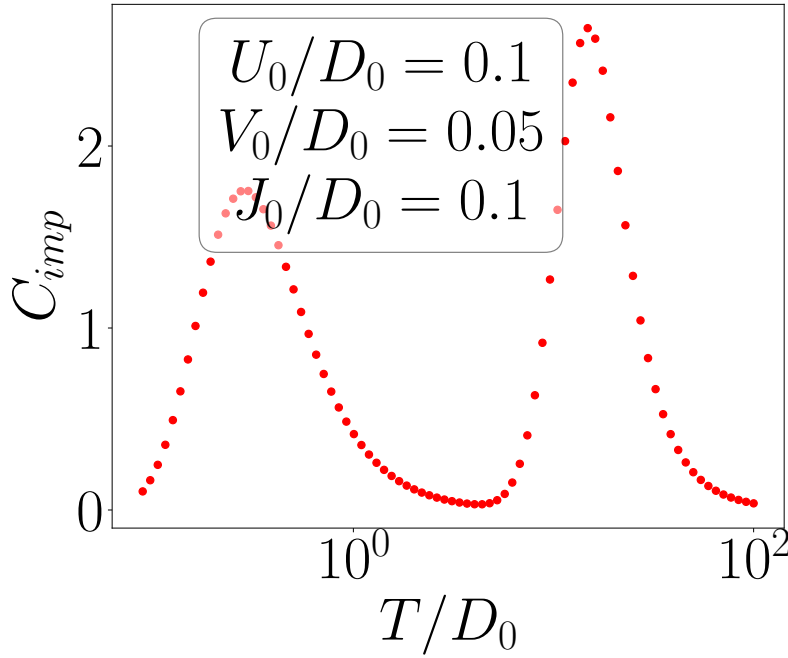


Figure 5.9: Impurity specific heat

5.9 Renormalization of impurity spectral function

In this section we will obtain the impurity spectral function [10, 79, 80], which is defined in terms of the impurity Green's function as

$$\mathcal{A}(\omega) = -\frac{1}{\pi} \text{Im} [G_{dd}^{\sigma}(\omega)] \quad (5.9.1)$$

The zero temperature retarded Green's function for the impurity, in the frequency domain, can be written as (see Appendix. A)

$$\mathcal{A}(\omega) = \frac{1}{d_0} \sum_{n,0} \left[\|\langle 0 | \mathcal{O}_\sigma | n \rangle\|^2 \delta(\omega + E_0 - E_n) + \|\langle n | \mathcal{O}_\sigma | 0 \rangle\|^2 \delta(\omega - E_0 + E_n) \right] \quad (5.9.2)$$

where $\mathcal{O}_\sigma = c_{d\sigma} + S_d^- c_{0\bar{\sigma}} + S_d^z c_{0\sigma}$ is the excitation whose spectral function we are interested in. The excitations defined in \mathcal{O} incorporates both single-particle excitations brought about by the hybridisation as well as two-particle spin excitations brought about by the spin-exchange term. Since this is in terms of the exact eigenstates, it is a discrete sum of delta-functions. In practice, we get a continuous distribution. To compare with experiment, we need to convert the discrete sum into a continuous function. Following [10], we replace the delta-functions at $\pm x_n \equiv \pm(E_n - E_0)$ by normalized Gaussian functions

$$\delta(\omega \pm x_n) \rightarrow \frac{1}{\eta_n \sqrt{\pi}} e^{-\left(\frac{\omega \pm x_n}{\eta_n}\right)^2} \quad (5.9.3)$$

The parameter η_n determines the height and width of the Gaussian, and is chosen such that the higher energy poles are broader than the lower energy ones:

$$\eta_n = 4\Delta + \frac{1}{2}|x_n| \quad (5.9.4)$$

$\Delta = \pi\rho(0)V^2$ is the relevant energy scale for the non-interacting ($U = 0$) problem, $\rho(0)$ being the density of states of the conduction bath at the Fermi energy. As a result, the function that we will numerically compute and plot is

$$\mathcal{A}(\omega) = \sum_{n,0} \frac{1}{d_0 \sqrt{\pi} \eta_n} \left[\|\langle 0 | c_{d\sigma} | n \rangle\|^2 e^{-\left(\frac{\omega - x_n}{\eta_n}\right)^2} + \|\langle n | c_{d\sigma} | 0 \rangle\|^2 e^{-\left(\frac{\omega + x_n}{\eta_n}\right)^2} \right] \quad (5.9.5)$$

From the results of Langreth [81], we know that the spectral function at zero frequency is fixed by the occupancy of the impurity. Since we are in the particle-hole symmetric regime, this occupancy is fixed at 1, and hence so is the spectral function height at $\omega = 0$. This result has been used to fix the spectral function height at the center during the computations. The fixed-point Hamiltonian H^* is diagonalized numerically to obtain $\{E_n, |n\rangle\}$, for various values of the couplings. The intention here is to get an idea of how the spectral function morphs under the RG. Doing an actual reverse RG (described in 5.15) would require us to diagonalize a huge Hamiltonian. We take the simpler route of tuning the U from zero to some large value. This should mimic the journey from the IR theory ($U = 0$) to the UV theory ($U \gg 0$).

The spectral function is plotted for three sets of values in fig. 5.10. For low values of U , the profile is that of a single peak at zero frequency. This is expected because at the low energy effective theory, the high energy Hubbard side bands have been integrated out. As U increases, shoulder-like structures appear on either side of the peak, which finally, at larger U , develop into two side-peaks. This is the microscopic theory, where high energy features are also relevant. The physics of the three peaks can now be looked into. Since the central peak is at zero energy, it has to do with excitations that do not cost any energy. There are two such excitations: excitations within the spin sector and within the charge sector.

$$\begin{array}{ccc} JS_d^- & & KC_d^- \\ |\uparrow\rangle \rightleftharpoons |\downarrow\rangle, & & |\uparrow\rangle \rightleftharpoons |\downarrow\rangle \\ JS_d^+ & & KC_d^+ \end{array} \quad (5.9.6)$$

The thick arrow \uparrow represents the charge isospin. At particle-hole symmetry, both the spin configurations has energy of ϵ_d , while the charge configurations have energy of $2\epsilon_d + U = 0$ and 0 . Hence, no energy is required for these excitations, which is why we see a macroscopic number of cloud electrons resonating with the impurity at the Fermi surface. Also note that if \hat{S}_i and \hat{C}_j are two operators of the spin and charge sector ($i, j \in \{x, y, z\}$), then

$$\hat{S}_i \hat{C}_j = \hat{C}_j \hat{S}_i = 0 \quad (5.9.7)$$

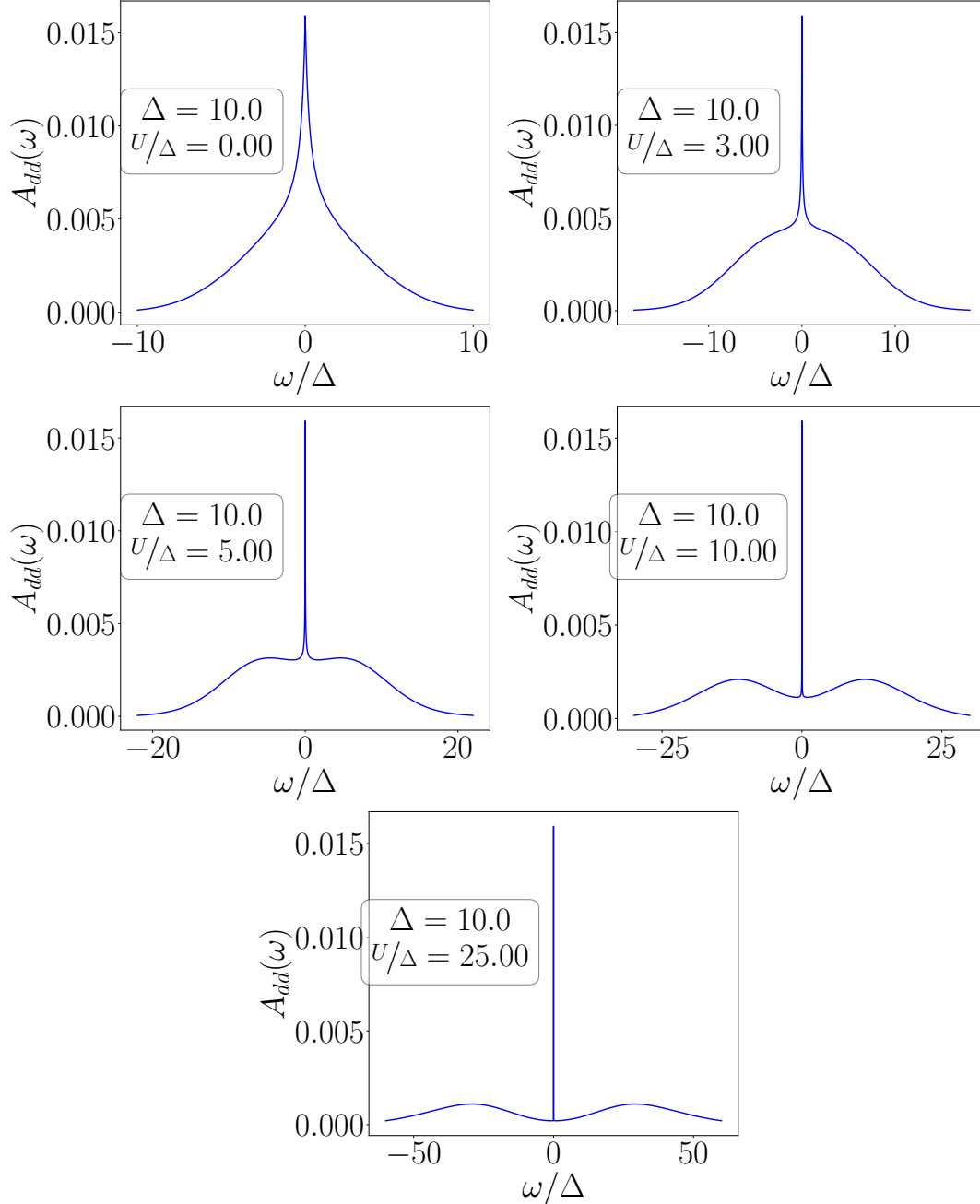


Figure 5.10: Impurity spectral function for multiple values of U . The increase in value of U is accompanied by the appearance of the side-peaks.

We can see this by applying that operator on a basis state. Since the set of four states

$$|\hat{S}_i = \pm \frac{1}{2}, \hat{C}_j = 0\rangle, |\hat{S}_i = 0, \hat{C}_j = \pm \frac{1}{2}\rangle \quad (5.9.8)$$

are all independent, they form a basis. If we apply the operator on these states:

$$\begin{aligned} \hat{S}_i \hat{C}_j |\hat{S}_i\rangle &= 0, & \hat{C}_j \hat{S}_i |S_i\rangle &= S_i \hat{C}_j |S_i\rangle = 0 \\ \hat{C}_j \hat{S}_i |C_j\rangle &= 0, & \hat{S}_i \hat{C}_j |\hat{C}_j\rangle &= C_j \hat{S}_i |\hat{C}_j\rangle = 0 \end{aligned} \quad (5.9.9)$$

This shows that each operator acts only on its own subspace. S_i does not act on the charge sector, and vice-versa.

There is no single-particle excitation here.

The physics of the side-peaks is that of single number fluctuations on the impurity. These are brought about by the term $V c_{0\sigma}^\dagger c_{d\sigma} + \text{h.c.}$

$$(\epsilon_d) |\sigma\rangle \xrightleftharpoons[V c_{d\bar{\sigma}}/V c_{d\sigma}^\dagger]{V c_{d\bar{\sigma}}^\dagger/V c_{d\sigma}} |n_d = 2, 0\rangle (0) \quad (5.9.10)$$

These transitions involve energy transfer of the order of ϵ_d . This is why, at very small U , they remain absorbed inside the central peak. These transitions do not involve any spin or charge-flip, rather they take the impurity between the spin and charge sectors.

5.10 Effective Hamiltonian for excitations of the Kondo cloud

To find an effective Hamiltonian for the excitations of the Kondo cloud, we will integrate out the impurity part of the wavefunction. The Schrodinger equation for the $J > K$ ground state is

$$\begin{aligned} E_g & \left[c_-^s (|\uparrow, \downarrow\rangle - |\downarrow, \uparrow\rangle) + c_-^c (|\uparrow\downarrow, 0\rangle + |0, \uparrow\downarrow\rangle) \right] \\ &= \mathcal{H} \left[c_-^s (|\uparrow, \downarrow\rangle - |\downarrow, \uparrow\rangle) + c_-^c (|\uparrow\downarrow, 0\rangle + |0, \uparrow\downarrow\rangle) \right] \\ &= \mathcal{H}_0^* \left[c_-^s (|\uparrow, \downarrow\rangle - |\downarrow, \uparrow\rangle) + c_-^c (|\uparrow\downarrow, 0\rangle + |0, \uparrow\downarrow\rangle) \right] \\ &+ V \sum_{\beta} \left[c_{2\beta}^\dagger c_{1\beta} - c_{2\beta} c_{1\beta}^\dagger \right] \left[c_-^s (|\uparrow, \downarrow\rangle - |\downarrow, \uparrow\rangle) + c_-^c (|\uparrow\downarrow, 0\rangle + |0, \uparrow\downarrow\rangle) \right] \\ &+ J \vec{S}_d \cdot \vec{s} \left[c_-^s (|\uparrow, \downarrow\rangle - |\downarrow, \uparrow\rangle) + c_-^c (|\uparrow\downarrow, 0\rangle + |0, \uparrow\downarrow\rangle) \right] \\ &+ K \vec{C}_d \cdot \vec{c} \left[c_-^s (|\uparrow, \downarrow\rangle - |\downarrow, \uparrow\rangle) + c_-^c (|\uparrow\downarrow, 0\rangle + |0, \uparrow\downarrow\rangle) \right] \end{aligned} \quad (5.10.1)$$

The last two lines gives

$$\begin{aligned} \frac{1}{2} J c_-^s & \left[s^z (|\uparrow, \downarrow\rangle + |\downarrow, \uparrow\rangle) + s^+ |\downarrow, \downarrow\rangle - s^- |\uparrow, \uparrow\rangle \right] + \frac{1}{2} K c_-^c \left[c^z (|\uparrow\downarrow, 0\rangle - |0, \uparrow\downarrow\rangle) + c^+ |0, 0\rangle \right. \\ & \left. + c^- |2, 2\rangle \right] \end{aligned} \quad (5.10.2)$$

The second line gives

$$\begin{aligned} & V c_{2\uparrow}^\dagger \left[c_-^s (|0, \downarrow\rangle) + c_-^c (|\downarrow, 0\rangle) \right] + V c_{2\downarrow}^\dagger \left[c_-^s (-|0, \uparrow\rangle) + c_-^c (|\uparrow, 0\rangle) \right] \\ & - V c_{2\uparrow} \left[c_-^s (-|\uparrow\downarrow, \uparrow\rangle) + c_-^c (|\uparrow, \uparrow\downarrow\rangle) \right] - V c_{2\downarrow} \left[c_-^s (-|\uparrow\downarrow, \downarrow\rangle) + c_-^c (|\downarrow, \uparrow\downarrow\rangle) \right] \end{aligned} \quad (5.10.3)$$

We will now write down four equations by comparing the coefficients of $|\uparrow\rangle, |\downarrow\rangle, |0\rangle$ and $|2\rangle$ of the impurity sector:

$$\begin{aligned} (E_g - H_0^*) c_-^s |\downarrow\rangle &= V c_-^c (c_{2\downarrow}^\dagger |0\rangle - c_{2\uparrow}^\dagger |2\rangle) + \frac{1}{2} J c_-^s (s^z |\downarrow\rangle - s^- |\uparrow\rangle) \quad [\text{eq. from } |\uparrow\rangle] \\ (-E_g + H_0^*) c_-^s |\uparrow\rangle &= V c_-^c (c_{2\uparrow}^\dagger |0\rangle - c_{2\downarrow}^\dagger |2\rangle) + \frac{1}{2} J c_-^s (s^z |\uparrow\rangle + s^+ |\downarrow\rangle) \quad [\text{eq. from } |\downarrow\rangle] \\ (E_g - H_0^*) c_-^c |2\rangle &= V c_-^s (c_{2\uparrow}^\dagger |\downarrow\rangle - c_{2\downarrow}^\dagger |\uparrow\rangle) + \frac{1}{2} K c_-^c (-c^z |2\rangle + c^+ |0\rangle) \quad [\text{eq. from } |0\rangle] \\ (E_g - H_0^*) c_-^c |0\rangle &= V c_-^s (c_{2\uparrow}^\dagger |\uparrow\rangle + c_{2\downarrow}^\dagger |\downarrow\rangle) + \frac{1}{2} K c_-^c (c^z |0\rangle + c^- |2\rangle) \quad [\text{eq. from } |2\rangle] \end{aligned} \quad (5.10.4)$$

These can be rearranged into

$$\begin{aligned}
\left(E_g - H_0^* - \frac{1}{2}Js^z\right) |\downarrow\rangle &= V\lambda^{-1} \left(c_{2\downarrow}^\dagger |0\rangle - c_{2\uparrow} |2\rangle\right) - \frac{1}{2}Js^- |\uparrow\rangle \\
\left(E_g - H_0^* + \frac{1}{2}Js^z\right) |\uparrow\rangle &= V\lambda^{-1} \left(c_{2\downarrow} |2\rangle - c_{2\uparrow}^\dagger |0\rangle\right) - \frac{1}{2}Js^+ |\downarrow\rangle \\
\left(E_g - H_0^* + \frac{1}{2}Kc^z\right) |2\rangle &= V\lambda \left(c_{2\uparrow}^\dagger |\downarrow\rangle - c_{2\downarrow}^\dagger |\uparrow\rangle\right) + \frac{1}{2}Kc^+ |0\rangle \\
\left(E_g - H_0^* - \frac{1}{2}Kc^z\right) |0\rangle &= V\lambda \left(c_{2\uparrow} |\uparrow\rangle + c_{2\downarrow} |\downarrow\rangle\right) + \frac{1}{2}Kc^- |2\rangle
\end{aligned} \tag{5.10.5}$$

where $\lambda = \frac{c^s}{c^c}$. We want to find the effective Hamiltonian in the subspace of $|\downarrow\rangle$. We first eliminate the charge sector from these equations:

$$\begin{aligned}
|0\rangle &= V\lambda \left[\frac{1}{A_-^K} c_{2\uparrow} + \frac{K}{2} \frac{1}{A_-^K} c^- \frac{1}{A_+^K - \left(\frac{K}{2}\right)^2 c^+ \frac{1}{A_-^K} c^-} \left(\frac{K}{2} c^+ \frac{1}{A_-^K} c_{2\uparrow} - c_{2\downarrow}^\dagger \right) \right] |\uparrow\rangle \\
&\quad + V\lambda \left[\frac{1}{A_-^K} c_{2\downarrow} + \frac{K}{2} \frac{1}{A_-^K} c^- \frac{1}{A_+^K - \left(\frac{K}{2}\right)^2 c^+ \frac{1}{A_-^K} c^-} \left(c_{2\uparrow}^\dagger + \frac{K}{2} c^+ \frac{1}{A_-^K} c_{2\downarrow} \right) \right] |\downarrow\rangle \\
|2\rangle &= \frac{V\lambda}{A_+^K - \left(\frac{K}{2}\right)^2 c^+ \frac{1}{A_-^K} c^-} \left[\left(c_{2\uparrow}^\dagger + \frac{K}{2} c^+ \frac{1}{A_-^K} c_{2\downarrow} \right) |\downarrow\rangle + \left(\frac{K}{2} c^+ \frac{1}{A_-^K} c_{2\uparrow} - c_{2\downarrow}^\dagger \right) |\uparrow\rangle \right]
\end{aligned} \tag{5.10.6}$$

where

$$A_\pm^K = E_g - H_0^* \pm \frac{1}{2}Kc^z \tag{5.10.7}$$

For ease of labeling, we will think of these equations as

$$|0\rangle = a_0^\uparrow |\uparrow\rangle + a_0^\downarrow |\downarrow\rangle, |2\rangle = a_2^\uparrow |\uparrow\rangle + a_2^\downarrow |\downarrow\rangle \tag{5.10.8}$$

The remaining two equations can then be written as

$$\begin{aligned}
A_-^J |\downarrow\rangle &= \frac{V}{\lambda} \left[c_{2\downarrow}^\dagger \left(a_0^\uparrow |\uparrow\rangle + a_0^\downarrow |\downarrow\rangle \right) - c_{2\uparrow} \left(a_2^\uparrow |\uparrow\rangle + a_2^\downarrow |\downarrow\rangle \right) \right] - \frac{J}{2} s^- |\uparrow\rangle \\
A_+^J |\uparrow\rangle &= \frac{V}{\lambda} \left[c_{2\downarrow} \left(a_2^\uparrow |\uparrow\rangle + a_2^\downarrow |\downarrow\rangle \right) - c_{2\uparrow}^\dagger \left(a_0^\uparrow |\uparrow\rangle + a_0^\downarrow |\downarrow\rangle \right) \right] - \frac{J}{2} s^+ |\downarrow\rangle
\end{aligned} \tag{5.10.9}$$

where

$$A_\pm^J = E_g - H_0^* \pm \frac{1}{2}Js^z \tag{5.10.10}$$

Eliminating $|\downarrow\rangle$ and solving for $|\uparrow\rangle$ gives

$$\begin{aligned}
A_+^J |\uparrow\rangle &= \frac{V}{\lambda} \left(c_{2\downarrow} a_2^\uparrow - c_{2\uparrow}^\dagger a_0^\uparrow \right) |\uparrow\rangle + \left(\frac{V}{\lambda} c_{2\downarrow} a_2^\downarrow - \frac{V}{\lambda} c_{2\uparrow}^\dagger a_0^\downarrow - \frac{J}{2} s^+ \right) |\downarrow\rangle \\
&= \frac{V}{\lambda} \left(c_{2\downarrow} a_2^\uparrow - c_{2\uparrow}^\dagger a_0^\uparrow \right) |\uparrow\rangle \\
&\quad + \left[\frac{V}{\lambda} \left(c_{2\downarrow} a_2^\downarrow - c_{2\uparrow}^\dagger a_0^\downarrow \right) - \frac{J}{2} s^+ \right] \frac{1}{A_-^J - \frac{V}{\lambda} \left(c_{2\downarrow}^\dagger a_0^\downarrow - c_{2\uparrow} a_2^\downarrow \right)} \left[\frac{V}{\lambda} \left(c_{2\downarrow}^\dagger a_0^\uparrow - c_{2\uparrow} a_2^\uparrow \right) - \frac{J}{2} s^- \right] |\uparrow\rangle
\end{aligned} \tag{5.10.11}$$

The effective Hamiltonian for the $|\uparrow\rangle$ state is

$$H_0^* - \frac{J}{2}s^z + \frac{V}{\lambda} \left(c_{2\downarrow}a_2^\uparrow - c_{2\uparrow}a_0^\uparrow \right) + \left[\frac{V}{\lambda} \left(c_{2\downarrow}a_2^\downarrow - c_{2\uparrow}a_0^\downarrow \right) - \frac{J}{2}s^+ \right] \frac{1}{A_-^J - \frac{V}{\lambda} \left(c_{2\downarrow}a_0^\downarrow - c_{2\uparrow}a_2^\downarrow \right)} \times \left[\frac{V}{\lambda} \left(c_{2\downarrow}a_0^\uparrow - c_{2\uparrow}a_2^\uparrow \right) - \frac{J}{2}s^- \right] \quad (5.10.12)$$

To get a clearer picture of this effective Hamiltonian, we will keep up to two-particle interactions. We first write down the full forms of $a_{0,2}^\sigma$:

$$a_0^\sigma = V\lambda \left[\frac{1}{A_-^K} c_{2\sigma} + \frac{K}{2} \frac{1}{A_-^K} c^- \frac{1}{A_+^K - \left(\frac{K}{2}\right)^2 c^+ \frac{1}{A_-^K} c^-} \left(\frac{K}{2} c^+ \frac{1}{A_-^K} c_{2\sigma} - \sigma c_{2\sigma}^\dagger \right) \right] \quad (5.10.13)$$

$$a_2^\sigma = \frac{V\lambda}{A_+^K - \left(\frac{K}{2}\right)^2 c^+ \frac{1}{A_-^K} c^-} \left(-\sigma c_{2-\sigma}^\dagger + \frac{K}{2} c^+ \frac{1}{A_-^K} c_{2\sigma} \right)$$

We will first look at the special case of $K = 0$. There, the above expressions simplify to

$$a_0^\sigma = V\lambda \frac{1}{A_-^K} c_{2\sigma} = \frac{V\lambda}{E_g} \left[1 + \frac{1}{E_g} (H_0^*) + \frac{1}{E_g^2} (H_0^*)^2 \right] c_{2\sigma} + \mathcal{O}(H_0^{*3}) \quad (5.10.14)$$

$$a_2^\sigma = -\sigma V\lambda \frac{1}{A_+^K} c_{2-\sigma}^\dagger = -\sigma \frac{V\lambda}{E_g} \left[1 + \frac{1}{E_g} (H_0^*) + \frac{1}{E_g^2} (H_0^*)^2 \right] c_{2-\sigma}^\dagger + \mathcal{O}(H_0^{*3})$$

We will make use of the following commutators:

$$\begin{aligned} \left[(H_0^*)^m, c_{2\sigma} \right] &= - \sum_k \frac{\epsilon_k^m}{\sqrt{N^*}} c_{k\sigma}, & \left[(H_0^*)^m, c_{2\sigma}^\dagger \right] &= \sum_k \frac{\epsilon_k^m}{\sqrt{N^*}} c_{k\sigma}^\dagger, & m = 1, 2 \\ \left[(H_0^*)^m, s^+ \right] &= \sum_{kk'} (\epsilon_k^m - \epsilon_{k'}^m) c_{k\beta}^\dagger c_{k'\bar{\beta}}, & m = 1, 2 \\ \left[(s^z)^m, c_{2\sigma} \right] &= - \left(\frac{\sigma}{2} \right)^m c_{2\sigma}, & \left[(s^z)^m, c_{2\sigma}^\dagger \right] &= \left(\frac{\sigma}{2} \right)^m c_{2\sigma}^\dagger, & m = 1, 2 \\ \left[(c^z)^m, c_{2\sigma} \right] &= - \left(\frac{1}{2} \right)^m c_{2\sigma}, & \left[(c^z)^m, c_{2\sigma}^\dagger \right] &= \left(\frac{1}{2} \right)^m c_{2\sigma}^\dagger, & m = 1, 2 \end{aligned} \quad (5.10.15)$$

Now we evaluate the various terms in the effective Hamiltonian.

$$\begin{aligned} c_{2\downarrow}a_2^\uparrow &= -\frac{V\lambda}{E_g} c_{2\downarrow} \left[1 + \frac{1}{E_g} (H_0^*) + \frac{1}{E_g^2} (H_0^*)^2 \right] c_{2\downarrow}^\dagger \\ &= -\frac{V\lambda}{E_g} \left[c_{2\downarrow} + \frac{1}{E_g} (H_0^*) c_{2\downarrow} + \sum_k \frac{\epsilon_k}{E_g \sqrt{N^*}} c_{k\downarrow} + \frac{1}{E_g^2} (H_0^*)^2 c_{2\downarrow} + \sum_k \frac{\epsilon_k^2}{E_g^2 \sqrt{N^*}} c_{k\downarrow} \right] c_{2\downarrow}^\dagger \\ &= -\frac{V\lambda}{E_g} \left[1 + \frac{H_0^*}{E_g} + \left(\frac{H_0^*}{E_g} \right)^2 \right] c_{2\downarrow} c_{2\downarrow}^\dagger - \frac{V\lambda}{E_g N^*} \sum_{kk'} \left(\frac{\epsilon_k}{E_g} + \frac{\epsilon_k^2}{E_g^2} \right) c_{k\downarrow} c_{k'\downarrow}^\dagger \\ c_{2\uparrow}a_2^\downarrow &= -\frac{V\lambda}{E_g} \left[1 + \frac{H_0^*}{E_g} + \left(\frac{H_0^*}{E_g} \right)^2 \right] c_{2\uparrow} c_{2\uparrow}^\dagger - \frac{V\lambda}{E_g N^*} \sum_{kk'} \left(\frac{\epsilon_k}{E_g} + \frac{\epsilon_k^2}{E_g^2} \right) c_{k\uparrow} c_{k'\uparrow}^\dagger \end{aligned}$$

$$\begin{aligned}
c_{2\uparrow}^\dagger a_0^\uparrow &= c_{2\uparrow}^\dagger \frac{V\lambda}{E_g} \left[1 + \frac{1}{E_g} (H_0^*) + \frac{1}{E_g^2} (H_0^*)^2 \right] c_{2\uparrow} \\
&= \frac{V\lambda}{E_g} \left[1 + \frac{H_0^*}{E_g} + \left(\frac{H_0^*}{E_g} \right)^2 \right] c_{2\uparrow}^\dagger c_{2\uparrow} - \frac{V\lambda}{E_g N^*} \sum_{kk'} \left(\frac{\epsilon_k}{E_g} + \frac{\epsilon_k^2}{E_g^2} \right) c_{k\uparrow}^\dagger c_{k'\uparrow} \\
c_{2\downarrow}^\dagger a_0^\downarrow &= \frac{V\lambda}{E_g} \left[1 + \frac{H_0^*}{E_g} + \left(\frac{H_0^*}{E_g} \right)^2 \right] c_{2\downarrow}^\dagger c_{2\downarrow} - \frac{V\lambda}{E_g N^*} \sum_{kk'} \left(\frac{\epsilon_k}{E_g} + \frac{\epsilon_k^2}{E_g^2} \right) c_{k\downarrow}^\dagger c_{k'\downarrow} \\
c_{2\downarrow}^\dagger a_2^\downarrow &= \frac{V\lambda}{E_g} c_{2\downarrow}^\dagger \left[1 + \frac{1}{E_g} (H_0^*) + \frac{1}{E_g^2} (H_0^*)^2 \right] c_{2\uparrow}^\dagger \\
&= \frac{V\lambda}{E_g} \left[1 + \frac{1}{E_g} (H_0^*) \right] c_{2\downarrow}^\dagger c_{2\uparrow}^\dagger + \frac{V\lambda}{E_g N^*} \sum_{kk'} \left(\frac{\epsilon_k}{E_g} + \frac{\epsilon_k^2}{E_g^2} \right) c_{k\downarrow}^\dagger c_{k'\uparrow}^\dagger \\
c_{2\uparrow}^\dagger a_2^\uparrow &= -\frac{V\lambda}{E_g} \left[1 + \frac{1}{E_g} (H_0^*) \right] c_{2\uparrow}^\dagger c_{2\downarrow}^\dagger - \frac{V\lambda}{E_g N^*} \sum_{kk'} \left(\frac{\epsilon_k}{E_g} + \frac{\epsilon_k^2}{E_g^2} \right) c_{k\uparrow}^\dagger c_{k'\downarrow}^\dagger \\
c_{2\uparrow}^\dagger a_0^\downarrow &= \frac{V\lambda}{E_g} \left[1 + \frac{H_0^*}{E_g} \right] c_{2\uparrow}^\dagger c_{2\downarrow} - \frac{V\lambda}{E_g N^*} \sum_{kk'} \left(\frac{\epsilon_k}{E_g} + \frac{\epsilon_k^2}{E_g^2} \right) c_{k\uparrow}^\dagger c_{k'\downarrow} \\
c_{2\downarrow}^\dagger a_0^\uparrow &= \frac{V\lambda}{E_g} \left[1 + \frac{H_0^*}{E_g} \right] c_{2\downarrow}^\dagger c_{2\uparrow} - \frac{V\lambda}{E_g N^*} \sum_{kk'} \left(\frac{\epsilon_k}{E_g} + \frac{\epsilon_k^2}{E_g^2} \right) c_{k\downarrow}^\dagger c_{k'\uparrow} \\
c_{2\downarrow}^\dagger a_2^\uparrow - c_{2\uparrow}^\dagger a_0^\uparrow &= -\frac{V\lambda}{E_g} \left[1 + \frac{H_0^*}{E_g} + \left(\frac{H_0^*}{E_g} \right)^2 \right] \times 2 + \frac{V\lambda}{E_g N^*} \sum_{kk'} \left(\frac{\epsilon_k}{E_g} + \frac{\epsilon_k^2}{E_g^2} \right) (c_{k\uparrow}^\dagger c_{k'\uparrow} - c_{k\downarrow}^\dagger c_{k'\downarrow}) \\
c_{2\downarrow}^\dagger a_2^\downarrow - c_{2\uparrow}^\dagger a_0^\downarrow &= \frac{V\lambda}{E_g} \left[1 + \frac{1}{E_g} (H_0^*) \right] c_{2\downarrow}^\dagger c_{2\uparrow}^\dagger \times 2 + \frac{V\lambda}{E_g N^*} \sum_{kk'} \left(\frac{\epsilon_k}{E_g} + \frac{\epsilon_k^2}{E_g^2} \right) (c_{k\downarrow}^\dagger c_{k'\uparrow} + c_{k\uparrow}^\dagger c_{k'\downarrow}) \\
c_{2\downarrow}^\dagger a_0^\downarrow - c_{2\uparrow}^\dagger a_2^\downarrow &= \frac{V\lambda}{E_g N^*} \sum_{kk'} \left(\frac{\epsilon_k}{E_g} + \frac{\epsilon_k^2}{E_g^2} \right) (c_{k\uparrow}^\dagger c_{k'\uparrow} - c_{k\downarrow}^\dagger c_{k'\downarrow}) \\
c_{2\downarrow}^\dagger a_0^\uparrow - c_{2\uparrow}^\dagger a_2^\uparrow &= \frac{V\lambda}{E_g N^*} \sum_{kk'} \left(\frac{\epsilon_k}{E_g} + \frac{\epsilon_k^2}{E_g^2} \right) (c_{k\uparrow}^\dagger c_{k'\downarrow} - c_{k\downarrow}^\dagger c_{k'\uparrow})
\end{aligned}$$

In all the expressions, we have dropped terms that have more than 4 operators in product. Also, in the last four equations, we have substituted $\hat{n}_{2\uparrow} - \hat{n}_{2\downarrow} = 1$, because this is the effective Hamiltonian for the state with $s^z = \frac{1}{2}$.

We now substitute these expressions into the effective Hamiltonian:

$$\begin{aligned}
H_0^* - \frac{J}{2}s^z - \frac{2V^2}{E_g} \left[1 + \frac{H_0^*}{E_g} + \left(\frac{H_0^*}{E_g} \right)^2 \right] &+ \frac{V^2}{E_g N^*} \sum_{kk'} \xi_k \left(c_{k\uparrow}^\dagger c_{k'\uparrow} - c_{k\downarrow}^\dagger c_{k'\downarrow} \right) \\
&+ \left[\frac{V}{\lambda} \left(c_{2\downarrow} a_2^\downarrow - c_{2\uparrow}^\dagger a_0^\downarrow \right) \right] \frac{1}{A_-^J - \frac{V^2}{E_g N^*} \sum_{kk'} \xi_k \left(c_{k\uparrow}^\dagger c_{k'\uparrow} - c_{k\downarrow}^\dagger c_{k'\downarrow} \right)} \left[\frac{V}{\lambda} \left(c_{2\downarrow}^\dagger a_0^\uparrow - c_{2\uparrow} a_2^\uparrow \right) \right] \\
&+ \left[\frac{V}{\lambda} \left(c_{2\downarrow} a_2^\downarrow - c_{2\uparrow}^\dagger a_0^\downarrow \right) \right] \frac{1}{A_-^J - \frac{V^2}{E_g N^*} \sum_{kk'} \xi_k \left(c_{k\uparrow}^\dagger c_{k'\uparrow} - c_{k\downarrow}^\dagger c_{k'\downarrow} \right)} \left[-\frac{J}{2}s^- \right] \\
&+ \left[-\frac{J}{2}s^+ \right] \frac{1}{A_-^J - \frac{V^2}{E_g N^*} \sum_{kk'} \xi_k \left(c_{k\uparrow}^\dagger c_{k'\uparrow} - c_{k\downarrow}^\dagger c_{k'\downarrow} \right)} \left[\frac{V}{\lambda} \left(c_{2\downarrow}^\dagger a_0^\uparrow - c_{2\uparrow} a_2^\uparrow \right) \right] \\
&+ \frac{J^2}{4} \left[s^+ \right] \frac{1}{A_-^J - \frac{V^2}{E_g N^*} \sum_{kk'} \xi_k \left(c_{k\uparrow}^\dagger c_{k'\uparrow} - c_{k\downarrow}^\dagger c_{k'\downarrow} \right)} \left[s^- \right]
\end{aligned} \tag{5.10.16}$$

where $\xi_k = \frac{\epsilon_k}{E_g} + \frac{\epsilon_k^2}{E_g^2}$. We first consider only zeroth order terms of the central propagator.

$$\begin{aligned}
H_0^* - \frac{J}{2} \underbrace{s^z}_{\frac{1}{2}} - \frac{2V^2}{E_g} \left[1 + \frac{H_0^*}{E_g} + \left(\frac{H_0^*}{E_g} \right)^2 \right] &+ \frac{V^2}{E_g N^*} \sum_{kk'} (\xi_k) \left(c_{k\uparrow}^\dagger c_{k'\uparrow} - c_{k\downarrow}^\dagger c_{k'\downarrow} \right) \\
&+ \frac{V^4}{E_g^2 N^{*2} \left(E_g + \frac{J}{4} \right)} \sum_{kk'} (\xi_{k'} + 2 - \xi_k) c_{k\uparrow}^\dagger c_{k'\downarrow} \sum_{kk'} (\xi_k + \xi_{k'}) c_{k\downarrow}^\dagger c_{k'\uparrow} \\
&+ \frac{V^2 J}{2E_g \left(E_g + \frac{J}{4} \right) N^*} \sum_{kk'} (\xi_{k'} + 2 - \xi_k) c_{k\uparrow}^\dagger c_{k'\downarrow} \sum_{kk'} c_{k\downarrow}^\dagger c_{k'\uparrow} \\
&+ \frac{J V^2}{2E_g \left(E_g + \frac{J}{4} \right) N^*} \sum_{kk'} c_{k\uparrow}^\dagger c_{k'\downarrow} \sum_{kk'} (\xi_k + \xi_{k'}) c_{k\downarrow}^\dagger c_{k'\uparrow} \\
&+ \frac{J^2}{4 \left(E_g + \frac{J}{4} \right)} \underbrace{s^+ s^-}_{s^z + \frac{1}{2} = 1}
\end{aligned} \tag{5.10.17}$$

We have set $s^z = -\frac{1}{2}$ in the denominator, hence the $E_g = \frac{J}{4}$. If we also consider the first and second order terms from the central propagator, note that they will produce terms of more than quartic interactions in the first three terms. For the last term, we get

$$\frac{J^2}{4 \left(E_g + \frac{J}{4} \right)} s^+ \left[\frac{H_0^*}{E_g + \frac{J}{4}} + \left(\frac{H_0^*}{E_g + \frac{J}{4}} \right)^2 \right] s^- \tag{5.10.18}$$

Using the commutator of H_0^* with s^+ to bring H_0^* to the left, and using $s^+ s^- = s^z + \frac{1}{2} = 1$, we get

$$\frac{J^2}{4 \left(E_g + \frac{J}{4} \right)} \left[\frac{H_0^*}{E_g + \frac{J}{4}} + \left(\frac{H_0^*}{E_g + \frac{J}{4}} \right)^2 - \sum_{kk'qq'} \left(\xi_k^J - \xi_{k'}^J \right) c_{k\uparrow}^\dagger c_{k'\downarrow} c_{q\downarrow}^\dagger c_{q'\uparrow} \right] \tag{5.10.19}$$

where $\xi_k^J = \frac{\epsilon_k}{E_g + \frac{J}{4}} + \frac{\epsilon_k^2}{(E_g + \frac{J}{4})^2}$. The full effective Hamiltonian, for $K = 0$, up to quartic interactions, is

$$\begin{aligned} H_0^* + \frac{J}{4} \left(\frac{J}{E_g + \frac{J}{4}} - 1 \right) - \frac{2V^2}{E_g} + \frac{V^2}{E_g N^*} \sum_{kk'} (\xi_k) (c_{k\uparrow}^\dagger c_{k'\uparrow} - c_{k\downarrow} c_{k'\downarrow}^\dagger) - \frac{2V^2}{E_g} \left[\frac{H_0^*}{E_g} + \left(\frac{H_0^*}{E_g} \right)^2 \right] \\ + \frac{J^2}{4 \left(E_g + \frac{J}{4} \right)} \left[\frac{H_0^*}{E_g + \frac{J}{4}} + \left(\frac{H_0^*}{E_g + \frac{J}{4}} \right)^2 \right] + \sum_{kk'qq'} F_{kk'qq'} c_{k\uparrow}^\dagger c_{k'\downarrow} c_{q\downarrow}^\dagger c_{q'\uparrow} \end{aligned} \quad (5.10.20)$$

The coefficient $F_{kk'qq'}$ is

$$\begin{aligned} F_{kk'qq'} = \frac{V^2}{E_g N^* (E_g + \frac{J}{4})} \left[\frac{V^2}{E_g N^*} (\xi_{k'} + 2 - \xi_k) (\xi_q + \xi_{q'}) + \frac{J}{2} (\xi_{k'} + 2 - \xi_k + \xi_q + \xi_{q'}) \right] \\ + \frac{J^2}{4 \left(E_g + \frac{J}{4} \right)} (\xi_{k'}^J - \xi_k^J) \end{aligned} \quad (5.10.21)$$

There are two main types of interactions that gets generated upon integrating out the impurity. One is the Fermi liquid type interactions arising from the H_0^{*2} terms. The Fermi liquid part of the Hamiltonian is

$$\begin{aligned} \left[\frac{J^2}{4 \left(E_g + \frac{J}{4} \right)^2} - \frac{2V^2}{E_g^2} \right] H_0^* + \left[\frac{J^2}{4 \left(E_g + \frac{J}{4} \right)^2} - \frac{2V^2}{E_g^3} \right] H_0^{*2} \\ = \left[\frac{J^2}{4 \left(E_g + \frac{J}{4} \right)^2} - \frac{2V^2}{E_g^2} \right] \left[H_0^* + \sum_{kk'\sigma\sigma'} f_{kk'} \hat{n}_{k\sigma} \hat{n}_{k'\sigma'} \right] \end{aligned} \quad (5.10.22)$$

where the Landau parameter is given by

$$f_{kk'} = \left[\frac{J^2}{4 \left(E_g + \frac{J}{4} \right)^2} - \frac{2V^2}{E_g^2} \right]^{-1} \left[\frac{J^2}{4 \left(E_g + \frac{J}{4} \right)^3} - \frac{2V^2}{E_g^3} \right] \epsilon_k \epsilon_{k'} \quad (5.10.23)$$

The more interesting interaction is the off-diagonal term

$$\sum_{kk'qq'} F_{kk'qq'} c_{k\uparrow}^\dagger c_{k'\downarrow} c_{q\downarrow}^\dagger c_{q'\uparrow} \quad (5.10.24)$$

This interaction arises from the enhanced entanglement between the impurity and the conduction electrons; removing the impurity from the singlet and the triplet generates these off-diagonal scatterings. As such, this is an indicator of the macroscopic entanglement of the singlet formed at the IR fixed point, and plotted in fig. 5.13.

We also wish to point out that this scattering is a signature of the change in Luttinger's count in going from the free orbital or local moment fixed point to the strong coupling fixed point, as shown in eq. (5.14.22). Both this off-diagonal scattering as well as the change in Luttinger's count are a direct consequence of the non-number conserving term $V c_k^\dagger c_d$ in the full Hamiltonian. The topological change of Luttinger's count is concomitant with the presence of the off-diagonal scattering term in the effective Hamiltonian. *Just the Fermi liquid piece in eq. (5.10.23) will give neither the enhanced mutual information nor the change in Luttinger's count.*

5.11 Obtaining the real space low energy Hamiltonian: the local Fermi liquid

The next step is to obtain the lowest excitations of the fixed point Hamiltonian, in real space. We will work in the $U > 0$ regime. For $V, J \gg 1$, the impurity couples very strongly with the zeroth site, and at zeroth order, it suffices to say that the zeroth site decouples from the rest of the lattice. This zeroth Hamiltonian then consists of two sites interacting with each other through V and J (the two site problem analysed before).

$$H_0^* = \sum_{\sigma} \left(V^* c_{0\sigma}^{\dagger} c_{d\sigma} + \text{h.c.} \right) + J^* \vec{S}_d \cdot \vec{s} - \frac{1}{2} U^* \left(\hat{n}_{d\uparrow} - \hat{n}_{d\downarrow} \right)^2 \quad (5.11.1)$$

$$|\Psi\rangle_1 = c_s \frac{1}{\sqrt{2}} (|\uparrow, \downarrow\rangle - |\downarrow, \uparrow\rangle) + c_c \frac{1}{\sqrt{2}} (|\uparrow\downarrow, 0\rangle + |0, \uparrow\downarrow\rangle), \quad E_1 = -V^* \sqrt{\gamma^2 + 4} - \frac{1}{4} U^* - \frac{3}{8} J^* \quad (5.11.2)$$

These were obtained in eq. (5.4.5). The quantities γ and $c_{s,c}$ were defined in and around eq. (5.4.6).

We start with the ground state $|\Psi\rangle_1$ and the star graph as the zeroth level ground state and Hamiltonian, and then add a nearest-neighbour hopping term as a perturbation of the zeroth Hamiltonian. We know that the ground state for the interacting part is predominantly the spin-singlet (it was shown while calculating the ground states of the effective zero-mode Hamiltonian that the ground state is a mixture of singlet and triplet, and the triplet part dies out at large system sizes, see eq. (5.5.1)), so we will take that as our reference state and treat the hopping part that connects the origin to the first site,

$$H_X = t \sum_{\vec{r}_1, \sigma} c_{0\sigma}^{\dagger} c_{\vec{r}_1, \sigma} + \text{h.c.} \equiv v^{\dagger} + v \quad (5.11.3)$$

as a weak perturbation. \vec{r}_1 here sums over the sites that are nearest to the origin. Once this perturbation is taken care of up to a certain order, we will have a decoupled singlet formed by the impurity and the zeroth site, and the rest of the lattice formed by $N - 1$ sites along with the interaction induced by the perturbation. To be precise, the goal is to integrate out the perturbation and generate an effective Hamiltonian in the subspace of the minimal energy states of the two site Hamiltonian, and this effective Hamiltonian will therefore describe the lowest excitations on top of the ground state $|\Psi\rangle_1$. The minimal energy subspace is given by the states:

$$|\Phi\rangle_i = |\Psi\rangle_1 \otimes |\hat{n}_{1\uparrow}, \hat{n}_{1\downarrow}\rangle, \quad \text{where } i \in \begin{cases} 0: & \hat{n}_{1\uparrow} = \hat{n}_{1\downarrow} = 0 \\ 1: & 1 - \hat{n}_{1\uparrow} = \hat{n}_{1\downarrow} = 0 \\ 2: & \hat{n}_{1\uparrow} = 1 - \hat{n}_{1\downarrow} = 0 \\ 3: & 1 - \hat{n}_{1\uparrow} = 1 - \hat{n}_{1\downarrow} = 0 \end{cases} \quad (5.11.4)$$

The effective Hamiltonian will be calculated using perturbation theory in $\frac{H_X^n}{H_0^{*n-1}}$. Since an odd number of scattering processes cannot bring the initial state back to itself, such orders will be absent from the effective Hamiltonian.

5.11.1 Second order effective Hamiltonian

We first consider the case of $n = 2$. The renormalisation of the effective Hamiltonian in the ground state subspace, at this order, is given by

$$\Delta H = \sum_{ij, n} |\Phi\rangle_i \langle \Phi_i| H_X |\Psi\rangle_n \frac{1}{E_{\text{gs}} - E_n} \langle \Psi|_n H_X |\Phi\rangle_j \langle \Phi_j| = \sum_{ij} |\Phi\rangle_i \langle \Phi_j| \langle \Phi_i| v + v^{\dagger} |\Psi\rangle_n \frac{1}{E_{\text{gs}} - E_n} \langle \Psi|_n v + v^{\dagger} |\Phi\rangle_j. \quad (5.11.5)$$

Here, $|\Psi\rangle_n$ are the eigenstates of the two site problem, with eigenvalue E_n . The total scattering process can be described as H_X acting on $|\Phi\rangle_j$ to excite to $|\Psi\rangle_n$, and then a subsequent H_X acting on $|\Psi\rangle_n$ to decay back to $|\Phi\rangle_j$ and into the ground state manifold. Since $|\Phi\rangle_{i,j}$ are eigenstates of the two site Hamiltonian, they are all eigenstates of the total number operator $\hat{n}_{d0} = \sum_{\sigma} (\hat{n}_{d\sigma} + \hat{n}_{0\sigma})$ for the two site model, with eigenvalue 2. Since we are to finally return to the ground state manifold, only those processes in H_X^2 are allowed that conserve \hat{n}_{d0} . These processes are v, v^{\dagger} and v^{\dagger}, v . This also means that the total number of particles on site 1 will remain constant in

the process, and we will have $|\Phi\rangle_i = |\Phi\rangle_j$.

$$\Delta H = \sum_i |\Phi\rangle_i \langle \Phi|_i \frac{1}{E_{\text{gs}} - E_n} \left(\langle \Phi_i | v^\dagger | \Psi \rangle_n \langle \Psi |_n v | \Phi \rangle_i + \langle \Phi_i | v | \Psi \rangle_n \langle \Psi |_n v^\dagger | \Phi \rangle_i \right). \quad (5.11.6)$$

If we define the matrix element $v_{ni} \equiv \langle \Psi |_n v | \Phi \rangle_i$ of v and the excitation energy $\delta E_n = E_n - E_{\text{gs}}$, we can write the renormalisation as

$$\Delta H = \sum_{i,n} \frac{|v_{ni}|^2 + |v_{in}|^2}{-\delta E_n} |\Phi\rangle_i \langle \Phi|_i. \quad (5.11.7)$$

We now look at each $|\Phi_i\rangle$ separately. For $|\Phi_i\rangle = |\Phi\rangle_0 = |\Psi\rangle_1 \otimes |0, 0\rangle$, we can write

$$v^\dagger |\Phi\rangle_i = 0, \quad v |\Phi\rangle_i = \frac{t}{\sqrt{2}} \sum_{\sigma} \bar{\sigma} \left(c_s^- |\sigma, 0\rangle + c_c^- |0, \sigma\rangle \right) |\bar{\sigma}\rangle \quad (5.11.8)$$

The first relation gives $v_{in} = \langle \Phi |_i v | \Psi \rangle_n = \left(\langle \Psi |_n v^\dagger | \Phi \rangle_i \right)^* = 0$. The set of states that give non-zero v_{in}^\dagger are specific elements of the set of eigenstates that have a total of either 1 or 3 electrons on the impurity and zeroth sites:

$$|\Psi\rangle_n = |\Psi\rangle_{\pm, \sigma}^{s, p} = -\sqrt{2} \left(a_{1, \pm} |\sigma, p\rangle + a_{2, \pm} |p, \sigma\rangle \right) \otimes |s\rangle, \quad \sigma = \uparrow, \downarrow, \quad E_{\pm, \sigma}^{s, p} = -\frac{U}{4} \pm \frac{1}{2} \Delta; \quad (5.11.9)$$

here, s is a string from the set $\{0, \uparrow, \downarrow, 2\}$ and represents the configuration of the first site $|s\rangle$ in direct product with the impurity and zeroth site entangled composite state, and p is either 2 or 0 such that $p+1 (= 1 \text{ or } 3)$ represents the total number of electrons on the impurity and zeroth sites. For $|\Phi\rangle_0$, only $s = \bar{\sigma}$ and $p = 0$ give non-zero inner product. The coefficients are defined as $a_{1, \pm} = \frac{4V}{\sqrt{2}\mathcal{N}_{\pm}}$, $a_{2, \pm} = \frac{U \pm 2\Delta}{\sqrt{2}\mathcal{N}_{\pm}}$. The inner product is

$$v_{\pm \sigma, i} = \langle \Psi_{\pm, \sigma}^{\bar{\sigma}, 0} | v | \Phi_i \rangle = \sigma t \left[a_{1, \pm} c_s^- + a_{2, \pm} c_c^- \right] \quad (5.11.10)$$

$\mathcal{N}_{\pm} = \sqrt{16V^2 + (U \pm 2\Delta)^2}$ is the normalisation factor and $\Delta = \frac{1}{2} \sqrt{U^2 + 16V^2}$. The renormalisation for this value of i then becomes

$$(\Delta H)_{i=0} = |\Phi\rangle_0 \langle \Phi|_0 \sum_n \frac{|v_{ni}|^2}{-\delta E_n} = |\Phi\rangle_0 \langle \Phi|_0 \sum_{\sigma, \pm} \frac{|v_{\pm \sigma, i}|^2}{-\delta E_{\pm}^{\sigma}} = -|\Phi\rangle_0 \langle \Phi|_0 2t^2 \sum_{\pm} \frac{[a_{1, \pm} c_s^- + a_{2, \pm} c_c^-]^2}{\delta E_{\pm}^{\sigma}} \quad (5.11.11)$$

where $\delta E_{\pm}^{\sigma} = E_{\pm}^{\sigma} - E_{\text{gs}}$.

For $i = 1$, we have $|\Phi\rangle_1 = |\Psi\rangle_1 \otimes |\uparrow\rangle$. Carrying out a similar calculation above, we get

$$v |\Phi\rangle_1 = t \frac{1}{\sqrt{2}} \left(c_s^- |\uparrow, 0, 2\rangle + c_c^- |0, \uparrow, 2\rangle \right), \quad |\psi\rangle_n = |\Psi\rangle_{\pm, \uparrow}^{2, 0}, \quad v_{ni} = -t \left(c_s^- a_{1, \pm} + c_c^- a_{2, \pm} \right) \quad (5.11.12)$$

$$v^\dagger |\Phi\rangle_1 = t \frac{1}{\sqrt{2}} \left(c_s^- |\uparrow, 2, 0\rangle - c_c^- |2, \uparrow, 0\rangle \right), \quad |\psi\rangle_n = |\Psi\rangle_{\pm, \uparrow}^{0, 2}, \quad v_{in} = -t \left(c_s^- a_{1, \pm} - c_c^- a_{2, \pm} \right) \quad (5.11.13)$$

$$(\Delta H)_{i=1} = -|\Phi\rangle_1 \langle \Phi|_1 2t^2 \sum_{\pm} \frac{a_{1, \pm}^2 c_s^{-2} + a_{2, \pm}^2 c_c^{-2}}{\delta E_{\pm}^{\sigma}} \quad (5.11.14)$$

The total Hamiltonian $H_0^* + H_X$ is invariant under the transformations $c_\sigma^\dagger \rightarrow c_\sigma, t \rightarrow -t$. Since the renormalisation only involves even powers of t , we can conclude that the renormalisation for $i = 2$ and $i = 3$ will be the

same as that of $i = 1$ and $i = 0$ respectively. The total renormalisation at second order is

$$\begin{aligned}\Delta H &= - \sum_{i=0}^3 |\Phi\rangle_i \langle \Phi|_i 2t^2 \sum_{\pm} \frac{a_{1,\pm}^2 c_s^{-2} + a_{2,\pm}^2 c_c^{-2}}{\delta E_{\pm}^{\sigma}} - \left(|\Phi\rangle_0 \langle \Phi|_0 + |\Phi\rangle_3 \langle \Phi|_3 \right) 4t^2 \sum_{\pm} \frac{a_{1,\pm} a_{2,\pm} c_s^{-} c_c^{-}}{\delta E_{\pm}^{\sigma}} \\ &= - \sum_{i=0}^3 |\Phi\rangle_i \langle \Phi|_i t^2 \sum_{\pm} \frac{1}{\mathcal{N}_{\pm}^2} \frac{\left(4V c_s^{-} \right)^2 + (U \pm 2\Delta)^2 c_c^{-2}}{\delta E_{\pm}^{\sigma}} - \left(|\Phi\rangle_0 \langle \Phi|_0 + |\Phi\rangle_3 \langle \Phi|_3 \right) \sum_{\pm} \frac{t^2}{\mathcal{N}_{\pm}^2} \frac{8V c_s^{-} (U \pm 2\Delta) c_c^{-}}{\delta E_{\pm}^{\sigma}}\end{aligned}\quad (5.11.15)$$

Since the $|\hat{n}_{1\sigma}, \hat{n}_{1\bar{\sigma}}\rangle$ form a complete set, we have $\sum_{i=0}^3 |\Phi\rangle_i \langle \Phi|_i = |\Psi\rangle_1 \langle \Psi|_1$, and the first term becomes a constant. The second term is a local Fermi liquid term on the first site:

$$\begin{aligned}\Delta H &= |\Psi\rangle_1 \langle \Psi|_1 \left[\text{constant} - \left\{ \hat{n}_{1\uparrow} \hat{n}_{1\downarrow} + (1 - \hat{n}_{1\uparrow}) (1 - \hat{n}_{1\downarrow}) \right\} \sum_{\pm} \frac{t^2}{\mathcal{N}_{\pm}^2} \frac{8V c_s^{-} (U \pm 2\Delta) c_c^{-}}{\delta E_{\pm}^{\sigma}} \right] \\ &= |\Psi\rangle_1 \langle \Psi|_1 \left[\text{constant} + (\hat{n}_{1\uparrow} - \hat{n}_{1\downarrow})^2 \sum_{\pm} \frac{t^2}{\mathcal{N}_{\pm}^2} \frac{8V c_s^{-} (U \pm 2\Delta) c_c^{-}}{\delta E_{\pm}^{\sigma}} \right]\end{aligned}\quad (5.11.16)$$

In the strong coupling regime, we have $J, V \gg U$, and we can then approximate:

$$\delta E_{\pm}^{\sigma} \simeq \frac{3J}{8} + \sqrt{4V^2 - \left(\frac{3J}{8} \right)^2} \mp V, \quad U \pm 2\Delta \simeq \pm 4V, \quad \text{and} \quad \mathcal{N}_{\pm}^2 \simeq 32V^2 \quad (5.11.17)$$

Substituting this gives

$$\Delta H = |\Psi\rangle_1 \langle \Psi|_1 \left[\text{constant} - (\hat{n}_{1\uparrow} - \hat{n}_{1\downarrow})^2 \frac{2t^2 V c_s^{-} c_c^{-}}{2 \left(\frac{3J}{8} \right)^2 + 3V^2 + \frac{3J}{4} \sqrt{4V^2 - \left(\frac{3J}{8} \right)^2}} \right] \quad (5.11.18)$$

5.11.2 Fourth order effective Hamiltonian

Using fourth order perturbation theory, we can write the effective Hamiltonian renormalisation at that order in the form

$$\begin{aligned}\Delta H &= - \sum_i |\Phi\rangle_i \langle \Phi|_i \left[\sum_{lmn} \frac{\langle \Phi_i | H_X | \Psi_l \rangle \langle \Psi_l | H_X | \Psi_m \rangle \langle \Psi_m | H_X | \Psi_n \rangle \langle \Psi_n | H_X | \Phi_i \rangle}{\delta E_l \delta E_m \delta E_n} + \Delta^{(2)} H \sum_n \frac{|\langle \Psi_n | H_X | \Phi_i \rangle|^2}{(\delta E_n)^2} \right], \\ &= - \sum_i |\Phi\rangle_i \langle \Phi|_i \left[\sum_m \frac{1}{\delta E_m} \left\| \sum_n \frac{1}{\delta E_n} (H_X)_{mn} (H_X)_{ni} \right\|^2 + \Delta^{(2)} H \sum_n \frac{1}{(\delta E_n)^2} \left\| (H_X)_{ni} \right\|^2 \right].\end{aligned}\quad (5.11.19)$$

We can have at most two successive v^\dagger or two successive v act on a particular state. Any more would lead to $c_\sigma^\dagger |\hat{n}_\sigma = 2\rangle = 0$. This limits the possible scattering processes (in the first term) to the following channels:

$$a. vv^\dagger vv^\dagger, \quad b. v^\dagger vv^\dagger v, \quad c. vvv^\dagger v^\dagger, \quad d. v^\dagger v^\dagger vv. \quad (5.11.20)$$

We start with $i = 0$. Out of the four channels a through d , only b and d survive. For $i = 0$, we already know the relevant $|\Psi\rangle_n$ and hence the $(H_X)_{ni} = v_{ni}$, from eq. (5.11.10).

$$v_{\pm\sigma,i} = \langle \Psi_{\pm,\sigma}^{\bar{\sigma},0} | v | \Phi_i \rangle = \sigma t \left[a_{1,\pm} c_s^{-} + a_{2,\pm} c_c^{-} \right] = \sigma t \mathcal{S}_{\pm}^{-} \quad (5.11.21)$$

where we have defined the sum and difference $\mathcal{S}_{\pm}^{\pm} = a_{1,\pm} c_s^{\pm} + a_{2,\pm} c_c^{\pm}$, $\mathcal{D}_{\pm}^{\pm} = a_{1,\pm} c_s^{\pm} - a_{2,\pm} c_c^{\pm}$. For channel b , we

then proceed as follows:

$$|\Psi\rangle_{\pm,\sigma}^{\bar{\sigma},0} = -\sqrt{2} \left(a_{1,\pm} |\sigma, 0\rangle + a_{2,\pm} |0, \sigma\rangle \right) \otimes |\bar{\sigma}\rangle \quad (5.11.22)$$

$$v^\dagger |\Psi\rangle_n = v^\dagger |\Psi\rangle_{\pm,\sigma}^{\bar{\sigma},0} = \sqrt{2}t \left(a_{1,\pm} |\sigma, \bar{\sigma}\rangle + a_{2,\pm} |0, \sigma\bar{\sigma}\rangle \right) \otimes |0\rangle \quad (5.11.23)$$

$$|\Psi\rangle_m = \begin{cases} \frac{1}{\sqrt{2}} (|\uparrow, \downarrow\rangle + |\downarrow, \uparrow\rangle) \otimes |0\rangle \\ \frac{1}{\sqrt{2}} (|2, 0\rangle - |0, 2\rangle) \otimes |0\rangle \\ \left[\frac{c_s^+}{\sqrt{2}} (|\uparrow, \downarrow\rangle - |\downarrow, \uparrow\rangle) + \frac{c_c^+}{\sqrt{2}} (|\uparrow\downarrow, 0\rangle + |0, \uparrow\downarrow\rangle) \right] \otimes |0\rangle \end{cases} \implies (H_X)_{m,\pm\sigma} = \begin{cases} ta_{1\pm} \\ \bar{\sigma}ta_{2\pm} \\ \sigma t (a_{1\pm}c_s^+ + a_{2\pm}c_c^+) = \sigma t\mathcal{S}_\pm^+ \end{cases} \quad (5.11.24)$$

$$\frac{1}{\delta E_m} \left\| \sum_n \frac{1}{\delta E_n} (H_X)_{mn} (H_X)_{ni} \right\|^2 = \begin{cases} \frac{1}{\delta E_{ST}} \left(\sum_{\sigma,\pm} \frac{t^2}{\delta E_\pm} \sigma a_{1\pm} \mathcal{S}_\pm^- \right)^2 = 0 \\ \frac{1}{\delta E_{CS}} \left(\sum_{\pm,\sigma} \frac{t^2}{\delta E_\pm} a_{2\pm} \mathcal{S}_\pm^- \right)^2 = \frac{4t^4}{\delta E_{CS}} \left(\sum_\pm \frac{1}{\delta E_\pm} a_{2\pm} \mathcal{S}_\pm^- \right)^2 \\ \frac{1}{\delta E_2} \left(-\sum_{\pm,\sigma} \frac{t^2}{\delta E_\pm} \mathcal{S}_\pm^+ \mathcal{S}_\pm^- \right)^2 = \frac{4t^4}{\delta E_2} \left(\sum_\pm \frac{1}{\delta E_\pm} \mathcal{S}_\pm^+ \mathcal{S}_\pm^- \right)^2 \end{cases} \quad (5.11.25)$$

E_{ST} , E_{CS} and E_2 are the energies of the spin triplet zero, charge singlet and spin singlet+charge triplet excited states of the set $|\Psi\rangle_m$ in eq. (5.11.24).

We now turn to channel d :

$$v |\Psi\rangle_n = v |\Psi\rangle_{\pm,\sigma}^{\bar{\sigma},0} = \sqrt{2}t\sigma a_{2\pm} |0, 0\rangle \otimes |2\rangle, \quad |\Psi\rangle_m = |0, 0, 2\rangle, \quad (H_X)_{m,\pm\sigma} = \sqrt{2}t\sigma a_{2\pm} \quad (5.11.26)$$

$$\frac{1}{\delta E_m} \left\| \sum_n \frac{1}{\delta E_n} (H_X)_{mn} (H_X)_{ni} \right\|^2 = \frac{8t^4}{\delta E_{00}} \left(\sum_\pm \frac{1}{\delta E_\pm} a_{2\pm} \mathcal{S}_\pm^- \right)^2 \quad (5.11.27)$$

E_{00} is the energy of the state $|0, 0, 2\rangle$.

Having accounted for both channels, we will calculate the second part of the effective Hamiltonian in eq. (5.11.19), the part involving $\Delta^{(2)}H$. We already know, from eq. (5.11.11), that

$$\Delta^{(2)}H_{i=0} = -2t^2 \sum_\pm \frac{1}{\delta E_\pm} \left(\mathcal{S}_\pm^- \right)^2 \quad (5.11.28)$$

Also, from the expression of $v_{\pm\sigma,i}$, we get

$$\sum_n \frac{1}{(\delta E_n)^2} \left\| (H_X)_{ni} \right\|^2 = \sum_\pm \frac{2t^2}{(\delta E_\pm)^2} \left(\mathcal{S}_\pm^- \right)^2 \quad (5.11.29)$$

Combining it all, the total renormalisation in $i = 0$ is

$$-|\Phi\rangle_0 \langle \Phi|_0 4t^4 \left[\left(\frac{1}{\delta E_{CS}} + \frac{2}{\delta E_{00}} \right) \left(\sum_\pm \frac{a_{2\pm} \mathcal{S}_\pm^-}{\delta E_\pm} \right)^2 + \frac{1}{\delta E_2} \left(\sum_\pm \frac{\mathcal{S}_\pm^+ \mathcal{S}_\pm^-}{\delta E_\pm} \right)^2 - \sum_\pm \frac{(\mathcal{S}_\pm^-)^2}{\delta E_\pm} \sum_\pm \left(\frac{\mathcal{S}_\pm^-}{\delta E_\pm} \right)^2 \right] \quad (5.11.30)$$

We now come to $i = 1$: $|\Phi\rangle_1 = |\Psi\rangle_1 \otimes |\uparrow\rangle$. Channels a and b are non-zero here. We start with channel b : $v^\dagger v v^\dagger v$. We already know, from eq. (5.11.12), that

$$v |\Phi\rangle_1 = t \frac{1}{\sqrt{2}} \left(c_s^- |\uparrow, 0, 2\rangle + c_c^- |0, \uparrow, 2\rangle \right), \quad |\psi\rangle_n = |\Psi\rangle_{\pm,\uparrow}^{2,0} = -\sqrt{2} \left(a_{1,\pm} |\uparrow, 0\rangle + a_{2,\pm} |0, \uparrow\rangle \right) \otimes |2\rangle, \quad (H_X)_{ni} = -t\mathcal{S}_\pm^- \quad (5.11.31)$$

Moving forward:

$$v^\dagger |\Psi\rangle_n = \sqrt{2}t \left(a_{1,\pm} |\uparrow, \uparrow\rangle \otimes |\downarrow\rangle - a_{1,\pm} |\uparrow, \downarrow\rangle \otimes |\uparrow\rangle - a_{2,\pm} |0, 2\rangle \otimes |\uparrow\rangle \right) \quad (5.11.32)$$

$$|\Psi\rangle_m = \begin{cases} \frac{1}{\sqrt{2}} (|\uparrow, \downarrow\rangle + |\downarrow, \uparrow\rangle) \otimes |\uparrow\rangle \\ \frac{1}{\sqrt{2}} (|2, 0\rangle - |0, 2\rangle) \otimes |\uparrow\rangle \\ \left[\frac{c_s^+}{\sqrt{2}} (|\uparrow, \downarrow\rangle - |\downarrow, \uparrow\rangle) + \frac{c_c^+}{\sqrt{2}} (|\uparrow\downarrow, 0\rangle + |0, \uparrow\downarrow\rangle) \right] \otimes |\uparrow\rangle \\ |\uparrow, \uparrow\rangle \otimes |\downarrow\rangle \end{cases} \implies (H_X)_{m,\pm} (H_X)_{\pm,i} = \begin{cases} t^2 a_{1\pm} \mathcal{S}_{\pm}^- \\ -t^2 a_{2\pm} \mathcal{S}_{\pm}^- \\ t^2 \mathcal{S}_{\pm}^+ \mathcal{S}_{\pm}^- \\ -\sqrt{2} t^2 a_{1\pm} \mathcal{S}_{\pm}^- \end{cases} \quad (5.11.33)$$

$$\frac{1}{\delta E_m} \left\| \sum_n \frac{1}{\delta E_n} (H_X)_{mn} (H_X)_{ni} \right\|^2 = \begin{cases} \frac{t^4}{\delta E_{ST}} \left(\sum_{\pm} \frac{1}{\delta E_{\pm}} a_{1\pm} \mathcal{S}_{\pm}^- \right)^2 \\ \frac{t^4}{\delta E_{CS}} \left(\sum_{\pm} \frac{1}{\delta E_{\pm}} a_{2\pm} \mathcal{S}_{\pm}^- \right)^2 \\ \frac{t^4}{\delta E_2} \left(\sum_{\pm} \frac{1}{\delta E_{\pm}} \mathcal{S}_{\pm}^+ \mathcal{S}_{\pm}^- \right)^2 \\ \frac{2t^4}{\delta E_{\uparrow\uparrow}} \left(\sum_{\pm} \frac{1}{\delta E_{\pm}} a_{1\pm} \mathcal{S}_{\pm}^- \right)^2 \end{cases} \quad (5.11.34)$$

$E_{\uparrow\uparrow}$ is the energy of the upwards polarised state $|\uparrow, \uparrow\rangle \otimes |\downarrow\rangle$.

Next is channel $a : vv^\dagger vv^\dagger$. Using eq. (5.11.13) and following the same steps as above, we get:

$$v^\dagger |\Phi\rangle_1 = t \frac{1}{\sqrt{2}} \left(c_s^- |\uparrow, 2, 0\rangle - c_c^- |2, \uparrow, 0\rangle \right), \quad |\Psi\rangle_n = |\Psi\rangle_{\pm, \uparrow}^{0,2} = -\sqrt{2} \left(a_{1,\pm} |\uparrow, 2\rangle + a_{2,\pm} |2, \uparrow\rangle \right) \otimes |0\rangle, \quad (H_X)_{ni} = -t \mathcal{D}_{\pm}^- \quad (5.11.35)$$

$$v |\Psi\rangle_n = \sqrt{2} t \left(a_{1,\pm} |\uparrow, \uparrow\rangle \otimes |\downarrow\rangle - a_{1,\pm} |\uparrow, \downarrow\rangle \otimes |\uparrow\rangle + a_{2,\pm} |2, 0\rangle \otimes |\uparrow\rangle \right) \quad (5.11.36)$$

$$|\Psi\rangle_m = \begin{cases} \frac{1}{\sqrt{2}} (|\uparrow, \downarrow\rangle + |\downarrow, \uparrow\rangle) \otimes |\uparrow\rangle \\ \frac{1}{\sqrt{2}} (|2, 0\rangle - |0, 2\rangle) \otimes |\uparrow\rangle \\ \left[\frac{c_s^+}{\sqrt{2}} (|\uparrow, \downarrow\rangle - |\downarrow, \uparrow\rangle) + \frac{c_c^+}{\sqrt{2}} (|\uparrow\downarrow, 0\rangle + |0, \uparrow\downarrow\rangle) \right] \otimes |\uparrow\rangle \\ |\uparrow, \uparrow\rangle \otimes |\downarrow\rangle \end{cases} \implies (H_X)_{m,\pm} (H_X)_{\pm,i} = \begin{cases} t^2 a_{1\pm} \mathcal{D}_{\pm}^- \\ -t^2 a_{2\pm} \mathcal{D}_{\pm}^- \\ t^2 \mathcal{D}_{\pm}^+ \mathcal{D}_{\pm}^- \\ -\sqrt{2} t^2 a_{1\pm} \mathcal{D}_{\pm}^- \end{cases} \quad (5.11.37)$$

$$\frac{1}{\delta E_m} \left\| \sum_n \frac{1}{\delta E_n} (H_X)_{mn} (H_X)_{ni} \right\|^2 = \begin{cases} \frac{1}{\delta E_{ST}} \left(\sum_{\pm} \frac{t^2}{\delta E_{\pm}} a_{1\pm} \mathcal{D}_{\pm}^- \right)^2 \\ \frac{t^4}{\delta E_{CS}} \left(\sum_{\pm} \frac{1}{\delta E_{\pm}} a_{2\pm} \mathcal{D}_{\pm}^- \right)^2 \\ \frac{t^4}{\delta E_2} \left(\sum_{\pm} \frac{1}{\delta E_{\pm}} \mathcal{D}_{\pm}^+ \mathcal{D}_{\pm}^- \right)^2 \\ \frac{2t^4}{\delta E_{\uparrow\uparrow}} \left(\sum_{\pm} \frac{1}{\delta E_{\pm}} a_{1\pm} \mathcal{D}_{\pm}^- \right)^2 \end{cases} \quad (5.11.38)$$

For the final part, we again use $\Delta^{(2)} H_{i=1} = -t^2 \sum_{\pm} \frac{1}{\delta E_{\pm}} \left[(\mathcal{S}_{\pm}^-)^2 + (\mathcal{D}_{\pm}^-)^2 \right]$. Also, since $(H_X)_{ni} = (v + v^\dagger)_{ni}$, we have

$$\sum_n \frac{1}{(\delta E_n)^2} \left\| (H_X)_{ni} \right\|^2 = t^2 \sum_{\pm} \left[\left(\frac{\mathcal{S}_{\pm}^-}{\delta E_{\pm}} \right)^2 + \left(\frac{\mathcal{D}_{\pm}^-}{\delta E_{\pm}} \right)^2 \right] \quad (5.11.39)$$

Combining all the terms, we get

$$\begin{aligned}
& -|\Phi\rangle_1 \langle\Phi|_1 4t^4 \left[\left(\frac{1}{\delta E_{\text{ST}}} + \frac{2}{\delta E_{\uparrow\uparrow}} \right) \left\{ \left(\frac{1}{2} \sum_{\pm} \frac{a_{1\pm} \mathcal{S}_{\pm}^-}{\delta E_{\pm}} \right)^2 + \left(\frac{1}{2} \sum_{\pm} \frac{a_{1\pm} \mathcal{D}_{\pm}^-}{\delta E_{\pm}} \right)^2 \right\} + \frac{1}{\delta E_{\text{CS}}} \left\{ \left(\frac{1}{2} \sum_{\pm} \frac{a_{2\pm} \mathcal{S}_{\pm}^-}{\delta E_{\pm}} \right)^2 \right. \right. \\
& \quad \left. \left. + \left(\frac{1}{2} \sum_{\pm} \frac{a_{2\pm} \mathcal{D}_{\pm}^-}{\delta E_{\pm}} \right)^2 \right\} + \frac{1}{\delta E_2} \left\{ \left(\frac{1}{2} \sum_{\pm} \frac{\mathcal{S}_{\pm}^+ \mathcal{S}_{\pm}^-}{\delta E_{\pm}} \right)^2 + \left(\frac{1}{2} \sum_{\pm} \frac{\mathcal{D}_{\pm}^+ \mathcal{D}_{\pm}^-}{\delta E_{\pm}} \right)^2 \right\} \right. \\
& \quad \left. - \sum_{\pm} \frac{1}{\delta E_{\pm}} \frac{1}{2} \left\{ (\mathcal{S}_{\pm}^-)^2 + (\mathcal{D}_{\pm}^-)^2 \right\} \sum_{\pm} \frac{1}{2} \left\{ \left(\frac{\mathcal{S}_{\pm}^-}{\delta E_{\pm}} \right)^2 + \left(\frac{\mathcal{D}_{\pm}^-}{\delta E_{\pm}} \right)^2 \right\} \right] \quad (5.11.40)
\end{aligned}$$

If we define some quantities: $F_{(1,2)} = \sum_{\pm} \frac{a_{(1,2)\pm} \mathcal{S}_{\pm}^-}{\delta E_{\pm}}$, $G_{(1,2)} = \sum_{\pm} \frac{a_{(1,2)\pm} \mathcal{D}_{\pm}^-}{\delta E_{\pm}}$, $P = \sum_{\pm} \frac{\mathcal{S}_{\pm}^+ \mathcal{S}_{\pm}^-}{\delta E_{\pm}}$, $Q = \sum_{\pm} \frac{\mathcal{D}_{\pm}^+ \mathcal{D}_{\pm}^-}{\delta E_{\pm}}$, $X_n = \sum_{\pm} \frac{(\mathcal{S}_{\pm}^-)^2}{(\delta E_{\pm})^n}$, $Y_n = \sum_{\pm} \frac{(\mathcal{D}_{\pm}^-)^2}{(\delta E_{\pm})^n}$, the total renormalisation from second and fourth order can be written as

$$\begin{aligned}
& -(|\Phi\rangle_0 \langle\Phi|_0 + |\Phi\rangle_3 \langle\Phi|_3) 4t^4 \left[\frac{1}{2t^2} X_1 + \left(\frac{1}{\delta E_{\text{CS}}} + \frac{2}{\delta E_{00}} \right) F_2^2 + \frac{1}{\delta E_2} P^2 - X_1 X_2 \right] \\
& -(|\Phi\rangle_1 \langle\Phi|_1 + |\Phi\rangle_2 \langle\Phi|_2) t^4 \left[\frac{1}{t^2} (X_1 + Y_1) + \left(\frac{1}{\delta E_{\text{ST}}} + \frac{2}{\delta E_{\uparrow\uparrow}} \right) (F_1^2 + G_1^2) + \frac{1}{\delta E_{\text{CS}}} (F_2^2 + G_2^2) \right. \\
& \quad \left. + \frac{1}{\delta E_2} (P^2 + Q^2) - (X_1 + Y_1) (X_2 + Y_2) \right] \quad (5.11.41)
\end{aligned}$$

The excitation energies are given by

$$\delta E_{\text{CS}} = \delta E_{00} = \frac{3J}{8} + \frac{U}{4} + \alpha, \quad \delta E_{\uparrow\uparrow} = \delta E_{\text{ST}} = -\frac{U}{4} + \frac{5J}{8} + \alpha, \quad \delta E_2 = 2\alpha, \quad \delta E_{\pm} = \frac{3J}{8} + \alpha \pm \frac{1}{2}\Delta, \quad \alpha \equiv \sqrt{V^2 \gamma^2 + 4V^2} \quad (5.11.42)$$

where $V\gamma = \frac{3J}{8} + \frac{U}{4}$ and $\Delta = \sqrt{\frac{U^2}{4} + 4V^2}$. The effective Hamiltonian can be expressed in the general form

$$H_{\text{eff}} = |\Psi\rangle_1 \langle\Psi|_1 \otimes \left[\text{constant} + \alpha_{\text{spin}} \hat{\mathcal{P}}_{\text{spin}} + \alpha_{\text{charge}} \hat{\mathcal{P}}_{\text{charge}} \right] \quad (5.11.43)$$

$\hat{\mathcal{P}}_{\text{charge}}$ and $\hat{\mathcal{P}}_{\text{spin}}$ are projection operators for, respectively, the charge ($\hat{n}_1 \neq 1$) and spin ($\hat{n}_1 = 1$) sectors of the first site. Since $\hat{\mathcal{P}}_{\text{charge}} + \hat{\mathcal{P}}_{\text{spin}} = 1$, we can eliminate one of the terms and rewrite the effective Hamiltonian in the simpler form

$$H_{\text{eff}} = |\Psi\rangle_1 \langle\Psi|_1 \otimes \left[\text{constant} + \mathcal{F} \hat{\mathcal{P}}_{\text{charge}} \right] \quad (5.11.44)$$

where $\mathcal{F} \equiv \alpha_{\text{charge}} - \alpha_{\text{spin}}$ is the net energy of the charge sector above the spin sector.

We will now look at the extreme strong coupling regime $J \gg V \gg U, t$. There, all the expressions simplify:

$$\begin{aligned}
V\gamma & \simeq \frac{3J}{8}, \quad \Delta \simeq 2V, \quad \alpha \simeq \frac{3J}{8}, \quad c_s^+ = -c_c^- \simeq 0, \quad c_s^- = c_c^+ \simeq 1, \quad \mathcal{N}_{\pm} \simeq 4\sqrt{2}V, \quad a_{1,\pm} \simeq \frac{1}{2}, \quad a_{2,\pm} \simeq \pm \frac{1}{2}, \\
\delta E_{\pm} & \simeq \delta E_{\text{CS}} = \delta E_{00} = \delta E_2 \simeq \frac{3J}{4}, \quad \delta E_{\text{ST}} = \delta E_{\uparrow\uparrow} \simeq J, \quad \mathcal{S}_{\pm}^- = \mathcal{D}_{\pm}^- \simeq \frac{1}{2}, \quad \mathcal{S}_{\pm}^+ = -\mathcal{D}_{\pm}^+ \simeq \pm \frac{1}{2}, \\
F_1 & = G_1 \simeq \frac{2}{3J}, \quad F_2 = G_2 \simeq 0, \quad P = Q \simeq 0, \quad X_1 = Y_1 \simeq \frac{2}{3J}, \quad X_2 = Y_2 \simeq \frac{8}{9J^2} \quad (5.11.45)
\end{aligned}$$

The effective Hamiltonian becomes

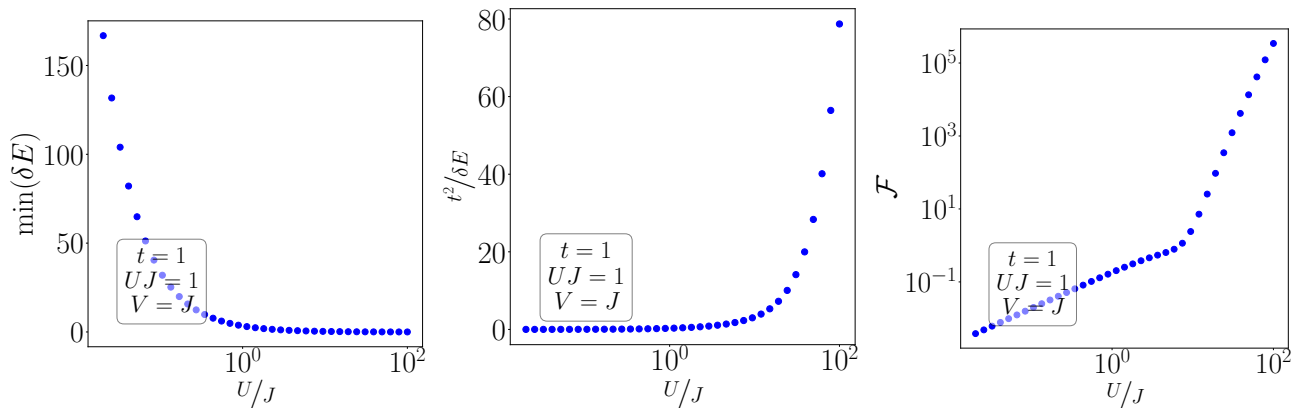
$$\begin{aligned}
& - \left(|\Phi\rangle_0 \langle\Phi|_0 + |\Phi\rangle_3 \langle\Phi|_3 \right) \frac{4t^2}{3J} \left[1 - \frac{16t^2}{9J^3} \right] - \left(|\Phi\rangle_1 \langle\Phi|_1 + |\Phi\rangle_2 \langle\Phi|_2 \right) \frac{4t^2}{3J} \left[1 + \frac{2t^2}{9J^2} \right] \\
& = - \frac{4t^2}{3J} \sum_i |\Phi\rangle_i \langle\Phi|_i + \left(|\Phi\rangle_0 \langle\Phi|_0 + |\Phi\rangle_3 \langle\Phi|_3 \right) \frac{64t^4}{27J^3} - \left(|\Phi\rangle_1 \langle\Phi|_1 + |\Phi\rangle_2 \langle\Phi|_2 \right) \frac{8t^4}{27J^3} \\
& = |\Psi\rangle_1 \langle\Psi|_1 \left[\text{constant} + \frac{64t^4}{27J^3} \mathcal{P}_{\text{charge}} - \frac{8t^4}{27J^3} \mathcal{P}_{\text{spin}} \right]
\end{aligned} \tag{5.11.46}$$

$\mathcal{P}_{\text{spin}}$ and $\mathcal{P}_{\text{charge}}$ project, respectively, onto the spin and charge sectors of the first site. The fact that the charge sector comes with a positive factor means that the holon-doublon states are repulsive, and this renormalisation of the states generates an effective particle-hole symmetric Fermi liquid interaction on the first site - also known as the local Fermi liquid (LFL) [16].

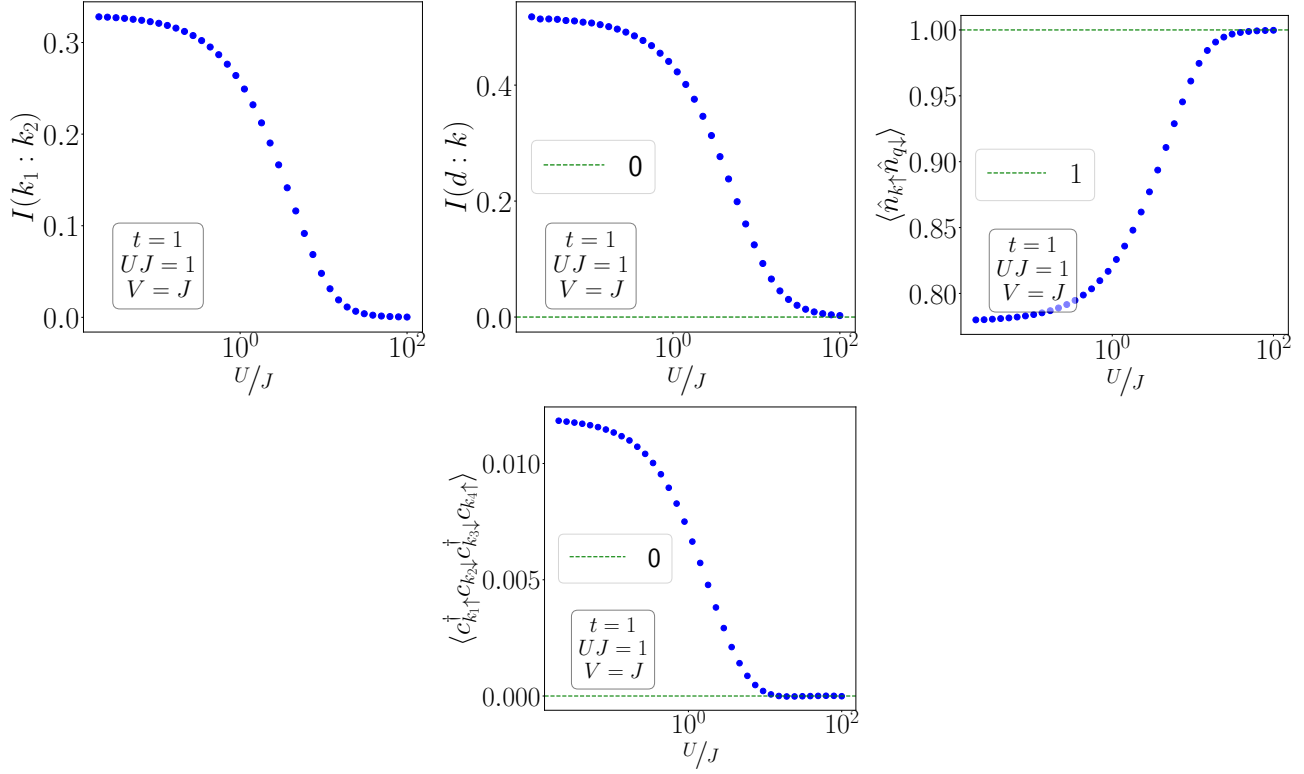
5.12 Destruction of the Abrikosov-Suhl resonance: passage from strong coupling to local moment

We will now tune the parameters of the fixed point Hamiltonian and study the variation of quantities related to the effective Hamiltonian like the local FL strength \mathcal{F} , the gap in the spectrum of the zeroth Hamiltonian H_0^* and the value of the small parameter $t^2/\delta E$, as well as various measures of entanglement like entanglement entropy, mutual information and spin-spin correlations between various sets of members of the real-space impurity+lattice construction. We will trace a specific path through the space of values of fixed point couplings: we will start from the strong coupling regime $U \ll J, V$ and go towards the local moment regime $U \gg J, V$. The context of this study is that the technique of dynamical mean-field theory (DMFT) obtains a metal-insulator transition in the 2D Hubbard model by studying the Anderson impurity model as the auxiliary system for the Hubbard; there, the local moment regime of the impurity corresponds to the insulator in the bulk. Our goal here is to study what precisely happens in the effective Hamiltonian in the journey from the metal to the insulator, and draw a concrete connection between this modification of the effective Hamiltonian, and the simultaneous change of the impurity spectral function in fig. 5.10. This is done with the knowledge that the local moment phase of the extended SIAM is never RG-stable.

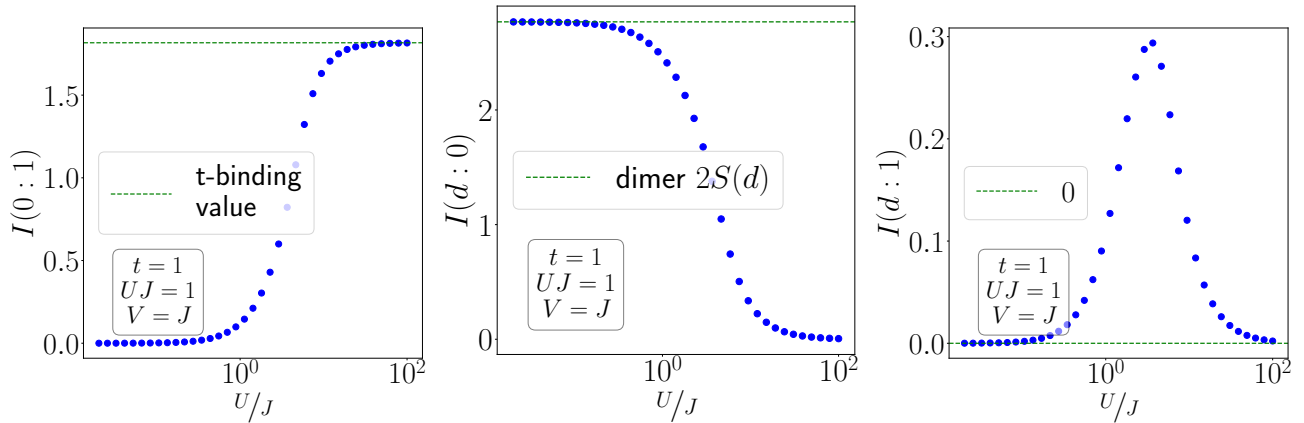
Perturbation theory parameters



The vanishing of the gap and the growth of the small parameter indicates the breakdown of perturbation theory around the singlet; this simply shows that there is a degeneracy in the local moment regime, and the effective Hamiltonian will have to be obtained using degenerate perturbation theory. The presence of degeneracy also suggests that the effective Hamiltonian will be of the non-Fermi liquid type.

k -space correlations within the Kondo cloud

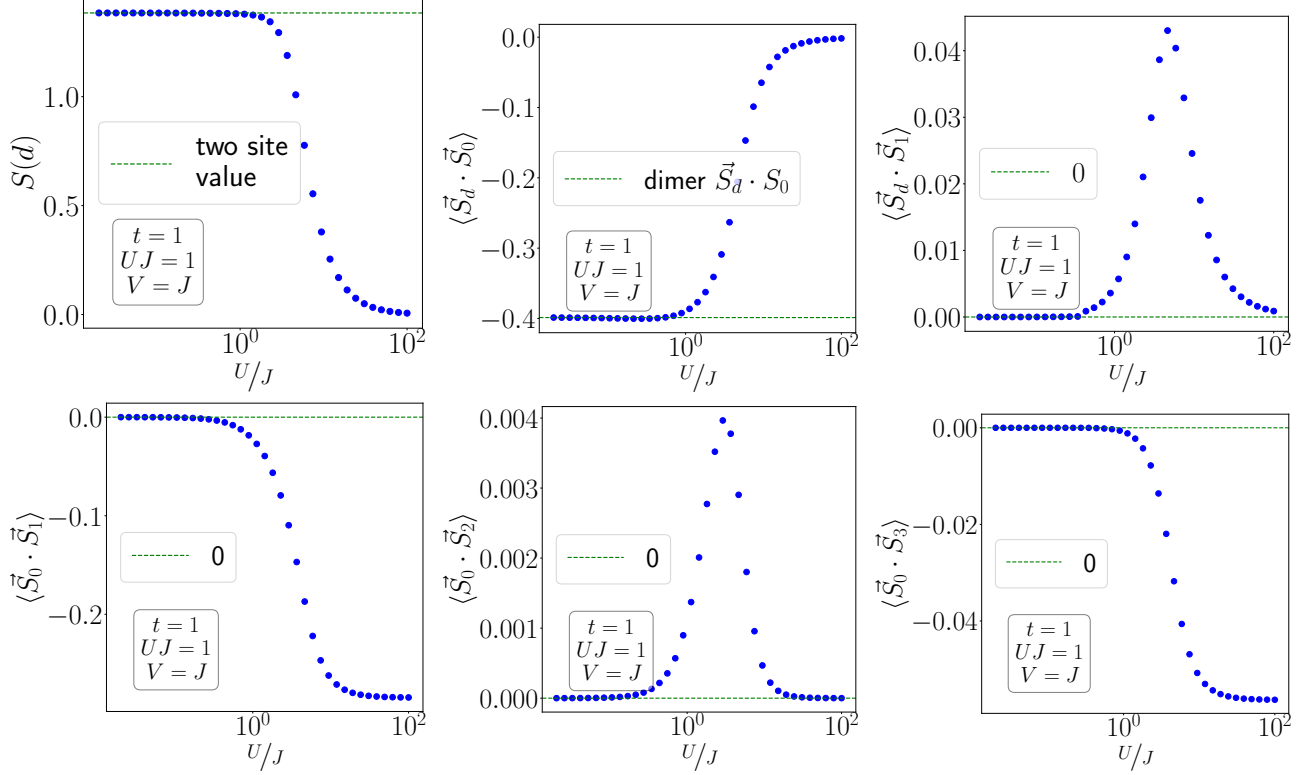
The mutual information $I(d : k)$ between the impurity and the cloud vanishes as U/J is increased. This is a signature of the loss of entanglement and the breakdown of the singlet. The reduction of the mutual information within the cloud, $I(k_1 : k_2)$, shows that the Kondo cloud is being killed as U/J is increased; it ultimately drops to zero, characteristic of a decoupled tight-binding chain. The four-Fermion off-diagonal term also vanishes as U/J increases and this is again a signature of the reduction in the spin-flip processes. The diagonal correlation $\langle \hat{n}_{k\uparrow} \hat{n}_{q\downarrow} \rangle$ increasing to 1 shows the formation of a filled Fermi sea.

Mutual information between various real space members

The impurity-zeroth site mutual information $I(d : 0)$ remains unchanged at the maximum for an appreciable range of values, and this shows the stability of the singlet. Meanwhile, the mutual information between the zeroth site and the site nearest to it ($I(0 : 1)$) grows, because when the singlet weakens, the zeroth site is able to entangle more with the other sites. It finally saturates to its maximum value, which is the value produced as result of the tight-binding hopping. The mutual information between the impurity and sites beyond the zeroth site ($I(d : 1)$)

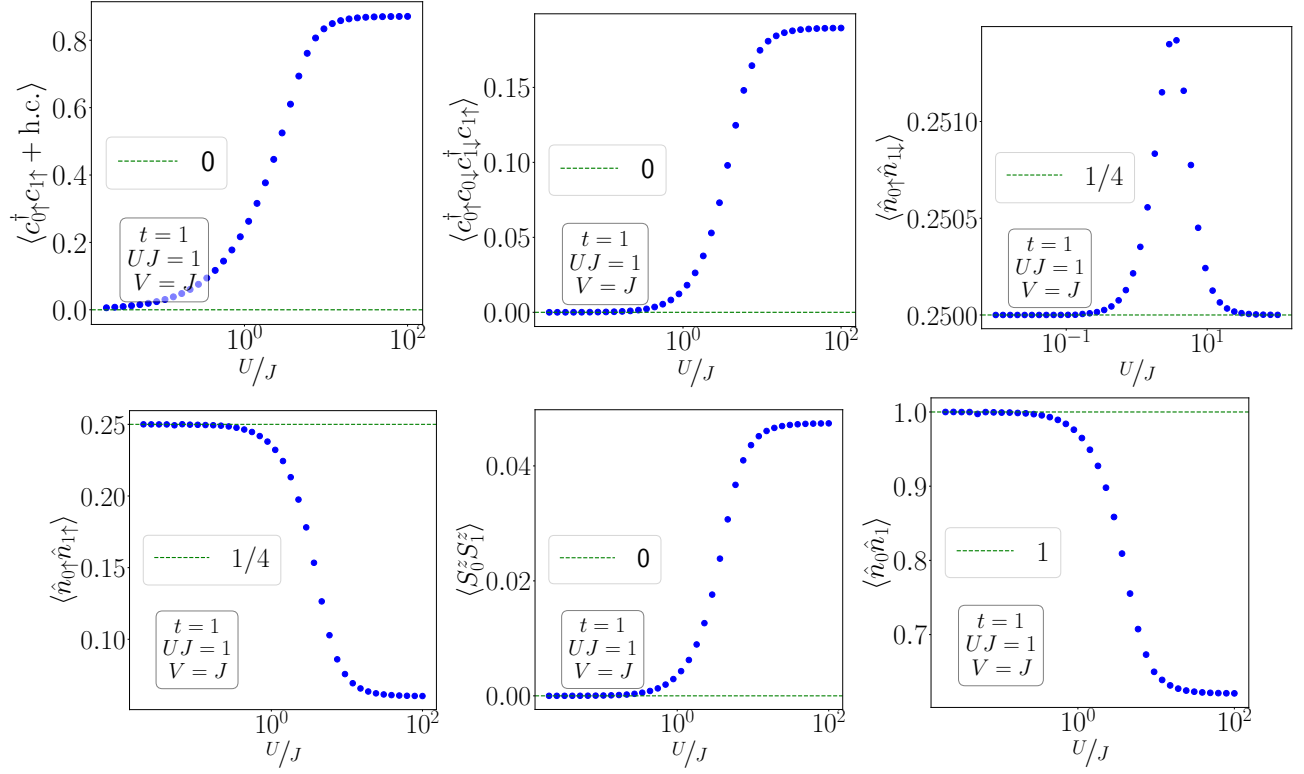
show a non-monotonic behaviour; it first increases as the entanglement that was initially restricted to just the impurity and the zeroth sites begins "seeping" into the other sites as well. Beyond a critical value of U/J , $I(d : 1)$ starts dropping, because the entanglement has now mostly shifted out of the singlet and into the conduction bath.

Impurity entanglement entropy and spin-spin correlations



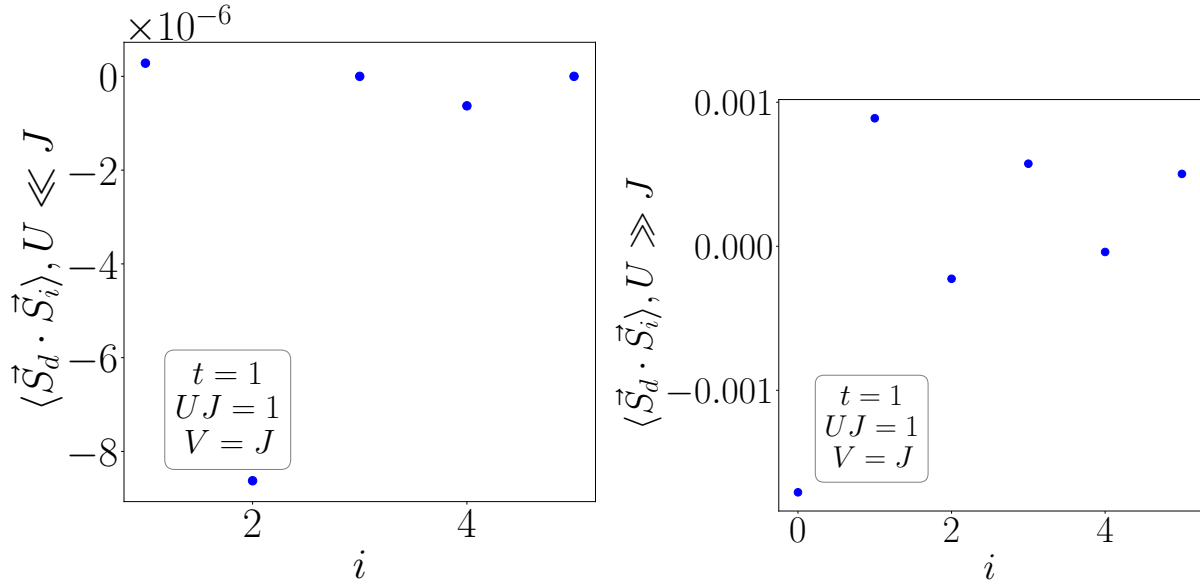
The von-Neumann entanglement entropy $S(d)$ of the impurity shows pretty straightforward behaviour. It is maximum for $U \ll J$ because it is in a singlet configuration. For $U \gg J$, the singlet weakens and the impurity begins to decouple from the bath, leading to a reduction in $S(d)$. At sufficiently low values of J/U , the impurity decouples from the zeroth site and the total system can be factorised into a local moment in product with a tight-binding chain, so that the impurity site will now have zero entanglement entropy. The spin-spin correlation $\tilde{S}_d \cdot \tilde{S}_0$ is most negative at large J , showing maximum screening at strong-coupling. It decreases to 0 as the singlet breaks. This reduction in the spin-spin correlation between the impurity and the zeroth site is accompanied by the appearance of antiferromagnetic spin-spin correlation $\tilde{S}_0 \cdot \tilde{S}_1, \tilde{S}_0 \cdot \tilde{S}_3$ between the zeroth site and odd-numbered sites like 1 and 3. This can be understood on the following grounds: since the tight-binding hopping only connects same spin states, an electron on the first site has to have spin opposite to that on the zeroth site in order to hop onto that site. This requirement of opposite spin is what induces an antiferromagnetic superexchange interaction J_1 between the zeroth site and the first site. This interaction strength increases as J is decreased, because $J_1 \sim t^2/J$. By the same argument, a ferromagnetic superexchange interaction is induced between the impurity site and the first site, as well as between the zeroth site and the other even-numbered sites. These are also seen in the plots.

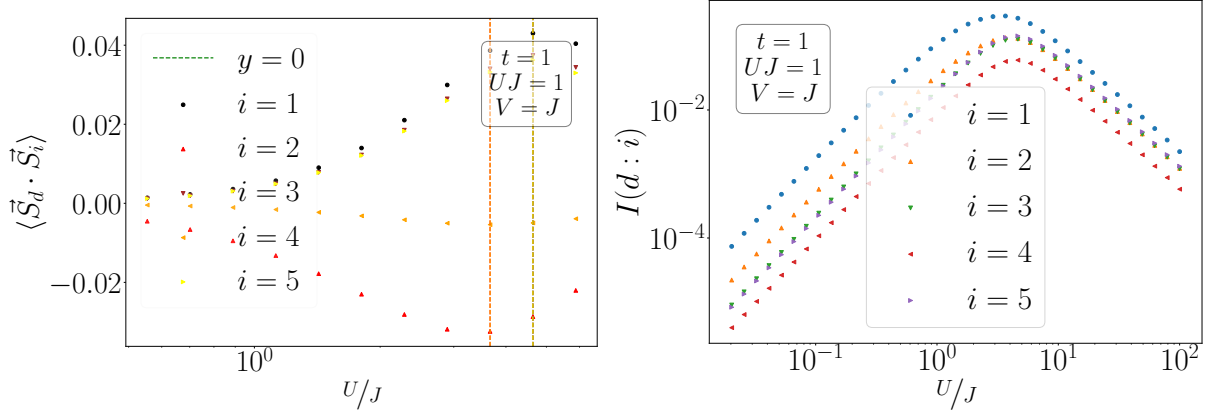
Real-space correlations



The increase of single-particle hopping correlation is another signature of the "handover" of entanglement from the singlet to the tight-binding chain. Exactly the same can be said for the four-Fermion interaction as well.

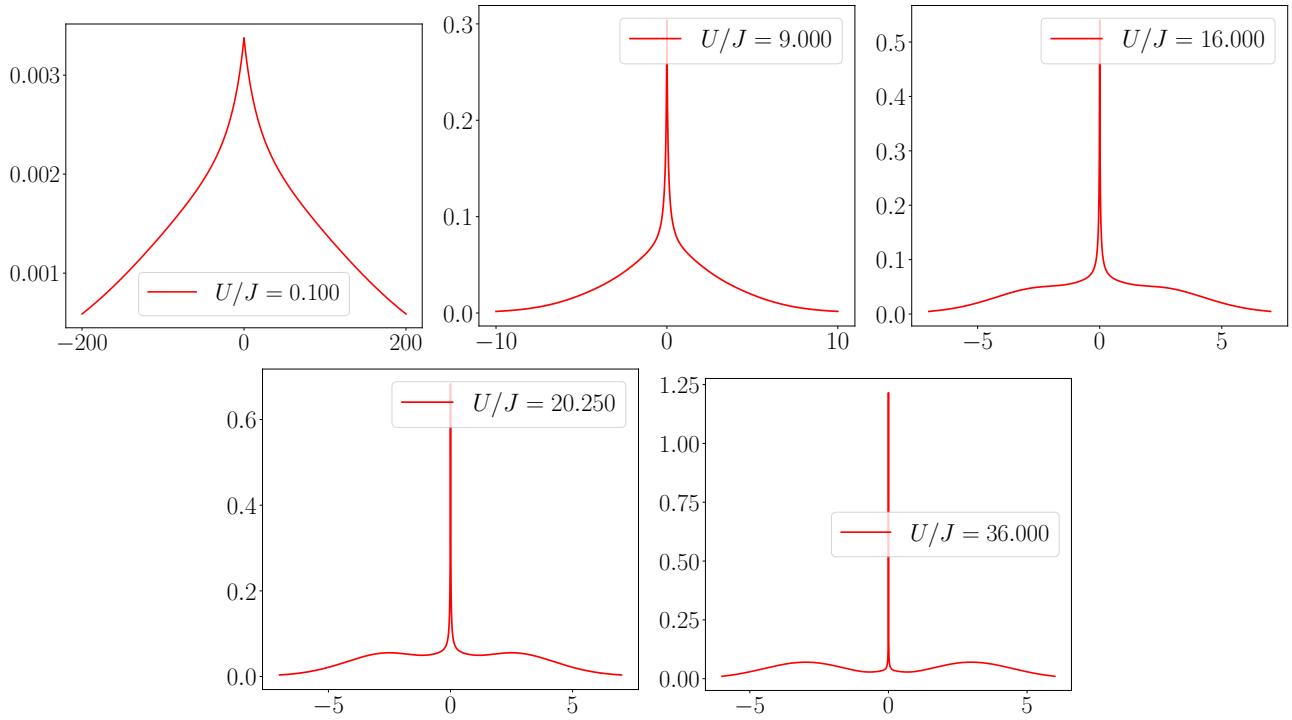
Real-space correlations as function of distance





The first thing to note in the first two figures is the difference in the order of magnitudes; the correlations are very small in the first figure, because the impurity is being screened almost completely by the zeroth site at $J \gg U$. This changes in the second figure where, because $U \gg J$, the singlet has become entangled with the other sites, and the impurity is being screened by multiple sites. The mutual information all vary similarly with distance in the bottom right figure.

Impurity spectral function



5.13 Calculating the $T = 0$ Wilson ratio from low energy excitations

The total system now consists of two decoupled parts - the singlet composed of the impurity and the zeroth site, and the remaining lattice composed of $N-1$ sites with a tight-binding dispersion and a local interaction at the 1-th site. The effective Hamiltonian for the remaining lattice is

$$\sum_{\sigma} \sum_{i=1}^{\infty} t \left(c_{i\sigma}^{\dagger} c_{i+1\sigma} + c_{i+1\sigma}^{\dagger} c_{i\sigma} \right) + u \hat{n}_{1\uparrow} \hat{n}_{1\downarrow} \quad (5.13.1)$$

We have rewritten the holon term in terms of the spin and doublon operators. We will now invoke the mean-field

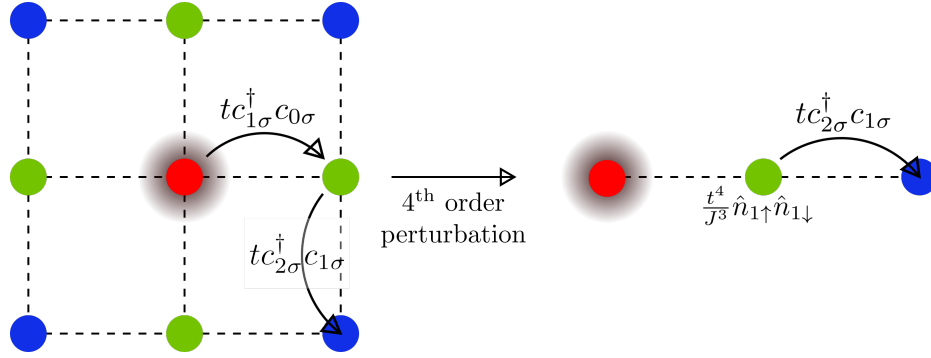


Figure 5.11: *Left*: The nearest-neighbor hopping described by the effective Hamiltonian. The red circle is the impurity. The black cloud at the center demarcates the collection of electrons at the origin of the lattice (which couple to the impurity). The green circles represent lattice sites that are nearest to the origin. The blue circles represent next-nearest sites. *Right*: After treating the hopping between origin and its nearest neighbors as perturbation, we get a system consisting of two decoupled parts: one part is the impurity+cloud singlet, the other part is the rest of the lattice sites. The effect of the hopping between the origin and the green sites is a repulsion term on the green sites.

approximation in simplifying this term. We will be dealing with thermodynamic quantities soon, so the operators will be replaced by their thermodynamic values, that is, the values that minimize the free energy functional.

$$\hat{n}_{1\uparrow}\hat{n}_{1\downarrow} \rightarrow \langle \hat{n}_{1\uparrow}\hat{n}_{1\downarrow} \rangle = \langle \delta n_{1\uparrow} \delta n_{1\downarrow} \rangle + \langle n_{1\uparrow} \rangle \langle n_{1\downarrow} \rangle \quad (5.13.2)$$

where $\delta n_{1\sigma} \equiv n_{1\sigma} - \langle n_{1\sigma} \rangle$ is the fluctuation of the particle number above the ground state. The mean-field approximation then involves dropping the first term which is a quadratic fluctuation - since we are interested in values of quantities at $T \rightarrow 0$, this quadratic fluctuation is very small. The interaction we are left with is

$$u \langle n_{1\uparrow} \rangle \langle n_{1\downarrow} \rangle = \sum_{kq\sigma} f_{kq} \langle n_{k\sigma} \rangle \langle n_{q\bar{\sigma}} \rangle \quad (5.13.3)$$

This interaction converts the problem to that of a Landau Fermi liquid, with the quasiparticle energy functional being given by

$$\epsilon_{k\sigma} = \epsilon_k + \sum_q f_{kq} \langle \hat{n}_{q\bar{\sigma}} \rangle \quad (5.13.4)$$

From the form of the quasiparticle energy functional, we can see that there is no spin-parallel term, so we can write

$$f_{kk'\sigma\sigma} = 0, f_{kk'\sigma\bar{\sigma}} = f_{kk'} \quad (5.13.5)$$

We will now use this Fermi liquid form to extract the Wilson ratio. We will make use of the following definitions/results:

$$dn_{k\sigma} = \frac{\partial n}{\partial \epsilon_{k\sigma}} (d\epsilon_{k\sigma} - d\mu) \quad [\text{follows from differentiating FD distribution}] \quad (5.13.6)$$

$$C_V = \frac{d\epsilon}{dT}, \quad \chi^{s,c} = \frac{d}{d(B, \mu)} (n_{\uparrow} \mp n_{\downarrow}), \quad 2f_0^{s,a} = \sum_k (f_{kk'\uparrow\uparrow} \pm f_{kk'\uparrow\downarrow}), \quad F_0^{s,a} = \rho(0)f_0^{s,a} \quad (5.13.7)$$

5.13.1 Low- T Specific heat

$$\begin{aligned}
C &= \frac{d}{dT} \sum_{k\sigma} \epsilon_{k\sigma} n_{k\sigma} \\
&\approx \sum_{k\sigma} \epsilon_{k\sigma}^0 \frac{dn_{k\sigma}}{dT} \quad [\text{no quasiparticles at ground state}] \\
&\approx \sum_{k\sigma} \epsilon_{k\sigma}^0 \frac{dn_{k\sigma}}{dT} \quad [\text{same expression as Fermi gas but with modified distribution function}] \\
&= \rho(0)T
\end{aligned} \tag{5.13.8}$$

where ρ is the total quasiparticle DOS with contributions from conduction bath and impurity.

$$\rho \sim \text{Im Trace } [G] = \text{Im} \sum_{d\sigma} G_{dd}^\sigma + \text{Im} \sum_{k\sigma} G_{kk}^\sigma = \rho_0 + \rho_{\text{imp}} \tag{5.13.9}$$

which gives

$$C_{\text{imp}} \equiv C - C_0 = \rho_{\text{imp}}(0)T \tag{5.13.10}$$

5.13.2 Low- T Charge Susceptibility

$$\chi^c = \frac{dN}{d\mu} \tag{5.13.11}$$

Due to change in chemical potential, $\delta\epsilon_{k\sigma}$ is isotropic and SU(2)-symmetric. Hence

$$\begin{aligned}
d\epsilon_{k\sigma} &= \sum_{k'\sigma'} f_{kk'\sigma\sigma'} dn_{k'\sigma'} \\
&= dn \sum_{k'} (f_{kk'\uparrow\uparrow} + f_{kk'\uparrow\downarrow}) \quad [dn = dn_{k'\uparrow} = dn_{k'\downarrow}] \\
&= 2dn f_0^s
\end{aligned} \tag{5.13.12}$$

Therefore,

$$\begin{aligned}
dN &= \sum_{k\sigma} dn_{k\sigma} = \sum_{k\sigma} \frac{\partial n}{\partial \epsilon_{k\sigma}} (d\epsilon_{k\sigma} - d\mu) = \sum_{k\sigma} -\frac{1}{2} \rho (2dn f_0^s - d\mu) = -\rho(0) dN f_0^s + d\mu \rho(0) \\
&\approx d\mu \rho(0) - \rho(0) f_0^s d\mu \rho(0) \quad [\text{substitute } dN \text{ back into itself}] \\
\Rightarrow \frac{dN}{d\mu} &= \rho(0) (1 - \rho(0) f_0^s) \Rightarrow \chi_{\text{imp}}^c = \rho(0)_{\text{imp}} - \rho(0) f_0^s
\end{aligned} \tag{5.13.13}$$

At an intermediate state, we substituted dN back into itself and kept only the leading order term. This is justified because $f_{kk'}$ goes as $\frac{1}{NJ}$. At the fixed point and for a thermodynamically large system, both J and N are very large, so keeping only the leading order suffices.

From a previous calculation, we know that the charge susceptibility at $T = 0$ is zero (eq. (5.7.9)), so we can write down the following relation:

$$f_0^s = \frac{\rho(0)_{\text{imp}}}{\rho(0)} \tag{5.13.14}$$

5.13.3 Low- T Spin Susceptibility

$$\chi^s = \frac{dm}{d\mu} \tag{5.13.15}$$

Due to change in magnetic field, change in $\epsilon_{k\sigma}$ should be isotropic and SU(2)-antisymmetric. Hence

$$\begin{aligned} d\epsilon_{k\sigma} &= -\frac{1}{2}dB\sigma + \sum_{k'\sigma'} f_{kk'\sigma\sigma'} dn_{k'\sigma'} \\ &= -\frac{1}{2}dB\sigma + dn_\sigma \sum_{k'} \left(f_{kk'\uparrow\uparrow} - f_{kk'\uparrow\downarrow} \right) \quad \left[dn_{k'\uparrow} = -dn_{k\downarrow} \right] \\ &= -\frac{1}{2}dB\sigma + 2dn_\sigma f_0^a \end{aligned} \quad (5.13.16)$$

Since the total number remains constant, $\mu = 0$. Therefore,

$$\begin{aligned} dm &= \sum_k \left(dn_{k\uparrow} - dn_{k\downarrow} \right) = -\frac{1}{2} \sum_k \rho \left(d\epsilon_{k\uparrow} - d\epsilon_{k\downarrow} \right) = -\frac{1}{2} \sum_k \rho \left(-dB + 2f_0^a \left(dn_{k\uparrow} - dn_{k\downarrow} \right) \right) \\ &= dB\rho(0) - dm\rho(0)f_0^a \approx dB\rho(0) - \rho(0)f_0^a B\rho(0) \quad [\text{substitute } dm \text{ back into itself}] \\ \implies \frac{dm}{dB} &= \rho(0) (1 - \rho(0)f_0^a) \implies \chi_{imp}^s = \rho(0)_{imp} - \rho(0)f_0^a \end{aligned} \quad (5.13.17)$$

5.13.4 Wilson ratio

The Wilson ratio for the impurity [9, 16, 69] is defined as

$$R = \frac{\chi_{imp}^s}{\frac{C_{imp}}{T}} \quad (5.13.18)$$

From eq. (5.13.5), we have $f_0^s = -f_0^a$, which, when combined with eq. (5.13.14), gives

$$\chi_{imp}^s = 2\rho(0)_{imp} \quad (5.13.19)$$

The Wilson ratio becomes

$$R = \frac{2\rho(0)_{imp}}{\rho(0)_{imp}} = 2 \quad (5.13.20)$$

5.14 Luttinger's and Friedel's sum rules

In this section, we will compute Luttinger's sum for the various fixed-point theories. Luttinger's sum is essentially the volume enclosed by the Fermi surface [82–84], and Luttinger's theorem states that this volume counts the number of electrons in the system [82–84].

We first consider the strong-coupling fixed point Hamiltonian, which is essentially just a resonant-level model:

$$\mathcal{H}_{\text{res}} = \sum_{k\sigma} \epsilon_k \hat{n}_{k\sigma} + \sum_{k\sigma} \left(V_k c_{k\sigma}^\dagger c_{d\sigma} + \text{h.c.} \right) \quad (5.14.1)$$

The impurity Green's function is given by [69, 85, 86]

$$G_d(z) = \frac{1}{z - \Sigma_d} |d\sigma\rangle \langle d\sigma|, \quad \Sigma_d = \sum_k \frac{V^2}{z - \epsilon_k} \quad (5.14.2)$$

$\Sigma_d(z)$ is zero at the free orbital fixed point. The conduction electron Green's function is

$$G_k(z) = G_k^0(z) + \left[G_k^0(z) V_k \right]^2 G_d(z), \quad G_k^0 = \frac{1}{z - \epsilon_k}, \quad G_c^0(z) = \sum_k G_k^0(z) |k\rangle \langle k|, \quad (5.14.3)$$

$$G_c(z) = \sum_k G_k(z) |k\rangle \langle k| = G_c^0 + \left[G_k^0(z) V_k \right]^2 G_d(z) |k\rangle \langle k| \quad (5.14.4)$$

The total number of electrons is given by the sum of the number of electrons in the conduction bath and at the

impurity [69, 81]:

$$N = \oint \frac{dz}{2\pi i} n_F(z) \text{Tr} [G_d(z) + G_c(z)] = \oint \frac{dz}{2\pi i} n_F(z) \text{Tr} \left[G_d(z) + G_c^0(z) + [G_k^0(z)V_k]^2 G_d(z) |k\rangle \langle k| \right] \quad (5.14.5)$$

Since the eigenstates of the system are situated at real poles, the contour Γ encloses only the real axes and hence picks out those real poles to count the total number of particles.

Since $1/G_c^0(z) = z - \sum_k \epsilon_k \hat{n}_k$, we can write $\text{Tr} [G_c^0(z)] = \text{Tr} \left[G_c^0 \frac{\partial}{\partial z} (1/G_c^0) \right]$ and hence

$$\text{Tr} [G_c(z)] = \frac{\partial}{\partial z} \left[\ln \text{Det} (1/G_c^0) \right] + \sum_k [G_k^0(z)V_k]^2 G_d(z) \quad (5.14.6)$$

The impurity part can, on the other hand, be written as

$$\text{Tr} [G_d(z)] = \text{Tr} \left[\frac{|d\rangle \langle d|}{z - \Sigma_d(z)} \right] = \text{Tr} \left[\frac{|d\rangle \langle d|}{z - \Sigma_d(z)} \frac{\partial(z)}{\partial z} \right] = \text{Tr} \left[G_d(z) \frac{\partial G_d^{-1}(z)}{\partial z} \right] + \text{Tr} \left[G_d(z) \frac{\partial \Sigma_d(z)}{\partial z} \right] \quad (5.14.7)$$

The first term can be written as $\text{Tr} \left[G_d(z) \frac{\partial G_d^{-1}(z)}{\partial z} \right] = \frac{\partial}{\partial z} [\ln \text{Det} G_d^{-1}(z)]$. The second part can be written as $\frac{\partial}{\partial z} \Sigma_d(z) = -\sum_k V^2 G_k^{02}$. Together, we get

$$\text{Tr} [G_d(z)] = \frac{\partial}{\partial z} [\ln \text{Det} (1/G_d)] - \text{Tr} \left[G_d(z) \sum_k V^2 G_k^{02} \right] \quad (5.14.8)$$

Substituting eqs. 5.14.6 and 5.14.8 into eq. 5.14.5, we get

$$N = \oint \frac{dz}{2\pi i} n_F(z) \left[\frac{\partial}{\partial z} [\ln \text{Det} (1/G_d)] + \frac{\partial}{\partial z} [\ln \text{Det} (1/G_c^0)] \right] \quad (5.14.9)$$

At $T = 0$, n_F is defined as 1 below the FS, $\frac{1}{2}$ at the FS and 0 above it.

$$N = \left[\oint_{\Gamma_-} + \frac{1}{2} \oint_{\Gamma_0} \right] \frac{dz}{2\pi i} \left[\frac{\partial}{\partial z} \ln \text{Det} \{1/G_d(z)\} + \frac{\partial}{\partial z} \ln \text{Det} \{1/G_c^0(z)\} \right] \quad (5.14.10)$$

Following Seki and Yunoki [84], we can define a winding number for a Green's function $G(z)$:

$$n_{\text{Det } G^{-1}}(C) = \oint_C \frac{dz}{2\pi i} \frac{\partial \ln \text{Det } G^{-1}(z)}{\partial z} = \oint_{\text{Det } G^{-1}(C)} \frac{d \text{Det } G^{-1}}{\text{Det } G^{-1}} \quad (5.14.11)$$

Since $n_{\text{Det } G^{-1}(C)}$ counts the number of times the curve $\text{Det } G^{-1}(C)$ winds around the origin, it is integer-valued and topological. Seki and Yunoki also show that this number is given by

$$n_{\text{Det } G^{-1}(C)} = P_{\text{Det } G}(C) - Z_{\text{Det } G}(C) \quad (5.14.12)$$

where $P_{f(z)}(C)$ is the number of poles of $f(z)$ enclosed by the contour C , and Z is the corresponding number of

zeros. The total number of particles in the resonant level model can thus be written as

$$\begin{aligned}
N &= \underbrace{P_{\text{Det } G_d}(\Gamma_<) - Z_{\text{Det } G_d}(\Gamma_<)}_{N_{\text{imp}}^<} + \frac{1}{2} \underbrace{\left[P_{\text{Det } G_d}(\Gamma_0) - Z_{\text{Det } G_d}(\Gamma_0) \right]}_{N_{\text{imp}}^0} + \underbrace{P_{\text{Det } G_c^0}(\Gamma_<) - Z_{\text{Det } G_c^0}(\Gamma_<)}_{N_L^<} \\
&\quad + \frac{1}{2} \underbrace{\left[P_{\text{Det } G_c^0}(\Gamma_0) - Z_{\text{Det } G_c^0}(\Gamma_0) \right]}_{N_L^0} \\
&= N_{\text{imp}}^< + \frac{1}{2} N_{\text{imp}}^0 + N_L^< + \frac{1}{2} N_L^0
\end{aligned} \tag{5.14.13}$$

The average number of particles can thus be expressed purely in terms of the number of real poles and real zeros of the impurity and the conduction electron Green's functions. $N_{\text{imp}}^< \left(N_{\text{imp}}^< \right)$ is the number of poles minus the number of zeros of the impurity Greens function inside (on) the Fermi surface. $N_{\text{imp}} = N_{\text{imp}}^0 + \frac{1}{2} N_{\text{imp}}^0$ therefore gives the total number of localised eigenstates of the system. Similarly, $N_L^< \left(N_L^0 \right)$ gives the number of real poles in the conduction electron Greens function minus the number of real zeros, and $N_L = N_L^< + \frac{1}{2} N_L^0$ gives the total number of delocalised eigenstates of the system.

$$N = N_{\text{imp}} + N_L \tag{5.14.14}$$

Note that this also holds at the free orbital fixed point, because it is a special case of the strong-coupling fixed point with $V = 0$.

If we are the local moment fixed point with particle-hole symmetry, we instead have the Hamiltonian

$$\mathcal{H}_{\text{lm}} = \sum_{k\sigma} \epsilon_k \hat{n}_{k\sigma} + H_{\text{imp}} \tag{5.14.15}$$

where $H_{\text{imp}} = -(U/2)\hat{n}_d + U\hat{n}_{d\uparrow}\hat{n}_{d\downarrow}$ is the impurity Hamiltonian. In this atomic limit, the impurity Greens function is given by [87]

$$G_d = \frac{1}{z - \Sigma_d(z)}, \quad \Sigma_d = \frac{U^2}{4} \frac{1}{z} \tag{5.14.16}$$

Since $V = 0$ at this fixed point, the total number of particles is given by

$$N = \oint \frac{dz}{2\pi i} n_F(z) \text{Tr} \left[G_d(z) + G_c^0(z) \right] \tag{5.14.17}$$

We again use eq. 5.14.7 to write

$$\text{Tr} \left[G_d(z) \right] = \text{Tr} \left[G_d(z) \frac{\partial G_d^{-1}(z)}{\partial z} \right] + \text{Tr} \left[G_d(z) \frac{\partial \Sigma_d(z)}{\partial z} \right] = \frac{\partial}{\partial z} \left[\ln \text{Det} (1/G_d) \right] + \text{Tr} \left[G_d(z) \frac{\partial \Sigma_d(z)}{\partial z} \right] \tag{5.14.18}$$

Performing the integral for the second term gives

$$\left(\int_{\Gamma_<} + \frac{1}{2} \int_{\Gamma_0} \right) \frac{dz}{2\pi i} \text{Tr} \left[G_d(z) \frac{\partial \Sigma_d(z)}{\partial z} \right] = 0 \tag{5.14.19}$$

Here we used the form of Σ_d in eq. 5.14.16. Repeating the same steps as before, we recover eq. 5.14.14.

We now compare the Luttinger volume across the fixed points. At the local moment fixed point, the impurity Greens function has a single pole at $z < 0$ and a zero at $z = 0$, so $N_{\text{imp}} = 1 - 1/2 = 1/2$, and eq. 5.14.14 becomes

$$N = 1/2 + N_L^{LM} \tag{5.14.20}$$

The same thing happens at the free orbital fixed point; there, G_d has a single pole at $z = 0$, so $N_{\text{imp}} = 1/2$ and we again get $N = 1/2 + N_L^{FO}$. The change happens when we go to the strong-coupling resonant-level fixed point.

There, the impurity self-energy can be written as [69, 85, 86]

$$\Sigma_d^{\text{sc}} = \text{Re} [\Sigma_d^{\text{sc}}] - i\Delta \quad (5.14.21)$$

That is, the self-energy becomes imaginary, so the real pole that existed at the free orbital fixed point moves off the real axis. We therefore have $N_{\text{imp}} = 0$. Assuming the number of particles N remained constant, we obtain $N = N_L^{\text{SC}}$. The change in the Fermi volume in going from the local moment to the strong coupling fixed point is therefore by $1/2$. If one defines new a Luttinger volume $\mathcal{N}_L = 2N_L$ to also account for the spin degeneracy, we can write:

$$\Delta\mathcal{N}_L = 1 \quad (5.14.22)$$

This is a specific case of the more general result for Kondo lattices obtained by Oshikawa using flux-insertion arguments [83].

The scattering phase shift suffered by the conduction electrons at the Fermi surface, off the impurity, can be calculated from the impurity occupancy, using the Friedel sum rule. From the ground state wavefunction, we can calculate the average number of particles on the impurity:

$$\langle n_d \rangle = \langle \Psi |_1 \sum_{\sigma} \hat{n}_{d\sigma} | \Psi \rangle_1 \quad (5.14.23)$$

$|\Psi\rangle_1$ is the lower energy state in eq. (5.4.5). Performing the inner product gives

$$\langle n_d \rangle = \left(c_s^-\right)^2 + \left(c_c^-\right)^2 = 1 \quad (5.14.24)$$

The phase shift is thus

$$\frac{1}{\pi} \sum_{\sigma} \delta_{\sigma}(0) = \langle n_d \rangle \implies \delta_{\sigma}(0) = \frac{\pi}{2} \quad (5.14.25)$$

There we used $\delta_{\uparrow} = \delta_{\downarrow}$ because the model is SU(2)-symmetric. This line of arguments was first presented for the Kondo model in [88].

The change in Luttinger's number also allows us to calculate the Wilson ratio of the system, from eq. (??).

$$R = 1 + \sin^2 \left(\frac{\pi}{2} \Delta\mathcal{N}_L \right) = 1 + \sin^2 \frac{\pi}{2} = 2 \quad (5.14.26)$$

5.15 Reverse RG analysis

The goal here is to chart the journey starting from the IR fixed point towards the UV regime, by following one particular wavefunction. We will start with a very simple IR ground state wavefunction, and then go back towards the UV ground state by applying the inverse unitary operator U^{\dagger} :

$$\begin{aligned} U : \underbrace{|1, 2, \dots, N\rangle}_{\text{UV ground state}} &\rightarrow |1, 2, \dots, N-1\rangle |N\rangle \rightarrow \dots \rightarrow \underbrace{|1, 2, \dots, N^*\rangle |N^*+1\rangle \dots |N\rangle}_{\text{IR ground state}} \\ U^{\dagger} : \underbrace{|1, 2, \dots, N^*\rangle |N^*+1\rangle \dots |N\rangle}_{\text{IR ground state}} &\rightarrow |1, 2, \dots, N^*+1\rangle |N^*+2\rangle \dots |N\rangle \rightarrow \dots \rightarrow \underbrace{|1, 2, \dots, N\rangle}_{\text{UV ground state}} \end{aligned}$$

The first process is the forward RG which we used to obtain the scaling equations. The second process is the reverse RG which we will undertake now. The method has already been applied to study the renormalisation of entanglement in various models of strong correlation [60, 89, 90]. In general, we start with an IR wavefunction that consists a certain number of momentum states n_1 still entangled with the impurity, and the remaining momentum states n_2 disentangled from the impurity. The former are said to be part of the emergent Kondo cloud, while the latter are said to be part of the integrals of motion (IOMs) and appear in direct product with the cloud+impurity system in the ground state wavefunction. Each momentum state is tagged with two conduction bath levels, one above the Fermi surface and one below. These will be represented as k, \pm . If we represent the emergent cloud

momentum states as $\{k_i\}$ and the IOM states as $\{q_i\}$, the ground state wavefunction can be written as

$$|\Psi\rangle_0 = \left(\otimes_{i=1}^{n_2} |q_i, -, \uparrow\rangle |q_i, -, \downarrow\rangle \right) |\Phi\rangle_{\text{cloud}} \left(\otimes_{i=1}^{n_2} |q_i, +, \uparrow\rangle |q_i, +, \downarrow\rangle \right) \quad (5.15.1)$$

Throughout, we have assumed that the IOMs below the Fermi surface are occupied while those above are unoccupied. This means:

$$|\Psi\rangle_0 = \left(\otimes_{i=1}^{n_2} |\hat{n}_{q_i, -, \uparrow} = 1\rangle |\hat{n}_{q_i, -, \downarrow} = 1\rangle \right) |\Phi\rangle_{\text{cloud}} \left(\otimes_{i=1}^{n_2} |\hat{n}_{q_i, +, \uparrow} = 0\rangle |\hat{n}_{q_i, +, \downarrow} = 0\rangle \right) \quad (5.15.2)$$

$|\Phi\rangle_{\text{cloud}}$ will be obtained by diagonalising a small system of n_1 conduction bath k states. This completes the construction of the IR ground state $|\Psi\rangle_0$. The algorithm of reverse RG then involves applying unitary transformations on this IR wavefunction; the unitary transformations will be the inverse of those that were applied during the forward RG algorithm. Since the forwards RG transformations decoupled k states and transformed them into the IOMS, the inverse transformations will take the momentum states in the IOMS and re-entangle them with the impurity+cloud system, one at a time. This is shown in fig. 5.12.

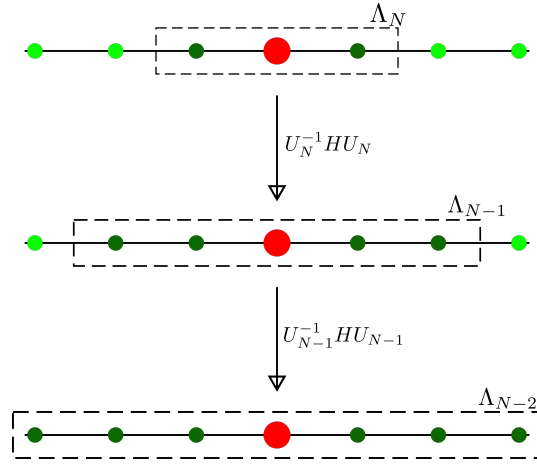


Figure 5.12: We start with a Hamiltonian with an impurity site (red) coupled with two conduction electrons (dark green), with four other decoupled electrons (bright green). The dotted rectangle represents the emergent window $(-\Lambda_j, \Lambda_j)$ at each step; the electrons inside that rectangle are still entangled with the impurity, while the ones inside have been decoupled. The next step of reverse RG involves applying the inverse transformation on the Hamiltonian, which will couple two more electrons from the IOMS (hence four dark green circles in the second step), leading to an enlargement of the emergent window. The unitary varies for each step, hence the notation U_j .

The next step is to write down the unitaries that will take us from the IR ground state to the UV ground state. In the forward RG, we used the following unitary for decoupling the shell ϵ_q and spin β is

$$U_{q\beta} = \frac{1}{\sqrt{2}} \left[1 + \eta_{0\beta} + \eta_{1\beta}^\dagger \right] . \quad (5.15.3)$$

Here, the subscripts 0 and 1 indicate it decouples an electron above and below the Fermi surface respectively. The inverse transformation for re-entangling $q\beta$ is

$$U_{q\beta}^\dagger = \frac{1}{\sqrt{2}} \left[1 + \eta_{0\beta}^\dagger + \eta_{1\beta} \right] . \quad (5.15.4)$$

In the $U > 0$ regime, the η s are given by

$$\begin{aligned} \eta_{0\beta}^\dagger &= V \left[\frac{1}{d_0} \left(1 - \hat{n}_{d\bar{\beta}} \right) + \frac{1}{d_1} \hat{n}_{d\bar{\beta}} \right] c_{q\beta}^\dagger c_{d\beta} + \frac{1}{d_2} \frac{J}{2} \sum_k \left(S_{d\beta}^z c_{q\beta}^\dagger c_{k\beta} + c_{d\bar{\beta}}^\dagger c_{d\beta} c_{q\beta}^\dagger c_{k\bar{\beta}} \right) , \\ \eta_{1\beta} &= V \left[\frac{1}{d_1} \left(1 - \hat{n}_{d\bar{\beta}} \right) + \frac{1}{d_0} \hat{n}_{d\bar{\beta}} \right] c_{d\beta}^\dagger c_{q\beta} + \frac{1}{d_2} \frac{J}{2} \sum_k \left(S_{d\beta}^z c_{k\beta}^\dagger c_{q\beta} + c_{d\beta}^\dagger c_{d\bar{\beta}} c_{k\bar{\beta}}^\dagger c_{q\beta} \right) ; \end{aligned} \quad (5.15.5)$$

since K is irrelevant, we have set $K = 0$ here. The denominators have already been defined in eq. (5.2.5).

$$d_0 = \omega - \frac{D}{2} - \frac{U}{2} + \frac{K}{4}, \quad d_1 = \omega - \frac{D}{2} + \frac{U}{2} + \frac{J}{4}, \quad d_2 = \omega - \frac{D}{2} + \frac{J}{4}, \quad d_3 = \omega - \frac{D}{2} + \frac{K}{4} \quad (5.15.6)$$

The wavefunction after reversing one step of the RG will thus be

$$|\Psi\rangle_1 = U_{q\uparrow}^\dagger U_{q\downarrow}^\dagger |\Psi\rangle_0 \quad (5.15.7)$$

Here, q is the first momentum state immediately outside the emergent cloud. Re-entangling further momentum states using their respective unitaries lead to the sequence of wavefunctions $|\Psi\rangle_2, |\Psi\rangle_3$ and so on.

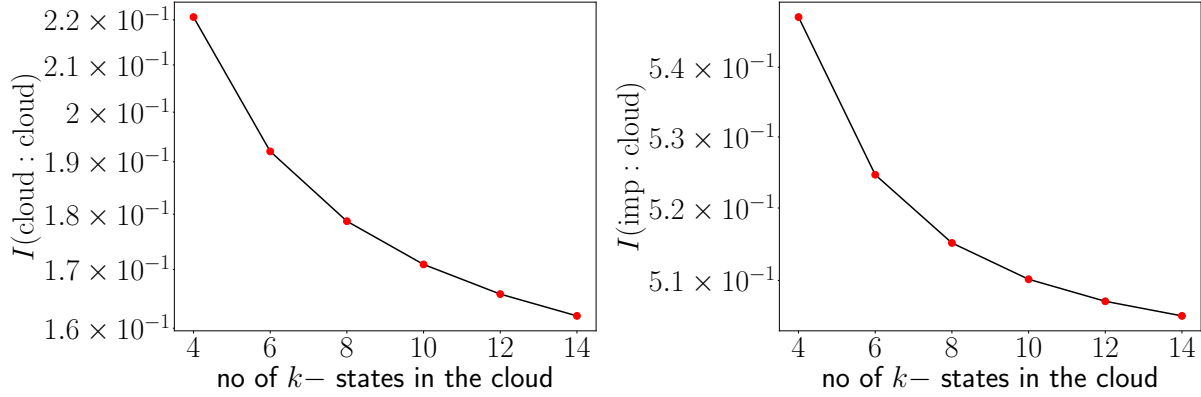


Figure 5.13: *Left*: Mutual information between two conduction electrons inside the cloud. *Right*: Mutual information between a conduction electron inside the cloud and an impurity electron. Both the measures increase towards the strong coupling fixed point, because of the distillation of the Kondo cloud brought about by the RG flow.

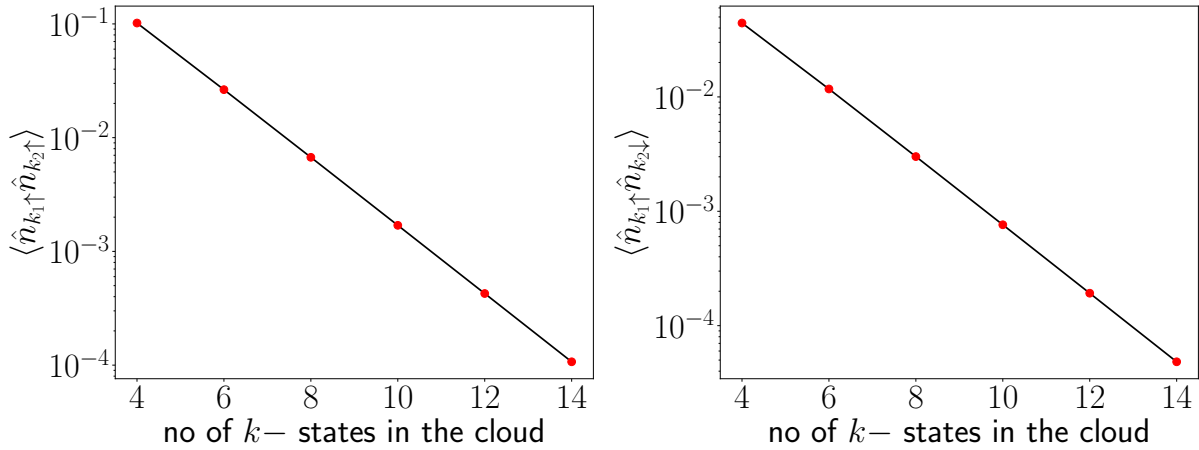


Figure 5.14: Increase in the diagonal correlation functions between cloud electrons under RG flow towards the strong coupling fixed point. This is consistent with the Fermi liquid pieces generated in the k -space effective Hamiltonian of the Kondo cloud.

The results of the reverse RG study are depicted in the following plots. We have used two types of quantities in the process - mutual information and correlation functions. The mutual information between two subsystems A and B in a wavefunction with many subsystems is defined as

$$I(A : B) = S_A + S_B - S_{AB} \quad (5.15.8)$$

where $S_{ij..q}$ is the von-Neumann entropy of the reduced density matrix obtained after tracing out all degrees of freedom except those in the subscript of S .

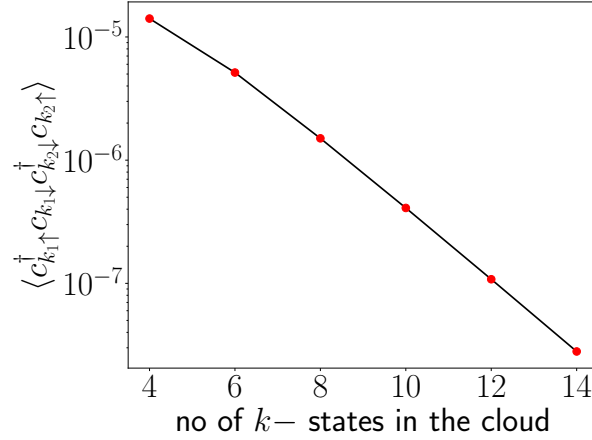


Figure 5.15: Growth of the off-diagonal correlation function between Kondo cloud electrons towards the strong coupling fixed point. This is the direct cause of the screening of the impurity spin, and is a reflection of the off-diagonal two-particle scattering terms in the k -space effective Hamiltonian of the Kondo cloud.

The mutual information between two electrons inside the entangled cloud increases as we go towards the IR fixed point. This can be understood in the following manner; as the wavefunction flows towards a smaller sized emergent cloud, the entanglement between those electrons gets distilled out.

We have also computed some correlation functions. All of them increase towards the IR fixed point. The increase in the correlation function $\langle \hat{n}_{k_1\uparrow} \hat{n}_{k_2\downarrow} \rangle$ arises from the crystallization of the spin singlet at the fixed point. The increase in the correlation function $\langle \hat{n}_{k\uparrow} \hat{n}_{k\downarrow} \rangle$ arises from the charge triplet content of the wavefunction, showing the increase of the charge contribution on the momenta. The increase in the off-diagonal correlation function $\langle c_{k\uparrow}^\dagger c_{k'\downarrow} c_{q\downarrow}^\dagger c_{q'\uparrow} \rangle$ shows that there is a large and non-trivial interaction between the electrons of the cloud that is being mediated by the impurity electron. This interaction is not of the Fermi liquid type, but instead was obtained in the effective Hamiltonian for the Kondo cloud.

Chapter 6

Effect of minimal attractive correlation in the bath

6.1 The modified hamiltonian

We will include a local particle-hole symmetric correlation of strength U_b on the origin of the lattice:

$$\mathcal{H} = \sum_{k\sigma} \epsilon_k \tau_{k\sigma} + \epsilon_d \left(\hat{n}_{d\uparrow} - \hat{n}_{d\downarrow} \right)^2 + \sum_{k\sigma} \left(V_k c_{k\sigma}^\dagger c_{d\sigma} + h.c. \right) + J \vec{S}_d \cdot \vec{s} - U_b \left(\hat{n}_{0\uparrow} - \hat{n}_{0\downarrow} \right)^2 \quad (6.1.1)$$

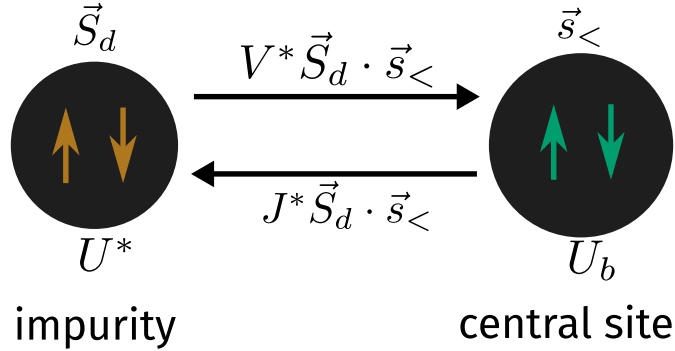


Figure 6.1: While we have studied the full model under renormalisation group, often we will turn to a simplified zero-bandwidth version of the model that is obtained by ignoring the kinetic energy part of the Hamiltonian. This zero-bandwidth model is effectively a two site model.

6.2 RG Equations

The derivation of the RG equations are shown in appendix B. . n_j is the number of k -states at the j^{th} isoenergetic shell.

$$\Delta U_b = 0, \quad \Delta U = 4V^2 n_j \left(\frac{1}{d_1} - \frac{1}{d_0} \right) - n_j \left(\frac{J^2}{d_2} - \frac{K^2}{d_3} \right), \quad (6.2.1)$$

$$\Delta V = -\frac{3n_j V}{8} \left[(J + 4U_b/3) \left(\frac{1}{d_2} + \frac{1}{d_1} \right) + (K + 4U_b/3) \left(\frac{1}{d_3} + \frac{1}{d_0} \right) \right], \quad (6.2.2)$$

$$\Delta J = -\frac{n_j J (J + 4U_b)}{d_2}, \quad \Delta K = -\frac{n_j K (K + 4U_b)}{d_3} \quad (6.2.3)$$

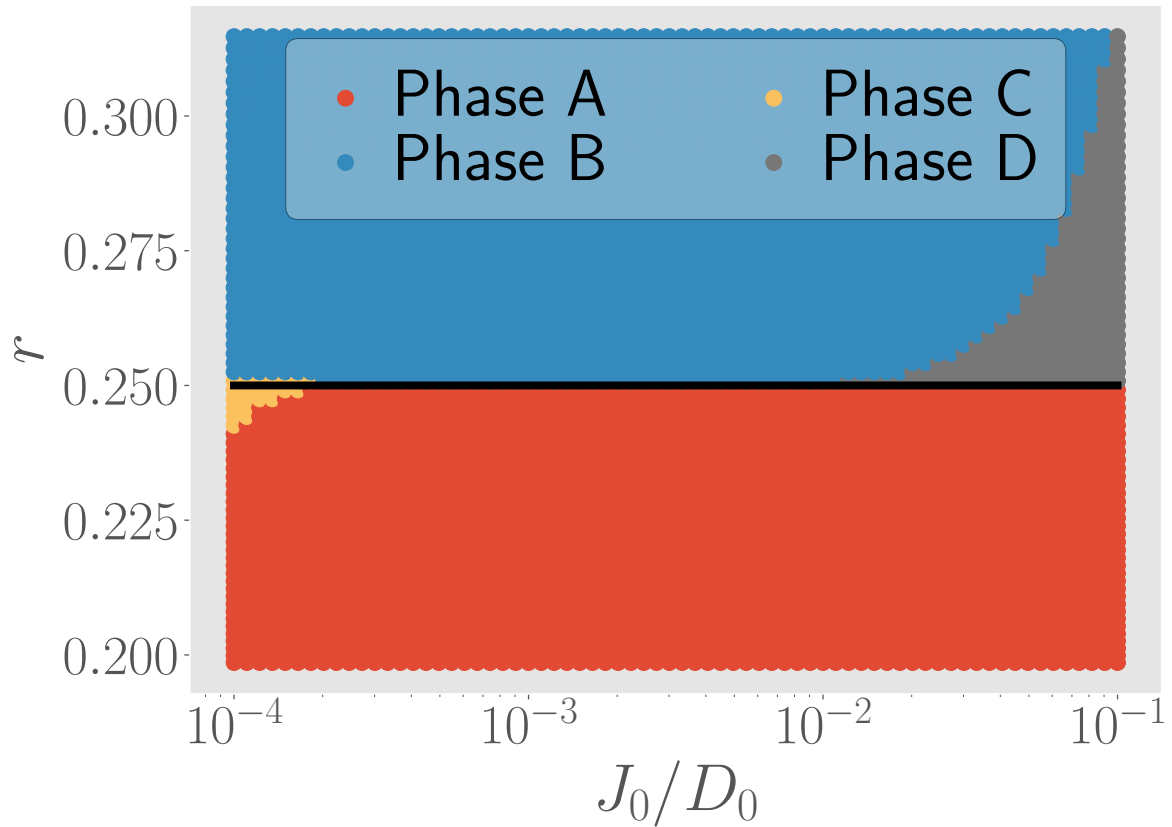
The denominators are

$$d_0 = \omega - \frac{D}{2} + \frac{U_b}{2} - \frac{U}{2} + \frac{K}{4}, \quad d_1 = \omega - \frac{D}{2} + \frac{U_b}{2} + \frac{U}{2} + \frac{J}{4}, \quad d_2 = \omega - \frac{D}{2} + \frac{U_b}{2} + \frac{J}{4}, \quad d_3 = \omega - \frac{D}{2} + \frac{U_b}{2} + \frac{K}{4} \quad (6.2.4)$$

Important points regarding notation

- The labels U_0, J_0, V_0 that may occur in the axes of the plots or anywhere else represent the bare values of the couplings U, J and V .
- Throughout the upcoming results, the bare value of U_b is set to the negative of the bare value of U_0 : $U_b = -U_0/10$. This means that whenever we vary U_0 along the axis of a plot, we are simultaneously varying U_b .

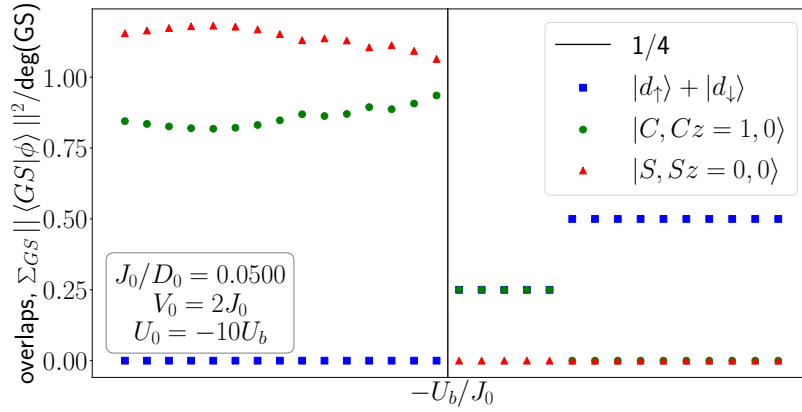
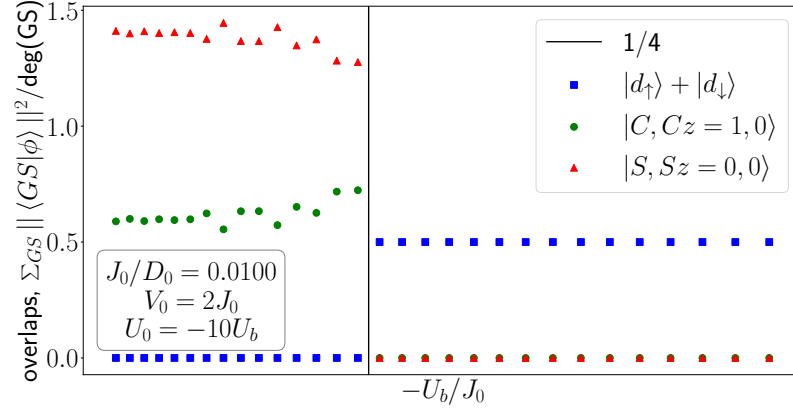
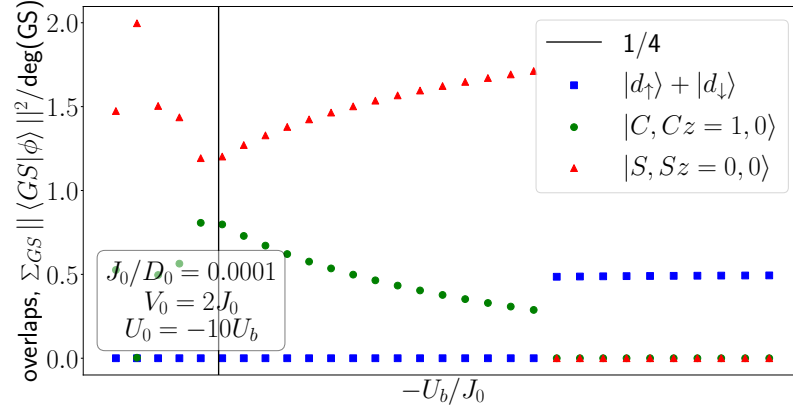
6.3 Phase diagram



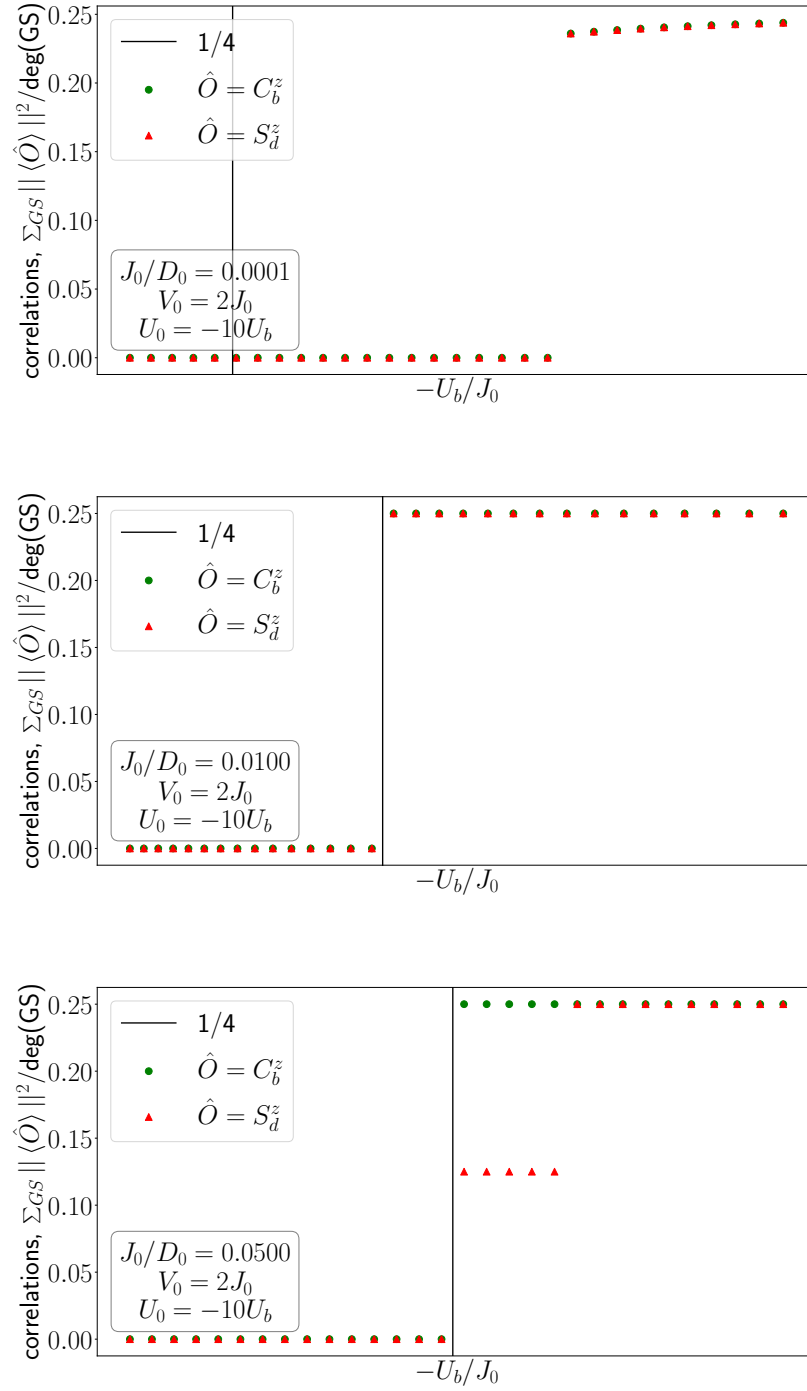
phase	RG flow	fixed point	GS	2-site GS
blue	$\Delta U < 0, \Delta J, \Delta V > 0$	$U^* \ll V^* \ll J^*$	SS	$ SS\rangle = \uparrow, \downarrow\rangle - \downarrow, \uparrow\rangle$
green	$\Delta U < 0, \Delta J < 0, \Delta V > 0$	$J^* < U^* \ll V^*$	SS + CT-0	$c SS\rangle + \sqrt{1-c^2} CT-0\rangle$
red	$\Delta U > 0, \Delta J, \Delta V < 0$	$U^* \gg 1, V^* = J^* = 0$	decoupled LM	$\{ \uparrow\rangle, \downarrow\rangle\} \otimes \{ 0\rangle, 2\rangle\}$
gray	$\Delta U, \Delta J, \Delta V < 0$	$U^* = V^* = J^* = 0$	lattice	$\{ \uparrow\rangle, \downarrow\rangle, 0\rangle, 2\rangle\} \otimes \{ 0\rangle, 2\rangle\}$

6.4 Evolution of the groundstate across the transition

Overlap of ground state against spin singlet and charge triplet zero states



Spin and charge correlations in ground state

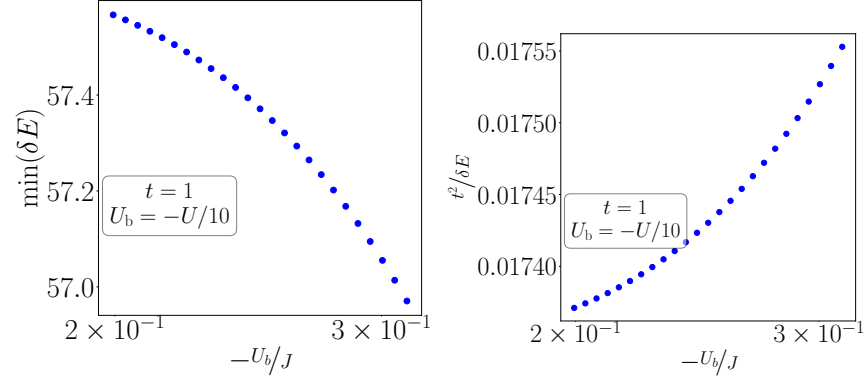


6.5 Evolution of various correlation measures and other quantities

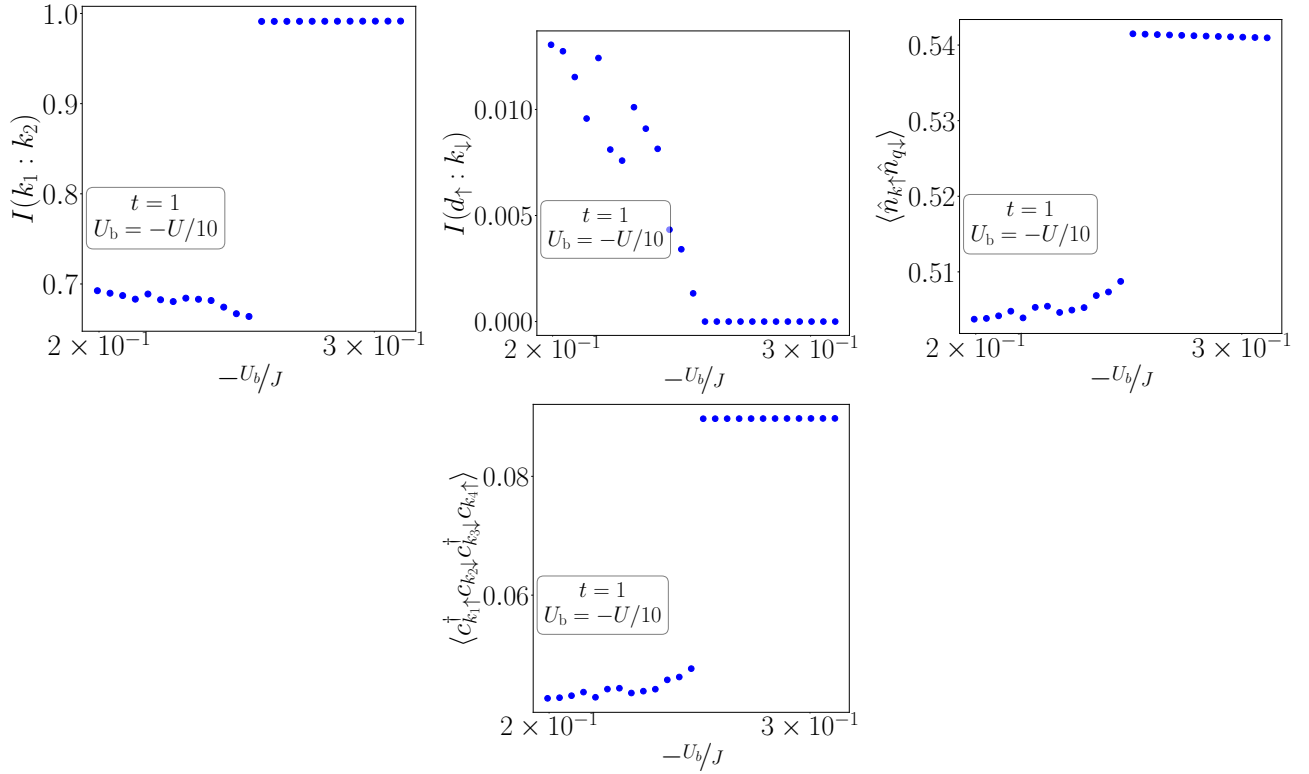
Perturbation theoretic terms

These quantities are related to the local Fermi liquid of the Kondo strong coupling fixed point and the perturbation theory associated with it. $\min(\delta E)$ is the gap in the spectrum of the two-site Hamiltonian; this which acts as the

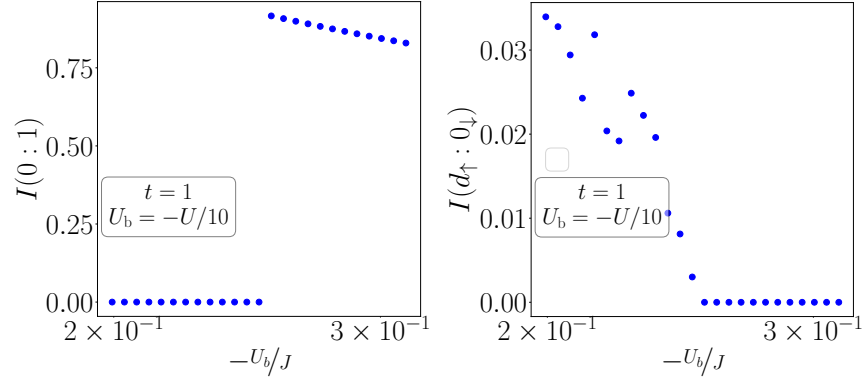
denominator for the perturbation theoretic calculations. $t^2/\delta E$ is the small parameter for the expansion, t being the tight-binding hopping.



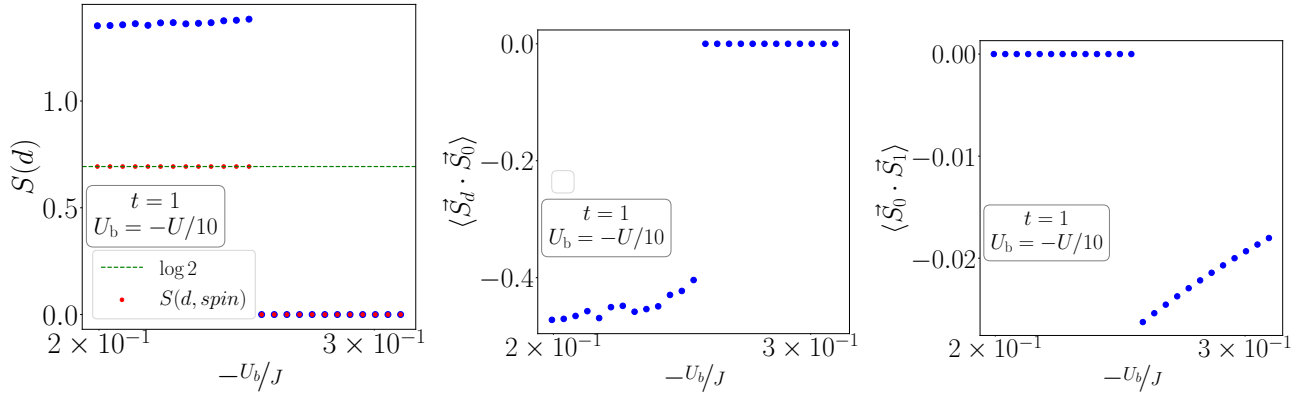
Correlation within the Kondo cloud



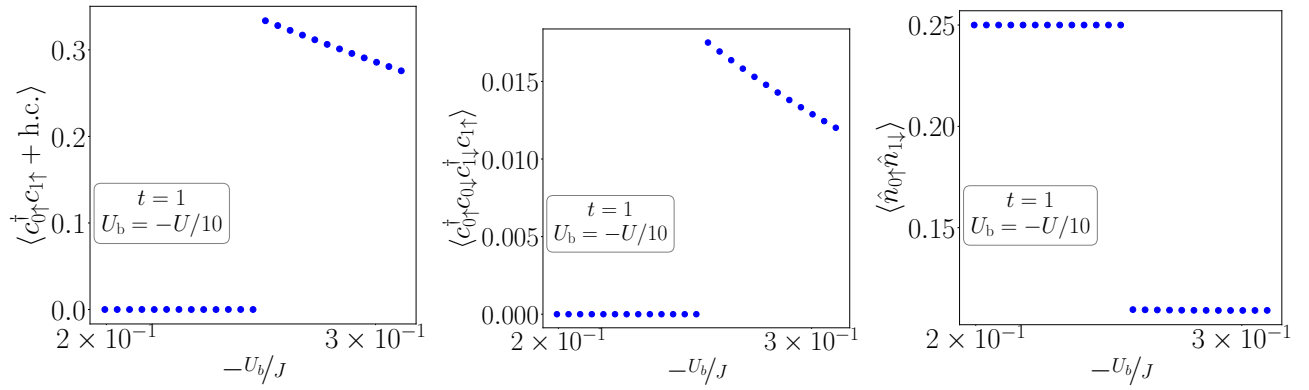
Mutual information between various real space members

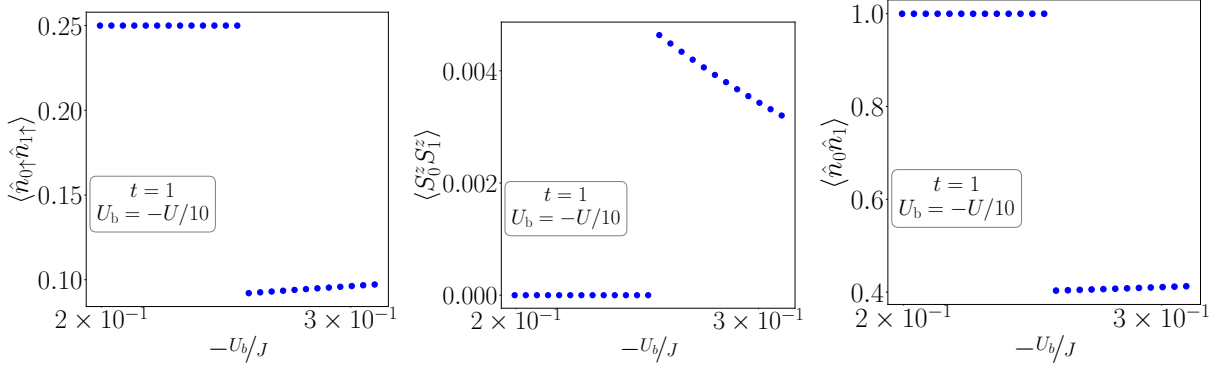


Impurity entanglement entropy and spin-spin correlations



Real-space correlations





6.6 Presence of sub-dominant pair fluctuations

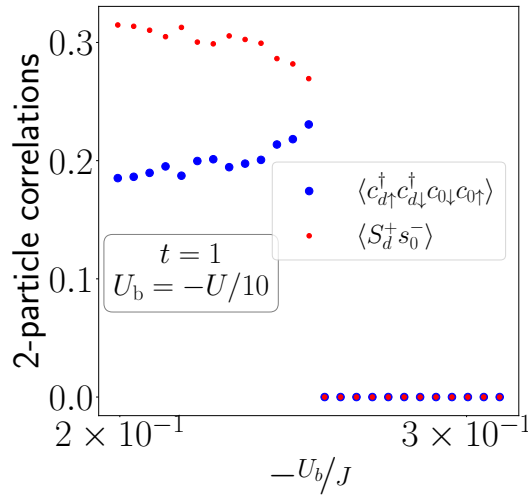


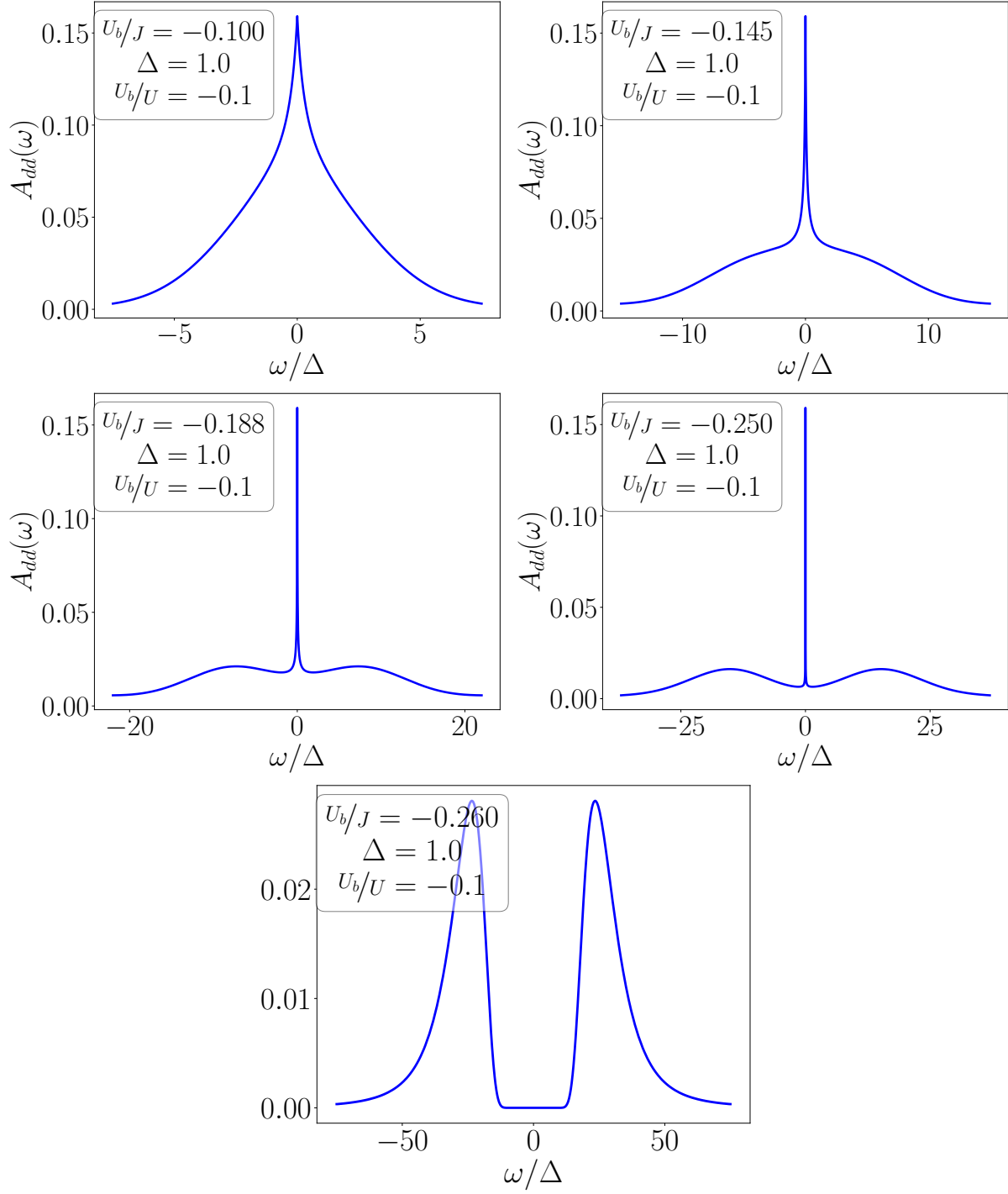
Figure 6.2: Growth of pair fluctuations $p_d^\dagger p_0$ between the impurity and the zeroth site towards the critical point, $p^\dagger = c_{\uparrow}^\dagger c_{\downarrow}^\dagger$ being the local pair creation operator. This comes at the cost of the spin-flip fluctuations $S_d^+ s_0^- + \text{h.c.}$ which decrease towards the transition.

The behaviour of the various kinds of correlation functions (for eg., the reduction of the impurity compensation $\vec{S}_d \cdot \vec{s}_0$) shown above indicate that the Kondo cloud that screens the impurity is getting destroyed as U_b/J increases in magnitude. To shed some light on the nature of the fluctuations that facilitate this process, we also plot the average pair fluctuation in the ground state as a function of U_b/J , in fig. 6.2. The pair fluctuations are terms that transfer an electron pair between the impurity and zeroth sites: $c_{d\uparrow}^\dagger c_{d\downarrow}^\dagger c_{0\downarrow} c_{0\uparrow}$. It can be seen from the figure that while the spin-flip fluctuations decrease (since the Kondo cloud is formed out of these spin-flip fluctuations, this is consistent with the destruction of the Kondo cloud discussed in this paragraph), the pair fluctuations pick up. Since the spin subspace and charge subspace cannot coincide on the same site, we can then conclude that it is the growth of these pair fluctuations brought about by the presence of the purely local interaction U_b that make the screening of the impurity spin very poor.

6.7 Spectral functions

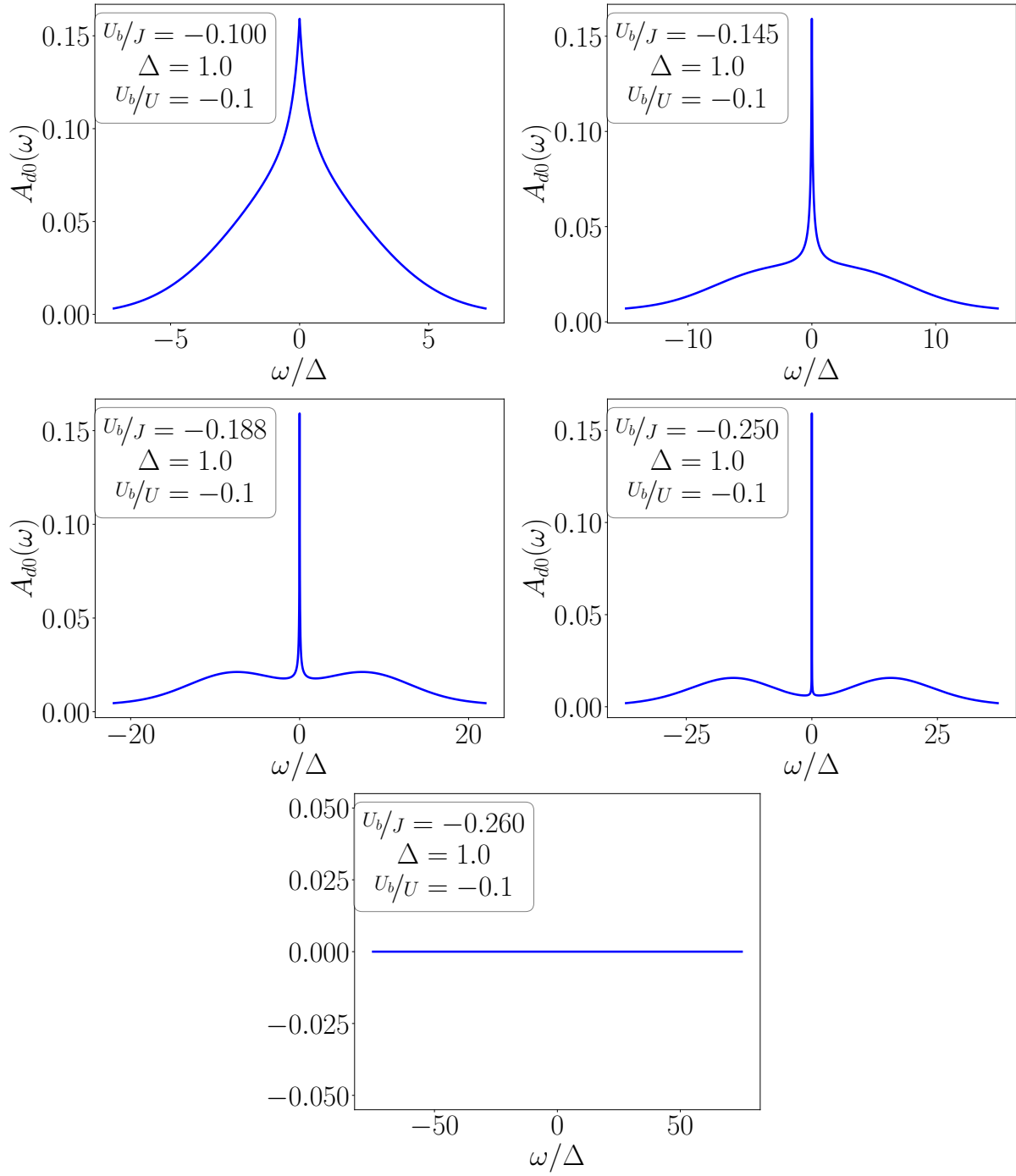
6.7.1 Impurity spectral function $A_{dd}(\omega)$

These are the frequency-domain spectral functions for the retarded propagator $-i\theta(t) \langle \{ c_{d\sigma}(t), c_{d\sigma}^\dagger \} \rangle$:

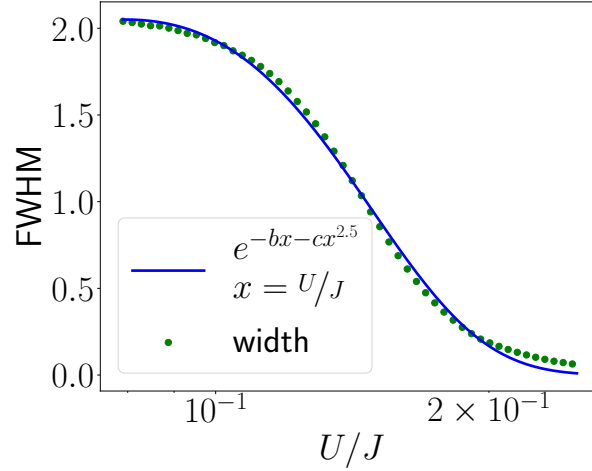


6.7.2 Impurity-bath off-diagonal spectral function $A_{dz}(\omega)$

These are the frequency-domain spectral functions for the off-diagonal retarded propagator $-i\theta(t) \left\langle \left\{ c_{d\sigma}(t), c_{0\sigma}^\dagger \right\} \right\rangle$:



6.7.3 Width of central peak of A_{dd}



6.8 Bath spectral function $A_{00}(\omega)$ and the relation to DMFT

In order to calculate the spectral function $A_{00}(\omega)$ of the site connected to the impurity (referred to as the zeroth site), we will use the following strategy. We will decouple the impurity states from the fixed point Hamiltonian using a single URG transformation. This will of course generate correlations on the zeroth site. The resulting Hamiltonian will be an Anderson impurity model with the hopping between the zeroth site and the rest of the chain acting as the effective hybridisation. Schematically, we will have

$$H^* = H_{\text{imp}} + V_{\text{imp-0}} + H_0 + H_{0-1} + H_{\text{rest}} \xrightarrow{\text{decouple imp.}} E_{\text{imp}} + \tilde{H}_0 + H_{0-1} + H_{\text{rest}} = H_{\text{new imp}} + V_{\text{new imp - rest}} + H_{\text{rest}} \quad (6.8.1)$$

Since the impurity is not coupled with any site beyond the zeroth site, the parts of the Hamiltonian that involve "rest" will not change in the process. This also means that the decoupling can be performed by looking at the smaller Hamiltonian

$$H_{\text{imp+0}} = H_{\text{imp}} + H_0 + V_{\text{imp-0}} = -\frac{U^*}{2} (\hat{n}_{d\uparrow} - \hat{n}_{d\downarrow})^2 - U_b (\hat{n}_{0\uparrow} - \hat{n}_{0\downarrow})^2 + J^* S_d^z S_0^z + V^* \sum_{\sigma} (c_{d\sigma}^\dagger c_{0\sigma} + \text{h.c.}) + \frac{J^*}{2} (c_{d\uparrow}^\dagger c_{d\downarrow} c_{0\downarrow}^\dagger c_{0\uparrow} + \text{h.c.}) \quad (6.8.2)$$

6.8.1 Renormalisation from V^*

From the off-diagonal term involving V^* , we generate the following term, in the particle sector for 0:

$$V^* \sum_{\sigma} c_{0\sigma}^\dagger c_{d\sigma} \frac{1}{\tilde{\omega} - H_d} V^* c_{d\sigma}^\dagger c_{0\sigma} = |V^*|^2 \sum_{\sigma} c_{0\sigma}^\dagger c_{d\sigma} \frac{1}{\tilde{\omega} + \frac{U^*}{2} (1 - \hat{n}_{d\bar{\sigma}})^2 + U_b \hat{n}_{0\bar{\sigma}} + \frac{J^*}{4} (1 - \hat{n}_{d\bar{\sigma}}) \hat{n}_{0\bar{\sigma}}} c_{d\sigma}^\dagger c_{0\sigma} \quad (6.8.3)$$

where $\tilde{\omega}$ is the quantum fluctuation operator for the impurity site and $H_d = -\frac{U^*}{2} (\hat{n}_{d\uparrow} - \hat{n}_{d\downarrow})^2 - U_b (\hat{n}_{0\uparrow} - \hat{n}_{0\downarrow})^2 + J^* S_d^z S_0^z$, is the diagonal part of the Hamiltonian for the imp+0 system. In order to resolve the operators in the denominator, we expand the unity in the numerator using the identity $1 = \hat{n}_{d\bar{\sigma}} \hat{n}_{0\bar{\sigma}} + \hat{n}_{d\bar{\sigma}} \hat{h}_{0\bar{\sigma}} + \hat{h}_{d\bar{\sigma}} \hat{n}_{0\bar{\sigma}} + \hat{h}_{d\bar{\sigma}} \hat{h}_{0\bar{\sigma}}$,

where $\hat{h} = 1 - \hat{n}$ is hole operator. On Substituting this, we get

$$\begin{aligned} \sum_{\sigma} V^* c_{0\sigma}^{\dagger} c_{d\sigma} \frac{1}{\tilde{\omega} - H_d} V^* c_{d\sigma}^{\dagger} c_{0\sigma} &= |V^*|^2 \sum_{\sigma} c_{0\sigma}^{\dagger} c_{d\sigma} \frac{\hat{h}_{d\bar{\sigma}} \hat{h}_{0\bar{\sigma}} + \hat{h}_{d\bar{\sigma}} \hat{n}_{0\bar{\sigma}} + \hat{n}_{d\bar{\sigma}} \hat{h}_{0\bar{\sigma}} + \hat{n}_{d\bar{\sigma}} \hat{n}_{0\bar{\sigma}}}{\tilde{\omega} + \frac{U^*}{2} \hat{h}_{d\bar{\sigma}} + U_b \hat{n}_{0\bar{\sigma}} + \frac{J^*}{4} \hat{h}_{d\bar{\sigma}} \hat{n}_{0\bar{\sigma}}} c_{d\sigma}^{\dagger} c_{0\sigma} \\ &= |V^*|^2 \sum_{\sigma} \hat{h}_{d\sigma} \hat{n}_{0\sigma} \left[\frac{\hat{h}_{d\bar{\sigma}} \hat{h}_{0\bar{\sigma}}}{\tilde{\omega}_{00} + \frac{U^*}{2}} + \frac{\hat{h}_{d\bar{\sigma}} \hat{n}_{0\bar{\sigma}}}{\tilde{\omega}_{01} + \frac{U^*}{2} + U_b + \frac{J^*}{4}} + \frac{\hat{n}_{d\bar{\sigma}} \hat{h}_{0\bar{\sigma}}}{\tilde{\omega}_{10}} + \frac{\hat{n}_{d\bar{\sigma}} \hat{n}_{0\bar{\sigma}}}{\tilde{\omega}_{11} + U_b} \right] \end{aligned} \quad (6.8.4)$$

$\tilde{\omega}_{(0,1),(0,1)}$ represents the quantum fluctuation scale corresponding to the configuration in the numerator.

In order to "freeze" the impurity dynamics, we will substitute $\hat{n}_{d\sigma} = \hat{n}_{d\bar{\sigma}} = \frac{1}{2}$, because of the \mathbb{Z}_2 symmetry and the particle-hole symmetry of the impurity levels. This gives

$$\frac{1}{4} |V^*|^2 \sum_{\sigma} \hat{n}_{0\sigma} \left[\frac{\hat{h}_{0\bar{\sigma}}}{\tilde{\omega}_{00} + \frac{U^*}{2}} + \frac{\hat{n}_{0\bar{\sigma}}}{\tilde{\omega}_{01} + \frac{U^*}{2} + U_b + \frac{J^*}{4}} + \frac{\hat{h}_{0\bar{\sigma}}}{\tilde{\omega}_{10}} + \frac{\hat{n}_{0\bar{\sigma}}}{\tilde{\omega}_{11} + U_b} \right] \quad (6.8.5)$$

The state that most closely represents the metallic ground state is $\tilde{\omega}_{10}$, we take that as the reference quantum fluctuation scale $\bar{\omega}$. It is of the order of $\bar{\omega} \sim -\frac{J^*}{4} - \frac{U^*}{2} - U_b$. We will now relate the other scales to $\bar{\omega}$ by expressing them in terms of the energy of the initial state:

$$\tilde{\omega}_{00} \sim -U_b = \bar{\omega} + \frac{J^*}{4} + \frac{U^*}{2}, \quad \tilde{\omega}_{01} \sim 0 = \bar{\omega} + \frac{J^*}{4} + \frac{U^*}{2} + U_b, \quad \tilde{\omega}_{11} \sim -\frac{U^*}{2} = \bar{\omega} + \frac{J^*}{4} + U_b \quad (6.8.6)$$

Substituting these gives

$$\frac{1}{4} |V^*|^2 \sum_{\sigma} \hat{n}_{0\sigma} \left[\hat{h}_{0\bar{\sigma}} \alpha_1 + \hat{n}_{0\bar{\sigma}} \alpha_2 \right] \quad (6.8.7)$$

where $\alpha_1 = \left(\bar{\omega} + U^* + \frac{J^*}{4} \right)^{-1} + (\bar{\omega})^{-1}$ and $\alpha_2 = \left(\bar{\omega} + U^* + 2U_b + \frac{J^*}{2} \right)^{-1} + \left(\bar{\omega} + 2U_b + \frac{J^*}{4} \right)^{-1}$.

Because of the particle-hole symmetry on the impurity as well as in the bath, the renormalisation from the hole sector is obtained simply by transforming $\hat{n} \leftrightarrow \hat{h}$:

$$\frac{1}{4} |V^*|^2 \sum_{\sigma} \hat{h}_{0\sigma} \left[\hat{n}_{0\bar{\sigma}} \alpha_1 + \hat{h}_{0\bar{\sigma}} \alpha_2 \right] \quad (6.8.8)$$

The total renormalisation arising from V is therefore

$$\frac{1}{4} |V^*|^2 \sum_{\sigma} \left[\alpha_1 \left(\hat{n}_{0\sigma} \hat{h}_{0\bar{\sigma}} + \hat{h}_{0\sigma} \hat{n}_{0\bar{\sigma}} \right) + \alpha_2 \left(\hat{n}_{0\sigma} \hat{n}_{0\bar{\sigma}} + \hat{h}_{0\sigma} \hat{h}_{0\bar{\sigma}} \right) \right] = \frac{1}{2} |V^*|^2 (\alpha_1 - \alpha_2) \left(\hat{n}_{0\uparrow} - \hat{n}_{0\downarrow} \right)^2 + \text{constant} \quad (6.8.9)$$

6.8.2 Renormalisation from J

The renormalisation arising from decoupling the Kondo coupling has two terms. The first term arises when the spin of the zeroth site is initially up:

$$\frac{J^{*2}}{4} c_{d\downarrow}^{\dagger} c_{d\uparrow} c_{0\uparrow}^{\dagger} c_{0\downarrow} \frac{1}{\tilde{\omega} - H_d} c_{0\downarrow}^{\dagger} c_{0\uparrow} c_{d\uparrow}^{\dagger} c_{d\downarrow} = c_{d\downarrow}^{\dagger} c_{d\uparrow} c_{0\uparrow}^{\dagger} c_{0\downarrow} \frac{J^{*2}/4}{\tilde{\omega} + \frac{U^*}{2} + U_b + \frac{J^*}{4}} c_{0\downarrow}^{\dagger} c_{0\uparrow} c_{d\uparrow}^{\dagger} c_{d\downarrow} = \frac{J^{*2}}{4} \frac{\hat{n}_{d\downarrow} \hat{h}_{d\uparrow} \hat{n}_{0\uparrow} \hat{h}_{0\downarrow}}{\tilde{\omega} + \frac{U^*}{2} + U_b + \frac{J^*}{4}} \quad (6.8.10)$$

The quantum fluctuation scale $\tilde{\omega}$ for this process can be similarly related to $\bar{\omega}$: $\tilde{\omega} \sim -\frac{U^*}{2} - U_b - \frac{J^*}{4} = \bar{\omega}$. This gives

$$\frac{J^{*2}}{4} \frac{\hat{n}_{d\downarrow} \hat{h}_{d\uparrow} \hat{n}_{0\uparrow} \hat{h}_{0\downarrow}}{\tilde{\omega} + \frac{U^*}{2} + U_b + \frac{3J^*}{4}} = \frac{J^{*2}}{16} \frac{\hat{n}_{0\uparrow} \hat{h}_{0\downarrow}}{\tilde{\omega} + \frac{U^*}{2} + U_b + \frac{J^*}{4}} \quad (6.8.11)$$

as the renormalisation for this configuration. At the final step, we substituted $\hat{n}_{d\sigma} = \hat{h}_{d\sigma} = \frac{1}{2}$. For the other configuration where the spin of the zeroth site is down, we get

$$\frac{J^{*2}}{16} \frac{\hat{n}_{0\downarrow} \hat{h}_{0\uparrow}}{\bar{\omega} + \frac{U^*}{2} + U_b + \frac{J^*}{4}} \quad (6.8.12)$$

Adding both sectors, we get

$$\frac{J^{*2}}{16} \frac{1}{\bar{\omega} + \frac{U^*}{2} + U_b + \frac{J^*}{4}} \left(\hat{n}_{0\uparrow} - \hat{n}_{0\downarrow} \right)^2 \quad (6.8.13)$$

6.8.3 Total renormalisation

Adding the contributions from both V^* and J^* , the net renormalisation is the generation of a local correlation term $-U_0 \left(\hat{n}_{0\uparrow} - \hat{n}_{0\downarrow} \right)^2$ on the zeroth site, where U_0 is given by

$$U_0 = -\frac{J^{*2}}{16} \frac{1}{\bar{\omega} + \frac{U^*}{2} + U_b + \frac{J^*}{4}} - \frac{1}{2} |V^*|^2 \left(\frac{1}{\bar{\omega} + U^* + \frac{J^*}{4}} + \frac{1}{\bar{\omega}} - \frac{1}{\bar{\omega} + U^* + 2U_b + \frac{J^*}{2}} - \frac{1}{\bar{\omega} + 2U_b + \frac{J^*}{4}} \right) \quad (6.8.14)$$

The effective Hamiltonian for the zeroth site is therefore

$$H_{0+\text{rest}} = \underbrace{-(U_0 + U_b) \left(\hat{n}_{0\uparrow} - \hat{n}_{0\downarrow} \right)^2}_{\text{new correlated impurity}} \underbrace{-t \sum_{\substack{j \in \text{n.n.} \\ \sigma}} \left(c_{0\sigma}^\dagger c_{j\sigma} + \text{h.c.} \right)}_{\text{hopping between new impurity \& new bath}} \underbrace{-t \sum_{\langle i,j \rangle} \left(c_{i\sigma}^\dagger c_{j\sigma} + \text{h.c.} \right)}_{\text{K.E. of new bath}} \quad (6.8.15)$$

6.8.4 Equivalence of the impurity site and the zeroth site: towards self-consistency

The fact that we end up with an Anderson impurity model shows that the behaviour of the zeroth site is equivalent to that of a correlated impurity interacting with a conduction bath through single-particle hopping. The correlation for this impurity is given by $U_{\text{eff}} = U_0 + U_b$, while the effective hybridisation for this new impurity into the conduction bath is given by $V = -t$. The new conduction bath is formed by all the sites of the lattice apart from the zeroth site. From Fig. 6.2, we know that the spin-flip correlations are quite dominant up to the transition, indicating that the largest energy scale in the system at low-energies is J^* . Using this, the effective correlation can be expressed to leading order as

$$U_{\text{eff}} \simeq \frac{J^*}{8} \quad (6.8.16)$$

This is simply a restatement of the fact that upto the transition, the impurity spectral function displays a central peak (Fig. 6.7.1); it is the dominant spin-flip scattering processes that lead to both the central peak as well as the induced repulsive correlation U_{eff} at the zeroth site. This also indicates that the bath spectral function will have a similar central peak, owing to the same scattering processes. We conclude that the spin-exchange coupling J acts as a mechanism of symmetrisation between the impurity and zeroth sites, leading to similar effective local correlations and similar local spectral functions. This also suggests that the self-consistency-based approach towards a bulk model, as used in DMFT, effectively involves finding the impurity model that has identical behaviour across the impurity and zeroth sites. Indeed, such an idea has been used in Ref. [91] to study the behaviour of the Hubbard model near the transition.

In the spirit of Ref. [91], near the transition, we can integrate out the charge degrees of freedom of the Anderson model via a canonical Schrieffer-Wolff transformation. Upto second order, this transformation removes the on site correlation U and the single-particle hybridisation V by generating an additional spin-exchange term $J' \sim \frac{V^2}{U+U_b}$. The total s-d coupling then becomes $\tilde{J} = J + J'$, and the effective Hamiltonian after the transformation is

$$H_{\text{Kondo}} = \tilde{J} \vec{S}_d \cdot \vec{S}_0 - U_b \left(\hat{n}_{0\uparrow} - \hat{n}_{0\downarrow} \right)^2 + H_{\text{K.E.}} \quad (6.8.17)$$

In this simplified model, the RG equations for \tilde{J} and U_b can be obtained simply by setting $U = V = 0$ in the more

general RG equations 6.2.1 through 6.2.3:

$$\Delta\tilde{J} = -\frac{n_j\tilde{J}(\tilde{J} + 4U_b)}{d_2}, \quad \Delta U_b = 0 \quad (6.8.18)$$

This makes it clear that the metal-insulator transition in this model is driven by the competition between Kondo screening generated by \tilde{J} and local pair correlation in the bath produced by $U_b = -|U_b|$. The fact that the only major impurity-bath interaction near the transition is of the spin-exchange kind reiterates the fact that the correlated spin-flip processes play the most important role in the model, and leads to the symmetrisation between the impurity and zeroth sites.

6.9 What, then, are the minimal ingredients for a metal-insulator transition?

We now return to the question posed at the very beginning in section 1.1: What is the minimal auxiliary model that can demonstrate a metal-insulator transition in the bulk? To answer this question, we first recall all the relevant RG equations in the positive U regime:

$$\Delta U_b = 0, \quad \Delta U = 4V^2 n_j \left(\frac{1}{d_1} - \frac{1}{d_0} \right) - n_j \frac{J^2}{d_2}, \quad (6.9.1)$$

$$\Delta V = -\frac{3n_j V}{8} \left[(J + 4U_b/3) \left(\frac{1}{d_2} + \frac{1}{d_1} \right) + 4U_b/3 \left(\frac{1}{d_3} + \frac{1}{d_0} \right) \right], \quad (6.9.2)$$

$$\Delta J = -\frac{n_j J (J + 4U_b)}{d_2}. \quad (6.9.3)$$

where $d_1 > d_2 > d_3 > d_0$. We now consider various models with increasing number of parameters.

6.9.1 Only impurity correlation and hybridisation U, V

If we had only U and V , the RG equations simplify to

$$\Delta U = 4V^2 n_j \left(\frac{1}{d_1} - \frac{1}{d_0} \right) < 0, \quad \Delta V = 0 \quad (6.9.4)$$

U is irrelevant while the hybridisation V is marginal, so the fixed point is where the impurity is screened. The bulk model will always be metallic. There is no transition in such a model.

6.9.2 Impurity correlation, hybridisation and spin-exchange between impurity and bath U, V, J

If we now add a spin-exchange coupling J between the impurity and the bath into the Hamiltonian, we obtain the extended SIAM studied in chapter 5. As discussed in that chapter, this is again similar to the previous case - the only stable fixed point is one of strong-coupling, and the bulk metal will never have an insulating phase.

6.9.3 Impurity correlation, hybridisation and local pairing interaction on the bath U, V, U_b

If we replace the J with an local interaction U_b on the bath, the RG equations undergo some changes:

$$\Delta U_b = 0, \quad \Delta U = 4V^2 n_j \left(\frac{1}{d_1} - \frac{1}{d_0} \right) = \frac{4V^2 U}{(\omega - D/2 + U_b/2)^2 - U^2/4}, \quad (6.9.5)$$

$$\Delta V = -n_j V U_b \left[\frac{\omega - D/2 + U_b/2}{(\omega - D/2 + U_b/2)^2 - U^2/4} + \frac{1}{\omega - D/2 + U_b/2} \right]. \quad (6.9.6)$$

This regime is interesting because it shows a variety of behaviour:

- For $U_b > 0$, the correlation U is irrelevant and V is relevant. This will produce a metal (see fig. 6.3).
- For $U_b < 0$, both U and V are irrelevant, but V decays much faster than U , and U saturates to a non-zero appreciable value which although lower than the bare value is much greater than 0 (see fig. 6.4). This behaviour is enhanced by making U_b more negative; V decays even faster to zero, while U saturates at higher values. If the bare bandwidth is increased, the fixed point value of U actually decreases, so it appears that on taking the thermodynamic limit, U renormalises to zero (see fig. 6.5).

Neither of these cases give rise to an insulator, because U never renormalises to a non-zero fixed point value in the thermodynamic limit.

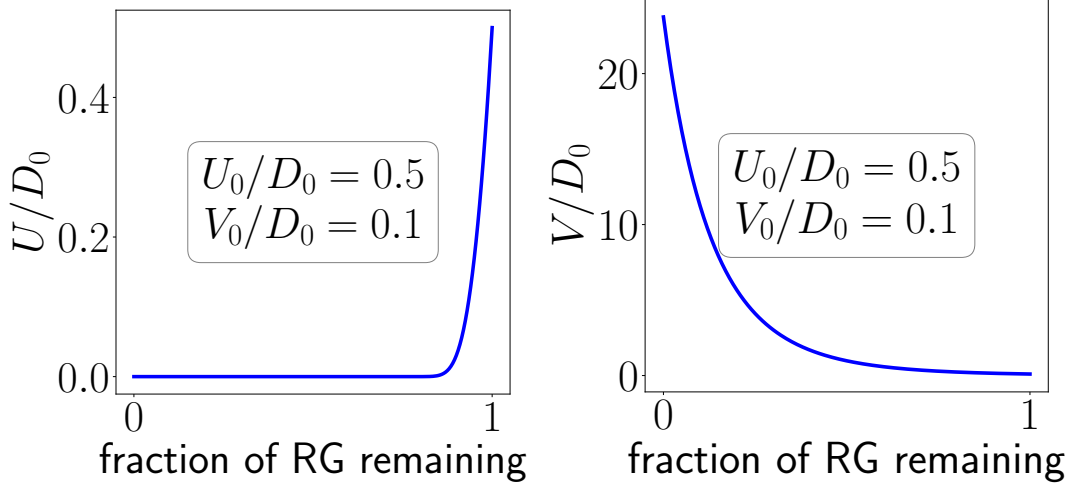


Figure 6.3: RG flows of U (left panel) and V (right panel) in the regime $U_b > 0$, for the auxiliary model with U, V, U_b . The impurity correlation U is irrelevant while the hybridisation V is relevant, leading to a metallic phase in the bulk.

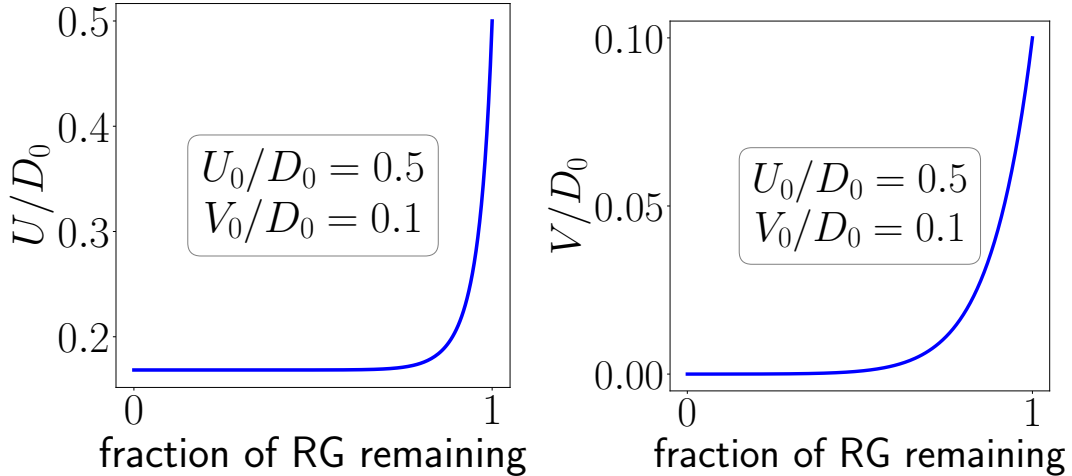


Figure 6.4: RG flows of U (left panel) and V (right panel) in the regime $U_b < 0$, for the auxiliary model with U, V, U_b . The hybridisation V is sharply irrelevant, renormalising to zero, while the impurity correlation U survives at the fixed point.

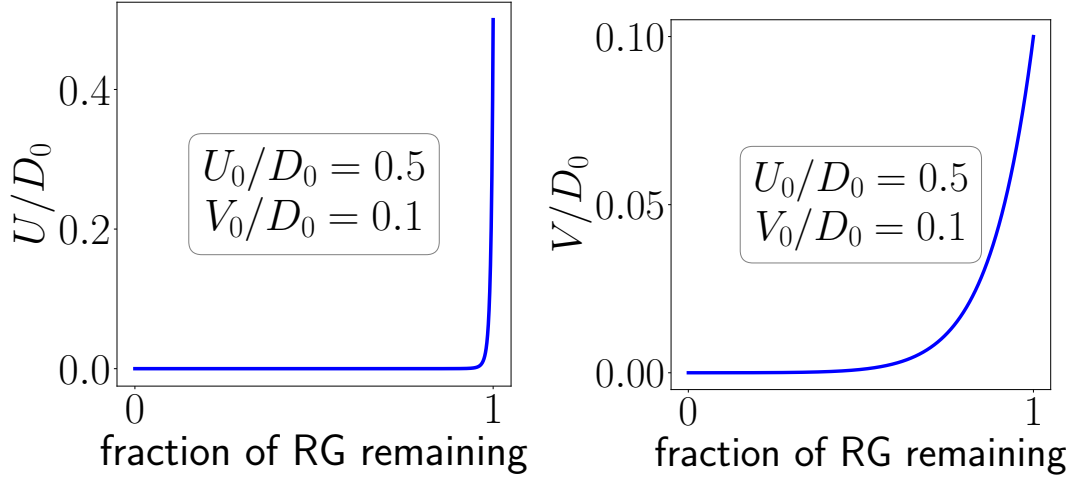


Figure 6.5: RG flows of U and V in the regime $U_b < 0$ at a larger bandwidth, for the auxiliary model with U, V, U_b . U now renormalises to zero, so an insulator is not possible in the thermodynamic limit.

6.9.4 Attractive correlation U_b instead of V : U, J, U_b

In the presence of these three couplings, the RG equations become

$$\Delta U = -n_j J^2 / d_2, \quad \Delta J = -n_j J(J + 4U_b) / d_2 \quad (6.9.7)$$

Since $J > 0$, ΔU is always positive, so U is always relevant. For $4U_b > -J$, ΔJ is also positive, and J is relevant. We end up in a metallic phase. However, for $4U_b < -J$, J becomes irrelevant, and the fixed point is that of a local moment decoupled from the bath, which describes an insulating state in the bulk.

6.9.5 The full model?

We are therefore ultimately led to a model with all four parameters. This was studied in chapter 6, and was shown to display both metallic and insulating phases. This makes it clear that *the minimal model must have all three kinds of correlation: magnetic (U, J), delocalisation (V) and pair formation (U_b).*

Appendices

Appendix A

Zero temperature Greens function in frequency domain

The impurity retarded Green's function (assuming the Hamiltonian to be time-independent, which it is) is defined as

$$G_{dd}^\sigma(t) = -i\theta(t) \left\langle \left\{ \mathcal{O}_\sigma(t), \mathcal{O}_\sigma^\dagger \right\} \right\rangle \quad (\text{A.0.1})$$

where the average $\langle \rangle$ is over a canonical ensemble at temperature T , and $\mathcal{O}_\sigma = c_{d\sigma} + S_d^- c_{0\bar{\sigma}} + S_d^z c_{0\sigma}$ is the excitation whose spectral function we are interested in. The excitations defined in \mathcal{O} incorporates both single-particle excitations brought about by the hybridisation as well as two-particle spin excitations brought about by the spin-exchange term. What follows is a standard calculation where we write the Green's function in the Lehmann representation. The ensemble average for an arbitrary operator \hat{M} can be written in terms of the exact eigenstates of the fixed point Hamiltonian:

$$H^* |n\rangle = E_n^* |n\rangle, \quad \langle \hat{M} \rangle \equiv \frac{1}{Z} \sum_n \langle n | \hat{M} | n \rangle e^{-\beta E_n^*} \quad (\text{A.0.2})$$

where $Z = \sum_n e^{-\beta E_n^*}$ is the fixed point partition function and $\{|n\rangle\}$ is the set of eigenfunctions of the fixed point Hamiltonian. We can therefore write

$$\begin{aligned} & \left\langle \left\{ \mathcal{O}_\sigma(t), \mathcal{O}_\sigma^\dagger \right\} \right\rangle \\ &= \frac{1}{Z} \sum_m e^{-\beta E_m} \langle m | \left\{ \mathcal{O}_\sigma(t), \mathcal{O}_\sigma^\dagger \right\} | m \rangle \\ &= \frac{1}{Z} \sum_{m,n} e^{-\beta E_m} \langle m | \left(\mathcal{O}_\sigma(t) |n\rangle \langle n| \mathcal{O}_\sigma^\dagger + \mathcal{O}_\sigma^\dagger |n\rangle \langle n| \mathcal{O}_\sigma(t) \right) | m \rangle \quad \left[\sum_n |n\rangle \langle n| = 1 \right] \\ &= \frac{1}{Z} \sum_{m,n} e^{-\beta E_m} \langle m | \left(e^{iH^*t} \mathcal{O}_\sigma e^{-iH^*t} |n\rangle \langle n| \mathcal{O}_\sigma^\dagger + \mathcal{O}_\sigma^\dagger |n\rangle \langle n| e^{iH^*t} \mathcal{O}_\sigma e^{-iH^*t} \right) | m \rangle \\ &= \frac{1}{Z} \sum_{m,n} e^{-\beta E_m} \left(e^{i(E_m - E_n)t} \langle m | \mathcal{O}_\sigma | n \rangle \langle n | \mathcal{O}_\sigma^\dagger | m \rangle + e^{i(E_n - E_m)t} \langle m | \mathcal{O}_\sigma^\dagger | n \rangle \langle n | \mathcal{O}_\sigma | m \rangle \right) \\ &= \frac{1}{Z} \sum_{m,n} e^{i(E_m - E_n)t} \|\langle m | \mathcal{O}_\sigma | n \rangle\|^2 \left(e^{-\beta E_m} + e^{-\beta E_n} \right) \end{aligned} \quad (\text{A.0.3})$$

The time-domain impurity Green's function can thus be written as (this is the so-called Lehmann representation)

$$G_{dd}^\sigma = -i\theta(t) \frac{1}{Z} \sum_{m,n} e^{i(E_m - E_n)t} \|\langle m | \mathcal{O}_\sigma | n \rangle\|^2 \left(e^{-\beta E_m} + e^{-\beta E_n} \right) \quad (\text{A.0.4})$$

We are interested in the frequency domain form.

$$\begin{aligned} G_{dd}^\sigma(\omega) &= \int_{-\infty}^{\infty} dt e^{i\omega t} G_{dd}^\sigma(t) \\ &= \frac{1}{Z} \sum_{m,n} ||\langle m | \mathcal{O}_\sigma | n \rangle||^2 \left(e^{-\beta E_m} + e^{-\beta E_n} \right) (-i) \int_{-\infty}^{\infty} dt \theta(t) e^{i(\omega + E_m - E_n)t} \end{aligned} \quad (\text{A.0.5})$$

To evaluate the time-integral, we will use the integral representation of the Heaviside function:

$$\theta(t) = \frac{1}{2\pi i} \lim_{\eta \rightarrow 0^+} \int_{-\infty}^{\infty} \frac{1}{x - i\eta} e^{ixt} dx \quad (\text{A.0.6})$$

With this definition, the integral in $G_{dd}^\sigma(\omega)$ becomes

$$\begin{aligned} (-i) \int_{-\infty}^{\infty} dt \theta(t) e^{i(\omega + E_m - E_n)t} &= (-i) \frac{1}{2\pi i} \lim_{\eta \rightarrow 0^+} \int_{-\infty}^{\infty} dx \frac{1}{x - i\eta} \int_{-\infty}^{\infty} dt e^{i(\omega + E_m - E_n + x)t} \\ &= (-i) \frac{1}{2\pi i} \lim_{\eta \rightarrow 0^+} \int_{-\infty}^{\infty} dx \frac{1}{x - i\eta} 2\pi \delta(\omega + E_m - E_n + x) \\ &= (-i) \frac{1}{i} \lim_{\eta \rightarrow 0^+} \frac{-1}{\omega + E_m - E_n - i\eta} \\ &= \frac{1}{\omega + E_m - E_n} \end{aligned} \quad (\text{A.0.7})$$

The frequency-domain Green's function is thus

$$G_{dd}^\sigma(\omega) = \frac{1}{Z} \sum_{m,n} ||\langle m | \mathcal{O}_\sigma | n \rangle||^2 \left(e^{-\beta E_m} + e^{-\beta E_n} \right) \frac{1}{\omega + E_m - E_n} \quad (\text{A.0.8})$$

The zero temperature Green's function is obtained by taking the limit of $\beta \rightarrow \infty$. In both the partition function as well as inside the summation, the only term that will survive is the exponential of the ground state energy E_0 .

$$Z \equiv \sum_m e^{-\beta E_m} \implies \lim_{\beta \rightarrow \infty} Z = d_0 e^{-\beta E_0}, \quad E_0 \equiv \min \{E_n\}$$

where d_0 is the degeneracy of the ground state. The Greens function then simplifies to

$$\begin{aligned} G_{dd}^\sigma(\omega, \beta \rightarrow \infty) &= \frac{1}{d_0 e^{-\beta E_0}} \sum_{m,n} ||\langle m | \mathcal{O}_\sigma | n \rangle||^2 \left[e^{-\beta E_m} \delta_{E_m, E_0} + e^{-\beta E_n} \delta_{E_n, E_0} \right] \frac{1}{\omega + E_m - E_n} \\ &= \frac{1}{d_0} \sum_{n,0} \left[||\langle 0 | \mathcal{O}_\sigma | n \rangle||^2 \frac{1}{\omega + E_0 - E_n} + ||\langle n | \mathcal{O}_\sigma | 0 \rangle||^2 \frac{1}{\omega - E_0 + E_n} \right] \end{aligned} \quad (\text{A.0.9})$$

The label 0 sums over all states $|0\rangle$ with energy E_0 . The spectral function is the imaginary part of this Green's function. To extract the imaginary part, we insert an infinitesimal imaginary part in the denominator:

$$G_{dd}^\sigma(\omega, \eta) = \frac{1}{d_0} \lim_{\eta \rightarrow 0^-} \sum_{n,0} \left[||\langle 0 | \mathcal{O}_\sigma | n \rangle||^2 \frac{1}{\omega + E_0 - E_n + i\eta} + ||\langle n | \mathcal{O}_\sigma | 0 \rangle||^2 \frac{1}{\omega - E_0 + E_n + i\eta} \right] \quad (\text{A.0.10})$$

The spectral function at zero temperature can then be written as

$$\begin{aligned}
\mathcal{A}(\omega) &= -\frac{1}{\pi} \text{Im} [G_{dd}^\sigma(\omega)] \\
&= \frac{1}{d_0} \frac{1}{\pi} \text{Im} \left[\lim_{\eta \rightarrow 0^-} \sum_{n,0} \left(\frac{-i\eta ||\langle 0 | \mathcal{O}_\sigma | n \rangle ||^2}{(\omega + E_0 - E_n)^2 + \eta^2} + \frac{-i\eta ||\langle n | \mathcal{O}_\sigma | 0 \rangle ||^2}{(\omega - E_0 + E_n)^2 + \eta^2} \right) \right] \\
&= \frac{1}{d_0} \frac{1}{\pi} \sum_{n,0} \left[||\langle 0 | \mathcal{O}_\sigma | n \rangle ||^2 \pi \delta(\omega + E_0 - E_n) + ||\langle n | \mathcal{O}_\sigma | 0 \rangle ||^2 \pi \delta(\omega - E_0 + E_n) \right] \\
&= \frac{1}{d_0} \sum_{n,0} \left[||\langle 0 | \mathcal{O}_\sigma | n \rangle ||^2 \delta(\omega + E_0 - E_n) + ||\langle n | \mathcal{O}_\sigma | 0 \rangle ||^2 \delta(\omega - E_0 + E_n) \right]
\end{aligned} \tag{A.0.11}$$

Appendix B

Derivation of RG equations for the impurity model with U, V, J, K, U_b, η

B.1 The full UV Hamiltonian

The Hamiltonian for the impurity problem is

$$\mathcal{H} = \sum_{k\sigma} \epsilon_k \tau_{k\sigma} - \frac{1}{2} U \left(\tau_{d\uparrow} - \tau_{d\downarrow} \right)^2 + \frac{1}{2} \eta \left(\tau_{d\uparrow} + \tau_{d\downarrow} \right) + \sum_{k\sigma} \left(V_k c_{k\sigma}^\dagger c_{d\sigma} + h.c. \right) + J \vec{S}_d \cdot \vec{s} + K \vec{C}_d \cdot \vec{C} - U_b \left(\tau_{0\uparrow} - \tau_{0\downarrow} \right)^2 \quad (\text{B.1.1})$$

where $\tau \equiv \hat{n} - \frac{1}{2}$. The first term is the kinetic energy term with a dispersion ϵ_k . The second term is the particle-hole symmetric impurity correlation term that sets the uncorrelated half-filled level $\tau_{d\uparrow} = -\tau_{d\downarrow} = \pm \frac{1}{2}$ at energy $-U/2$ below the Fermi surface, and the correlated doublon and holon states $\tau_{d\downarrow} = \tau_{d\uparrow} = \pm \frac{1}{2}$ at the Fermi surface. The particle-hole symmetry is in the fact that the term is invariant under $\tau_{d\sigma} \rightarrow -\tau_{d\sigma}$, and manifests in the symmetric positioning of the doublon and holon levels with respect to each other. The third term is the particle-hole asymmetry term that explicitly measures the deviation away from particle-hole symmetry - it is non-zero only when we are away from half-filling. The fourth, fifth and sixth terms describe various mechanisms in which the impurity can hybridise with the conduction bath. The first of these is a single-particle hopping V , the second mechanism is through spin-flip scattering, and the third is through isospin-flip scattering. The single-particle hybridisation V allows the impurity electron to tunnel into the conduction bath and this leads to a frequency-dependent self-energy renormalisation of the impurity, implying that the impurity electron can spend large amount of time in the bath [86]. $\vec{S}_d = \frac{1}{2} \sum_{\alpha\beta} \vec{\sigma}_{\alpha\beta} c_{d\alpha}^\dagger c_{d\beta}$ is the impurity spin, while $\vec{C}_d = \frac{1}{2} \sum_{\alpha\beta} \psi_\alpha^\dagger \vec{\sigma}_{\alpha\beta} \psi_\beta$ is the impurity isospin, where $\psi = \begin{pmatrix} c_{d\uparrow} & c_{d\downarrow}^\dagger \end{pmatrix}$ [77, 78]. The former acts on the 2-dimensional Hilbert-space formed by the magnetic up and down states on the impurity, while the latter acts on the 2-dimensional space formed by the doublon and holon states. The former reacts to a magnetic field, while the latter responds to a chemical potential. Such a chemical potential term that couples with the isospin is already present in the Hamiltonian - it is the asymmetry term η . In fact, that term can be rewritten as ηC_d^z , because $C_d^z = \frac{1}{2} (\hat{n}_{d\uparrow} + \hat{n}_{d\downarrow} - 1) = \frac{1}{2} (\tau_{d\uparrow} + \tau_{d\downarrow})$. The bath operators \vec{s} and \vec{C} are defined in the same way as the operator counterparts: $\vec{s} = \sum_{kk'\alpha\beta} \vec{\sigma}_{\alpha\beta} c_{k\alpha}^\dagger c_{k'\beta}$, $\vec{C} = \sum_{kk'\alpha\beta} \psi_\alpha^{k\dagger} \vec{\sigma}_{\alpha\beta} \psi_\beta^{k'}$, where $\psi^k = \begin{pmatrix} c_{k\alpha} & c_{k'\beta}^\dagger \end{pmatrix}$. The final seventh term is a local particle-hole symmetric correlation on the zeroth site of the bath. For $U_b > 0$, this term promotes half-filling on the zeroth site, while for $U_b < 0$, a doublon or holon is more favourable on that site.

We first Fourier transform the U_b -term to k -space. In k -space, the diagonal contribution (to H_D) coming from this term is the single-particle self-energy $-U_b \left(\hat{n}_{q\beta} \right)^2$ which can be made particle-hole symmetric in the form:

$$-U_b \left(\tau_{q\beta} \right)^2 \quad (\text{B.1.2})$$

where q is the k -state being decoupled and $\tau \equiv \hat{n} - 1/2$. In the initial state $|\Psi\rangle_i$, we have $\langle \hat{n}_{q\beta} \rangle = 1/2 \implies \tau_{q\beta} = 0$, so the contribution of U_b to that state is 0. For both hole excitations $c_{q\beta} |\Psi\rangle_i$ as well as particle excitations $c_{q\beta}^\dagger |\Psi\rangle_i$,

the intermediate state energy lowers to $-U_b/4$.

The off-diagonal part is

$$-\frac{U_b}{2} \sum_{kk'\sigma} c_{k\sigma}^\dagger c_{k'\sigma} + U_b \sum_{k_1, k_2, k'_1, k'_2} c_{k_1\uparrow}^\dagger c_{k_2\uparrow} c_{k'_1\downarrow}^\dagger c_{k'_2\downarrow} \quad (\text{B.1.3})$$

We ignore the potential scattering arising from the first term.

B.2 Renormalisation in the absence of U_b

B.2.1 Renormalisation of the impurity energy levels

A single site has four degrees of freedom arising from the spin-degeneracy, and can be represented by the Hamiltonian

$$H = \epsilon_0 |0\rangle \langle 0| + \epsilon_1 \sum_{\sigma} |\sigma\rangle \langle \sigma| + \epsilon_2 |2\rangle \langle 2| \quad (\text{B.2.1})$$

$|0\rangle, |2\rangle$ are the holon and doublon states, while $|\sigma\rangle$ is the state where the site is singly-occupied by a particle of spin σ . We will obtain the renormalisation to the energy levels ϵ_0, ϵ_1 and ϵ_2 , and thereby calculate the renormalisation in U and η . This can be done by noting that $\epsilon_1 = -\frac{U}{2}$, and $\epsilon_2 = \eta$. A qualifier is, however, needed here. In the bare Hamiltonian, the energies of the doublon and holon states are negatives of each other, and this would correspond to requiring $\epsilon_2 = -\epsilon_0$. This may not hold true under renormalisation, and the way we account for this is that at each step of the RG, we subtract a constant energy from the Hamiltonian so as to set the energy of the holon state to 0. This means that the energy of the singly-occupied and doublon states become $\epsilon_1 - \epsilon_0$ and $\epsilon_2 - \epsilon_0$. And since we have identified ϵ_1 and ϵ_2 as $-\frac{U}{2}$ and η respectively, we can use $\Delta U = -2(\Delta\epsilon_1 - \Delta\epsilon_0)$, $\Delta\eta = \Delta\epsilon_2 - \Delta\epsilon_0$.

We need to look at three kinds of scattering vertices here: V^2 , J^2 and K^2 . We will consider these processes one after another. We define n_j as the number of states being decoupled on each side of the Fermi surface, at the j^{th} RG step. In order to treat both spin and isospin exchanges democratically, we take $|\Psi\rangle_i = \frac{1}{2}(|0\rangle + |q\uparrow\rangle + |q\downarrow\rangle + |q\uparrow, q\downarrow\rangle)$ as the *initial* state for the scattering processes. The intermediate states $|\Psi\rangle_{\text{int}}$ in the particle sector $(c_{q\beta}|\Psi\rangle_i)$ and hole sector $(c_{q\beta}^\dagger|\Psi\rangle_i)$ will then have both spin and isospin excitations which can couple with the corresponding impurity degree of freedom. We will assume that states $q > k_F$ ($\epsilon_q > 0$) above the Fermi surface can have only particle excitations and states below the Fermi surface can only have hole excitations. The kinetic energy part $\epsilon_q \tau_{q\beta}$ of H_D for $|\Psi\rangle_i$ is then zero, whereas it is always $D/2$ for $|\Psi\rangle_{\text{int}}$. To demonstrate this for a typical $q < k_F$, the hole excitation is $c_{q\uparrow}|\Psi\rangle_i = \frac{1}{\sqrt{2}}(|0\rangle + |q\downarrow\rangle)$. This has an isospin term in the form of the *holon* and a spin term in the form of the down state. Since $\tau_{q\uparrow} = -\frac{1}{2}$ in the excited state, the kinetic energy for $|\Psi\rangle_{\text{int}}$ is $\epsilon_q \tau_{q\uparrow} = (-D) \times \left(-\frac{1}{2}\right) = D/2$.

The renormalisation arising from the first kind of terms, in the particle sector, is

$$\sum_{q\beta} c_{q\beta}^\dagger c_{d\beta} \frac{V^2}{\omega - H_D} c_{d\beta}^\dagger c_{q\beta} = \sum_{q\beta} V^2 \hat{n}_{q\beta} (1 - \hat{n}_{d\beta}) \left(\frac{1 - \hat{n}_{d\bar{\beta}}}{\omega - E_0} + \frac{\hat{n}_{d\bar{\beta}}}{\omega' - E_1} \right) = V^2 n_j \sum_{\beta} (1 - \hat{n}_{d\beta}) \left(\frac{1 - \hat{n}_{d\bar{\beta}}}{\omega_0 - E_0} + \frac{\hat{n}_{d\bar{\beta}}}{\omega_1 - E_1} \right) \quad (\text{B.2.2})$$

q runs over the momentum states that are being decoupled at this RG step: $|q| = \Lambda_j$. $E_{1,0}$ are the diagonal parts of the Hamiltonian at $\hat{n}_{d\bar{\beta}} = 1, 0$ respectively. We have $\hat{n}_{d\beta} = 1$ in the intermediate state because of the $c_{d\beta}^\dagger$ in front of the Greens function. Applying $c_{q\beta}$ on the initial state $|\Psi\rangle_i$ leaves us with $C_q^z = -\frac{1}{2}$ and $s_q^z = \frac{1}{2}\bar{\beta}$. We also know that

$$\hat{n}_{d\beta} = 1, \begin{cases} \hat{n}_{d\bar{\beta}} = 0 & \implies S_d^z = \frac{1}{2}\beta, C_d^z = 0, \epsilon_d (\hat{n}_{d\uparrow} - \hat{n}_{d\downarrow})^2 = \epsilon_d \\ \hat{n}_{d\bar{\beta}} = 1 & \implies S_d^z = 0, C_d^z = \frac{1}{2}, \epsilon_d (\hat{n}_{d\uparrow} - \hat{n}_{d\downarrow})^2 = 0 \end{cases} \quad (\text{B.2.3})$$

Combining all this, we can write $E_1 = \frac{D}{2} - \frac{K}{4}$ and $E_0 = \frac{D}{2} + \epsilon_d - \frac{J}{4}$. In order to relate ω_0 with ω_1 with the common fluctuation scale ω for the conduction electrons, we will replace these quantum fluctuation scales by the current renormalised values of the single-particle self-energy for the initial state from which we started scattering. For $\hat{n}_{d\bar{\beta}} = 0$, there is no additional self-energy because the impurity does not have any spin: $\omega_0 = \omega$. For $\hat{n}_{d\bar{\beta}} = 1$, we have an additional self-energy of ϵ_d arising from the correlation on the impurity: $\omega_1 = \omega + \epsilon_d$. Substituting the

values of $E_{0,1}$ and $\omega_{0,1}$, we get

$$V^2 n_j \sum_{\beta} \left(1 - \hat{n}_{d\beta}\right) \left(\frac{1 - \hat{n}_{d\bar{\beta}}}{\omega - \frac{D}{2} - \epsilon_d + \frac{J}{4}} + \frac{\hat{n}_{d\bar{\beta}}}{\omega - \frac{D}{2} + \epsilon_d + \frac{K}{4}} \right) \quad (\text{B.2.4})$$

Performing a similar calculation for the hole sector gives the contribution:

$$V^2 n_j \sum_{\beta} \hat{n}_{d\beta} \left(\frac{1 - \hat{n}_{d\bar{\beta}}}{\omega - \frac{D}{2} + \epsilon_d + \frac{K}{4}} + \frac{\hat{n}_{d\bar{\beta}}}{\omega - \frac{D}{2} - \epsilon_d + \frac{J}{4}} \right) \quad (\text{B.2.5})$$

We now come to the second type of terms: spin-spin. We first look at the particle sector:

$$\frac{J^2}{4} \sum_{q\beta} c_{d\bar{\beta}}^{\dagger} c_{d\beta} c_{q\beta}^{\dagger} c_{-q\bar{\beta}} \frac{1}{\omega - H_D} c_{d\beta}^{\dagger} c_{d\bar{\beta}} c_{q\bar{\beta}}^{\dagger} c_{q\beta} = \frac{J^2}{4} n_j \frac{1}{\omega - \frac{D}{2} + \frac{J}{4}} \sum_{\beta} \hat{n}_{d\bar{\beta}} (1 - \hat{n}_{d\beta}) \quad (\text{B.2.6})$$

The diagonal part in the denominator was simple to deduce in this case, because the nature of the scattering requires the spins S_d^z and $\frac{\beta}{2} (\hat{n}_{q\beta} - \hat{n}_{q\bar{\beta}})$ to be anti-parallel. This ensures that the intermediate state has an energy of $E = \frac{D}{2} + \epsilon_d - \frac{J}{4}$, and the quantum fluctuation scale is $\omega' = \omega + \epsilon_d$, such that $\omega' - E = \omega - \frac{D}{2} + \frac{J}{4}$. In the hole sector, we have

$$\frac{J^2}{4} n_j \frac{1}{\omega - \frac{D}{2} + \frac{J}{4}} \sum_{\beta} \hat{n}_{d\beta} (1 - \hat{n}_{d\bar{\beta}}) \quad (\text{B.2.7})$$

The final kind of scattering is the K^2 type. Similar to the J^2 term, we get the following contribution:

$$\frac{K^2}{4} \sum_{q\beta} c_{q\beta}^{\dagger} c_{q\bar{\beta}}^{\dagger} c_{d\bar{\beta}} c_{d\beta} \frac{1}{\omega - H_D} c_{d\beta}^{\dagger} c_{d\bar{\beta}}^{\dagger} c_{q\bar{\beta}} c_{q\beta} = \frac{K^2}{2} n_j \frac{1}{\omega - \frac{D}{2} + \frac{K}{4}} (1 - \hat{n}_{d\uparrow}) (1 - \hat{n}_{d\downarrow}) \quad (\text{B.2.8})$$

in the particle sector. This is again because $E = \frac{D}{2} - \frac{K}{4}$ in the intermediate state and $\omega' = \omega$. In the hole sector, we get

$$\frac{K^2}{2} n_j \frac{1}{\omega - \frac{D}{2} + \frac{K}{4}} \hat{n}_{d\uparrow} \hat{n}_{d\downarrow} . \quad (\text{B.2.9})$$

We now have all possible renormalisation to the impurity energy ϵ_d . To actually compute the renormalisation, we will first calculate the renormalisation in the energies ϵ_0, ϵ_1 and ϵ_2 of the impurity states $|\hat{n}_d = 0\rangle, |\hat{n}_d = 1\rangle, |\hat{n}_d = 2\rangle$ respectively. The renormalisation of these states are given by the following terms:

- $\Delta\epsilon_0$ is given by the renormalisation of the term $(1 - \hat{n}_{d\uparrow}) (1 - \hat{n}_{d\downarrow})$
- $\Delta\epsilon_1$ is given by the renormalisation of either $(1 - \hat{n}_{d\uparrow}) \hat{n}_{d\downarrow}$ or $(1 - \hat{n}_{d\downarrow}) \hat{n}_{d\uparrow}$
- $\Delta\epsilon_2$ is given by the renormalisation of $\hat{n}_{d\uparrow} \hat{n}_{d\downarrow}$

From eqs. B.2.4, B.2.5, B.2.6, B.2.7, B.2.8 and B.2.9, we write

$$\Delta\epsilon_0 = \Delta\epsilon_2 = \frac{2V^2 n_j}{\omega - \frac{D}{2} - \epsilon_d + \frac{J}{4}} + \frac{K^2 n_j / 2}{\omega - \frac{D}{2} + \frac{K}{4}}, \quad \Delta\epsilon_1 = \frac{2V^2 n_j}{\omega - \frac{D}{2} + \epsilon_d + \frac{K}{4}} + \frac{J^2 n_j / 2}{\omega - \frac{D}{2} + \frac{J}{4}} \quad (\text{B.2.10})$$

We had started with a particle-hole symmetric Hamiltonian ($2\epsilon_d + U = 0$); the fact that $\Delta\epsilon_0 = \Delta\epsilon_2$ means the RG transformation has preserved that symmetry. The renormalisation of ϵ_d is simply the renormalisation in the energy difference between the singly-occupied and vacant impurity levels: $\Delta\epsilon_d = \Delta\epsilon_1 - \Delta\epsilon_0$. This gives our first RG equation:

$$\Delta\epsilon_d = 2V^2 n_j \left(\frac{1}{\omega - \frac{D}{2} + \epsilon_d + \frac{K}{4}} - \frac{1}{\omega - \frac{D}{2} - \epsilon_d + \frac{J}{4}} \right) + \frac{n_j}{2} \left(\frac{J^2}{\omega - \frac{D}{2} + \frac{J}{4}} - \frac{K^2}{\omega - \frac{D}{2} + \frac{K}{4}} \right) \quad (\text{B.2.11})$$

B.2.2 Renormalisation of the hybridisation V

Renormalisation of V happens through two kinds of processes: VJ and VK . In order words, the two vertices involve one single-particle scattering and one spin or isospin exchange respectively. We first look at the vertices that involve a spin-exchange scattering.

Within spin-exchange, the scattering can be either via S_d^z or through S_d^\pm . For the first kind, we have the following contribution in the particle sector:

$$\sum_{q\beta} V c_{q\beta}^\dagger c_{d\beta} \frac{1}{\omega - H_D} \frac{1}{4} J \sum_k \left(\hat{n}_{d\beta} - \hat{n}_{d\bar{\beta}} \right) c_{k\beta}^\dagger c_{q\beta} = \frac{1}{4} V J n_j \frac{1}{2} \left(\frac{1}{\omega'_1 - E} + \frac{1}{\omega'_2 - E} \right) \sum_{k\beta} \left(1 - \hat{n}_{d\bar{\beta}} \right) c_{d\beta} c_{k\beta}^\dagger \quad (\text{B.2.12})$$

The transformation from $\frac{1}{\omega - H_D}$ to $\frac{1}{2} \left(\frac{1}{\omega'_1 - E} + \frac{1}{\omega'_2 - E} \right)$ is made so that we can account for both the initial state and the final state energies through the two fluctuation scales ω'_1 and ω'_2 respectively; we calculate the denominators for both the initial and final states, and then take the mean of the two (hence the factor of half in front). This was not required previously because in the earlier scattering processes, the impurity returned to its initial state at the end, at least in terms of $\epsilon_d \left(\hat{n}_{d\uparrow} - \hat{n}_{d\downarrow} \right)^2$, and so we had $\omega'_1 = \omega'_2 = \omega'$.

Note that the $c_{d\beta}$ in front of the Greens function resulted in $\left(\hat{n}_{d\beta} - \hat{n}_{d\bar{\beta}} \right) \rightarrow \left(1 - \hat{n}_{d\bar{\beta}} \right)$. The intermediate state is characterised by $\hat{n}_{d\beta} = 1 - \hat{n}_{d\bar{\beta}} = 1$, which means that $E = \frac{D}{2} + \epsilon_d - \frac{J}{4}$. Moreover, the initial state gives $\omega'_1 = \omega + \epsilon_d$ while the final state gives $\omega'_2 = \omega$. Therefore, the renormalisation becomes

$$- \frac{n_j}{4} V J \frac{1}{2} \left(\frac{1}{\omega - \frac{D}{2} + \frac{J}{4}} + \frac{1}{\omega - \frac{D}{2} - \epsilon_d + \frac{J}{4}} \right) \sum_{k\beta} \left(1 - \hat{n}_{d\bar{\beta}} \right) c_{k\beta}^\dagger c_{d\beta} \quad (\text{B.2.13})$$

One can generate another such process by exchanging the single-particle process and the spin-exchange process:

$$\sum_{q\beta} \frac{1}{4} J \sum_k \left(\hat{n}_{d\beta} - \hat{n}_{d\bar{\beta}} \right) c_{q\beta}^\dagger c_{k\beta} \frac{1}{\omega - H_D} V c_{d\beta}^\dagger c_{q\beta} \quad (\text{B.2.14})$$

This is simply the Hermitian conjugate of the previous contribution. Combining this with the previous then gives

$$- \frac{n_j}{8} V J \left(\frac{1}{\omega - \frac{D}{2} + \frac{J}{4}} + \frac{1}{\omega - \frac{D}{2} - \epsilon_d + \frac{J}{4}} \right) \sum_{k\beta} \left(1 - \hat{n}_{d\bar{\beta}} \right) \left(c_{d\beta}^\dagger c_{k\beta} + \text{h.c.} \right) \quad (\text{B.2.15})$$

We now consider the spin-exchange processes involving S_d^\pm :

$$\sum_{q\beta} V c_{q\beta}^\dagger c_{d\beta} \frac{1}{\omega - H_D} \frac{1}{2} J \sum_k c_{d\beta}^\dagger c_{d\bar{\beta}} c_{k\bar{\beta}}^\dagger c_{q\beta} = \frac{1}{2} V J n_j \frac{1}{2} \left(\frac{1}{\omega'_1 - E} + \frac{1}{\omega'_2 - E} \right) \sum_{k\beta} \left(1 - \hat{n}_{d\beta} \right) c_{d\bar{\beta}} c_{k\bar{\beta}}^\dagger \quad (\text{B.2.16})$$

We again have $E = \frac{D}{2} + \epsilon_d - \frac{J}{4}$, $\omega'_1 = \omega + \epsilon_d$ and $\omega'_2 = \omega$, which gives

$$- \frac{1}{4} V J n_j \left(\frac{1}{\omega - \frac{D}{2} + \frac{J}{4}} + \frac{1}{\omega - \frac{D}{2} - \epsilon_d + \frac{J}{4}} \right) \sum_{k\beta} \left(1 - \hat{n}_{d\beta} \right) c_{k\bar{\beta}}^\dagger c_{d\bar{\beta}} \quad (\text{B.2.17})$$

Combining this with the Hermitian conjugate obtained from exchanging the processes gives

$$- \frac{1}{4} V J n_j \left(\frac{1}{\omega - \frac{D}{2} + \frac{J}{4}} + \frac{1}{\omega - \frac{D}{2} - \epsilon_d + \frac{J}{4}} \right) \sum_{k\beta} \left(1 - \hat{n}_{d\beta} \right) \left(c_{k\bar{\beta}}^\dagger c_{d\bar{\beta}} + \text{h.c.} \right) \quad (\text{B.2.18})$$

The contributions from the hole sector are obtained making the transformation $\hat{n}_{d\bar{\beta}} \rightarrow 1 - \hat{n}_{d\bar{\beta}}$ on the particle

sector contributions. The total renormalisation to V from VJ processes are

$$-\frac{3n_j}{8}VJ\left(\frac{1}{\omega - \frac{D}{2} + \frac{J}{4}} + \frac{1}{\omega - \frac{D}{2} - \epsilon_d + \frac{J}{4}}\right)\sum_{k\beta}\left(c_{d\beta}^\dagger c_{k\beta} + \text{h.c.}\right) \quad (\text{B.2.19})$$

We now look at the VK processes. The first one is

$$\sum_{q\beta}Vc_{q\beta}^\dagger c_{d\beta}\frac{1}{\omega - H_D}\frac{1}{4}K\sum_k(\hat{n}_d - 1)c_{k\beta}^\dagger c_{q\beta} = -\frac{1}{8}VKn_j\left(\frac{1}{\omega - \frac{D}{2} + \frac{K}{4}} + \frac{1}{\omega - \frac{D}{2} + \epsilon_d + \frac{K}{4}}\right)\sum_{k\beta}\hat{n}_{d\bar{\beta}}c_{k\beta}^\dagger c_{d\beta} \quad (\text{B.2.20})$$

The exchanged process again gives the Hermitian conjugate, so the combined contribution is

$$-\frac{1}{8}VKn_j\left(\frac{1}{\omega - \frac{D}{2} + \frac{K}{4}} + \frac{1}{\omega - \frac{D}{2} + \epsilon_d + \frac{K}{4}}\right)\sum_{k\beta}\hat{n}_{d\bar{\beta}}\left(c_{k\beta}^\dagger c_{d\beta} + \text{h.c.}\right) \quad (\text{B.2.21})$$

The isospin-flip vertex gives

$$\sum_{q\beta}Vc_{q\beta}^\dagger c_{d\beta}\frac{1}{\omega - H_D}\frac{1}{2}K\sum_k c_{d\beta}^\dagger c_{d\bar{\beta}}^\dagger c_{k\bar{\beta}} c_{q\beta} = \frac{1}{4}KVn_j\left(\frac{1}{\omega - \frac{D}{2} + \frac{K}{4}} + \frac{1}{\omega - \frac{D}{2} + \epsilon_d + \frac{K}{4}}\right)\sum_{k\beta}(1 - \hat{n}_{d\beta})c_{d\bar{\beta}}^\dagger c_{k\bar{\beta}}. \quad (\text{B.2.22})$$

Combining with Hermitian conjugate gives

$$\frac{1}{4}KVn_j\left(\frac{1}{\omega - \frac{D}{2} + \frac{K}{4}} + \frac{1}{\omega - \frac{D}{2} + \epsilon_d + \frac{K}{4}}\right)\sum_{k\beta}(1 - \hat{n}_{d\beta})\left(c_{d\bar{\beta}}^\dagger c_{k\bar{\beta}} + \text{h.c.}\right). \quad (\text{B.2.23})$$

After obtaining the hole sector contributions, the total renormalisation from VK processes is

$$-\frac{3n_j}{4}VK\left(\frac{1}{\omega - \frac{D}{2} + \frac{K}{4}} + \frac{1}{\omega - \frac{D}{2} + \epsilon_d + \frac{K}{4}}\right)\sum_{k\beta}\left(c_{d\beta}^\dagger c_{k\beta} + \text{h.c.}\right). \quad (\text{B.2.24})$$

The RG equation for V is

$$\Delta V = -\frac{3n_j V}{8}\left[J\left(\frac{1}{\omega - \frac{D}{2} + \frac{J}{4}} + \frac{1}{\omega - \frac{D}{2} - \epsilon_d + \frac{J}{4}}\right) + K\left(\frac{1}{\omega - \frac{D}{2} + \frac{K}{4}} + \frac{1}{\omega - \frac{D}{2} + \epsilon_d + \frac{K}{4}}\right)\right] \quad (\text{B.2.25})$$

B.2.3 Renormalisation of the exchange couplings J and K

We will just note the renormalisation in J^z , which will be equal to J^\pm due to spin-rotation symmetry. The terms that renormalise J^z are of the form $S_d^\pm S_d^\mp$. In the particle sector, we have

$$\sum_q \sum_{kk'} \frac{1}{4}J^2 S_d^\pm c_{q\mp}^\dagger c_{k'\pm} \frac{1}{\omega - H_D} S_d^\mp c_{k\pm}^\dagger c_{q\mp} = -n_j \frac{1}{4}J^2 \left(\frac{1}{2} \pm S_d^z\right) \sum_{kk'} c_{k\pm}^\dagger c_{k\pm} \frac{1}{\omega - \frac{D}{2} + \frac{J}{4}}. \quad (\text{B.2.26})$$

The denominator is determined using $E = \frac{D}{2} + \epsilon_d - \frac{J}{4}$ and $\omega' = \omega + \epsilon_d$. In the hole sector, we similarly have

$$\sum_q \sum_{kk'} \frac{1}{4}J^2 S_d^\mp c_{k\pm}^\dagger c_{q\mp} \frac{1}{\omega - H_D} S_d^\pm c_{q\mp}^\dagger c_{k'\pm} = n_j \frac{1}{4}J^2 \left(\frac{1}{2} \mp S_d^z\right) \sum_{kk'} c_{k\pm}^\dagger c_{k\pm} \frac{1}{\omega - \frac{D}{2} + \frac{J}{4}}. \quad (\text{B.2.27})$$

Adding all four expressions and dropping the constant part, we get

$$-n_j \frac{1}{2}J^2 S_d^z \sum_{kk'} \left(c_{k\uparrow}^\dagger c_{k'\uparrow} - c_{k\downarrow}^\dagger c_{k'\downarrow}\right) \frac{1}{\omega - \frac{D}{2} + \frac{J}{4}}. \quad (\text{B.2.28})$$

We can now directly read off the RG equation for J :

$$\Delta J = -\frac{n_j J^2}{\omega - \frac{D}{2} + \frac{J}{4}} \quad (\text{B.2.29})$$

Since the spin and charge degrees of freedom are treated on an equal footing in the model, we obtain the RG equation for K by simply changing $J \rightarrow K$:

$$\Delta K = -\frac{n_j K^2}{\omega - \frac{D}{2} + \frac{K}{4}} \quad (\text{B.2.30})$$

B.3 Renormalisation in the presence of U_b

We first Fourier transform the U_b -term to k -space. In k -space, the diagonal contribution (to H_D) coming from this term is the single-particle self-energy $-U_b \left(\hat{n}_{q\beta} \right)^2$ which can be made particle-hole symmetric in the form:

$$-U_b \left(\tau_{q\beta} \right)^2 \quad (\text{B.3.1})$$

where q is the k -state being decoupled and $\tau \equiv \hat{n} - 1/2$. In the initial state $|\Psi\rangle_i$, we have $\langle \hat{n}_{q\beta} \rangle = 1/2 \implies \tau_{q\beta} = 0$, so the contribution of U_b to that state is 0. For both hole excitations $c_{q\beta} |\Psi\rangle_i$ as well as particle excitations $c_{q\beta}^\dagger |\Psi\rangle_i$, the intermediate state energy lowers to $-U_b/4$.

The off-diagonal part is

$$-\frac{U_b}{2} \sum_{k k' \sigma} c_{k\sigma}^\dagger c_{k'\sigma} + U_b \sum_{k_1, k_2, k'_1, k'_2} c_{k_1\uparrow}^\dagger c_{k_2\uparrow} c_{k'_1\downarrow}^\dagger c_{k'_2\downarrow} \quad (\text{B.3.2})$$

We ignore the potential scattering arising from the first term.

B.3.1 Renormalisation of U_b

U_b can renormalise only via itself. The relevant renormalisation term in the particle sector is

$$U_b^2 \sum_{q\beta} \sum_{k_1, k_2, k_3, k'_1, k'_2, k'_3} c_{q\beta}^\dagger c_{k_1\beta} c_{k_3\beta}^\dagger c_{k'_1\beta} \frac{1}{\omega - H_D} c_{k'_2\beta}^\dagger c_{k'_3\beta} c_{k_2\beta}^\dagger c_{q\beta} \quad (\text{B.3.3})$$

In order to renormalise U_b , we need to contract one more pair of momenta. There are two choices. The first is by setting $k_3 = k'_3 = q$. The two internal states, then, are $q\beta$ and $q\bar{\beta}$. As discussed above, the intermediate state energy is $-U_b/4$. We therefore have

$$\frac{U_b^2 n_j}{\omega - D/2 + U_b/4} \sum_{\beta} \sum_{k_1, k_2, k'_1, k'_2} c_{k_1\beta} c_{k'_1\bar{\beta}} c_{k_2\beta}^\dagger c_{k'_2\beta} = \frac{U_b^2 n_j}{\omega - D/2 + U_b/4} \sum_{\beta} \sum_{k_1, k_2, k'_1, k'_2} c_{k'_2\bar{\beta}}^\dagger c_{k'_1\bar{\beta}} c_{k_2\beta}^\dagger c_{k_1\beta} \quad (\text{B.3.4})$$

Another way to contract the momenta is by setting $k'_1 = k'_2 = q$, which gives a renormalisation of

$$\frac{U_b^2 n_j}{\omega - D/2 + U_b/4} \sum_{\beta} \sum_{k_1, k_2, k_3, k'_3} c_{k_1\beta} c_{k_3\bar{\beta}}^\dagger c_{k_2\beta}^\dagger c_{k'_3\bar{\beta}} = -\frac{U_b^2 n_j}{\omega - D/2} \sum_{\beta} \sum_{k_1, k_2, k_3, k'_3} c_{k_3\bar{\beta}}^\dagger c_{k'_3\bar{\beta}} c_{k_2\beta}^\dagger c_{k_1\beta} \quad (\text{B.3.5})$$

The two contributions cancel each other. The same cancellation happens in the hole sector as well.

B.3.2 Renormalisation of U

U_b does not have any new renormalisation term on account of U_b . U_b does however modify the existing RG equation for U , by shifting the denominator. The existing RG equation is

$$\Delta U = -4V^2 n_j \left(\frac{1}{\omega - \frac{D}{2} + \epsilon_d + \frac{K}{4}} - \frac{1}{\omega - \frac{D}{2} - \epsilon_d + \frac{J}{4}} \right) - n_j \left(\frac{J^2}{\omega - \frac{D}{2} + \frac{J}{4}} - \frac{K^2}{\omega - \frac{D}{2} + \frac{K}{4}} \right). \quad (\text{B.3.6})$$

On accounting for the contribution of U_b to the denominator, we get

$$\Delta U = -4V^2 n_j \left(\frac{1}{\omega - \frac{D}{2} + \frac{U_b}{4} + \epsilon_d + \frac{K}{4}} - \frac{1}{\omega - \frac{D}{2} + \frac{U_b}{4} - \epsilon_d + \frac{J}{4}} \right) - n_j \left(\frac{J^2}{\omega - \frac{D}{2} + \frac{U_b}{4} + \frac{J}{4}} - \frac{K^2}{\omega - \frac{D}{2} + \frac{U_b}{4} + \frac{K}{4}} \right). \quad (\text{B.3.7})$$

B.3.3 Renormalisation of V

The single-particle hybridisation V renormalises through terms of VU_b and U_bV kind. The first term gives

$$\begin{aligned} & \sum_{q\beta} \sum_k U_b V c_{q\beta}^\dagger c_{k\beta} \hat{n}_{q\bar{\beta}} \frac{1}{\omega - H_D} c_{d\beta}^\dagger c_{q\beta} \\ &= n_j U_b V \sum_{k\beta} c_{k\beta} \left[\frac{\hat{n}_{d\bar{\beta}}}{2} \left(\frac{1}{\omega_1 - E_1} + \frac{1}{\omega'_1 - E_1} \right) + \frac{1 - \hat{n}_{d\bar{\beta}}}{2} \left(\frac{1}{\omega_0 - E_0} + \frac{1}{\omega'_0 - E_0} \right) \right] c_{d\beta}^\dagger \end{aligned} \quad (\text{B.3.8})$$

E_1 and E_0 are the intermediate state energies for $\hat{n}_{d\bar{\beta}} = 1$ and 0 respectively. $\omega_{1,0}$ are the quantum fluctuation scales for the corresponding initial states. $\omega'_{1,0}$ are the fluctuation scales for the corresponding final states. The intermediate energies are $E_1 = D/2 - U_b/4 - K/4$, $E_0 = D/2 - U_b/4 - U/2 - J/4$. The fluctuation scales are $\omega_1 = \omega - U/2 = \omega'_0$, $\omega'_1 = \omega = \omega_0$. Substituting these gives

$$\begin{aligned} & -n_j U_b V \sum_{k\beta} c_{d\beta}^\dagger c_{k\beta} \left[\frac{\hat{n}_{d\bar{\beta}}}{2} \left(\frac{1}{\omega - \frac{D}{2} - \frac{U}{2} + \frac{U_b}{4} + \frac{K}{4}} + \frac{1}{\omega - \frac{D}{2} + \frac{U_b}{4} + \frac{K}{4}} \right) \right. \\ & \quad \left. + \frac{1 - \hat{n}_{d\bar{\beta}}}{2} \left(\frac{1}{\omega - \frac{D}{2} + \frac{U_b}{4} + \frac{U}{2} + \frac{J}{4}} + \frac{1}{\omega - \frac{D}{2} + \frac{U_b}{4} + \frac{J}{4}} \right) \right] \end{aligned} \quad (\text{B.3.9})$$

The second term is of the form

$$\sum_{q\beta} \sum_k U_b V c_{q\beta}^\dagger c_{d\beta} \frac{1}{\omega - H_D} \hat{n}_{q\bar{\beta}} c_{k\beta}^\dagger c_{q\beta} \quad (\text{B.3.10})$$

and this is just the Hermitian conjugate of the previous term, so these two terms together lead to

$$\begin{aligned} & -n_j U_b V \sum_{k\beta} \left(c_{d\beta}^\dagger c_{k\beta} + \text{h.c.} \right) \left[\frac{\hat{n}_{d\bar{\beta}}}{2} \left(\frac{1}{\omega - \frac{D}{2} - \frac{U}{2} + \frac{U_b}{4} + \frac{K}{4}} + \frac{1}{\omega - \frac{D}{2} + \frac{U_b}{4} + \frac{K}{4}} \right) \right. \\ & \quad \left. + \frac{1 - \hat{n}_{d\bar{\beta}}}{2} \left(\frac{1}{\omega - \frac{D}{2} + \frac{U_b}{4} + \frac{U}{2} + \frac{J}{4}} + \frac{1}{\omega - \frac{D}{2} + \frac{U_b}{4} + \frac{J}{4}} \right) \right] \end{aligned} \quad (\text{B.3.11})$$

In the hole sector, we have

$$\begin{aligned} & \sum_{q\beta} \sum_k U_b V \hat{n}_{q\bar{\beta}} c_{k\beta}^\dagger c_{q\beta} \frac{1}{\omega - H_D} c_{q\beta}^\dagger c_{d\beta} \\ & - \sum_{q\beta} \sum_k U_b V \left(1 - \hat{n}_{q\bar{\beta}} \right) c_{k\beta}^\dagger c_{q\beta} \frac{1}{\omega - H_D} c_{q\beta}^\dagger c_{d\beta} \\ &= -n_j U_b V \sum_{k\beta} c_{k\beta} \left[\frac{\hat{n}_{d\bar{\beta}}}{2} \left(\frac{1}{\omega_1 - E_1} + \frac{1}{\omega'_1 - E_1} \right) + \frac{1 - \hat{n}_{d\bar{\beta}}}{2} \left(\frac{1}{\omega_0 - E_0} + \frac{1}{\omega'_0 - E_0} \right) \right] c_{d\beta} \end{aligned} \quad (\text{B.3.12})$$

$E_1 = D/2 - U_b/4 - U/2 - J/4$, $E_0 = D/2 - U_b/4 - K/4$. The fluctuation scales are $\omega_1 = \omega = \omega'_0$, $\omega'_1 = \omega - U/2 = \omega_0$.

Substituting these gives

$$\begin{aligned}
 -n_j U_b V \sum_{k\beta} c_{d\beta}^\dagger c_{k\beta} & \left[\frac{1 - \hat{n}_{d\bar{\beta}}}{2} \left(\frac{1}{\omega - \frac{D}{2} - \frac{U}{2} + \frac{U_b}{4} + \frac{K}{4}} + \frac{1}{\omega - \frac{D}{2} + \frac{U_b}{4} + \frac{K}{4}} \right) \right. \\
 & \left. + \frac{\hat{n}_{d\bar{\beta}}}{2} \left(\frac{1}{\omega - \frac{D}{2} + \frac{U_b}{4} + \frac{U}{2} + \frac{J}{4}} + \frac{1}{\omega - \frac{D}{2} + \frac{U_b}{4} + \frac{J}{4}} \right) \right]
 \end{aligned} \tag{B.3.13}$$

The other term, obtained by exchanging V and U_b , gives the Hermitian conjugate, so the overall contribution from the hole sector is the same as the total contribution from the particle sector, but with $\hat{n}_{d\bar{\beta}} \rightarrow 1 - \hat{n}_{d\bar{\beta}}$. Combining both the sectors, we get

$$\begin{aligned}
 -n_j U_b V \sum_{k\beta} (c_{d\beta}^\dagger c_{k\beta} + \text{h.c.}) & \frac{1}{2} \left[\left(\frac{1}{\omega - \frac{D}{2} - \frac{U}{2} + \frac{U_b}{4} + \frac{K}{4}} + \frac{1}{\omega - \frac{D}{2} + \frac{U_b}{4} + \frac{K}{4}} \right) \right. \\
 & \left. + \left(\frac{1}{\omega - \frac{D}{2} + \frac{U_b}{4} + \frac{U}{2} + \frac{J}{4}} + \frac{1}{\omega - \frac{D}{2} + \frac{U_b}{4} + \frac{J}{4}} \right) \right]
 \end{aligned} \tag{B.3.14}$$

Combining with the already existing RG equations, the complete RG equation for V becomes

$$\begin{aligned}
 \Delta V &= -\frac{3n_j V}{8} \left[\left(\frac{J}{\omega - \frac{D}{2} + \frac{U_b}{4} + \frac{J}{4}} + \frac{J}{\omega - \frac{D}{2} + \frac{U_b}{4} + \frac{U}{2} + \frac{J}{4}} \right) + K \left(\frac{K}{\omega - \frac{D}{2} + \frac{U_b}{4} + \frac{K}{4}} + \frac{K}{\omega - \frac{D}{2} + \frac{U_b}{4} - \frac{U}{2} + \frac{K}{4}} \right) \right] \\
 & - \frac{n_j U_b}{2} \left[\left(\frac{V}{\omega - \frac{D}{2} - \frac{U}{2} + \frac{U_b}{4} + \frac{K}{4}} + \frac{V}{\omega - \frac{D}{2} + \frac{U_b}{4} + \frac{K}{4}} \right) + \left(\frac{V}{\omega - \frac{D}{2} + \frac{U_b}{4} + \frac{U}{2} + \frac{J}{4}} + \frac{V}{\omega - \frac{D}{2} + \frac{U_b}{4} + \frac{J}{4}} \right) \right] \\
 & = -\frac{n_j V}{8} \left[\left(\frac{3J + 4U_b}{\omega - \frac{D}{2} + \frac{U_b}{4} + \frac{J}{4}} + \frac{3J + 4U_b}{\omega - \frac{D}{2} + \frac{U_b}{4} + \frac{U}{2} + \frac{J}{4}} \right) + \left(\frac{3K + 4U_b}{\omega - \frac{D}{2} + \frac{U_b}{4} + \frac{K}{4}} + \frac{3K + 4U_b}{\omega - \frac{D}{2} + \frac{U_b}{4} - \frac{U}{2} + \frac{K}{4}} \right) \right]
 \end{aligned} \tag{B.3.15}$$

B.3.4 Renormalisation of J and K

We will track the entire renormalisation purely from that of J^+ , by virtue of the $\text{SU}(2)$ symmetry. J^+ renormalises through the JU_b terms. One of the terms is

$$\frac{1}{2} JU_b \sum_q \sum_{k,k'} S_d^+ c_{q\downarrow}^\dagger c_{k\uparrow} \frac{1}{\omega - H_D} \hat{n}_{q\uparrow} c_{k'\downarrow}^\dagger c_{q\downarrow} = -\frac{1}{2} \frac{JU_b n_j}{\omega - \frac{D}{2} + \frac{U_b}{2} + \frac{J}{4}} \sum_{k,k'} S_d^+ c_{k'\downarrow}^\dagger c_{k\uparrow} \tag{B.3.16}$$

The factor of half in front is the same half factor that appears in front of the $S_1^+ S_2^-, S_1^- S_2^+$ terms when we rewrite $\vec{S}_1 \cdot \vec{S}_2$ in terms of S^z, S^\pm . Another term is obtained by switching J and U_b :

$$\frac{1}{2} JU_b \sum_q \sum_{k,k'} \hat{n}_{q\downarrow} c_{q\uparrow}^\dagger c_{k\uparrow} \frac{1}{\omega - H_D} S_d^+ c_{k'\downarrow}^\dagger c_{q\uparrow} = -\frac{1}{2} \frac{JU_b n_j}{\omega - \frac{D}{2} + \frac{U_b}{2} + \frac{J}{4}} \sum_{k,k'} S_d^+ c_{k'\downarrow}^\dagger c_{k\uparrow} \tag{B.3.17}$$

The corresponding terms in the hole sector are

$$\frac{1}{2} JU_b \sum_q \sum_{k,k'} S_d^+ c_{k'\downarrow}^\dagger c_{q\uparrow} \frac{1}{\omega - H_D} \hat{n}_{q\downarrow} c_{q\uparrow}^\dagger c_{k\uparrow} = -\frac{1}{2} \frac{JU_b n_j}{\omega - \frac{D}{2} + \frac{U_b}{2} + \frac{J}{4}} \sum_{k,k'} S_d^+ c_{k'\downarrow}^\dagger c_{k\uparrow} \tag{B.3.18}$$

$$\frac{1}{2} JU_b \sum_q \sum_{k,k'} \hat{n}_{q\uparrow} c_{k'\downarrow}^\dagger c_{q\downarrow} \frac{1}{\omega - H_D} S_d^+ c_{q\downarrow}^\dagger c_{k\uparrow} = -\frac{1}{2} \frac{JU_b n_j}{\omega - \frac{D}{2} + \frac{U_b}{2} + \frac{J}{4}} \sum_{k,k'} S_d^+ c_{k'\downarrow}^\dagger c_{k\uparrow} \tag{B.3.19}$$

Adding all these terms and combining with the existing RG equation, we get the updated RG equation for J :

$$\Delta J = -J n_j \frac{4U_b + J}{\omega - \frac{D}{2} + \frac{U_b}{2} + \frac{J}{4}} \quad (\text{B.3.20})$$

We will follow the same strategy with K - we will calculate the renormalisation in K^+ . The first term is

$$\frac{1}{2} K U_b \sum_q \sum_{k, k'} \hat{n}_{q\downarrow} c_{q\uparrow}^\dagger c_{k'\uparrow} \frac{1}{\omega - H_D} C_d^+ c_{k\downarrow} c_{q\uparrow} = -\frac{1}{2} \frac{K U_b n_j}{\omega - \frac{D}{2} + \frac{U_b}{2} + \frac{K}{4}} \sum_{k, k'} C_d^+ c_{k\downarrow} c_{k'\uparrow} \quad (\text{B.3.21})$$

The second term in the same sector is obtained by flipping the spins of k and q :

$$\frac{1}{2} K U_b \sum_q \sum_{k, k'} \hat{n}_{q\uparrow} c_{q\downarrow}^\dagger c_{k'\downarrow} \frac{1}{\omega - H_D} C_d^+ c_{q\downarrow} c_{k\uparrow} = -\frac{1}{2} \frac{K U_b n_j}{\omega - \frac{D}{2} + \frac{U_b}{2} + \frac{K}{4}} \sum_{k, k'} C_d^+ c_{k\downarrow} c_{k'\uparrow} \quad (\text{B.3.22})$$

The terms in the hole sector give identical contributions. The RG equation for K is

$$\Delta K = -K n_j \frac{4U_b + K}{\omega - \frac{D}{2} + \frac{U_b}{2} + \frac{K}{4}} \quad (\text{B.3.23})$$

Bibliography

- [1] N. F. Mott, “The basis of the electron theory of metals, with special reference to the transition metals,” *Proceedings of the Physical Society. Section A*, vol. 62, pp. 416–422, jul 1949.
- [2] K. Held, R. Peters, and A. Toschi, “Poor man’s understanding of kinks originating from strong electronic correlations,” *Phys. Rev. Lett.*, vol. 110, p. 246402, Jun 2013.
- [3] P. Anderson, “A poor man’s derivation of scaling laws for the kondo problem,” *Journal of Physics C: Solid State Physics*, vol. 3, no. 12, p. 2436, 1970.
- [4] J. Schrieffer and P.A.Wolff, “Relation between the anderson and kondo hamiltonians,” *Phys. Rev.*, vol. 149, p. 491, 1966.
- [5] J. Kondo, “Resistance minimum in dilute magnetic alloys,” *Progress of theoretical physics*, vol. 32, no. 1, pp. 37–49, 1964.
- [6] Y. hui Zhang, S. Kahle, T. Herden, C. Stroh, M. Mayor, U. Schlickum, M. Ternes, P. Wahl, and K. Kern, “Temperature and magnetic field dependence of a kondo system in the weak coupling regime,” *Nature Communications*, vol. 4, July 2013.
- [7] P. W. Anderson and G. Yuval, “Exact results in the kondo problem: equivalence to a classical one-dimensional coulomb gas,” *Physical Review Letters*, vol. 23, no. 2, p. 89, 1969.
- [8] P. W. Anderson, G. Yuval, and D. Hamann, “Exact results in the kondo problem. ii. scaling theory, qualitatively correct solution, and some new results on one-dimensional classical statistical models,” *Physical Review B*, vol. 1, no. 11, p. 4464, 1970.
- [9] K. G. Wilson, “The renormalization group: Critical phenomena and the kondo problem,” *Rev. Mod. Phys.*, vol. 47, pp. 773–840, Oct 1975.
- [10] R. Bulla, T. Costi, and T. Pruschke, “Numerical renormalisation group method for quantum impurity systems,” *Rev. Mod. Phys.*, vol. 80, p. 395, 2008.
- [11] N. Andrei, K. Furuya, and J. H. Lowenstein, “Solution of the kondo problem,” *Rev. Mod. Phys.*, vol. 55, p. 331, 1983.
- [12] A. M. Tsvelick and P. B. Wiegmann, “Exact results in the theory of magnetic alloys,” *Adv. in Phys.*, vol. 32, p. 453, 1983.
- [13] I. Affleck, “Conformal field theory approach to the kondo effect,” *Acta Phys.Polon.B*, vol. 26, no. 1869, 1995.
- [14] I. Affleck and A. W. Ludwig, “Exact conformal-field-theory results on the multichannel kondo effect: Single-fermion green’s function, self-energy, and resistivity,” *Physical Review B*, vol. 48, no. 10, p. 7297, 1993.
- [15] E. Fradkin, C. von Reichenbach, and F. A. Schaposnik, “Bosonization of the kondo problem,” *Nuclear Physics B*, vol. 316, no. 3, pp. 710–734, 1989.
- [16] P. Nozieres, “A “fermi-liquid” description of the kondo problem at low temperatures,” *Journal of Low Temperature Physics*, vol. 17, p. 31, 1974.
- [17] M. Nozaki, S. Ryu, and T. Takayanagi, “Holographic geometry of entanglement renormalization in quantum field theories,” *Journal of High Energy Physics*, vol. 2012, no. 10, p. 193, 2012.
- [18] H. Krishnamurthy, C. Jayaprakash, S. Sarker, and W. Wenzel, “Mott-hubbard metal-insulator transition in nonbipartite lattices,” *Physical review letters*, vol. 64, no. 8, p. 950, 1990.
- [19] M. Hanl and A. Weichselbaum, “Local susceptibility and kondo scaling in the presence of finite bandwidth,” *Phys. Rev. B*, vol. 89, p. 075130, Feb 2014.
- [20] T. Arai, “Green’s function solution of the kondo problem and universality of the thermodynamic properties (invited),” *Journal of Applied Physics*, vol. 57, no. 8, pp. 3161–3165, 1985.
- [21] M. Gaass, A. K. Hüttel, K. Kang, I. Weymann, J. von Delft, and C. Strunk, “Universality of the kondo effect in quantum dots with ferromagnetic leads,” *Phys. Rev. Lett.*, vol. 107, p. 176808, Oct 2011.
- [22] E. S. Sørensen and I. Affleck, “Scaling theory of the kondo screening cloud,” *Phys. Rev. B*, vol. 53, pp. 9153–9167, Apr 1996.
- [23] I. Affleck and P. Simon, “Detecting the kondo screening cloud around a quantum dot,” *Phys. Rev. Lett.*, vol. 86, pp. 2854–2857, Mar 2001.
- [24] P. Simon and I. Affleck, “Kondo screening cloud effects in mesoscopic devices,” *Phys. Rev. B*, vol. 68, p. 115304, Sep 2003.
- [25] C. A. Busser, G. B. Martins, L. C. Ribeiro, E. Vernek, E. V. Anda, and E. Dagotto *Phys. Rev. B*, vol. 81, p. 045111, 2010.
- [26] L. C. Ribeiro, G. B. Martins, G. Gomez-Silva, and E. V. Anda *Phys. Rev. B*, vol. 99, p. 085139, 2019.

- [27] D. Goldhaber-Gordon, H. Shtrikman, D. Mahalu, D. Abusch-Magder, U. Meirav, and M. A. Kastner, “Kondo effect in a single-electron transistor,” *Nature*, vol. 391, pp. 156–159, Jan 1998.
- [28] S. M. Cronenwett, T. H. Oosterkamp, and L. P. Kouwenhoven, “A tunable kondo effect in quantum dots,” vol. 281, no. 5376, pp. 540–544, 1998.
- [29] J. Schmid, J. Weis, K. Eberl, and K. v. Klitzing, “A quantum dot in the limit of strong coupling to reservoirs,” vol. 256–258, pp. 182–185, Dec. 1998.
- [30] M. Pustilnik and L. Glazman, “Kondo effect in quantum dots,” vol. 16, pp. R513–R537, apr 2004.
- [31] I. V. Borzenets, J. Shim, J. C. H. Chen, A. Ludwig, A. D. Wieck, S. Tarucha, H.-S. Sim, and M. Yamamoto, “Observation of the kondo screening cloud,” *Nature*, vol. 579, pp. 210–213, Mar 2020.
- [32] N. Néel, J. Kröger, R. Berndt, T. O. Wehling, A. I. Lichtenstein, and M. I. Katsnelson, “Controlling the kondo effect in CoCu_n clusters atom by atom,” *Phys. Rev. Lett.*, vol. 101, p. 266803, Dec 2008.
- [33] A. Zhao, Q. Li, L. Chen, H. Xiang, W. Wang, S. Pan, B. Wang, X. Xiao, J. Yang, J. G. Hou, and Q. Zhu, “Controlling the kondo effect of an adsorbed magnetic ion through its chemical bonding,” *Science*, vol. 309, pp. 1542–1544, Sept. 2005.
- [34] A. Kaminski, Y. V. Nazarov, and L. I. Glazman, “Universality of the kondo effect in a quantum dot out of equilibrium,” *Phys. Rev. B*, vol. 62, pp. 8154–8170, Sep 2000.
- [35] H. R. Krishna-murthy, J. W. Wilkins, and K. G. Wilson, “Renormalization-group approach to the anderson model of dilute magnetic alloys. i. static properties for the symmetric case,” *Phys. Rev. B*, vol. 21, pp. 1003–1043, Feb 1980.
- [36] O. Sakai, Y. Shimizu, and T. Kasuya, “Single-particle and magnetic excitation spectra of degenerate anderson model with finite f-f coulomb interaction,” *Journal of the Physical Society of Japan*, vol. 58, no. 10, pp. 3666–3678, 1989.
- [37] T. Costi and A. Hewson, “A new approach to the calculation of spectra for strongly correlated systems,” *Physica B: Condensed Matter*, vol. 163, no. 1, pp. 179–181, 1990.
- [38] T. A. Costi, J. Kroha, and P. Wölfle, “Spectral properties of the anderson impurity model: Comparison of numerical-renormalization-group and noncrossing-approximation results,” *Phys. Rev. B*, vol. 53, pp. 1850–1865, Jan 1996.
- [39] J. Kroha and P. Wölfle, “Conserving diagrammatic approximations for quantum impurity models: Nca and ctma,” *Journal of the Physical Society of Japan*, vol. 74, no. 1, pp. 16–26, 2005.
- [40] T. A. Costi and A. C. Hewson, “Resistivity cross-over for the non-degenerate anderson model,” *Philosophical Magazine B*, vol. 65, no. 6, pp. 1165–1170, 1992.
- [41] Nozières, Ph. and Blandin, A., “Kondo effect in real metals,” *J. Phys. France*, vol. 41, no. 3, pp. 193–211, 1980.
- [42] J. Gan, N. Andrei, and P. Coleman, “Perturbative approach to the non-fermi-liquid fixed point of the over-screened kondo problem,” *Phys. Rev. Lett.*, vol. 70, pp. 686–689, Feb 1993.
- [43] V. J. Emery and S. Kivelson, “Mapping of the two-channel kondo problem to a resonant-level model,” *Phys. Rev. B*, vol. 46, pp. 10812–10817, Nov 1992.
- [44] J. Gan, “On the multichannel kondo model,” vol. 6, pp. 4547–4568, jun 1994.
- [45] A. M. Tsvelick and P. B. Wiegmann, “Solution of then-channel kondo problem (scaling and integrability),” *Zeitschrift für Physik B Condensed Matter*, vol. 54, pp. 201–206, Sep 1984.
- [46] A. M. Tsvelick and P. B. Wiegmann, “Exact solution of the multichannel kondo problem, scaling, and integrability,” *Journal of Statistical Physics*, vol. 38, pp. 125–147, Jan 1985.
- [47] O. Parcollet and A. Georges, “Transition from overscreening to underscreening in the multichannel kondo model: Exact solution at large N ,” *Phys. Rev. Lett.*, vol. 79, pp. 4665–4668, Dec 1997.
- [48] T. Kimura and S. Ozaki, “Fermi/non-fermi mixing in $\text{su}(n)$ kondo effect,” *Journal of the Physical Society of Japan*, vol. 86, no. 8, p. 084703, 2017.
- [49] D. Bensimon, A. Jerez, and M. Lavagna, “Intermediate coupling fixed point study in the overscreened regime of generalized multichannel $\text{SU}(n)$ kondo models,” *Phys. Rev. B*, vol. 73, p. 224445, Jun 2006.
- [50] D. L. Cox and M. Jarrell, “The two-channel kondo route to non-fermi-liquid metals,” vol. 8, pp. 9825–9853, nov 1996.
- [51] I. Affleck and A. W. Ludwig, “Critical theory of overscreened kondo fixed points,” *Nuclear Physics B*, vol. 360, no. 2, pp. 641–696, 1991.
- [52] P. Coleman, L. B. Ioffe, and A. M. Tsvelik, “Simple formulation of the two-channel kondo model,” *Phys. Rev. B*, vol. 52, pp. 6611–6627, Sep 1995.
- [53] S. Yasui and K. Sudoh, “Heavy-quark dynamics for charm and bottom flavor on the fermi surface at zero temperature,” *Phys. Rev. C*, vol. 88, p. 015201, Jul 2013.
- [54] K. Hattori, K. Itakura, S. Ozaki, and S. Yasui, “Qcd kondo effect: Quark matter with heavy-flavor impurities,” *Phys. Rev. D*, vol. 92, p. 065003, Sep 2015.
- [55] L. Fritz and M. Vojta, “The physics of kondo impurities in graphene,” vol. 76, p. 032501, feb 2013.
- [56] A. Principi, G. Vignale, and E. Rossi, “Kondo effect and non-fermi-liquid behavior in dirac and weyl semimetals,” *Phys. Rev. B*, vol. 92, p. 041107, Jul 2015.
- [57] A. K. Mitchell and L. Fritz, “Kondo effect in three-dimensional dirac and weyl systems,” *Phys. Rev. B*, vol. 92, p. 121109, Sep 2015.
- [58] S. Yasui and K. Sudoh, “Kondo effect of \bar{d}_s and \bar{d}_s^* mesons in nuclear matter,” *Phys. Rev. C*, vol. 95, p. 035204, Mar 2017.

- [59] S. Yasui, “Kondo effect in charm and bottom nuclei,” *Phys. Rev. C*, vol. 93, p. 065204, Jun 2016.
- [60] A. Mukherjee, A. Mukherjee, N. S. Vidhyadhiraja, A. Taraphder, and S. Lal, “Unveiling the kondo cloud: Unitary renormalization-group study of the kondo model,” *Phys. Rev. B*, vol. 105, p. 085119, Feb 2022.
- [61] R. Brockett, “Dynamical systems that sort lists, diagonalize matrices, and solve linear programming problems,” *Linear Algebra and its Applications*, vol. 146, pp. 79–91, 1991.
- [62] A. Mukherjee and S. Lal, “Unitary renormalisation group for correlated electrons-i: a tensor network approach,” *Nuclear Physics B*, vol. 960, p. 115170, 2020.
- [63] A. Mukherjee and S. Lal, “Unitary renormalisation group for correlated electrons-ii: insights on fermionic criticality,” *Nuclear Physics B*, vol. 960, p. 115163, 2020.
- [64] A. Mukherjee and S. Lal, “Scaling theory for mott–hubbard transitions: I. $t = 0$ phase diagram of the $1/2$ -filled hubbard model,” *New Journal of Physics*, vol. 22, p. 063007, jun 2020.
- [65] A. Mukherjee and S. Lal, “Scaling theory for mott–hubbard transitions-II: quantum criticality of the doped mott insulator,” *New Journal of Physics*, vol. 22, p. 063008, jun 2020.
- [66] K. Suzuki and R. Okamoto, “General structure of effective interaction in degenerate perturbation theory,” *Progress of Theoretical Physics*, vol. 71, no. 6, pp. 1221–1238, 1984.
- [67] F. Haldane, “Scaling theory of the asymmetric anderson model,” *Physical Review Letters*, vol. 40, no. 6, p. 416, 1978.
- [68] S. Patra, A. Mukherjee, A. Taraphder, N. Vidhyadhiraja, and S. Lal *Unpublished*, 2022.
- [69] A. C. Hewson, *The Kondo Problem to Heavy Fermions*. Cambridge University Press, 1993.
- [70] T. Chowdhury and K. Ingersent, “Critical charge fluctuations in a pseudogap anderson model,” *Phys. Rev. B*, vol. 91, p. 035118, Jan 2015.
- [71] R.-U.-H. Wani and V. N S, “Scaling analysis of the extended single impurity anderson model: Renormalization due to valence fluctuations,” 10 2017.
- [72] j h jefferson, “a renormalisation group approach to the mixed valence problem,” *journal of physics c: solid state physics*, vol. 10, pp. 3589–3599, sep 1977.
- [73] S. Kehrein, *The flow equation approach to many-particle systems*, vol. 217. Springer, 2007.
- [74] S. D. Glazek and K. G. Wilson, “Renormalization of hamiltonians,” *Physical Review D*, vol. 48, no. 12, p. 5863, 1993.
- [75] F. Wegner, “Flow-equations for hamiltonians,” *Annalen der physik*, vol. 506, no. 2, pp. 77–91, 1994.
- [76] R. Žitko and J. Bonča, “Spin-charge separation and simultaneous spin and charge kondo effect,” *Phys. Rev. B*, vol. 74, p. 224411, Dec 2006.
- [77] P. W. Anderson, “Random-phase approximation in the theory of superconductivity,” *Physical Review*, vol. 112, no. 6, p. 1900, 1958.
- [78] Y. Nambu, “Quasi-particles and gauge invariance in the theory of superconductivity,” *Phys. Rev.*, vol. 117, pp. 648–663, Feb 1960.
- [79] T. A. Costi, “Kondo effect in a magnetic field and the magnetoresistivity of kondo alloys,” *Phys. Rev. Lett.*, vol. 85, pp. 1504–1507, Aug 2000.
- [80] A. Rosch, T. A. Costi, J. Paaske, and P. Wölfle, “Spectral function of the kondo model in high magnetic fields,” *Phys. Rev. B*, vol. 68, p. 014430, Jul 2003.
- [81] D. C. Langreth, “Friedel sum rule for anderson’s model of localized impurity states,” *Phys. Rev.*, vol. 150, pp. 516–518, Oct 1966.
- [82] J. Luttinger, “Fermi surface and some simple equilibrium properties of a system of interacting fermions,” *Physical Review*, vol. 119, no. 4, p. 1153, 1960.
- [83] M. Oshikawa, “Topological approach to luttinger’s theorem and the fermi surface of a kondo lattice,” *Physical Review Letters*, vol. 84, no. 15, p. 3370, 2000.
- [84] K. Seki and S. Yunoki, “Topological interpretation of the luttinger theorem,” *Physical Review B*, vol. 96, no. 8, p. 085124, 2017.
- [85] P. W. Anderson, “Localized magnetic states in metals,” *Phys. Rev.*, vol. 124, pp. 41–53, Oct 1961.
- [86] P. Coleman, *Introduction to many-body physics*. Cambridge University Press, 2015. Chapter:18.
- [87] P. Phillips, *Advanced solid state physics*. Cambridge University Press, 2012.
- [88] R. M. Martin, “Fermi-surface sum rule and its consequences for periodic kondo and mixed-valence systems,” *Physical Review Letters*, vol. 48, no. 5, p. 362, 1982.
- [89] S. Patra and S. Lal, “Origin of topological order in a cooper-pair insulator,” *Phys. Rev. B*, vol. 104, p. 144514, Oct 2021.
- [90] A. Mukherjee and S. Lal, “Holographic entanglement renormalisation of topological order in a quantum liquid,” 2020.
- [91] G. Moeller, Q. Si, G. Kotliar, M. Rozenberg, and D. S. Fisher, “Critical behavior near the mott transition in the hubbard model,” *Phys. Rev. Lett.*, vol. 74, pp. 2082–2085, Mar 1995.